UNIVERSITY OF VENDA

Removal of cationic and anionic dyes from aqueous solution using a clay-based nanocomposite.

By

Tholiso Ngulube

Student No: 11601328

Student:	**T Ngulube**	**Signed**	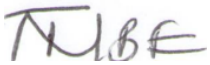	**Date 30/04/2019**
Promoter:	**Prof JR Gumbo**	**Signed**		**Date 30/04/2019**
Co - promoter:	**Dr V Masindi**	**Signed**		**Date 30/04/2019**
Co – promoter:	**Prof A Maity**	**Signed**	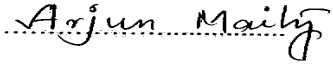	**Date 30/04/2019**

A PhD thesis submitted to the Department of Ecology and Resource Management in fulfillment of the requirements for the degree of Doctor of Philosophy in Environmental Sciences at the University of Venda

DEDICATION

This research is dedicated to my Creator, without his transmuting power, I would never have begun this journey, let alone finish it. He is faithful from the beginning to the end.

GRAPHICAL ABSTRACT

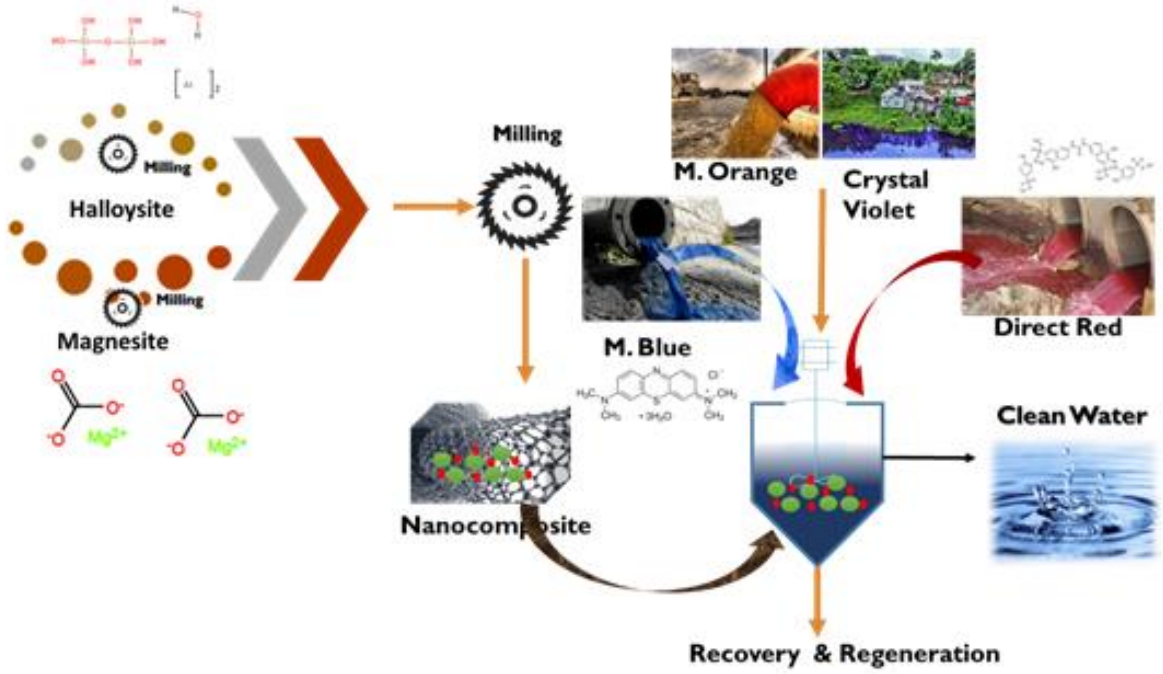

ABSTRACT

Some industries such as textiles, ceramics, paper and printing are known to use significant amounts of dye to colour their products and during the colouring process, certain quantities of dyes are absorbed by the products, and some of them end up in wastewater. Depending on their application, some synthetic dyes are designed to be chemically or biologically resistant and their presence in the environment can cause severe environmental problems because of their colour impartation to water bodies. Therefore, proper treatment is required to remove these pollutants from wastewater before discharge into the environment. In this thesis, the potential of dye removal from wastewater by calcined magnesite, halloysite nanoclay and calcined magnesite - halloysite nanoclay composite was evaluated. To this end, the study was subdivided to four segments.

The first segment of the study focused on evaluating the efficiency of using calcined magnesite to remove Methylene Blue (MB), Direct Red 81 (DR81), Methyl Orange (MO) and Crystal Violet (CV) dyes from aqueous systems using a batch study. To achieve that, several operational factors like residence time, adsorbent dosage, dye concentration and temperature were appraised. The adsorbent was subjected to different kinds of physicochemical characterization to determine the various characteristics that would assist in the dye uptake process. Characterization results showed that the adsorbent material was highly crystalline with magnesite, periclase, dolomite, and quartz as some of the crystalline phases. The batch study proved that calcined magnesite is effective in the treatment of dye contaminated water and moreover it performed well in terms of colour removal, though exceptional results were recorded for CV removal with complete decolourisation occurring in first few minutes of contact. In terms of experimental adsorption capacity, the performance of calcined magnesite was in the order CV (14.99 mg/g) > DR81 (12.56 mg/g) > MO (0.64 mg/g) > MB (0.39 mg/g). Mechanisms of adsorption where explained by fitting the experimental data into adsorption isotherms, kinetics, and thermodynamic parameters. Neither, the Langmuir, nor the Freundlich nor the Dubinin Radushkevich, nor the Temkin model could perfectly describe the adsorption of the four dyes onto calcined magnesite, however adsorption kinetics obeyed the pseudo second order model, implying that, the dye removal process was primarily a chemical process. In accordance with the results of this study, it can be concluded that calcined magnesite can be used effectively for the removal of dyes in aqueous solution and thus can be applied to treat wastewater containing dyes.

The second segment of the study focused on the removal of MB, DR81, MO and CV dyes by halloysite nanoclay. Physicochemical characterisation revealed that the nanoclay has a surface area of 42 m^2/g and its

morphology is predominated by tubular structures, which exhibit some hollow rod like structures. Various important parameters namely contact time, initial concentration of dyes, dosage, solution temperature and solution pH were optimized to achieve maximum adsorption capacity and it was observed that the effect of initial pH and temperature of the aqueous solution was neglibible on removal of the four dyes. The experimental adsorption capacities towards 40 mg/L of MB, DR81, MO and CV dyes were 17.51, 14.11, 0.38, and 4.75 mg/g respectively. The results indicate that natural halloysite nanoclay is an efficient material for the removal of the selected dyes. Due to its low cost and non-toxicity, halloysite nanoclay can be considered a good replacement option of other high cost materials used to treat coloured wastewater especially in developing countries like South Africa.

Having observed the performance of calcined magnesite and halloysite nanoclay individually in the removal of selected dyes, a third study was designed with the aim of preparing a nanocomposite adsorbent from the aforementioned adsorbent materials and then evaluating the synergistic influence of the mechanochemical modification by a ball miller on the removal of MB, DR81, MO and CV dyes. Physicochemical characterization was carried out to get an insight of pre- and -post adsorption characteristics of the nanocomposite material and results showed major changes which could be an indication of dye uptake by the nanocomposite material. According to the results, the nanocomposite material outcompeted its component individual constituent materials i.e (calcined magnesite and halloysite nanoclay material) in the removal of DR81, which in turn was the highest removal efficiency observed for the whole batch adsorption study recording a maximum adsorption capacity and percentage removal of 19.89 mg/g and 99.40% respectively. Experimental results fitted the Langmuir and pseudo-second order models perfectly hence demonstrating that adsorption took place on a homogenous adsorbent layer via chemisorption. In overall, the results suggested that the nanocomposite is a suitable adsorbent for decolourising industrial wastewater.

Based on the overall performance of the adsorbents in removing the four dyes, it was observed that the nanocomposite material had a high affinity for DR81 dye hence it was chosen as the model dye for further application in column studies. The effect of flow rate, bed height and initial dye concentration on the removal of DR81 was investigated. Maximum bed capacity and equilibrium dye uptake were determined and break through curves were plotted. Percentage dye removal increased with decrease in flow rate and increase in bed height. The maximum capacity of column was found to be about 51.73 mg DR81 per gram of the nanocomposite adsorbent for a flow rate of 3 mL/min, initial concentration of 10 mg/L and 4 cm bed height. Data from column studies was fitted to the Thomas model and Adams-Bohart models. The comparison of the R^2 values obtained from both models showed a better fit for the nanocomposite material than the individual halloysite nanoclay and calcined magnesite materials. The study revealed the applicability of calcined magnesite- halloysite nanoclay composite in fixed bed column for the removal of DR81 dye from aqueous solution.

The reuse of an adsorbent is essential in order to make the adsorption process economic and environmentally friendly. To recover the adsorbate and renew the adsorbent for further use, a chemical method of regeneration was applied by using 0.1 M NaOH as the desorbent. Regeneration with 0.1 M NaOH proved very efficient for some dyes and less efficient for others depending on the adsorbent material used at the time. The general observation was that the adsorption capacity of the adsorbent materials decreased with successive adsorption – desorption cycles. Furthermore, regeneration with NaOH, favoured the acidic dyes (DR81 and MO) more than the basic dyes (MB and CV) possibly due to electrostatic interactions between oppositely charged molecules allowing for reversible reactions to take place.

The three tested adsorbents namely calcined magnesite, halloysite nanoclay and their nanocomposite thereof were applied for the treatment of real wastewater effluent from a printing and ink industry. The adsorbents performed very well in terms of colour removal as recommended by the South African standards of wastewater discharge, However, in terms of pH, calcined magnesite and the nanocomposite produced a highly alkaline solution hence wastewater neutralisation by an acid is recommended before discharge. These findings show that the two natural clay-based materials (calcined magnesite and halloysite nanoclay) and their nanocomposite thereof have a great potential for application in dye wastewater remediation since the materials used in the process are inexpensive, abundant and require minimal modifications.

Key words: adsorption mechanisms, calcined magnesite, dyes, halloysite, nanocomposite, wastewater treatment.

DECLARATION

I declare that this is my own work and it contains no material which has been accepted for the award of any other degree or diploma in any university or other tertiary institutions. To the best of my knowledge I also believe that it contains no material previously published by another person except where due reference has been made.

I give consent to this copy of my thesis, when deposited in the University library being made available for loan and photocopying subject to the provisions of the Copyright Act 1978. I do acknowledge that copyright of published works contained within this thesis resides with the copyright holders of those published works.

Tholiso Ngulube February 2019

Signature … 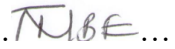 …

ACKNOWLEDGEMENTS

First and foremost, I would like to acknowledge my Creator, he bestowed me the courage and strength to pull throughout this PhD journey. Without which, I would have never completed.

To all the people who have helped me to sail in this boat, my sincere gratitude goes to you. To begin with, let me thank my promoters, Prof Gumbo J.R, Dr Masindi V and Prof Maity A for their academic guidance. Their support and faith in me allowed me to begin and to complete this project. It is because of them that this project is a success.

A special thank you goes to the Director of Research and Innovation, University of Venda, National Research Foundation and Water Research Commission. Thank you for the financial support from the beginning through to the end of my research. I never struggled with funds to run the project.

From my research group, my thanks go out to all who provided help along the way. I am endlessly grateful for the people who encouraged and poked me when I was down and was tempted to quit. However, special recognition must be made of the friends who stopped by the or called each time I did not show up to see whether my day was productive, Mudau M and Munyai L.F. More than anyone else, Mudau knows the days I barely achieved anything, yet he kept on encouraging me to persist.

I would also like to say a heartfelt thank you to Lebelo T.P. Towards the completion of this PhD, at some point I almost lost it and gave up, but you supported me spiritually throughout the challenging period. Profound gratitude to you.

Above all, many thanks go to my loving and supporting family. My mum Beria, those words of wisdom you would always say over the phone when things were tough, “the darkest hour is just before the dawn” how can I ever forget that. My sister, Thoko, just for being a shoulder to cry on, you are a rock and then my brother Khathu, this one is for you. You believe in me more than I believe in myself. If that is not inspiration enough, then I don’t know what is. Indeed, you guys are always a bedrock of support to me.

ACADEMIC OUTPUTS

Patent

1. Title: Method of Removing Dyes from wastewater. PTC Patent Application No: TBA. ZA Patent number: 2018/08369. Filing date 11/12/2018. Inventors: Gumbo J.R., Masindi V. & Ngulube T.

Published journal articles

1. Ngulube T., Gumbo J.R., Masindi V., Maity A., 2017. An update on synthetic dyes adsorption onto clay-based minerals: A state-of-art review. Journal of Environmental Management. 191, 35-57.
2. Ngulube T., Gumbo J.R., Masindi V., Maity A., 2018. Calcined magnesite as an adsorbent for cationic and anionic dyes: Characterization, adsorption parameters, isotherms and kinetics study. Heliyon. 4(10), e00838. doi: 10.1016/j.heliyon. 2018.e00838.
3. Ngulube T., Gumbo J.R., Masindi V., Maity A., 2019. Preparation and characterisation of high performing magnesite-halloysite nanocomposite and its application in the removal of methylene blue dye. Journal of Molecular Structure. In Press.doi.org/10.1016/j.molstruc.2019.02.043.

Manuscripts accepted for publication

1. Ngulube T., Gumbo J.R., Masindi V., Maity A., 2019. Evaluation of the efficacy of halloysite nanotubes in the removal of acidic and basic dyes from aqueous solution. Clay Minerals - Journal of Fine Particle Science.

Manuscript submitted and under review

1. Ngulube T., Gumbo J.R., Masindi V., Maity, A., 2018. Mechanochemical-synthesis of a super-performing nanocomposite and its application on the removal of cationic and anionic dyes. Chemical Sciences Journal.

Accepted book chapters

1. Ngulube T., Gumbo J.R., Masindi V., Maity A., 2018. Enhanced removal of Direct Red 81 dye from synthetic wastewater using ball-milled magnesia. Nova Science Publishers.

Published conference proceedings

1. Ngulube T., Gumbo J.R., Masindi V., Maity A., 2018. Insight into the removal of dyes from synthetic dye wastewater using magnesite. Fifth International Symposium on Green Chemistry, Sustainable Development and Circular Economy. Skiathos, Greece. Environmentally Benign processes and products. 109-117. ISBN:978 -618-5271-61-9.
2. Ngulube T., Gumbo J.R., Masindi V., Maity A., 2018. Synergistic approach in the removal of dyes from aqueous solution using magnesite-halloysite nanocomposite. Development and Identification of Novel green technologies, products and perspectives. 151-159. ISBN:978 -618-5271-61-9.

Conference Presentations

1. Ngulube T., Gumbo J.R., **Masindi V**., Maity, A., 2018. Insight into the removal of dyes from synthetic dye wastewater using magnesite. Fifth International Symposium on Green Chemistry, Sustainable Development and Circular Economy. Greece. **(Oral presentation).**
2. **Ngulube T**., Gumbo J.R., Masindi V., Maity A., 2018. The treatment of dye contaminated wastewater using cryptocrystalline magnesite. 18th Global Summit on Environmental Toxicology and Pharmacology. 17-18 September 2018, Singapore. **(Poster presentation).**
3. **Ngulube T**., Gumbo J.R., Masindi V., Maity A., 2018. Effective removal of methyl orange from aqueous solution using magnesia. First Pan African International Research Congress on Knowledge Generation and Knowledge Generation and Dissemination (PAIRC-2018). 18 - 22 June 2018. Kisumu, Kenya. **(Oral presentation).**
4. **Ngulube T**., Gumbo J.R., Masindi V., Maity A., 2018. Cryptocrystalline magnesite nano-adsorbent for dye removal in wastewater. The 7th international conference on Nanoscience and Nanotechnology in Africa. 22 – 25 April 2018. Durban, South Africa. **(Poster presentation).**
5. **Ngulube T**., Gumbo J.R., Masindi V., Maity A., 2017. Application of magnesite-halloysite composite for the treatment of coloured industrial wastewater. 18th WaterNett//WARFFSA//GWP -SA Symposium on Integrated Water Resources Development and Management: Innovative Technological Advances for Water Security in Eastern and Southern Africa, 25 – 27 October 2017. Swakopmund, Namibia. **(Oral presentation).**
6. **Ngulube T**., Gumbo J.R., Masindi V., Maity A., 2017. Treatment of crystal violet, a toxic dye, from industrial wastewater using cryptocrystalline magnesite. First Regional Conference and School on Climate Change, Water and Environmental Sanitation for Early Career Scientists Working in Africa. 28 – 31 August 2017. Accra – Ghana. **(Oral presentation).**

7. **Ngulube T**., Gumbo, J.R., Masindi, V., Maity, A., 2017. The treatment of dye wastewater using natural South African magnesite. J Pollut Eff Cont 2017, 5:2 (Suppl) DOI: 10.4172/2375-4397-C1-005. Australia. **(Oral presentation).**
8. **Ngulube T**., Gumbo, J.R., Masindi, V., Maity, A., 2016. Synthetic dye adsorption onto clay materials: A review. 2nd UNIVEN-WSU International Research Conference Galvanising development through research and innovation. 5 - 7 October 2016. Polokwane, South Africa. **(Poster presentation).**

ACRONYMS AND ABBREVIATIONS

BET	: Brunauer-Emmett-Teller method
COD	: Chemical Oxygen Demand
CV	: Crystal Violet
DR81	: Direct Red 81
DWA	: Department of Water Affairs
DWS	: Department of Water and Sanitation
EC	: Electrical conductivity
FTIR	: Fourier Transform Infrared
ICP-MS	: Inductively Coupled Plasma Mass Spectrometry
NTU	: Nephelometric Turbidity Unit
MB	: Methylene Blue
MO	: Methyl Orange
PZC	: Point of Zero Charge
SEM	: Scanning Electron Microscopy
SEM-EDS	: Scanning Electron Microscopy-Electron Dispersive Spectra
TEM	: Transmission Electron Microscopy
TDS	: Total Dissolved Solids
TGA	: Thermal Gravimetric Analysis
XRD	: X-ray Diffraction
WHO	: World Health Organization
WRC	: Water Research Commission

NB: Please refer to the periodic table of elements for the elements

TABLE OF CONTENTS

CHAPTER ONE

1.1 Background Information

Mother Nature expresses itself in different spectrums of colours all around us, such that the world today would be unimaginable without colours. Industries such as textiles, leather, paper-making, plastics, food, rubber, and cosmetics use different types of dyes, which also appear in the effluents discharged from some of these industries (Ngulube et al., 2018). Generally, dyes are stable to light, heat and oxidizing agents and are usually non-biodegradable (Kono, 2015). The presence of dyes in water bodies cannot be easily ignored because they impart colour to water bodies (Kant, 2012). The presence of colour in water bodies affects aquatic diversity by blocking the passage of sunlight which is needed for photosynthesis. This colour in water bodies also has an adverse aesthetic effect. Furthermore, dyes are known to have toxic effects to some organisms due to the presence of aromatics and metals in their structures (Yagub et al., 2014). A major concern in wastewater treatment is the release of dyes and their metabolites into the environment as some may be mutagens and carcinogens. Some of these dyes are considered to be xenobiotic in nature and aerobically recalcitrant to biodegradation (De Jagger, 2013), and thus pose a threat to the environment when wastewater is disposed off, untreated. In that regard, there is a need to find treatment technologies that can decolourise the water and at the same time reduce the toxic effects of the dyes to within permissible limits as stipulated by water quality guidelines.

Being among the most demanding environmental tasks of the modern day, the increasing amount of toxic industrial waste has led to the development of various decontamination methods and techniques (Chollom, 2014). Usually, industrial wastewater is treated by various methods like adsorption, precipitation, chemical degradation, advanced oxidation processes, biodegradation and chemical coagulation (Kobya et al., 2007; Mohan et al., 2007; Du et al., 2010). Although these methods have been widely applied, they have some shortcomings (Pajootan et al., 2012). For example, biological methods are time consuming and are often ineffective in removing dyes which are highly structured polymers with low biodegradability and cannot be applied to most textile wastewaters due to the toxicity of most commercial dyes to the organisms used (Buthelezi, 2012). Chemical coagulation causes extra pollution due to the undesired reactions in treated water and produces large amounts of sludge (Kobya et al., 2007). Chemical degradation by oxidative agents such as chlorine is the most effective method, but it produces some very toxic products such as organochlorine

compounds (Merzouk et al., 2011). Advanced oxidation processes such as ozonation, ultra violet and ozone–UV combined oxidation, photocatalysis, fenton reactive and ultrasonic oxidation are not economically feasible (Daneshvar et al., 2006). Furthermore, these methods are also usually expensive and treatment efficiency is inadequate because of the large variability of the composition of textile wastewaters (Drouiche et al., 2011).

Adsorption however seems to be one of the most preferable techniques used for water treatment because of low initial costs, simple design and ease of use and implementation even in small plants. Activated carbon adsorption has been widely used for industrial wastewater treatment but it has the disadvantage of high costs and difficulty of the regeneration process and a high waste disposal cost (Yagub et al., 2014). Because of very stringent laws regarding elimination of dyes from wastewaters before their discharge into water bodies and expensive conventional sorbents, there is an increasing tendency for the development of new, adequate, low-cost adsorbents with satisfactory adsorption properties and inexpensive to regenerate.

Various naturally occurring materials that are available and abundant have been explored as adsorbents for the removal of dyes from wastewater (Nandi et al., 2009; Rafatullah et al., 2010; Tehrani-Bagha et al., 2011; Ali et al, 2012; Ghosh and Reddy, 2013). A great interest has grown towards naturally occurring adsorbents, preferably the development of an adsorbent demonstrating both a high adsorption capacity and low cost for removing contaminants from polluted waters. Although a wide variety of adsorbents have been used for wastewater treatment, naturally available clays have been the adsorbents of choice in most developing countries (Weng and Pan, 2007; Nandi et al., 2009; Ali et al., 2012) It is extremely important to choose a technique that is cheap, requires only minor workloads and at the same time it should not be complicated. Obviously, the maintenance and repair should be easy and affordable. Using clays and earth minerals for industrial wastewater treatment fits well with all the above-mentioned parameters. This study, therefore, intends to synthesize a nanocomposite adsorbent (calcined magnesite - halloysite nanoclay composite) that can remove dyes from aqueous solution.

Halloysite clay is a low-cost adsorbent which can be used for wastewater treatment. Halloysite nanotubes (HNTs) are naturally occurring eco-friendly nanotubes that are harmless to humans (Yao et al., 2015). Halloysite nanotubes are unique and versatile nanomaterials composed of double layered aluminosilicate ($Al_2Si_2O_5(OH)_4.H_2O$ with 1:1 layer) minerals with a predominantly hollow tubular structure in submicron range (Liu et al., 2011). Halloysite has a similar composition to that of kaolinite except that it contains additional water molecules between the layers and most commonly has a tubular morphology. The presence of metal oxides and/or hydroxides in halloysite contribute towards anionic dye adsorption (Zhang et al., 2015). Halloysite nanotubes, a low-cost available clay mineral, were tested for the ability to remove dyes such as Neutral Red (Luo et al., 2011), Methylene blue (Yao et al., 2015) and Malachite Green (Kiani et al.,

2011) from aqueous solution and they performed well in dye removal. Natural halloysite nanotubules used as adsorbents showed that their adsorption potential increased with increase in the dose of adsorbent, initial pH, temperature and initial concentration (Luo et al., 2010; Liu et al., 2011).

Magnesium containing materials have been used by numerous researchers to remove dyes from wastewater due to the potential of this metal in adsorption processes (Tan et al., 2000; Gao et al., 2007). Research has shown that alkaline earth metal hydroxides/oxides have strong affinity for water pollutants and this makes them potential dye adsorbents (Wang et al., 2009). However, synthetic alkaline earth metals, are much expensive when compared to natural earth materials when used in the treatment of wastewater hence their application for such purposes is restricted. Naturally occurring alkaline earth metal salts such as magnesite and gypsum offer potential alternatives to be used for wastewater treatment. Magnesite is as a low-cost and locally available material and it has been used for the removal of metals in wastewater treatment (Masindi et al., 2014), defluoridation of groundwater (Masindi et al., 2015), the removal of metalloids (Masindi et al., 2015a), the removal of phosphates (Masindi et al., 2015b) and the remediation of acid mine drainage (Masindi et al., 2014c). Owing to its ability to remove inorganic contaminants from wastewater, the potential of calcined magnesite on the removal of dyes will be tested in this study.

Considering the fast development of nanomaterials, environmental nanotechnology has attracted a lot of interest from the science community. In the field of water treatment, nanotechnology exhibits a great potential in improving the performance and efficiency of water decontamination as well as providing a sustainable approach to secure water supply (Kanchi, 2014). Green nanotechnology aims at developing environmentally safe and less harmful nano products (Nath and Banerjee, 2013). Nanocomposites and nano powders are now emerging as trend setters in the wastewater treatment industry hence the need to modify naturally occurring materials to nanoscale level.

Many modification and synthetic methods exist for preparing nanocomposites but only a few are ‘green’ and less costly. Methods like pillaring and intercalation (Gupta and Bhattacharyya, 2006; 2008), acid activation (Gupta and Bhattacharyya, 2011) and mechanochemical activation (Vdović et al., 2010) can be applied to enhance the adsorption capacity of clays. Amongst these, mechanochemical activation has proved to be preferable due its low cost and environmentally friendly properties. Several researchers studied the effect of mechanochemical activation on structural and morphological variations of clays (Lee et al., 2007; Ramadan et al., 2010; Vdović et al., 2010), but only a few studies explored the use of milling on their adsorption properties (Nenadović et al., 2009; Kumrić et al., 2013). Destruction, alteration, fragmentation of the crystalline network and reduction of particle size together with increased surface area and amorphization, can lead to enhanced removal of contaminants by modified clays (Makó et al., 2001; Hrachová et al., 2007). To overcome the restrictions and weaknesses of using raw and chemically modified clays as adsorbents,

composite adsorbents can be prepared by way of grinding and/or milling. This is a novel study to evaluate the feasibility of applying mechanochemically synthesised clay-based nanocomposite for the decolouration of aqueous dye solutions.

Numerous studies have looked at the successful synthesis of adsorbent materials and their application in water treatment but there exist few studies that proceed to investigate what happens after the adsorbent material has been exhausted and can no longer be used for adsorption process. The available options currently used for managing post-sorbents are restricted to recovering the adsorbate, disposing of the adsorbent in a landfill and safe storage (Reddy et al., 2016). It should be highlighted that adsorption only transfers contaminants from one phase to the next and consequently generating sludge which must be regenerated, disposed off or managed by some other processes (Reddy et al., 2016a) which is a limitation as a method of removing dyes from aqueous solution. During the adsorption process, the physical structure of the adsorbent does not get altered much. When the adsorbent material is to be regenerated, the fate of the resultant concentrated sludge of dyes presents a problem of correct disposal (Guilane et al., 2016). Many adsorbent materials can be disposed off in landfills, however, this must be done in compliance with standard disposal regulations (McKay, 1995). Disposal of the adsorbent material is subject to certain requirements including using a landfill that demonstrates safe immobilisation of the absorbed liquid so as not to allow free liquid to leak into waste repositories (Feng et al., 2013). Apart from regenerating and disposing of spent adsorbents there are value added applications of spent adsorbents. It is essential to find sustainable ways of effectively using contaminant loaded adsorbents as value-added products to solve economic, management and toxicity issues associated with the spent adsorbent materials (Dodson et al., 2015).

Magnesite is widely used in industries for various applications including steel boiler additives, plastics, rubber, and pulp processing, adhesives, preparation of cement, fertilizer and animal feed (Kawasaki et al., 2006; Masindi et al., 2014). Magnesite is also used almost exclusively for refractory applications in the form of basic bricks and granular refractories. Basic magnesite bricks are used in furnaces, ladles and secondary refining vessels and in cement and glass making kilns (Chowdhury et al., 2013). Magnesite has a very high melting point amongst common refractory oxides and due to that, its application is extensive for high temperature processes in the steel industry. Other magnesite applications include thermal insulation and electrical insulation (electric ovens and appliances). These wide applications in the industry can be explored as post sorbent applications when calcined magnesite material becomes exhausted after adsorption.

Halloysite is a kaolin clay that can be used for a variety of clay-based applications in the industries. Clays have a variety of physicochemical characteristics that make them suitable for various industrial applications including making pottery, both utilitarian and decorative, and construction products, such as bricks, wall and floor tiles (Guggenheim and Martin, 1995). Different types of clay, when used with different minerals and

firing conditions, are used to produce earthenware, stoneware and porcelain. Clay can also be used as a filter medium and liners in landfills hence after adsorption process, halloysite clay can also be developed into various value-added post sorbent products.

1.2 Problem statement

Dye wastewater is complex and consists of concentrated waste process water which contains a wide and varied range of dyes and their metabolites (Shoukat et al., 2017). This wastewater contains non-biodegradable constituents and the impartation of colour to water bodies affects aquatic diversity by blocking the passage of sunlight. Due to the complexity of dye wastewater, some industrial companies do not meet environmental discharge standards, causing detrimental problems if the wastewater is discharged into the sewage system and eventually into the aquatic environment (Ngulube et al., 2017). Unless the wastewater is properly treated before it is discharged, it will contaminate the environment.

Three processes are used for the treatment of textile wastewater: biological, physical and chemical methods (Akram et al., 2017; Nouren et al., 2017). However, this manner of treating textile wastewater is not sufficient. Physical treatment methods and physico-chemical methods such as flocculation are limited due to the high electrolytic strength of the dye liquid (Kausar et al., 2018). Chemical methods such as ozonation are also used, however, degradation products which result from ozonation and chlorination increase in the recycled liquid and act as colourless dyes which obstruct the dyeing process (Iqbal and Bhatti, 2015). Some biological treatment methods are toxic to the microorganisms used and adsorption using activated carbon seems a very viable method; colour removal is limited because only a single dye can be treated in a run (Chollom, 2014).

Moreover, the cost of treating these effluents is on the increase. Consequently, most textile industries have their own effluent treatment plants where most of the waste coming from various processes is combined and treated prior to its discharge to the environment. Biological and chemical methods are usually applied for end-of-pipe treatment (Pirkarami et al., 2013). The effluents from different processes are collected and treated together. The mixture of these streams makes the characteristics of the effluent complex. Therefore, the water quality obtained from these treatments is not satisfactorily high because most of the compounds cannot be easily degraded (Martınez-Huitle and Brillas 2009). The reclaimed water still contains colour. In addition, these processes are unable to decrease salinity and most of them are expensive and require expertise in the operation of the equipment employed (Daneshvar et al., 2006; Drouiche et al., 2011). The conventional methods are therefore limited because the quality of water produced do not meet the water quality guidelines.

It is, therefore, imperative to use cheap treatment methods that can treat the effluent to water for reuse in order to save on the costs incurred by treating the effluents and disposing into rivers and reduce fresh water consumption. This can be done using the adsorption treatment option in the dyeing process such that the most

polluted streams are treated at the point of collection. Adsorption using clay-based materials is relatively cheap because it uses materials that are naturally available in abundance, the materials do not need pre-chemical treatment before use, and they are not toxic to the environment hence are very important products in the green nanoscale technology of wastewater treatment.

1.3 Aim and objectives

The main goal of this study is to evaluate the efficiency of calcined magnesite, halloysite nanoclay and their corresponding nanocomposite on the removal of selected cationic and anionic dyes from aqueous solution.

The project involves a major technological practice for wastewater treatment i.e. adsorption which encompasses numerous developmental stages which will be addressed by the following specific objectives.

I. To synthesize a nanocomposite adsorbent using calcined magnesite and halloysite nanoclay using a vibratory ball miller.

II. To identify the physicochemical characteristics of calcined magnesite, halloysite nanoclay and their corresponding nanocomposite using different characterization techniques.

III. To optimize conditions that are suitable for the removal of selected cationic and anionic dyes from aqueous solution via a batch study using calcined magnesite, halloysite and calcined magnesite – halloysite nanoclay composite and establish the mechanisms governing the removal of those dyes using different mathematical adsorption models.

IV. To optimize conditions that are suitable for the removal of a selected dye from aqueous solution via a column study using calcined magnesite, halloysite nanoclay and their nanocomposite thereof.

V. To determine the regeneration potential of the calcined magnesite, halloysite and their nanocomposite thereof.

1.4 Hypothesis

A nanocomposite prepared from calcined magnesite and halloysite nanoclay using a vibratory ball milling technique can successfully remove selected cationic and anionic dyes from aqueous solution.

1.5 Significance of study

Many investigations have been done on the remediation of dye wastewaters (Zhou et al., 2014; Han et al., 2016; Yang et al., 2018). However, environmentally friendly and low-cost techniques that can be used by small scale industries are hardly available. Conventional advanced wastewater treatment technologies such

as ozonation, membrane separation and electrolysis are costly and hence the driving force is to search for creative, low cost and environmentally sound ways of treating wastewater as environmental laws are becoming stringent (Yagub et al., 2014; Ngulube et al., 2017). Recently, the development of green nanotechnology in wastewater treatment is growing very fast (Karishma and Mehali, 2015). Green nanotechnology aims at developing environment safe and less harmful nano products from nanocomposites and nano powders.

Most conventional methods require high capital investment and are high in operational costs and create sludge disposal problems (Rafatullah et al., 2010). Although the adsorption technique is relatively cheap, there is a pressing need to replace commercial adsorbents like activated carbon, zeolite, activated alumina and silica gel with the low-cost adsorbents. The method of adsorption using commercial activated carbon is costly, especially for developing countries such as South Africa. Thus, ready to use adsorbent materials are desired considering the difficulties faced during commercial activated carbon regeneration and the disposal problems posed by regeneration solutions.

This calls for research efforts to develop an industrially feasible, cost effective and environmentally compatible adsorbent for wastewater treatment. Therefore, the viable option is to look for locally available and cost-effective adsorbents. Therefore, it is of utmost importance that naturally occurring materials be assessed for their potential in dye wastewater treatment hence, this study seeks to investigate the dye removal efficiency of a modified clay-based nanocomposite.

A greater motivation is the ability of the adsorbent to be used again after adsorption processes. The major drawback of adsorption is that it is a nondestructive technology where the materials do not degrade or disappear after use hence, they need safe disposal. However, post sorbent materials from naturally occurring earth materials like clays can be utilized in various value-added materials like sintered grains in ramming mixes, gunning mixes and bricks, insulator for high temperatures and as desiccants.

This work will provide textile and clothing industries which not only utilise large volumes of water, but also produce large quantities of wastewater containing dyes with the following options: 1) meeting the water quality discharge standards and reducing their discharge costs; 2) re-using the treated wastewater to reduce their carbon footprint by utilising less water from the municipality, thus reducing their impact on the environment; and 3) decreasing their annual expenditure on water, since the treated water would be available for re-use.

1.6 Novelty of the work and contribution to the body of knowledge

Much work on the use of various adsorbents for wastewater treatment has been reported by different researchers. This research is novel in the following aspects: At the inception of this research project, to date,

to the best of the author's knowledge, there were no reported investigations of the ability of calcined magnesite-halloysite nanocomposite to decolourize wastewater containing synthetic dyes. Magnesium based materials and halloysite have been used separately to remove dyes from aqueous solution but the synergistic effect of combining the two materials and assessing the performance on the removal of dyes has not yet been explored. This study will produce an optimised procedure for synthesising the nanocomposite as well as a procedure for decolourising water resources using a mechanochemically engineered nanocomposite. Although numerous dye removal studies exist, many researchers concentrate on the batch adsorption mode using different adsorbents. While adsorption capacity parameters obtained from batch experiments are useful in providing information about the effectiveness of the adsorbate - adsorbent system, the data is not applicable to most industrial treatment systems. Adsorption on continuous flow fixed bed columns is preferred since it can be up scaled from a laboratory set up to a field set up. Hence, there is a definite need to perform both batch and continuous flow experiments in a fixed bed. Many studies have been done on the removal of dyes using clay-based adsorbents under different experimental conditions. However, most of the studies focus on an individual dye and only focus on synthetic dye solutions. In this study, the adsorbents were tested for the removal of four different dyes (two cationic and two anionic). This provided an opportunity to deliver a comparative analysis on how the materials work with differently charged dyes under the same experimental conditions. Moreover, attempts have not been made to use clay-based adsorbents on real effluents, and to fill that gap, the performance of our adsorbent materials on real industrial effluent was also tested. Most of the research into these adsorbent materials has focused on improved performance and increased removal rates, whereas less emphasis has been placed on the storage, disposal and reuse of these adsorbents once they are spent. To fill that gap, this work discussed the use of post-adsorbents, which are adsorbents with bound materials applied to meet environmental, energy, agricultural and dietary needs. The key contributions to knowledge of this work is the synergistic interaction between halloysite nanoclay and calcined magnesite which led to the formation of a novel adsorbent with distinct structures possessing different adsorbent capabilities that gave rise to excellent removal of DR81 dye.

1.7 Thesis layout

The author has chosen to present the research results in the format of the manuscripts that have been published and those under review/submitted for publication. Due to this format, there will be some minor replication of the introduction and experimental sections. However, the results and discussion section will be specific to a particular chapter. In that regard, the thesis has been structured as follows:

Chapter 1: Introduction

Chapter 2: Literature review. This chapter has been published as: Ngulube T., Gumbo J.R., Masindi V., Maity A., 2017. An update on synthetic dyes adsorption onto clay-based minerals: A state-of-art review. Journal of Environmental Management. 191, 35-57.

Chapter 3: Application of calcined magnesite in the removal of dyes: A batch study. This chapter has been published as: Ngulube T., Gumbo J.R., Masindi V., Maity A., 2018. Calcined magnesite as an adsorbent for cationic and anionic dyes: Characterization, adsorption parameters, isotherms and kinetics study. Heliyon. 4(10), e00838. doi: 10.1016/j.heliyon. 2018.e00838. This chapter addresses objectives (ii), (iii) and (v).

Chapter 4: Application of halloysite in the removal of dyes: A batch study. This chapter has been accepted for publication in Clay Minerals - Journal of Fine Particle Science as: Ngulube T., Gumbo J.R., Masindi V., Maity A., 2019. Evaluation of the efficacy of halloysite nanotubes in the removal of acidic and basic dyes from aqueous solution. This chapter addresses objectives (ii), (iii) and (v).

Chapter 5: Application of calcined magnesite – halloysite nanocomposite in the removal of dyes: A batch study. This chapter is under review for publication in Chemical Sciences Journal as: Ngulub T., Gumbo, J.R., Masindi V., Maity A., 2018. Mechanochemical-synthesis of a super-performing nanocomposite and its application on the removal of cationic and anionic dyes. Chemical Sciences Journal. This chapter addresses objectives (i), (ii), (iii) and (v).

Chapter 6: Application of calcined magnesite, halloysite nanoclay and calcined magnesite – halloysite clay nanocomposite in the removal of dyes: A column study. This chapter has been prepared for submission to a peer reviewed journal as: Ngulube T., Gumbo J.R., Masindi V., Maity A., 2019. Exceptional removal of DR81 dye from aqueous solution: A fixed column study. This chapter addresses objective (v).

Chapter 7: Conclusions and Recommendations for future work

References

Akram A., Bhatti H.N., Iqbal M., Noreen S., Sada S., 2017. Biocomposite efficiency for Cr (VI) adsorption: kinetic, equilibrium and thermodynamics studies, J. Environ. Chem. Eng. 5, 400-411.

Ali I., Asim M., Khan T.A., 2012. Low cost adsorbents for the removal of organic pollutants from wastewater. J Environ Management. 113, 170–83.

Buthelezi S.P., Olaniran A.O., Pillay B., 2012. Textile Dye Removal from Wastewater Effluents Using Bioflocculants Produced by Indigenous Bacterial Isolates. Molecules. 17, 14260-14274.

Chollom M.N., 2014. Treatment and reuse of reactive dye effluent from textile industry using membrane technology. Unpublished thesis. Durban University of Technology.

Chowdhury AA., Rasul M.G., Khan MMK., 2013. Thermodynamic Processes and Characterisation of Dead Burned Magnesia: A Review. Recent advances in energy & environment. 344 – 349 ISBN: 978-960-474-159-5.

Daneshvar N., Oladegaragoze A., Djafarzadeh N., 2006. Decolourization of basic dye solutions by electrocoagulation: an investigation of the effect of operational parameters. J Hazard Mater. 129, 116–22.

De Jager D., 2013. Membrane bioreactor application within the South African textile industry: pilot to full-scale. Unpublished dissertation. Cape Peninsula University of Technology.

Dodson J.R., Parker H.L., Munoz G.A., Hicken A., Asemave K., Farmer T.J., et al. 2015. Bioderivedmaterials as a green route for precious and critical metal recovery and re-use. Green Chem.17, 1951–65.

Drouiche N., Aoudj S., Hecini M., Ouslimane T., 2011. Experimental design for the elimination of fluoride from pretreated photovoltaic wastewater by electrocoagulation. Chem Eng Trans. 24, 1207–1212.

Du L., Yang Y., Li G., Wang S., Jia X.M, Zhao Y., 2010. Optimization of heavy metal containing dye Acid Black 172 decolourisation by Pseudomonas sp DY1 using statistical designs. Int Bio deter Biodegr. 64, 566–73.

Feng Y., Dionysiou D.D., Wu Y., Zhou H., Xue L., He S., et al. 2013. Adsorption of dyestuff from aqueous solutions through oxalic acid-modified swede rape straw: adsorption process and disposal methodology of depleted bio adsorbents. Bio resour Technol. 138, 191–7.

Gao B.Y., Yue Q.Y., Wang Y., Zhou W.Z., 2007. Colour removal from dyecontaining wastewater by magnesium chloride. J. Environ. Manag. 82 (2), 167-172.

Ghosh R.K. and Reddy, D.D., 2014. Crop Residue Ashes as Adsorbents for Basic Dye (Methylene Blue) Removal: Adsorption Kinetics and Dynamics. CLEAN – Soil, Air, Water. 42(8), 1098–1105.

Guggenheim S., Martin R.T., 1995. Definition of clay and clay mineral: Journal report of the AIPEA nomenclature and CMS nomenclature committees. Clays and Clay Minerals. 43 (2), 255–256.

Guilane S., Hamdaoui O., 2016. Regeneration of exhausted granular activated carbon by low frequency ultrasound in batch reactor. Desalin Water Treat. 57, 15826–34.

Han H., Wei W., Jiang Z., Lu J., Zhu J., Xie J., 2016. Removal of cationic dyes from aqueous solution by adsorption onto hydrophobic/hydrophilic silica aerogel. Colloids and Surfaces A: Physicochemical and Engineering Aspects. 509, 539-549.

Iqbal M., Bhatti I.A., 2015. Gamma radiation/H_2O_2 treatment of a nonylphenol ethoxylates: degradation, cytotoxicity, and mutagenicity evaluation, J. Hazard. Mater. 299, 351–360.

Kanchi S., Nanotechnology for Water Treatment. International Journal of Environmental Analytical Chemistry. 1(2), 1000e102.

Kant R., 2012. Adsorption of Dye Eosin from an Aqueous Solution on Two Different Samples of Activated Carbon by Static Batch Method. Journal of Water Resource and Protection. 4, 93-98.

Karishma K.C., Mehali J.M., 2015. Applications of Nanotechnology in Wastewater Treatment. International Journal of Innovative and Emerging Research in Engineering. 2(1), 21-26.

Kawasaki S., Shinoda M., Iwai Y., Ogawa M., Hara T., Hattori Y., Kubota T., 2006. Mechanism of single-walled carbon nanotube growth on natural magnesite. Solid State Communications. 138(8), 382-385.

Kiani G., Dostal M.A., Khataee A.R., 2011. Adsorption studies on the removal of Malachite Green from aqueous solutions onto halloysite nanotubes. Applied Clay Science. 54, 1, 34-39.

Kobya M., Bayramoglu M., Eyvaz M., 2007. Techno-economical evaluation of electrocoagulation for the textile wastewater using different electrode connections. J Hazard Mater. 148, 311– 8.

Kono H., 2015. Preparation and Characterization of Amphoteric Cellulose Hydrogels as Adsorbents for the Anionic Dyes in Aqueous Solutions. Gels. 1, 94 -116.

Liu R., Zhang B., Mei D., Zhang H., Liu J., 2011. Adsorption of methyl violet from aqueous solution by Halloysite nanotubes. Desalination. 268 111 – 116.

Luo P., Zhao Y., Zhang B., Liu J., Yang Y., Liu J., 2010. Study on the adsorption of Neutral Red from aqueous solution onto halloysite nanotubes. Water research. 44, 1489 – 1497.

Martınez-Huitle C.A., Brillas E., 2009. Decontamination of wastewaters containing synthetic organic dyes by electrochemical methods: A general review. Appl. Catal. B: Environ. 87, 105–145.

Masindi V., Gitari M.W., Tutu H., De Beer M., 2014. Application of magnesite–bentonite clay composite as an alternative technology for removal of arsenic from industrial effluents, Toxicol. Environ. Chem. 96, 1435–1451.

Masindi V., Gitari W.M., Ngulube T., 2015. Kinetics and equilibrium studies for removal of fluoride from underground water using cryptocrystalline magnesite. Journal of Water Reuse and Desalination. 1, 282-292.

Masindi V., Gitari M.W., Tutu H., De Beer M., 2015a. Removal of boron from aqueous solution using magnesite and halloysite clay composite, Desalin. Water Treat. 1–11.

Masindi V., Gitari M.W., Pindihama K.G., 2015b. Synthesis of cryptocrystalline magnesite/bentonite clay composite and its application for removal of phosphate from municipal wastewaters, Environ. Technol. 1–10.

Masindi V., Gitari M.W., Tutu H., De Beer M., 2015c. Passive remediation of acid mine drainage using cryptocrystalline magnesite: A batch experimental and geochemical modelling approach. Water SA. 41 (5), 677-682

McKay G. 1995. Use of adsorbents for the removal of pollutants from wastewater. 1st edition. Taylor & Francis.

Merzouk B., Yakoubi M., Zongo I., Leclerc J.P., Paternotte G., Pontvianne S., 2011. Effect of modification of textile wastewater composition on electrocoagulation efficiency. Desalination. 275, 181– 6.

Mohan N., Balasubramanian N., Basha C.A., 2007. Electrochemical oxidation of textile wastewater and its reuse. J Hazard Mater. 147, 644–51.

Nandi B., Goswami A., Purkait M., 2009. Removal of cationic dyes from aqueous solutions by kaolin: kinetic and equilibrium studies. Appl Clay Sci. 42(3–4), 583–90.

Nath D., Banerjee P., 2013. Green nanotechnology – A new hope for medical biology. Environmental toxicology and pharmacology. 36, 997 – 1014.

Ngulube T., Gumbo J.R., Masindi V., Maity A., 2017. An update on synthetic dyes adsorption onto clay-based minerals: A state-of-art review. Journal of Environmental Management. 191, 35-57.

Nouren S., H.N., Bhatti Iqba, M., Bibi I., Kamal S., Sadaf S., Sultan M., Kausar A., Safa Y., 2017. By-product identification and phytotoxicity of biodegraded direct yellow 4 dye. Chemosphere. 169, 474–484.

Pajootan E., Arami M., Mohammad N., 2012. Binary system dye removal by electrocoagulation from synthetic and real coloured wastewaters. Journal of the Taiwan Institute of Chemical Engineers. 43, 282–290.

Pirkarami A., Olya M.E., Tabibian S., 2013. Treatment of coloured and real industrial effluents through electrocoagulation using solar energy, Journal of Environmental Science and Health, Part A. 48:10, 1243-1252.

Rafatullah M., Sulaiman O., Hashim R., Ahmad A., 2010. Adsorption of methylene blue on low-cost adsorbents: a review. J Hazard Mater. 177(1–3), 70–80.

Reddy D.H.K., Vijayaraghavan K., Kima J.E., Yun Y., 2016. Valorisation of post-sorption materials: Opportunities, strategies, and challenges. Advances in Colloid and Interface Science. DOI: 10.1016/j.cis.2016.12.002.

Reddy D.H.K., Yun Y.S., 2016a. Spinel ferrite magnetic adsorbents: alternative future materials for water purification? Coord Chem Rev. 315, 90–111.

Shoukat S., Bhatti H.N., Iqbal M., Noreen S., 2017. Mango stone biocomposite preparationand application for crystal violet adsorption: a mechanistic study. Microporous Mesoporous Mater. 239. 180–189.

Tan B.H., Teng T.T., Mohd-Omar A.K., 2000. Removal of dyes and industrial dye wastes by magnesium chloride. Water Res. 34(2), 597-601.

Tehrani-Bagha A., 2011. The sorption of cationic dyes onto kaolin: kinetic, isotherm and thermodynamic studies. Desalination. 266(1), 274 - 80.

Wang S., Boyjoo Y., Choueib A., Zhu Z.H., 2009. Removal of dyes from aqueous solution using fly ash and red mud. Water Res. 39,129-138.

Weng C.H., Pan Y., 2007. Adsorption of a cationic dye (methylene blue) onto spent activated clay. J Hazard Mater. 144(1), 355-62.

Yagub M.T., Sen T.K., Afroze S., Ang, H.M., 2014. Dye and its removal from aqueous solution by adsorption: A review. Advances in Colloid and Interface Science. 209, 172–184.

Yang R., Li D., Li A., Yang H., 2018. Adsorption properties and mechanisms of palygorskite for removal of various ionic dyes from water. Applied Clay Science. 151, 20–28.

Yao P., Zhong S., Shen Z., TiO_2/Halloysite Composites Codoped with Carbon and Nitrogen from Melamine and Their EnhancedSolar-Light-Driven Photocatalytic Performance. International Journal of Photoenergy. http://dx.doi.org/10.1155/2015/605690.

CHAPTER TWO

Literature review

This chapter has been published as: Ngulube T., Gumbo J.R., Masindi V., Maity A., 2017. An update on synthetic dyes adsorption onto clay-based minerals: A state-of-art review. Journal of Environmental Management. 191, 35-57.

Journal of Environmental Management 191 (2017) 35-57

Contents lists available at ScienceDirect

Journal of Environmental Management

journal homepage: www.elsevier.com/locate/jenvman

Review

An update on synthetic dyes adsorption onto clay based minerals: A state-of-art review

Tholiso Ngulube [a, *], Jabulani Ray Gumbo [b], Vhahangwele Masindi [c, d], Arjun Maity [e]

Department of Ecology and Resources Management, University of Venda, Private Bag X5050, Thohoyandou, 0950, Limpopo, South Africa
Department of Hydrology and Water Resources, School of Environmental Sciences, University of Venda, Private Bag X5050, Thohoyandou, 0950, Limpopo, South Africa
Council of Scientific and Industrial Research (CSIR), Building Science and Technology (BST), Built Environment, P.O Box 395, Pretoria, 0001, South Africa
Department of Environmental Sciences, School of Agriculture and Environmental Sciences, University of South Africa (UNISA), P. O. Box 392, Florida, 1710, South Africa
Smart Polymers Group, Polymers and Composites, Council for Scientific and Industrial Research (CSIR), Pretoria, South Africa

article info

Article history:
Received 20 September 2016
Received in revised form 8 December 2016
Accepted 12 December 2016

Keywords:
Clays
Dyes
Wastewater
Adsorption capacity and mechanisms

abstract

Dyes are growing to be a problematic class of pollutants to the environment. The disposal of dyes in water resources has bad aesthetic and health effects, hence the need to remove them from the environment. The need for treatment methods that are effective and low in price is rising hence a lot of research interest are being diverted towards adsorbents that are cheap, preferable naturally occurring materials like clays. In most reported dye adsorption studies, limited information on the relationship between characterization results with adsorbent performance on dye removal has been given. This review article seeks to report on the link between the adsorption characteristics of the clays and their adsorption capacities and to gather information on the modifications done on clays to improve their adsorption capacities. A critical analysis of the different mechanisms involved during the decolouration process and their application for dye removal has been discussed in detail in this up-to-date review. From a wide range of consulted literature review, it is evident that some clays have appreciable adsorption capacities apart from being widely available. It was also noted that several parameters like contact time, dosage, concentration, temperature and pH affect the removal of dyes. Furthermore, the application of clay minerals for decolourising water represents economic viable and locally available materials that can be used substantially for pollution control and management. Conclusions were also drawn and suggestions for future research perspectives are proposed.

Contents

Corresponding author.
E-mail address: tholisongulube@gmail.com (T. Ngulube).

http://dx.doi.org/10.1016/j.jenvman.2016.12.031
0301-4797/

1. Introduction

Different classes of dyes are used in numerous industries including rubber, textiles, cosmetics, plastics, leather, food and paper making. The variability of these dyes is seen in wastewaters discharged from these industries. "Generally, dyes are stable to light, heat and oxidizing agents and are usually non-biodegradable" (Kono, 2015). Because these dyes give colour to the receiving water bodies hence degrading their aesthetic values, it is of paramount importance that their presence in a water body be managed (Kant, 2012).

The presence of colour in an aquatic ecosystem reduces the penetration of sunlight to benthic organisms thus limiting the process of photosynthesis. Dyes also affect the aesthetic value of an aquatic ecosystem due to colouration of water resources (Yagub et al., 2014). The key concern in the treatment of wastewater is the release of dyes and their metabolites into the environment, as some may be mutagens and carcinogens. Some of these dyes are xenobiotic in nature and aerobically recalcitrant to biodegradation (Gupta et al., 2013) and thus pose a threat when wastewater is disposed off to the adjacent environment without being treated. In that regard, there is a need to find treatment technologies that can decolourise the water and at the same time reduce the toxic effects of the dyes to within the recommended water quality guidelines.

Being among the most demanding environmental tasks of the modern day, the increasing amount of toxic industrial waste has led to the development of various methods for its eradication and removal from wastewaters (Chollom, 2014). Usually industrial effluents are treated by several methods including chemical degra-dation, advanced oxidation processes, adsorption, precipitation, biodegradation and chemical coagulation (Pajootan et al., 2012). These methods have been extensively applied, however they have some shortcomings (Kobya et al., 2007; Mohan et al., 2007). For instance, a lot of time is needed for the biological methods and more often than not, the biological methods are less effective when it comes to highly structured polymer dyes. Buthelezi et al. (2012) reported that dyes are non-biodegradable by nature, as such, bio-logical methods will be inapplicable, and their applicability is limited to few dyes because many dyes in the market are toxic to the organisms used hence the biological methods cannot be applied to treat those dyed wastewaters.

Chemical coagulation processes produce huge amounts of sludge thereby causing a lot of pollution as a result of the different chemical reactions that would have taken place during the waste-water treatment processes (Balik and Aydin, 2016). Merzouk et al. (2011) reported that the most effective and important treatment method is chemical degradation using oxidative agents like chlo-rine, however the disadvantage of this method is the production of highly toxic products like organochlorine compounds. Amongst other oxidation processes, there are more advanced processes not limited to some of the following: fenton reactive and ultrasonic oxidation, UV and ozone-UV combined oxidation and photo-catalysis. These oxidation processes are said to be not economically feasible (Daneshvar et al., 2006). The great variability of the wastewater composition often leads to inefficiencies or inadequate treatment of the dye effluents (Drouiche et al., 2011). Having pointed out the above, adsorptions seems to be among the most favoured wastewater treatment technique because of its environmental and economic sustainability.

2. Dyes

Dyes can be defined as organic compounds that have colour and are used to give colour to different substrates like cosmetics, paper, drugs, leather, fur, greases hair, waxes, plastics and textile materials. "Dyes are basically chemical compounds that can connect themselves to surfaces or fabrics to impart colour" (Yagub et al., 2014). Dyes can be classified according to where they are derived. They can be from natural or synthetic sources. Natural dyes are extracted from sources including plants, animals and minerals. Natural dyes were used mostly during early textile industry and these include Jackfruit, Onion, eucalyptus, Turmeric, Weld and henna (Dawood and Sen, 2014). However, because of population increase and industrial activities, people are moving away from natural dyes because they are failing to meet the industrial demand hence their application nowadays is mostly found in the food industry. Synthetic dyes have replaced natural dyes almost completely particularly in the fabrics and textile industry. Several types of dyes are used in numerous industries and these include basic, acid, reactive, direct, vat and disperse dyes (Chen et al., 2016). All these dyes are soluble in water except for disperse and vat dyes. Dyes also contain traces of metals like chromium, copper, lead, zinc, and cobalt apart

from vat and disperse dyes. Dye effluents from industries are known for their organic content, high colour and are harmful as well (Gupta et al., 2013).

2.1. Physico-chemical properties of dyes

Normally dyes are soluble in water or water dispersible organic compounds that are capable of being absorbed into the substrate destroying the crystal structure of the substance (Hunger, 2003). Molecules of dyes are chemically bonded to the surface and after application to a material they become a part of it. For dyes to be marketable in the commercial industry, they should have high colour intensity and the colour must not fade away with time. The intensity of the colour depends on how strongly it absorbs radiation in the visible region (Zollinger, 1987). The structures in dyes that give colour (unsaturated groups that can undergo $\pi - \pi$ and n - π transitions) are called chromophores (see Figs. 1 and 2):

There is also another group of structures that cause colour intensification and these structures are called auxochromes. Unlike chromophores, auxochromes cannot undergo $\pi - \pi$ transitions, but instead can undergo n electrons transition. The following are examples of chromophores: -OH, -OR, $-NH_2$, -NHR, $-NR_2$ and -X.

3. Dye effluent treatment methods

Several technologies to treat dye wastewater have been developed and these include coagulation, adsorption, membrane sepa-ration process, precipitation, electrochemical, chemical oxidation and biological processes (Yagub et al., 2014). The several methods mentioned however can be divided into three major types which are: biological, chemical and physical and their major strengths and weaknesses are shown in Table 1.

The biodegradation of synthetic dyes by microorganisms is a common and simple method of wastewater treatment by operation but the processes involved in the biological degradation can be complex. A number of microorganisms have been used for the decolouration of dyes. These methods of biological

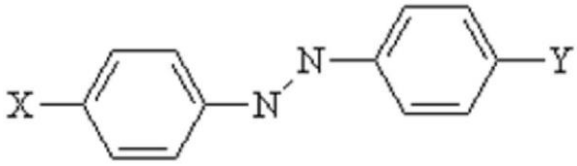

Fig. 2. Example of a chromophores.

treatment include colour removal by Sphingomonas, white rot fungi, pseudo-monas strains, and microbial cultures, under aerobic and anaerobic or mixed conditions as well as adsorption using living and dead biomass (Adensola et al., 2016; Babarinde and Onyiaocha, 2016; Tahir et al., 2016). Most of these dye compounds are however very stable and resistant to biological degradation. The isolation of new strains or the adaptation of existing ones to the decomposition of dyes will probably increase the efficacy of bioremediation of dyes in the near future. The biodegradation of dye effluents by the use of microorganisms is an acceptable and easy method by operation (Buthelezi et al., 2012).

Chemical wastewater treatment methods include precipitation, flocculation, coagulation, flotation and filtration, electrokinetic coagulation, oxidation methods, electroflotation, irradiation or electrochemical processes (Pajootan et al., 2012). The effectiveness of chemical methods depends on the interaction between the contaminants in the wastewater and the nature of chemical used (Iqbal et al., 2014). The chemicals treat the wastewater by way of either assisting in the separation process or helping to ruin and neutralise some of the detrimental effects caused by the pollutants (Mohan et al., 2007). These techniques are good at decolourizing water but at the same time are expensive and disadvantageous because they create a lot of sludge after use and therefore lead to a sludge disposal problem (Kobya et al., 2007). Moreover, secondary pollution problem can arise because of too much chemical use. Oxidation processes generate powerful oxidizing agents like as hydroxyl radicals and these have been used successfully for degrading pollutants but they are also

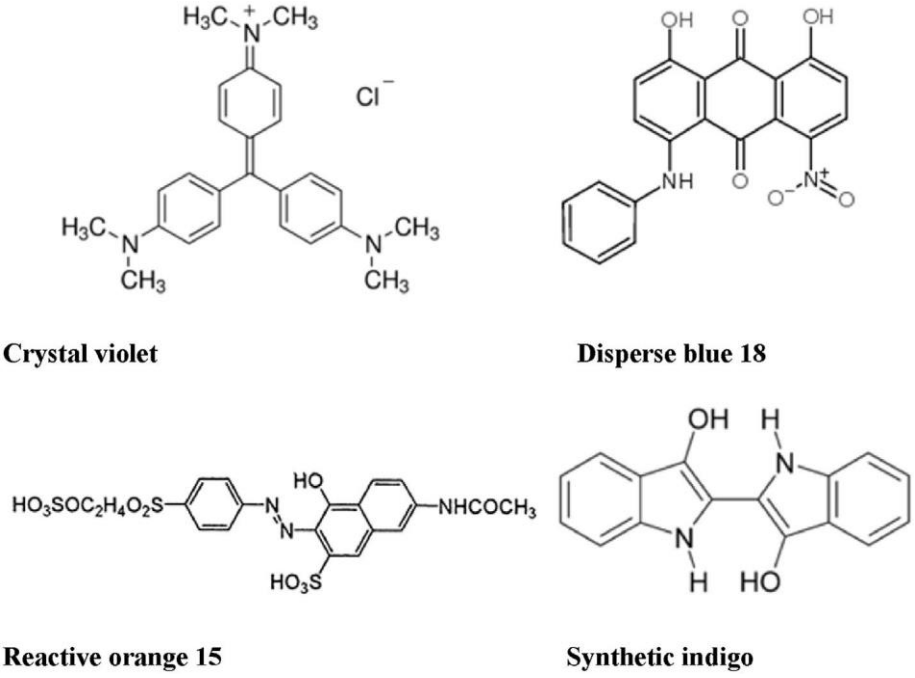

Fig. 1. The chemical structures of some synthetic dyes (Hunger, 2003).

Table 1
The pros and cons of wastewater treatment methods (Robinson et al., 2001).

Treatment Method	Pros	Cons
Ion-exchange	Adsorbent can be regenerated and therefore used for several times	Only effective for certain types of dyes.
Membrane processes	Reuse of water salts and heat	Handling and disposal of concentrate stream, flux decline
Electrochemical processes	Breakdown compounds and are non-hazardous	Economically less feasible because high electricity costs
Photochemical	No sludge production	Formation of by products
Ozonation processes	Applied in gaseous state: no modification of volume	Ozonation processes have a very short half-life
Coagulation/flocculation	Insoluble dyes can be removed and it is economically feasible	The amount of sludge produced is high.

very expensive and commercially unattractive because of high consumption of chemicals and electrical energy demand (Bilal et al., 2014; Jamal et al., 2015; Qureshi et al., 2015).

Physical methods are also extensive and these include adsorption techniques, reverse osmosis, electrodialysis, membrane-filtration processes and nanofiltration (Khan et al., 2015; Shon et al., 2013). The main drawback of the membrane processes is the short period of use before the membrane starts fouling and the various costs coming as a result of constant replacement of the membranes eventually leading to membrane processes being economically unviable (Shamraiz et al., 2016). According to documented studies, adsorption is one of the most widespread wastewater treatment approach that has been proven effective and efficient in depollution science since it can remove contaminants and decolour the water resources (Gomes et al., 2015; Mu and Wang, 2016; Tahir et al., 2016; Srinivasan, 2011). If a treatment plant is given a proper adsorption process design, it produces a high quality treated effluent. Adsorption processes offer an attractive alternative treatment method for contaminated waters, particularly in cases where the adsorbent is inexpensive, locally available, abundant and requires less additional pre-treatment step before it is used (Crini, 2006).

Although, the adsorption process has been deemed to offer an attractive alternative treatment technology for polluted waters, it also has its drawbacks. Adsorption is known to produce highly concentrated sludge that lead to a problem of sludge disposal. It has also been reported to be less effective for some dyes, especially the highly concentrated dyes. Moreover, it can be very expensive when using high cost adsorbents like activated carbon which are also costly to regenerate. A number of investigations have shown that several factors affect the adsorption process but worth to note is that adsorption is vastly dependent on the pH media, basically meaning that to attain maximum adsorption capacities, the pH has to be adjusted in most cases. Besides that, the physical and chemical characteristics of the adsorbent can have an intense influence on the capacity and rate of the adsorption process. e.g low surface area for some adsorbents leads to low adsorption capacity (Benefield et al., 1982).

4. The adsorption process

Oremusova (2007) defines adsorption as "a process that occurs when a gas or liquid solute accumulates on the surface of a solid or a liquid (adsorbent), forming a molecular or atomic film (the adsorbate)". Generally, the adsorbent has a fixed total uptake, where a particular solute is replaced by another for example, in ion exchange processes. When an adsorbent is contacted with liquid containing an absorbable solute, adsorption occurs until equilibrium is achieved or when the surface of an adsorbent is saturated with an adsorbate (Kalibantonga, 2004).

The adsorption process can be divided into two main types, namely, physical and chemical both sometimes referred to as physisorption and chemisorption respectively. The difference between the two types of adsorption is that, in physical adsorption the adsorbate sticks to the surface through weak intermolecular interactions like such as Van der Waals forces, hydrophobicity, hydrogen bonding, polarity, static interactions, dipole-dipole interactions and π-π interactions (Dawood and Sen, 2014). On the other hand, in chemisorption, molecules stick to the surface by forming a chemical bond through electron exchange (Artioli, 2008). Some of the differences between physisorption and chemisorption are shown in Table 2.

In adsorption processes, the contaminated water is passed through a sorbent bed. The adsorbent material will retain the contaminants by either chemical, physical or ion exchange mechanisms. After a certain period of time of operation, the adsorbent gets saturated and will require regeneration/replacement depending on regeneration feasibility (Chapman and Siebold, 1912).

Worch (2012) pointed out that the extent of adsorption is directly proportional to the specific area of the adsorbent. The specific area is that part of the entire area available for adsorption. It is related to the grain size of the adsorbent. The choice of particle size is made by considering the following factors:

- ❖ the ease of mass transfer from the fluid to the surface,
- ❖ creation of as much interfacial surface area as possible and reduction of antiparticle diffusion path length, all of which favor smaller particles
- ❖ maintenance of a low pressure drop, which favors larger particles (Worch, 2012).

For an adsorbent to be selected as favorable, a number of factors are looked at. These include ease of operation, cost of the medium, adsorption capacity, potential for reuse and likelihood of regeneration (Worch, 2012). Various naturally occurring materials that are both readily available and abundant have been explored as adsorbents for the removal of dyes from wastewater (Ghosh and Reddy, 2014; Ali et al., 2012; Tehrani-Bagha et al., 2011; Rafatullah et al., 2010). A great interest has grown towards naturally occurring adsorbents, preferably developing sorbents that have a high adsorption capacity and has low cost for removing pollutants from contaminated waters. Although a wide variability of sorbents have been used for wastewater treatment, naturally available clays have been the adsorbents of choice in most developing countries (Ali et al., 2012; Hajjaji et al., 2016; Mu and Wang, 2016; Santos and Boaventura, 2016).

5. Clays

"Clays are hydrous aluminosilicates broadly defined as those minerals that make up the colloid fraction of soils, sediments, rocks and water and may be composed of mixtures of fine grained clay minerals and clay-sized crystals of other minerals such as quartz, carbonate and metal oxides" (Pinnavaia, 1983). Clay materials possess structures that are organized in layers and they are categorized by those different layered structures (Ajbary et al., 2013; Li et al., 2013;

Table 2
Comparison between physiosorption and chemisorption (Jaafar, 2006).

Physisorption	Chemisorption
Weak intermolecular forces like van der Waals forces	Strong covalent bonding involving electron exchange
Low enthalpy: ΔH < 20 kJ/mol	High enthalpy: ΔH ~ 400 kJ/mol
Multilayer adsorption	Monomolecular adsorption
Low temperature, constantly lower than the adsorbate critical temperature	High temperatures
Low activation energy	High activation energy
Reversible	Non-reversible.
Nonselective surface attachment	Selective surface attachment

Savic et al., 2014). Clay materials fall under various types like pyrophyllite - talc, smectites - montmorillonite, mica - illite, kaolinite, serpentine, vermiculite and sepiolite (Shichi and Takaqi, 2000). Fig. 3 shows the structure of a typical clay.

5.1. Clays and adsorption: physicochemical characteristics favouring adsorption

The chemistry which occurs on the surfaces of clay gives them high flexibility in adsorption processes. The surface chemistry involves the structure, ion exchange capacity, specific surface area, mechano-chemical stability, water holding capacity and reactivity of the surface which influences physical and chemical properties of clay minerals (Eren, 2010). Usually, these clay materials are used without being chemically modified. Nonetheless, chemical modification can improve the clay‘s adsorption capacity leading to its widespread use in novel technologies (Liang et al., 2013).

According to Elmoubarki et al. (2015), clay adsorption capacities are usually dependent on the net negative charge found on the clay minerals. The negative charge contributes to the clay's ability to adsorb positively charged ions.

Furthermore, clays' adsorption characteristics arise from their large pore sizes and surface area (Yan et al., 2015). Generally, clays have exchangeable ions on their surface (Eren, 2010). This characteristic leads to clays playing a crucial role in the environment by being natural pollutant scavengers by way of cations and anions take up through adsorption and ion exchange. Ions that are usually found on surfaces of the clay include H^+, K^+, Na^+, Ca^{2+}, Mg^{2+}, NH_4^+ and Cl, SO_4^{2-} , PO_4^{3-} , NO_3^- . Cation exchange occurs readily without affecting the clay mineral's structure (Huang et al., 2011).

Clay minerals display a strong attraction to cationic and anionic dyes (Crini, 2006; Hajjaji et al., 2016; Santos et al., 2016; Sarma et al., 2016; Yan et al., 2015; Yu et al., 2015). Nevertheless, the adsorption capability for basic dyes is comparable greater than that of acid dyes as shown in Table 2. From Table 2, it can be seen that the adsorption capacities recorded on basic dye like Methylene Blue and Malachite Green were approximately three times higher than that recorded for acid dyes like Congo Red and Methyl Orange. The main reason behind the differences in adsorption capacities is the charges on the dyes and surface characteristics of clay materials. As stated earlier by Elmoubarki et al. (2015), clay minerals have a net negative charge hence they will strongly attract positively charged basic dyes.

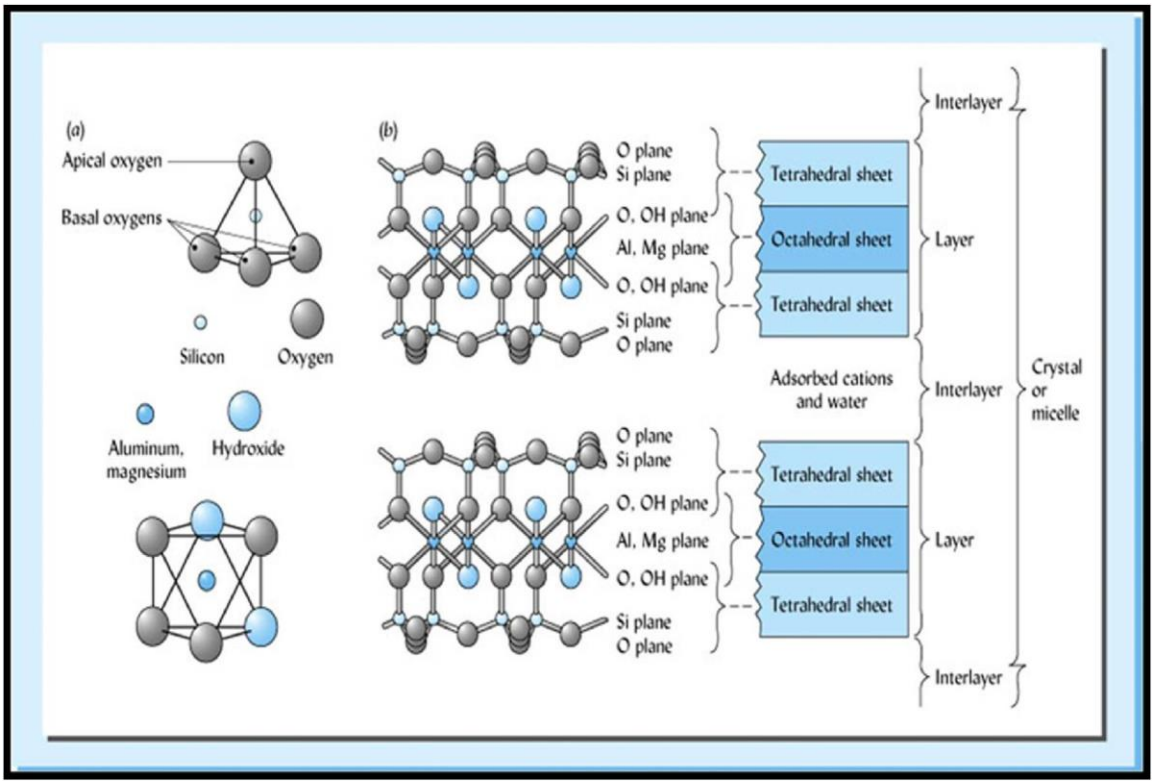

Fig. 3. Structure of a typical clay material (Masindi et al., 2014).

Nonetheless, adsorption capacities can differ even though the dyes have the same charge. Yu et al. (2015) explored the effect of molecular structure on the adsorption of basic dyes, where the adsorption behaviour of methylene blue (MB) and crystal violet (CV) onto natural vermiculite were studied. CV and MB have an ionic charge of +1, so CV was used as a comparative dye, but it has a triangular molecular structure that is considerably different from the molecular structure of MB which is linear. The isotherm modelling results indicated that MB's equilibrium adsorption capacity at 25 ºC decreased from 0.076 to 0.053 mmol/g with increase in initial dye concentration from 0.3 to 0.5 mmol/L. A similar phenomenon was observed by Almeida et al. (2009). Results of this study demonstrate that even though dyes have the same charge, their molecular structure can also play a vital role in the adsorption processes. The decrease of MB's adsorption at high initial concentrations could be due to its molecular structure. The linear structure of MB might have had a steric effect on the adsorbate - adsorbate medium more than that of CV causing an equilibrium adsorption density decrease (Yu et al., 2015).

It is also important to note that, is not always the case that clays have a higher adsorption capacity towards basic dyes than acid dyes. This generalisation is made solely depending on the net negative charges of clays but there are instances where clays soils exhibited a much higher adsorption capacity towards acid dyes compared to basic dyes. Santos and Boaventura (2016) reported on the removal of a basic and acid dye on sepiolite clay and their results showed the amount of dye adsorbed was higher for the acid dye than that of the basic day. They investigated the removal of Basic Red 46 (BR) and Direct Blue 85 (DB) and the obtained maximum adsorption capacities at 25 ºC and pH 9, were 110 and 232 mg/g, respectively. Ideally, it would be expected that the results show a vice versa trend because of the nature of clays. The authors explained these results in terms of other variables that can affect dye adsorption like temperature and pH. They reported that, in the case of basic red adsorption, the increase in temperature and pH favoured the adsorption extent (from 25 to 35 ºC). Regarding the direct blue dye, the adsorption was not influenced by temperature (15-35 ºC), but a significant effect of pH was observed, with a sharp decrease in the uptake capacity for strong alkaline conditions. The main reason why sepiolite clay showed a tendency to adsorb acidic dyes than basic dyes was explained in terms of sepiolite's point of zero net proton charge (PZNPC) (Santos and Boaventura, 2016). To estimate the ranges where the clay surface charge is positive or negative, usually the pH of zero charge is determined using electrolytes of different concentrations. When a common intersection point is obtained for the curves resulting from different electrolyte concentrations, the intersection point is not dependent on the ionic concentration and it can be designated as a zero point of charge. The results for sepiolite however showed three distinct intersection points which are referred to as the PZNPC rather than one inter-section for PZC. This observation is due to the dual nature of surface charge in minerals, where two different surface charges are pre-sent: a permanent negative charge (resulting from the structural isomorphous substitutions) and a pH-dependent charge (primarily related to the dissociation of hydroxyl groups). The high PZNPC values allow to predict a higher propensity of sepiolite to adsorb the anionic dye in pH conditions up to 10. The different pH effects observed for BR (cationic) and DB (anionic) have been also reported for other cationic (Han et al., 2014) and anionic species (Han et al., 2014; Tabak et al., 2009; Tümsek and Avci, 2013).

Many studies have been done using several types of clays in the removal of dyes like cationic, anionic and azo dyes and clays exhibited different adsorption capacities varying from as low as 7 mg/g to as high as about 200 mg/g. Some of the dye removed by various types of clays include: Acid Orange 7 dye by clay and red mud mixes (Hajjaji et al., 2016); Brilliant green dye by red clay (Rehman et al., 2013); methylene blue and methyl orange by bentonite (Fosso-Kankeu et al., 2014); Congo red by a mixture of Kaolin and Bentonite clay (Vimonses et al., 2009) and Reactive red 120 by raw clay (Errais et al., 2012). Table 3 shows various adsorption capacities obtained by different clays for the treatment of various dyes.

5.2. The relationship between clay surface area, size/mesh and adsorption capacity

The major reason for the high adsorption capacity of clay ma-terials is their high surface areas. If a particular clay has a higher surface area, it means that it will also have a higher adsorption capacity compared to clays with lower surface areas (Cadena et al., 1990). However, this notion may not always be the case for some clays but a number of studies have proved that the surface area of a clay is directly proportional to the adsorption capacity of the clay (Sarma et al., 2016; Santos and Boaventura, 2016; Elmoubarki et al., 2015; Auta and Hameed, 2013).

Elass et al. (2011) investigated the removal of methyl violet from aqueous solution using Moroccan clays. Their study showed that the fine mineral fraction had a surface area of 137 m^2/g. As it is expected of high surface area clays, the Morrocan clays had an adsorption capacity of 625 mg/g. The adsorption capacities of other clay based adsorbents for dyes obtained by some other investigators are presented in Table 3. Comparing of these values with the one obtained by Elass et al. (2011) shows that the stevensite-rich clay from Morocco has a comparable higher surface area and high adsorption capacity too. The authors however made an overall conclusion that the mechanisms of adsorption could be explained by electrostatic attraction between the surfaces of the clay which are negatively charged and the dye molecules which are positively charged and not highly dependent on the high surface area of the clay. However, as the clays have a notable higher surface area, the fact that the higher surface area contributed to the high adsorption capacity cannot be ruled out.

On a different study by Yan et al. (2015), the notion that if a particular clay has a higher surface area, means that it will also have a higher adsorption capacity does not hold true. Their study focused on using cetyltrimethyl ammonium bromide (CTMAB) modified organobentonite to remove acid dyes from aqueous solution. The BET results showed that the specific surface area of the modified clay which was measured to be 4.42 m^2/g is comparable lower than that of other adsorbents (Table 3) and even lower than that of raw bentonite (10.2 m^2/g). According to Yan et al. (2015), the reduction in surface area indicates the entrance of organic molecules into bentonite interlayers leading to the blockage of layer channels and thus reducing the surface area. A similar phenomenon was reported by Heinz et al. (2007). Even though CTMAB-Bent recorded a very low surface area it showed very interestingly high adsorption capacities for different dyes. From the Langmuir isotherm results, the maximum adsorption capacities of CTMAB-Bent for Acid Blue 25, Acid Blue 93 Acid Turquoise Blue A, Acid Turquoise Blue A and Acid Golden Yellow G are 360.8 mg/g, 226.0 mg/g, 487.2 mg/g and 304.7 mg/g, respectively. For a clay with a surface area of below 5 m^2/g, the reported adsorption capacities are obviously very high and therefore it can be established that other characteristics of the soil other than its surface area played a vital role in the adsorption of the four dyes.

The surface area of an adsorbent including its pore size are largely important in the description of adsorbent quality because they directly affect their analyte retention abilities and for that reason it becomes imperative to choose adsorbents with high surface area before conducting studies. In a bid to increase

Table 3
Adsorption capacities of different clays.

Type of clay	Dye removed	Adsorption capacity (mg/g)	Reference
Sepiolite clay	Direct Blue	106	Santos and Boaventura, 2016
Palygorskite	Methylene blue	132.72	Mu and Wang, 2016
Red mud	Acid Orange 7	32.36	Hajjaji et al., 2016
Acid Activated Kaolinite	Congo Red	12.36	Hai et al., 2015
Bis-imidazolium modified bentonite	Telon dyes	108	Makhoukhi et al., 2015
Montmorillonite	Methylene blue	74	Zhou et al., 2014
Acid modified clay beads	Methylene blue	223.19	Auta and Hameed, 2012
Safi decanted clays	Malachite green	88.70	Elmoubarki et al., 2015
Modified natural bentonite	Di azo dye	7.14	Toor and Jin, 2012
Modified montmorillonite	Methyl Orange	24	Chen et al., 2011

the surface areas of clays, researchers tend to chemically modify their adsorbents to increase their surface areas (Hai et al., 2015). Auta and Hameed (2012) reported on the effects of modifying surface areas of Raw Ball Clay (RBC) by H_2SO_4. The RBC and Modified Ball Clay (MBC) BET surface area, pore width and total pore volume were found to be 10 m^2/g, 19.62 nm, 0.0519 cm^3/g and 92 m^2/g, 9.54 nm, 0.2183 cm^3/g, respectively. The surface area and pore volume of MBC were expectedly higher than those of RBC. A possible explanation to this is the leaching and loss of some ions during the acid treatment and calcinations processes. Watanabe et al. (2011) reported similar results after ultrasonically treating SP (0.0)-cal which led to an increase in both surface area and sphere pore volume. Auta and Hameed (2012) reported an 82% increase in surface area which then led to a 188.60% in adsorption capacity with MBC. Results of all these studies show that indeed some chemical treatments to raw clay can increase surface areas and ultimately leading to increased adsorption capacities of modified clays.

The vital part played by surface area on adsorption processes has been shown by various studies on the adsorption of dyes by different clays including kaolinite, montmorillonite and smectites. Table 3 shows numerous clays used for dye adsorption, their sur-face areas and their adsorption capacities. From Table 4 we can derive a clear relationship between surface areas and adsorption capacities.

The size of clay particles plays an indispensable role in all interphase interactions in clays including ion-exchange and adsorption processes (Mandzhieva et al., 2014). Therefore, the evaluation of the effect of the particle size on the adsorption properties of soils is a vital mission in adsorption processes. Small particle sizes cause equilibrium to be achieved more easily and near maximum adsorption capability can be attained because they reduce internal diffusion and mass transfer limitation to the penetration of the adsorbate inside the adsorbent.

To examine the effect of the particle size on basic green 4 adsorption by granular organo-inorgano pillared clays (GOICs) in column reactor, Cheknane et al. (2016), varied particle size ranges of GOICs from 300-400 μm to100-1200 μm. Results show that a decrease in particle size improves the performance of the adsorption column from 221 to 428 mg/g. According to their previous work, the adsorption capacities of dye depended strongly on granulation and particle size of the granule pillared clay (Cheknane et al., 2010; 2012). On the other hand, the comparison between the adsorption capacities of BG4 (mg/g) determined from respective batch and continuous reactors, showed increase of adsorption capacity with the size of particles.

The authors explained the observed behavior using the following mechanism: Firstly, the limitation of active mass of pillared clay to the external surface of granular organo-inorgano pillared clay was influenced by the silicone used for granulating the powder organo-inorgano pillared clay (Cheknane et al., 2010; 2012). Secondly, the interparticle porosity of the adsorption beds are reduced for the small particle size ranges. The column packed with larger particle sized GOICs had lower adsorption efficiencies lower than the one packed with smaller diameter GOICs.

Jaafar (2006) also stipulates that small particle sizes of the clay adsorbent enhance the adsorption capacity of the adsorbent. A study using diatomite for the removal of SB showed that the decreasing of particle size of diatomite from 300 to 60 μm increased the adsorption rate of SB. This is because increasing the external surface area of the diatomite particle exposes more active sites to SB molecules. There is a slight effect of particle size of diatomite on adsorption of textile dyes (Ozcan and Ozcan, 2004).

5.3. The role of clay morphology in the adsorption process

It is well known that the adsorption capacity of clays depends on their

Table 4
Surface area of different clays used in the adsorption of dye.

Clay type	Dye adsorbed	Surface area (m^2/g)	Adsorption capacity (mg/g)	Reference
Red mud	Acid Orange 7	74	32.36	Hajjaji et al., 2016
Sepiolite clay	Direct Blue	108	332	Santos and Boaventura, 2016
Safi raw clays	Malachite green	34.07	156.43	Elmoubarki et al., 2015
Halloysite	Direct orange 34	20	7.75	Chaari et al., 2015
Montmorillonite K10	Crystal violet	173	370.37	Sarma et al., 2016
Acid-activated kaolinite	Azo dyes	358.6	12.36	Hai et al., 2015
Raw clay beads	Methylene blue	58.02	19.32	Auta and Hameed 2013
Modified clay beads	Methylene blue	223.19	101	Auta and Hameed 2013
Raw bentonite	Acid dyes	10.2	-	Yan et al., 2015
CTMAB-Bentonite	Acid Turquoise Blue A	4.42	487.2	Yan et al., 2015
Raw bentonite	Diazo dye	25.7	-	Toor and Jin (2012)
Acid bentonite	Diazo dye	84.6	69.44	Toor and Jin (2012)
Swelling clays	Methylene blue	65	-	Li et al., 2011

chemical composition and structure (Mu and Wang, 2016). The structure of clay includes crystalline unit growth mechanics, crystallites interlocking and interpenetration, crystal habits including helical growth, twinning, and tapotaxis (Bohor and Randall, 1970). The Scanning Electron Microscope (SEM) is uniquely suited for studying the structure of clays because it magnifies the three dimensional view of clay surfaces with great depth of focus. It brings out the configuration, texture and fabric of clay samples. Fig. 4(a)-(g) shows how SEM can solve the problem of determining the morphology of clay powders. Figures (a) and (b) show Suzhou kaolin with a typical sheet structure and a Longyan kaolin containing tubular Halloysite particles respectively (Zhang et al., 2016). Figures (c) and (d) show natural and Al/Fe oxide-modified diatomaceous earth (DE) respectively and different pores sizes and DE appearance before and after modification can be seen. The modified DE pores appear to be packed by the deposition of Al/Fe oxide as compared to the clear, net-like pores in the natural DE. The proximate closure of the pores of the modified DE is evidence that natural DE was modified (Izuagie et al., 2016). Figure (e) shows a highly magnified view of a bentonite clay sample and the platy-like features characteristic of clay minerals are seen. Protruding rodlike structures are clearly visible in the montmorillonite rich bentonite clay (Masindi et al., 2015). Figure (g) shows a natural soil sample of smectite rich soils from Limpopo, South Africa. At lower magnifications, the smectite rich clay soils showed irregular porous structure that is a good characteristic of a good adsorbent material (Mudzielwana et al., 2016).

Mu and Wang (2016) postulate that the effect of different clay origins (which lead to different morphological structures) on adsorption properties of clays is rarely studied. Hence the researchers selected three representative samples of palygorskite (PAL) from Gansu, Anhui and Jiangsu provinces of China to study the effect of different origins on MB adsorption (Zhang et al., 2016). The results revealed that the Mg-poor sample of Jiangsu characterised by short rods and a dioctahedral structure exhibited the highest adsorption capacity for MB, whereas the Mg-rich sample from Anhui characterised by long rods and an intermediate struc-ture of trioctahedral and dioctahedral phyllosilicates exhibited lesser adsorption capacity for MB. From this study we can clearly see how the structures of the selected PAL samples affected their adsorption capacity, showing that it is not only the chemical composition that affects adsorption capacity but morphology. Clays rich in Mg recorded a low adsorption capacity but clays with lower Mg concentrations had a higher adsorptive removal towards MB. Furthermore, it is worth noting that although the maximum adsorption of natural palygorskite toward dyes far exceeded the

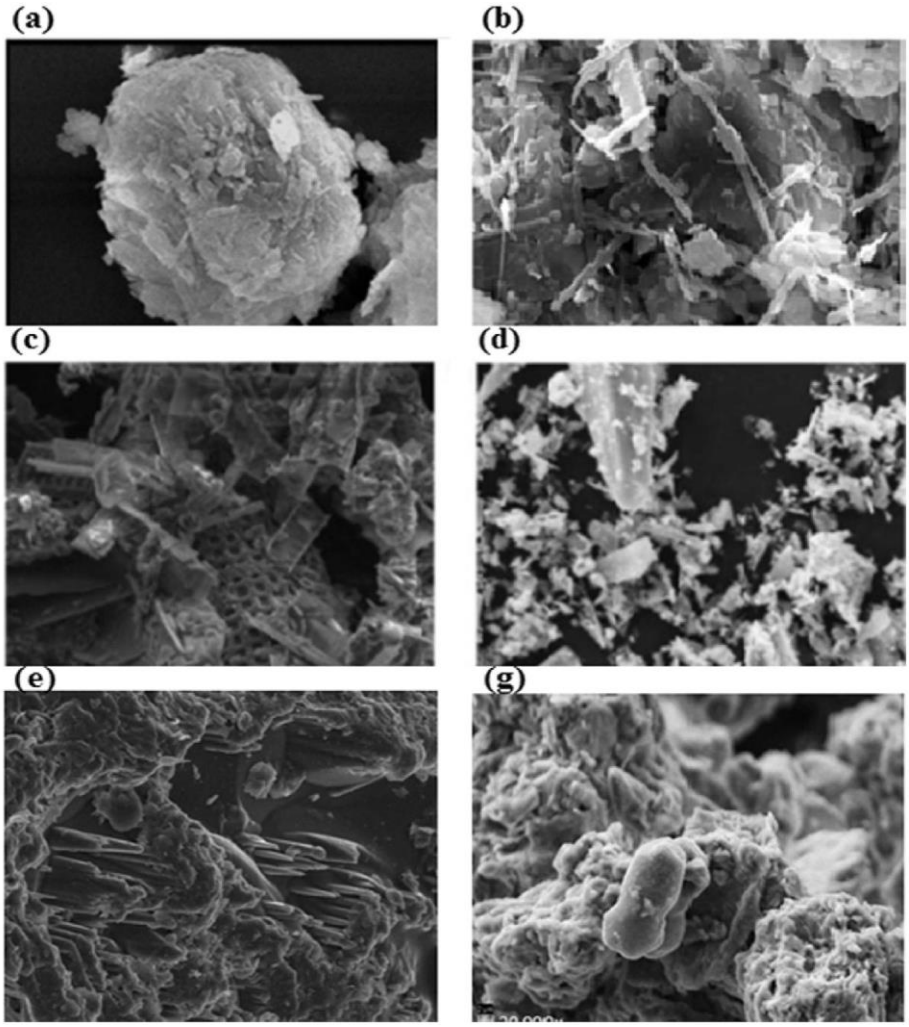

Fig. 4. Clay particles SEM images: (a) - Suzhou kaolin (Zhang et al., 2016); (b) - Longyan kaolin (Zhang et al., 2016); (c) - raw diatomaceous earth (Izuagie et al., 2016); (d) - Al/Fe oxide-modified diatomaceous earth (Izuagie et al., 2016); (e) - bentonite clay (Masindi et al., 2015); (g) - Mukondeni smectite rich clay (Mudzielwana et al., 2016).

cation exchange capacity of palygorskite, it is difficult to completely release the adsorption capacity of palygorskite toward dyes due to the existence of the bulk crystal bundles or aggregates originated from the interparticle Van der Waals' and hydrogen bonding interactions.

Another common structural feature characteristic of clay soils is their fibrous and porous nature. It is interesting to note the differ-ence in adsorption capacities with respect to different dyes on fibrous clays. Sarma et al. (2016) used raw and acid-treated mont-morillonite to adsorb CV. With a more similar structure to montmorillonite is bentonite which was studied by Chinoune et al., 2016 for the removal of Procion blue HP (PB) and Remazol brilliant blue R (RB), both anionic reactive dyes. The SEM images of montmorillonite showed that the clay had a fluffy appearance of different shapes and sizes with some bigger particles appearing broken down into small and medium sized particles with no particular shape. On the other hand, bentonite appeared either as thin, ul-trafine, leaf-like crystals forming dense aggregates or in a more open honeycomb texture. The Langmuir monolayer adsorption capacities of PB and RB on bentonite in aqueous solution were estimated to be 40.22 and 66.90 mg/g, respectively while the Langmuir monolayer adsorption capacity of raw montmorillonite was found to be 370.37 mg/g. It is very interesting to note how much the adsorption capacities of more or less similar fibrous clays are so different with montmorillonite having an adsorption capacity almost 7 times greater than that of bentonite. The fibrous surface topography of the clays is expected to increase the degree of unsaturation of the surface with dangled bonds and free valences, thus amassing the total surface area of the clay. The lower adsorption capacity of the bentonite clay compared to that of montmorillonite could be due to the dense aggregates in the clays that did not create enough pores to allow for adsorption compared to the broken down particles that appeared on the montmorillonite.

5.4. The role of electrical charges in the adsorption process: point of zero charge (pHpzc), point of zero net proton charge (PZNPC), zeta potential and charge density

Point of zero charge (pHpzc) is among the significant factors which can help indicate the type of surface active centres on the adsorbent and the adsorption ability of the surface (Yagub et al., 2014). The point of zero charge (pzc) is the pH at which the net surface charge is zero and is typically used to define the electro-kinetic characteristics of a surface. The value of pH is used to describe pzc only for systems in which H^+/OH^- are the potential determining ions. Studies on point of zero charge (pHpzc) of a number of clay adsorbents have been conducted in order to understand the adsorption mechanism in relation to pzc (Ghaedi et al., 2011; Shirsath et al., 2013; Tümsek and Avci, 2013). Cationic dye adsorption is high at pH > pHpzc because of the presence of functional groups like OH while, anionic dye adsorption is high at pH < pHpzc when the surface is positively charged.

Chemical characterization of red clay by Rehman et al. (2013) showed that it had a point of zero charge at pH 6.8. It is well known that dye adsorption is dependent on pH of the solution because the surface charge of the adsorbent and the degree of ionization of the adsorbate and degree of dissociation of functional groups differ with various pHs (Nandi et al., 2009; Ghaedi et al., 2011). The adsorption of Brilliant Green dye by red clay was higher at circumneutral pH. However, the highest adsorption efficiency (97%) and capacity (121 mg/g) was recorded at pH 7. The information on pHpzc of red clay best explains the impact that solution pH has on the adsorption of BG. As stated earlier, the pzc of red clay was established to be 6.8 and the results show That BG adsorption is favoured at pH 7. Electrostatic forces operate because the RC surface will be negatively charged at pH > pHZPC, and BG molecules are positively charged. At high pH there is charge neutralization on RC surfaces leading to enhanced adsorption of BG (Ghaedi et al., 2011). At pH > 7 there was no significant adsorption. Nandi et al. (2009) and Shirsath et al. (2013) also studied the adsorption of BG by kaolin clay at pH 7 and they described the same results. However, high BG adsorption capacity (108.4 mg/g) at pH 4 revealed that BG dye adsorption was not only due to electrostatic attraction.

Besides the point of zero charge there is also the pH at which there is a zero net adsorption of H^+/OH^-, designated as points of zero net proton charge (PZNPC) (Avena and De Pauli, 1998). A study using sepiolite clay on the adsorption of cationic and anionic azo dyes by Santos and Boaventura (2016) determined the PZNPC at three different ionic strengths by the pH-drift method (Lazarevic et al., 2007). The results showed three distinct intersection points for different ionic concentrations: 10.4; 10.0 and 9.8, respectively for NaCl 0.001 M, 0.01 M and 0.1 M. The authors concluded that this observation was due to the dual nature of surface charge in minerals. Where two different surface charges are present: a permanent negative charge (resulting from the structural isomorphous substitutions) and a pH-dependent charge (primarily related to the dissociation of hydroxyl groups). The authors further on reported that the intersection points obtained, corresponding to zero net adsorption of H^+/OH^- should be named as PZNPC, instead of PZC, since they represent the conditions where the pH-dependent charge is null (Avena and De Pauli, 1998) and not the conditions under which the total charge is null. The high PZNPC values allowed for the prediction of a higher tendency of sepiolite to adsorb the anionic dye in pH conditions up to 10. The different pH effects observed by Santos and Boaventura (2016) for cationic and anionic species (Han et al., 2014; Tumsek et al., 2013; Tabak et al., 2009) and are explained by the electrostatic attraction. With the increase in pH, the dependent charge tends to be more negative and hence amenable to adsorb cationic species and less to adsorb anionic ones. The PZNPC of sepiolite occurs at pH 10 and then a significant increase in BR dye adsorption was observed from an equilibrium pH 8.5-8.7 to 9.2-9.5; in turn, a sharp decrease in the DB uptake was observed from final pH 9.3 to 9.8.

Greenwood and Kendall (1999) define zeta potential as "the electric potential in the interfacial double layer (DL) at the location of the slipping plane versus a point in the bulk fluid away from the interface". Zeta potential is an important parameter because its value helps to determine colloidal dispersion stability. It indicates the degree of repulsion between particles with similar charges in a dispersion. So, colloids with high negative or positive zeta potential values are said to be electrically stabilized whereas those with low zeta potential values have a tendency to flocculate (Hanaor et al., 2012). The zeta potential of clays also plays a very important role in dye adsorption and this can be seen when the effect of pH on dye adsorption is investigated (Fayazi et al., 2015).

Zeta potentials of modified sepiolite (MS) and natural sepiolite (NS) at various pHs were determined and it was established that NS and MS isoelectric points were around 6.8 and 7.9, respectively. Comparable values, between pH 3.2 and 7.4 have also been reported by other researchers (Lazarevic et al., 2007; Sabah et al., 2007) for the isoelectric point of natural sepiolite, and 7.7 to 8.5 for that of iron-coated sep (Liu et al., 2014; Lazarevic et al., 2010). The sepiolite used in the various studies had different mineralogical composition and clay mineral preparation methods for electro kinetic measurements differ hence we see a wide range of values for sepiolite. (Fayazi et al., 2015). The surface charges of adsorbent materials are usually influenced by pH because of the effect it has on the degree of ionization of the adsorbate. When pH is less than 7.9, the MS

nanocomposite surface is positively charged because of surface functional groups protonation and when pH is greater than 7.9 the surface is negatively charged due to the dehydroxylation of the MS surface groups. In acidic conditions, the H^+ compete with positively charged dye molecules for available adsorption sites, hence the decrease in removal efficiency. As pH increases, there is also a rise in removal efficiency due to electrostatic attraction between the negatively charged surface of the MS nanocomposites and cationic safranin molecules. Given the above, we can then say pH has a very important role to play in adsorption processes.

5.5. Clay charge density and swelling properties: effect on the adsorption process

The reactivity of clay minerals is commonly due to a charge they carry. The presence of this charge is the basis of their exchange capacity and consequently swelling. The relationship between clay charge and swelling lies in the fact that as clay charge density increases, the attraction energies on the clay predominate and therefore the clay does not swell, whereas the vice versa is true with decrease in charge density (Miyamoto et al., 2000). There are three main groups of clay minerals which are kaolinite, illite and smectites (Liu and Zhang, 2007). Nevertheless, the most commonly used clays in dye adsorption processes are smectites and kaolinites. Structurally, illite clays are similar to muscovite, but are typically deficient in alkalis, with less Al substitution for Si and because of possible charge imbalance, Ca and Mg can also sometimes substitute for K. The K, Ca or Mg interlayer cations prevent the entrance of H_2O into the structure hence making this type of clay to be non-expanding clays (Moore and Reynolds, 1997). Just like illite clays, kaolinite also does not absorb water and does not expand when it comes in contact with water. However, smectites or montmorillonites show a different behavior when contacted with water. Smectites are weakly linked by cations like Na^+, Ca^{2+} which result in the high swelling/shrinking potential of this type of clay. The interlayer in smectites is not only hydrated, but it is also expansible and because of this, they are often referred to as “swelling clays” (Grim, 1962).

The charge densities of clay minerals are important not only for structural studies but in the application of clays in the adsorption processes. Whether or not a clay becomes totally dissociated or not, depends on the available interlayer cations and the layer charge (Liu and Zhang, 2007). For example, vermiculites have a high charge and for that reason, they will not completely dissociate. Essentially, without a charge, kaolinites are never separated to start with, because they do not have interlayer cations that hydrate. However, they can undergo interparticle swelling as opposed to intraparticle swelling. Unlike the other two types of clays, smectites will undergo complete dissociation by osmotic swelling when saturated with cations possessing a hydration energy greater than or equal to Na^+ (Moore and Reynolds, 1997).

Numerous clay adsorption properties can be associated with the layer charge density (Mermut, 1994). Bujdak and Komadel (1997) studied the interaction between modified clays with different layer charges and the cationic dye (methylene blue) in aqueous suspension. The authors concluded that the strong aggregation and redistribution of the molecules in the clays with higher layer charge was due to the proximity of the negative sites in the clay surfaces and the different coverage of the clay surfaces. This suggests that MB is initially adsorbed only on a minor fraction of the clay, followed by a redistribution with passing time. The higher layer charges on the particles of the studied montmorillonites resulted in a larger aggregation of the dye. The higher charge holds together the layers of the clay more tightly, preventing the movement of the dye molecules to the interlamellar region. The effect of layer charge density in the adsorption of dyes by numerous layered silicates was also examined by other authors (Miyamoto et al., 2000; Bujdak et al., 2010).

Bentonite possesses an excess negative charge on its lattice and is characterized by a three-layer structure having two silicate layers covering an aluminate layer (Adeyemo et al., 2015). This comes as a result of the partial replacement of tetravalent Si with trivalent Al that leads to the replacement of trivalent Al with divalent Ca. Since opposite charges attract, the negatively charged surface lattice of the bentonite clay may have an affinity for cationic dye. Therefore, it can be expected that bentonite clay exhibits a greater capacity to take up cationic dyes. On the other hand, kaolinite has a heterogeneous surface charge. The basal surface of kaolinites is believed to carry a constant structural charge, which is attributed to the isomorphous substitution of Si^{4+} by Al^{3+}. The presence of a charge on the edges is a result of protonation/deprotonation of surface hydroxyl groups and therefore depends on the solution pH (Zhou and Gunter, 1992). Kaolinite is reported to be the least reactive clay (Suraj et al., 1998). However, it's high dependency on pH increases or constrains the adsorption of dyes according to the pH of the solution (Mitchell, 1993). Adsorption may also take place on the flat exposed planes of the silica and the alumina sheets (Spark et al., 1995).

Extensive studies have been done utilising swelling clays to eliminate cationic dyes from aqueous media. Many of these studies sought to evaluate the applicability and feasibility of using basic dyes adsorption for cation exchange capacity (CEC) and specific surface area (SSA) determination. Li et al. (2011) did a study to explain the mechanism of MB adsorption on low-charge montmorillonite as a swelling clay. The stoichiometric desorption of exchangeable cations from the clays associated with MB adsorption together with the close match between the CEC of the clays and adsorption capacity established cation exchange as the central mechanism for MB elimination. XRD and TG-DTG analyses indicated interlayer adsorption, hence, intercalation of MB molecules. FTIR analyses indicated that hydrogen bonding might not be a major interaction in the adsorption of MB. The results confirmed that the charge density, rather than the SSA was the limiting factor for MB adsorption. The authors concluded that for the treatment of wastewater having cationic dyes, swelling clays with a high CEC values would be efficient adsorbents.

Another study by Lv et al. (2011) also confirmed that with low charge swelling clays, CEC is the single most important mechanism for dye removal from water. Lv and coworkers investigated the adsorption of acridine orange (AO), a cationic dye, on low charge montmorillonite to better understand the mechanism behind AO removal using swelling clays. The proportional desorption of exchangeable cations from the clays followed by AO adsorption established cation exchange as the most leading mechanism for AO removal. Moreover, FTIR analyses confirmed the presence of cationic dye AOH^+ on the surface and in the interlayer of the swelling clays. XRD and TG-DTG results also showed interlayer adsorption, thus, intercalation of AO molecules with different conformations at low and higher AO adsorption levels. The authors then concluded that the amount of AO adsorbed far exceeded the CEC of the low charge swelling clays and that was seen as an advantage of using swelling clays to remove cationic dyes from water. They further reported that the uptake of AO was attributed to cation exchange when the amount of AO adsorbed was less than the CEC.

6. Disadvantages of clays leading to modification to enhance their adsorption capacities

Although clays have shown to be good adsorbents for dyes, they have several

limitations which have led to several forms of modifications to enhance their adsorption capacities. Clay modification is the introduction of an alien material to clay matrices with the aim of improving its adsorption capacity for a given pollutant. There are different ways of clay modification which include pillaring, mech-anochemical modification, ion exchange, organo-modification and sonochemical treatment. A variety of studies have reported on the modifications of clay including chemical treatments such as $Mg(OH)_2$ coating of bentonite (Chinoune et al., 2016), clay ion-exchange using bis-imidazolium salts (Makhoukhi et al., 2015), quaternary ammonium cationic surfactants addition onto bentonite external surfaces (Yan et al., 2015), modifying bentonite by a cationic surfactant (Hexadecyltrimenthylammonium chloride) (Anirudhan and Ramachandran, 2015) and treating the clays with acid (Espantaleon et al., 2003; Ozcan and Ozcan, 2004).

6.1. Cationic and anionic surfactant modification

Generally, clays are applied in the elimination of basic dyes because they have a natural negative charge but chemical modifications to the surfaces of the clay can change the surface charge of clays from negative to positive (Errais et al., 2012). These alterations enhance the sorption of anionic dyes. Baskaralingam et al. (2006) stipulates that bentonite adsorbs acidic pollutants weakly because of repellant forces between the negatively charged surfaces and the anions. A number of authors have reported on the modification of bentonite with cationic surfactants for the removal of acidic dyes. They showed that the main mechanism of the acidic dye adsorption can be can be explained in terms of the anionic exchange between the excessive anions and the cations from the surfactant (Ceyhan and Baybas, 2001; Jovic-Jovicic et al., 2008; Ozcan et al., 2004). Ma et al. (2013) compared the performances of raw bentonite and surfactant-modified bentonite. Their findings showed that CTAB-modified bentonite has a comparable high adsorption capacity towards acid dyes, whereas the raw bentonite showed a lower adsorption capacity. The adsorbed amount of Cong Red was found to be 210.10 mg/g for CTABMBn and 37.10 mg/g for raw bentonite.

Clays are also known to have low organic carbon content and because of their hydrophilic surfaces, they are usually less effective in adsorbing nonionic organic contaminants in water (Boyd et al., 1998). However, simple ion-exchange reactions with surfactants causes the clay to be altered from being organophilic to being organophobic and hence enhancing nonionic organic contaminants adsorption. Studies have shown that cationic surfactants interca-lation does not only change the hydrophilic surface characteristics of the clay, but it also significantly increases the clay interlayer basal spacing. Many studies have investigated the modification of montmorillonite (MMT) by alkyl quaternary ammonium cationic surfactants like dodecyltrimethylammonium, benzyldimethylter-adecylammonium and cetyltrimethylammonium. Few studies have reported on anionic surfactant modification mainly because anionic surfactants have a negative charge thus making it difficult to enter into the interlayer spacing of the clays (Zhang et al., 2011).

Chen et al. (2011a) disclosed that surfactants that are anionic enter the interlayer space as pairs of ions with protons (H_3O^+ ions) or as counter ions (Na^+ and Ca^{2+}). Zhu and Chen (2000) studied the adsorption characteristics of MMT modified by an anion-cationic surfactant and they established that a combination of cationic and anionic surfactants form mixed micelles, producing organic com-pounds synergies solubilization. On another study Chen et al. (2011), modified MMT by anion-cationic, anionic and cationic surfactants by adding anionic surfactants cetyl trimethyl ammo-nium bromide (CTMAB) and anionic surfactants sodium stearate (SSTA) to MMT. The mechanisms of adsorption of methyl orange on anion-cationic modified MMT were compared. Their findings showed that CTMAB/10SSTA-MMT has a higher adsorption capacity than CTMAB-MMT and 10SSTA-MMT because of the formation of a highly effective partition medium by anion-cationic surfactant micelle.

Li et al. (2010) reported on the adsorption of a polymer loaded bentonite (EPIDMA) and raw bentonite for Acid Scarlet (AS GR) and Acid Dark Blue 2G (ADB 2G) dyes from aqueous solution. After the adsorption experiments, the adsorption capacities of raw bentonite, cationic surfactant cetyltrimethylammonium bromide (CTMAB) modified bentonite (CTMAB/bentonite) and cationic polymerpolydiallydimethylammonium (PDMDAAC) modified bentonite (PDMDAAC/bentonite) were compared. For AS GR, the observed adsorption capacities were 4.12, 30.28 and 42.72 mg/g for raw bentonite, CTMAB/bentonite and PDMDAAC/bentonite respectively whereas for ADB 2G the adsorption capacities were 3.67, 24.85 and 33.34, respectively for the three different adsor-bents. All the above mentioned adsorption capacities were lower than that of EPI-DMA/bentonite for AS GR and ADB 2G which recorded maximum adsorption capacities of 45.54 and 35.93 mg/g respectively. This comparison study confirmed that EPI-DMA/ bentonite is the best adsorbent for AS GR and ADB 2G among the selected adsorbents.

6.2. Magnetic modification

Due to their high dispersion, waste clay particles can prove difficult to remove from solution after adsorption. To overcome this limitation, magnetizing clays can be an option using a simple procedure referred to as magnetic separation which removes the clay particles from water (Xu et al., 2012; Gao et al., 2015; Wang et al., 2014). Magnetic materials such as ferrite (MFe_2O_4), where M = Co, Mn, Cu, Zn, etc), Fe_3O_4, Fe_2O_3 and so on have been used as adsorbents for the removal of toxic pollutants because they can be easily separated from the reaction medium by using an external magnetic field within a short time. Unfortunately, their low adsorption capacity and narrow pH range restrict their large-scale practical application (Li et al., 2016). Therefore, to improve adsorption performances, great efforts have been made to functionalize magnetic materials (Fan et al., 2012; Ge et al., 2012; Peng et al., 2012).

The introduction of magnetic particles in the nano scale industries is attracting the attention of numerous researchers (Hashem, 2013). Nano particles are exceptionally fine sized, and this property makes them favorable adsorbents. When the size of a particle is reduced, the surface of the particles becomes more accessible to atoms resulting in an increased surface area ultimately changing the surface morphologies and surface energies of the nanoparticles. The aforementioned factors modify the elementary properties and the chemical reactivity of nanomaterials (Hashemian, 2010). Hashem (2013) studied the effect of covering bentonite nanocomposite with magnetite on the removal of methylene blue. According to the author, the introduction of Fe_3O_4 magnetic nanoparticles into the surface of bentonite generates a porous surface with high surface area which is suitable for the adsorption of cationic dyes such as methylene blue. The findings of the batch adsorption experiments revealed that, increasing the initial pH of MB solutions as well as the contact time also increased the adsorption capacity. However, a different trend was observed with adsorbent dosage as the adsorption capacity decreased with increasing mass of the adsorbent. The maximum adsorption ca-pacity was 1600 mg/g.

Another reason why magnetic materials are preferred in the adsorption process is because they have been proved to have more advanced mesoporosity and microporosity compared to natural clays (Giakisikli and Anthemidis, 2013).

Ambasht and Sillanpa (2010) also stipulated that magnetic composites have high surface areas compared to natural clay and this makes them to produce fast adsorption kinetics i.e. comparatively little contact time is needed for the adsorption process to reach equilibrium. Determination of sorption properties of magnetic nanocomposite sorbents showed that the adsorption efficiency of nanocomposites is considerably greater than the separate phases of the composite. Moreover, studies have shown that all the residual composite magnetic sorbents can be successfully removed from aqueous solution by magnetic separation (Makarchuk et al., 2016). A study to assess the adsorption of MB by nanocomposite sorbents, saponite and magnetic liquid revealed that among the three tested adsorbents, the magnetic composite sorbents (MCS) were the most effective adsorbents. With respect to all dyes, the adsorption capacity of MCS increased as the magnetite content increased from 2 to 7 wt%. However, modifying saponite by magnetite by 10 wt% led to the decrease of MCS 10 sorption properties. These results corroborated with the characteristic of nanocomposites porous structure.

6.3. Mechanochemical modification of palygorskite

Mu and Wang (2016) compiled a comprehensive review on the modification of palygorskite with different physical or chemical methods and palygorskite-based composite used as adsorbents for the adsorption of dyes from aqueous solution. Traditionally grinding and extrusion methods were widely used on palygorskite to modify it to increase its adsorption capacity before use because of their simple operation process, low cost, and easy industrial application. However, the enhancement in the adsorption capacity of palygorsite toward dyes is limited by these traditional methods. Therefore, other treatments also have been adopted to activate palygorsite for the adsorption of dyes, such as acid or alkali-activation, thermal treatment, hydrothermal or solvothermal treatment. To have a full understanding on the various mechanisms involved in the dye removals and specifications in the modification processes, readers are advised to consult the review article by Mu and Wang (2016). However, Table 5 summarises some of the methods of palygorsite modifications that have been used and how these various modifications impacted the adsorption capability of the palygorsite. Because palygorsite is an example of a clay, the same modifications can be applied to some clays.

6.4. Structural and chemical changes after clay modification: effect on adsorption

To follow the structural and chemical changes made after various modifications, the adsorbents are usually characterised before and after modifications. Most modifications are aimed at increasing the surface area of the clay soils or adding the functional groups that are responsible for dye uptake and all this will be basically aimed at enhancing the adsorbent material's adsorption capacity. Sarma et al. (2016) reported on the treatment of montmorillonite (Mt) with 0.25 and 0.50 M sulfuric acid and how this treatment affected the adsorption capacity of the clay. Character-ization by BET showed that pore volume and surface area were greater than before acid treatment. The pore volume showed an increase from 0.1 cm^3/g to 0.8 cm^3/g after treatment and the surface area increased from 173.0 to 221.38 m^2/g and further to 228.95 $m^2/$ g on treatment with 0.25 M acid and 0.50 M acid respectively recording a 28 and 32.3% increase for the different acid molar concentrations respectively. This increase in surface area may have led to the increase in adsorption capacities as reported by the authors. The Langmuir data disclosed that the adsorption capacity of the untreated montmorillonite was 370.37 mg/g while that of 0.25 M and 0.50 M acid treated montmorillonite was 384.62 and 400.0 mg/g respectively at 303 K.

Treatment with acid removes impurities in the clay at the same time substituting exchangeable cations with H^+. Acid treatment can also lead to cation leaching some from the tetrahedral and octahedral sites opening up platelet edges. This may result in an increase in the surface area and the pore dimensions (Diaz and Santos, 2010; Auta and Hameed, 2013) subsequently leading to an enhanced adsorption capacity.

Anirudhan and Ramachandran (2015) used Hexadecyl-trimenthylammonium chloride as a cationic surfactant to modify bentonite clay. Characterization of the clay before and after modification showed significant changes in the chemical composition and surface properties of adsorbent. The changes included a decrease in Fe_2O_3 and Al_2O_3 content, implying that the surfactant adsorption was through the exchange of inorganic cations, the BET surface area of the organoclay was reduced from 36.5 to 27.9 m^2/g. Unlike surface area, the PZC and CEC of the bentonite increased after modification from 4.5-7.8 and 0.52-0.71(meq/g) respectively. The prepared organo bentonite clay was later evaluated for its adsorption behaviour for the basic dye removal CV, MB and Rhodiamine B (RB). The findings showed that the modified clay demonstrated better adsorption capacity for the removal of all the selected dyes. pH was found to play an imperative role in the adsorption process, moreover the removal of dyes was found to be dependent on initial dye concentration. The adsorption capacities for the dyes were established to be 399.74 mol/g for MB, 365.11 mol/g for CV and 324.36 mol/g for RB. The adsorption efficiency of the organobentonite was higher than the unmodified bentonite as expected. The results also showed that organoclay was 1.6, 1.7 and 1.75 times more effective than natural bentonite for MB, CV and RB adsorption respectively because after modification, the porosity of the clay increased. The authors attributed the mechanism of the adsorption process to the adsorption/partition model (Zhu and Chen, 2000). This study basically showed us that surfactant modification of clay can enhance their adsorption capacities.

In a study done by Chinoune et al. (2016), an effective brucite-coated bentonite was synthesised and assessed for anionic dye removal from water. The obtained results from this study showed that, coating bentonite clay with $Mg(OH)_2$ considerably improved the removal of reactive dyes. At a pH of 5, which was greater than the acidity constant, reactive dyes mainly existed as anions and were probable going to be repelled by the montmorillonite surfaces because they are negatively charged. The $BeMg(OH)_2$ contains more polar acid SieOe groups and basic Mg(OH) sites that have a tendency to react with organic compounds because they are polar in addition to several other functional groups. The ability of modified bentonite to take up dyes showed that van der Waals and $\pi-\pi$ interactions take place amongst OH ions available on the clay. pH had a major influence on the adsorption of ions on the com-posite surface, mainly on the extent of adsorbate ionization. The maximum dye removal was achieved at pH 2. This could be as a result of electrostatic interaction between cationic dye molecules and the negatively charged $BeMg(OH)_2$ surfaces. Nonetheless, the adsorption still took place in basic conditions, showing the occur-rence of intermolecular interaction.

On the work done on bentonite, Ozcan et al. (2004) proposed that natural bentonite surfaces make it less effective for taking up hydrophobic organic compounds owing to the electrical charges and hydrophilic surface. The authors recommended that raw bentonite can be treated by organic cations to yield a Dodecyl-trimethylammonium bromide-modified bentonite (DTMA-bentonite) thus considerably improving its ability of adsorbing hydrophobic pollutants from aqueous solution. A comparison of the findings with Na-bentonite revealed that Na-bentonite and DTMA- bentonite synthesized from

Table 5
Various palygorsite modifications for the adsorption of dyes.

Modification method	Dye removed	Effect of modification on adsorption capacity	Reason for change in adsorption capacity	References
Extrusion	Methylene blue	Adsorption capacity was observed to increase to 158 mg/g, 78 mg/g and 98 mg/g.	Partial disaggregation of crystal bundles of PAL.	Zhang et al., 2015a,b
Grinding	Methylene blue	Percentage dye removal increased by 25%	Specific surface area increased from 153 to 229 m^2/g.	Liu et al., 2012
High-pressure homogenization	Methylene blue	Percentage dye removal increased by 21%	Disaggregation of PAL crystal bundles.	Zhang et al., 2015a
Ion beam bombardment	Methylene blue	Better adsorption capacity in comparison to the raw PAL.	A larger interspace, better separation, higher pore-size (with micro/nano- scale) and porosity and doubling of the BET surface area of the PAL nanonetworks. Increase the surface area.	Cai et al., 2010 Zhang et al., 2013
Acid activation	Quinalizarin	Percentage dye removal increased by 50%		Frini-Srasra and Srasra, 2009 Wang et al., 2015
Alkali-activation	Methylene blue	Exhibited a far better adsorption capacity compared to that of raw PAL inferred from the colour of 200 mg/L MB.	No clear explanation because the rod-like morphology almost disappeared and BET specific surface area of PAL was highly reduced after the treatment with 5.0 M of NaOH solution.	
Thermal activation	Methylene blue	Adsorption capacity increased with calcination temperature and reached the maximum at 700 °C (about 78.1 mg/g), and then decreased with further increasing temperature.	Cation exchange was a main mechanism in the adsorption process.	Chen et al., 2011b
Hydrothermal or solvothermal treatment	Methylene blue	Adsorption properties of PAL for MB were evidently improved from 119 mg/g to 171 mg/g after modification	Disaggregation of crystal bundles, PAL nanorods became more uniform and an increase in pore size of adsorbent. Electrostatic attraction as well as van der Waals interaction.	Zhang et al., 2015b
Surfactant modification	Orange II	Adsorption capacities were observed to be 92 and 88 mg/g.		Sarkar et al., 2011
Silane coupling agent modification	Reactive Red 3BS, Reactive Blue KE-R and Reactive Black GR	34.24 mg/g, 38.60 mg/g, and 60.13 mg/g respectively. Percentage increase from 1.16 to 99.32%; 3.30-99.67% and 2.88-96.42% respectively.	Activity of the amino groups.	Xue et al., 2010 Xue et al., 2011
Polymer modification	Reactive yellow 3RS	Langmuir model was 71.38 mg/g which was much higher than that of the raw PAL (6.3 mg/g).	Cationicity	Peng et al., 2013

natural materials are able to remove acid blue 193 from aqueous solution. Nevertheless, DTMA bentonite displayed a greater removal capacity than raw bentonite. DTMA-bentonite had an adsorption capacity of 740.5 mg/g which is approximately 11 times greater than that of Na-bentonite (67.1 mg/g). Acid blue 193 was also adsorbed effectively by benzyltrimethylammonium (BTMA) chloride surfactant modified bentonite (Ozcan et al., 2005) . Furthermore, Ozcan et al. (2007) applied the DTMA-bentonite for the elimination of reactive blue 19 from water. The results showed that the modified bentonite had an adsorption capacity of 206.58 mg/g for DTMA-bentonite at pH of about 1.5. This suggested that electrostatic interactions occurred between bentonite's adsorption site and the anionic dye.

6.5. Clay composite materials: clay nanocomposites, clay/polymer nanocomposite and clay/polymer nanocomposite hydrogels

One promising approach to resolve the disadvantages of the low adsorption capacities of natural clay minerals is to mix it with other advanced adsorbents like polymers and/or activated carbon which have proven to be exceptionally efficient in the removal of organic compounds. In recent years, composite materials have received extensive interest for their potential applications in wastewater treatment because they can combine the properties and advantages of each component and may also exhibit some attractive perfor-mances (Mahdavinia et al., 2012a; Hosseinzadeh et al., 2015). A composite could be defined as a mixture of two or more materials possessing different physical and chemical properties with a very distinct interface.

Dye adsorption onto clay minerals is affected by different factors like exchangeable cations, the space between the clay inter layers, and whether or not there are water molecules between those layers. On the other hand, polymers are considered multipurpose materials because they can be easily manipulated, they are simple to produce and are highly flexible. However, there are cases where polymers need to be altered for them to achieve certain perfor-mance requirements. One way of modifying polymer properties is mixing them with solid fillers such as fibers, platelets, particles, other polymers, clays or clay minerals, resulting in polymeric composites or blends (Mahdavinia et al., 2012c). These polymeric blends can then be used for adsorption processes and studies have shown that they exhibit exceptionally good adsorption capacities (Table 3).

There are different types of polymers used for adsorption pro-cesses and hydrogels are amongst those polymer materials per-forming successfully in the removal of contaminants from aqueous solution. They are a group of polymers capable of absorbing a lot of water without dissolving because of the physical or chemical crosslinking of the hydrophilic polymer chains (Schacht, 2004). Hydrogels have functional groups that can ionize easily and therefore repel each other, capturing more water molecules. Additionally, these ionized functional groups let hydrogels absorb and trap different types of contaminants with the opposite ionic charges. As such, hydrogels, as potential adsorbents have attracted much attention in recent years for dye adsorption. Furthermore, hydrogels have a relatively low production cost and high adsorption capacity for some dyes (Wang et al., 2010).

Kamal et al. (2014) prepared copolymer hydrogels made up of Poly vinyl alcohol (PVA) and Poly acrylic acid (PAA) through γ-irradiation. This polymer was prepared having N,N' methylene bis- acrylamide (MBAM) as a

crosslinking agent. The adsorption experiments revealed that the adsorption of CV dye onto PVA/PAA and PVA/PAA/clay composite hydrogels depended on a number of variables like solution pH, initial dye concentration, PVA/PAA/clay composition, temperature of the solution and ionic strength amongst other variables. It can be concluded that the PVA/ PAA/clay composite hydrogel is a more efficient adsorbent than PVA/PAA hydrogel for CV dye, since its removal efficiency reached 92% for the composite hydrogel containing 4% clay and of composition 50/50 (wt%).

Clays like bentonite, laponite, sepiolite enhance the adsorption capacity and mechanical properties of hydrogels and in most cases nanocomposite hydrogels are loaded with such types of clays (Shirsath et al., 2011). A study that corroborate this findings was carried out by Li et al. (2012) where nanocomposites hydrogels were prepared by loading laponite clay into a poly(acryl amide) hydrogel via in situ polymerization to assess the adsorption prop-erties of the composite onto CV. The experimental results of the removal of cationic dye showed that, as the clay content in the hydrogel increased, the adsorption capacity of the hydrogel increased hence confirming the aforementioned statement about clays enhancing the adsorption capacity and mechanical properties of hydrogels. Li and coworkers also prepared another hydrogel nanocomposite (poly(acrylic acid)-bentonite-FeCo (PAA-B-FeCo)) through ultrasound assisted in situ emulsion polymerization. The incorporation of Fe-Co and exfoliated bentonite clay platelets also increased the stability and strength of hydrogel thereby aiding the dye adsorption process. The adsorption results showed that a pH of 11 produced the maximum dye adsorption because at that high pH, there is dissociation of COO ions which attracts cationic organic compounds.

Adsorption studies using a variety of composites including nanocomposites, polymer composites, clay nanocomposites hydrogels have acquired relevance due the potential it offers, as shown on Table 6.

7. The effect of variables and their interaction on dye adsorption

Dye adsorption studies using clays are usually carried out in a batch approach to evaluate the influence of experimental parameters including contact time, pH, adsorbent dose, initial dye concentration and temperature. Batch experiments investigate one factor a time in order to acquire optimum conditions of dye adsorption.

7.1. Effect of solution pH

By definition, pH is a measure of hydrogen ions concentration. The variability of the pH of the aqueous solution in which the adsorption process takes place, plays a vital role in the whole adsorption process (Elmoubarki et al., 2015). Generally, pH influences the dye adsorption because of change in surface characteristics of the adsorbent and that of the dye chemistry. Solution pH also determines the extent of protonation of the OH exchange sites and the extent of protonation of the adsorbate thus determining the specific charge of an exchange site and therefore ultimately the adsorption tendency of the substrate also (Tomar et al., 2014). Therefore, the adsorption capacity of the adsorbent will also depend on solution pH. In general, at low pH values (acidic conditions) there is an increase in the amount of anionic dye removal. This is due to the electrostatic attraction occurring between the anionic dye and the positively charged surface of the adsorbent. At high pH values (basic conditions), there is electrostatic repulsion between the negatively charged adsorbent surface and the anionic dye, therefore reducing the adsorption capacity and anionic dyes percentage removal (Han et al., 2014; Tümsek and Avci, 2013).

To corroborate the general trends shown by the effect of pH on dye adsorption, we looked at a few studies that investigated pH influence on the removal of dyes from solution. To study the effect of pH on adsorption, Anirudhan and Ramachandran (2015) performed batch experiments using organoclay on dyes with initial concentrations of 200 and 400 μmol/L solutions of Methylene Blue (MB), Reactive Blue (RB) and Crystal Violet (CV). The findings showed that increasing pH also increases the adsorption capacity. A possible explanation to this observation is that, increase in pH, decreases the positive charges on the surface thereby increasing the negatively charged sites. Negatively charged surfaces on the clay will favour the uptake of cationic dye molecules due to electrostatic attraction. Earlier we mentioned that cationic dye adsorption improves with a rise in pH. Results on the specific adsorption capacities of the clay for dyes were 99 and 97 μmol/g for MB, 95 and 184 μmol/g at initial concentrations of 200 and 400 μmol/L for CV and 90 and 174 μmol/g for RB, respectively at pH 9. The dyes were taken up in the order: MB > CV > RB. The authors reported that order of affinity could be explained on the basis that dyes have different molecular size, structure and functional groups hence electrostatic and other physical forces they experience will be different (Allen et al., 1989). Essentially most cationic dyes yield molecular cations (C^+) as well as reduced ions (CH^+) (Kavitha and Namasivayam, 2007). There is a decrease in dye adsorption in acidic conditions due to the electrostatic repulsion because the protonated adsorbent surface repel the cationic dye molecules. The adsorbent surface becomes positive after modification giving a pHpzc of 7.8 and the maximum removal occurred at pH 9. Beyond the pHpzc, the clay surface was negative, and adsorption occurred by electrostatic attraction between the negative surface of adsorbent and cationic dye species. These results show that indeed the surface characteristics of the adsorbent influence its adsorption capacity.

As it has already been indicated earlier, anionic dye adsorption strongly depends on pH, and low pH ranges are ideal for their removal when metal oxides are used as sorbents (Afkhami and Moosavi, 2010; Saha et al., 2011). Hai et al. (2015) also obtained similar results in their study. These researchers used acid-activated kaolinite with TiO_2 to remove azo dyes CR, Direct Fast Scarlet 4BS (4BS), and weak acid dark blue 5R (5R)) from aqueous solution and like many dye removal studies, they also investigated the effect of pH to see how it will influence the percentage dye removal. Their findings showed that all the three dyes were maximally removed in acidic conditions than basic conditions. To explain their findings, the authors stated that pH determines TiO_2 nanoparticles surface charges and the ionic nature of dyes. Anirudhan and Ramachandran (2015) also gave the same explanation for dye adsorption earlier on. CR, 4BS, and 5R are anionic dyes and are negatively charged, it was quite expected that their removal be greater in acidic conditions and the results came out as expected. However, the same explanation cannot be given in the case of metal oxide adsorbents. The increased adsorption of the dyes on the metal oxide modified ad-sorbents under acidic conditions was mainly attributed to the electrostatic attraction between the negatively charged dye ions and the positively charged Ti-OH_2^+. On the contrary, under basic conditions, OH groups on the surface of TiO_2 dissociates forming TiO and therefore TiO_2 nanoparticles surfaces become negatively charged causing electrostatic repulsion between the dye anions and the negatively charged TiO_2 nanoparticles, resulting in a decrease in dye adsorption.

It is worth noting that it is not always the fact that adsorption processes always depend on pH, sometimes the adsorption may totally be independent of pH though this is not always the case for most studies.

Table 6
Comparison of adsorption properties of different clay composite materials.

Clay polymer nanocomposites	Dye	Enhancement action of polymer system	References
Poly (acrylamide-co acrylic acid)/Kaolinite P(AAm-AAc/Kao) Clay composite	Bromophenol Blue	An increase in temperature resulted in increase in the amount of BPB dye adsorbed per unit mass of sorbents	El-Zahhar et al. (2014)
Chitosan/Modified Ball (MBC-CH) Clay composite	Methylene Blue	Adsorption of MB on MBC-CH was found to increase as the initial concentration, solution pH and temperature of the solution were increased.	Auta and Hameed (2014)
Poly(ethylene glycol-co-acrylic acid)/Bentonite Clay nanocomposite semi-IPN type hydrogel	Congo Red and Methyl Violet	The nanocomposites showed high adsorption capacity and removal-% of CR and MV at a solution pH of 7	Bhattacharyya and Kumar-Ray (2015)
Poly(Acrylamide)/k-Carrageenin/Sodium Alginate Sodium Montmorillonite (MMT) Clay hydrogel nanocomposite	Crystal Violet	Dye adsorption capacity of hydrogels was influenced by both clay content and biopolymers weight ratio. At acidic media, the dye adsorption capacity of nanocomposites was enhanced as the carrageenan and clay content were increased.	Reza-Mahdavinia et al. (2013)
Poly(acrylicacid)/Bentonite/FeCo particles (PAAc-BFeCo) hybrid hydrogel nanocomposite	Crystal Violet	Exfoliated bentonite clay and Fe-Co particles increased the strength and stability of hydrogel and assisted the adsorption of CV	Shirsath et al. (2011)
CarAlg/MMt nanocomposite hydrogels	crystal violet	The adsorption capacity of nanocomposites was enhanced as the clay content was increased.	Mahdavinia et al. (2013)
kappa-carrageenan-g-poly(acrylamide)/sepiolite nanocomposite hydrogels	crystal violet	The speed of adsorption of cationic CV dye onto obtained hydrogels was improved by introducing sepiolite nanoclay.	Mahdavinia and Asgari (2013)
Novel kappa-carrageenan/poly (vinyl alcohol)/ montmorillonite nanocomposite hydrogels	Crystal violet	Compared with clay-free hydrogel, the nanocomposites indicated a relatively improved adsorption capacity at the same batch system.	Hosseinzadeh et al. (2015)
Magnetic carboxymethyl chitosan-gpoly(acrylamide)/laponite RD nanocomposites	Crystal violet	By introducing magnetic laponite RD, the nanocomposites showed an enhanced adsorption capacity for CV dye.	Mahdavinia and Karami (2015)
carrageenan-based nanocomposite superabsorbents	Crystal violet	The rate of dye adsorption is enhanced by increasing the clay content up to 14 wt% of clay.	Mahdavinia et al. (2012a)
Novel carrageenan-based hydrogel nanocomposites containing laponite RD		The effect of carrageenan and clay contents on the speed of dye adsorption revealed that while the rate of dye adsorption is enhanced by increasing the clay content, it was depressed as the carrageenan content increased in nanocomposites composition.	Mahdavinia et al. (2012b)

Santos et al. (2016) evaluated the effect of pH on Basic Red 46 uptake by bentonite clay. Contrary to the usual findings on the effect of pH on dye removal, their results show that the amount of adsorbed dye was not considerably affected by pH. They reported that, for initial pH values between 2 and 6, the BR adsorbed amount was approximately 220 mg/g and pH did not have a considerable impact on that adsorption capacity. Chemical adsorbent charac-terization before the dye adsorption experiments showed that 0.1, 0.01 and 0.001 mol/L, NaCl concentrations recorded the PZNPC of the adsorbent as 9.6, 9.9 and 10.1 respectively. Considering those PZNPC results, at low pH values, there is a positive pH-dependent charge meaning that it is only the negative permanent constant charge that is in charge for BR adsorption. As pH was increased an increase of adsorption capacity from 220 mg/g at pH 6 - 319 mg/g at pH 10 was observed and in that basic solution, equilibrium pH values ranging from 8.7 to 9.3 and those values were closely similar to PZNPC values. The negative pH-dependent charge and the permanent charge, plays a pivotal role in the improved adsorption capacity. Similar tendencies were also reported for the cationic dye adsorption by montmorillonite and palygorskite (Al-Futaisi et al., 2007; Roulia and Vassiliadis, 2008). These findings clearly indicate that BR dye (a cationic dye) can be taken up extensively even under unfavourable (acidic) conditions and furthermore bentonite clay did not show the weakness of being strongly dependent on pH to perform well.

7.2. Effect of adsorbent dose

To determine a minimum adsorbent dosage that is economically viable in wastewater treatment processes, many studies have investigated the effectiveness of several sorbent dosages on the removal both anionic and cationic dyes (Anirudhan and Ramachandran, 2015; Chaari et al., 2015; Yan et al., 2015). Generally, the percentage removal of dye is directly proportional to the adsorbent dosage (as the adsorbent dosage increases, the percentage removal of the dye also increases). A possible explanation for such a trend is that, with increase in adsorbent dosage, adsorption sites that can take up dye ions become more available. When the adsorbent dosage is low the adsorption rate is quick because of the readily available active sites and when the adsorbent dosage is high, the dye ions cannot readily access the adsorption sites easily until the attainment of equilibrium (Sarma et al., 2016).

Acid Blue 25 (AB25), Acid Blue 93 (AB93), Acid Golden Yellow G (AGYG) and Acid Turquoise Blue A (ATBA were used as model dyes in a study by Yan et al. (2015). Raw bentonite and CTMAB-Bentonite were used to test the effect of adsorbent dosage for this particular study. As expected, the results followed the general trend with adsorbent dosage. Their findings revealed that the amount of dye uptake increased with the increasing amount of the modified adsorbent. An 80% removal was achieved for AB93 and AB25 with a 0.02 g dosage. For the other 2 dyes, there was a rapid adsorption, with the equilibrium state being achieved at 0.05 g. All four dyes recorded more than 88% removal with the modified clay, while for raw bentonite the percentage removals were all lower than 30%. The findings showed that the adsorption ability of CTMAB-Bent was strongly enhanced by surfactant modification, by changing the hydrophilic surface to hydrophobic. A similar trend of results was also reported by Chaari et al. (2015) on the interactions of C.I. direct orange 34 (DO34) with Tunisian raw clay. To assess the adsorption capability of the clay, the dosage was varied in the range 0.3-1.5 g/L.

The percent removal improved from 85 to 87% with dose increase from 0.3 to 1 g/L. The authors reported that this might have been ascribed to an improved surface area of the adsorbent and the availability of additional adsorption sites. Nonetheless, above 1 g/L dose, there was a reduction in dye adsorption, which might have been caused by the reduction of the available surface area due to the formation of agglomerates by the clay minerals thereby blocking some of the binding sites.

Rehman et al. (2013) are also among many researchers that investigated the adsorbent dose effect on dye removal and they also acknowledge that it is important to select a proper initial adsorbent dosage because it controls adsorption by way of available adsorption sites and surface area (Javaid et al., 2011; Safa and Bhatti, 2011). These authors studied the removal of Brilliant Green dye by red clay (RC) and they varied the adsorbent dosage between 0.3 and 1.5 g/L. Their results showed an inverse relationship between removal efficiency and adsorbent dosage. Dye adsorption rose from 67% to 94%, while the adsorption capacity declined from 117.3 to 31.4 mg/g at a dose of 0.3-1.5 g/L. Mane and Babu (2011) and Safa and Bhatti (2011) also described a similar performance of adsorption against adsorbent amount. Increasing the amount of RC increases the available adsorption sites up to a particular level against a fixed dye molecules number (Ghaedi et al., 2011).

7.3. Effect of initial dye concentration

To evaluate the amount of dye adsorbed and consequentially the percentage of dye removed from a solution, investigating effect of the initial dye concentration becomes imperative. Previous studies have shown a general trend wherein increasing the initial dye concentration leads to a decrease in the percentage of dye removal (Anirudhan and Ramachandran, 2015; Yu et al., 2015). Various authors have attributed this to the saturation of adsorption sites on the sorbent surface by the adsorbate species. The percentage of dye adsorption rises with increasing contact time at all initial dye concentrations (Dawood and Sen, 2014). What happens is that a driving force to overcome the resistance to the mass transfer of dye is provided by the initial dye concentration between the aqueous and the solid phase (Rafatullah et al., 2010).

This phenomenon of saturation of sorption sites on the sorbent surface by the adsorbate species was also observed by Ogunmodede et al. (2015). They studied the removal of acid dye from using a combination of bentonite and kaolin clay and among other variables, also investigated the effect of initial dye concen-tration on dye uptake. The adsorption efficiency of kaolin-bentonite improved as the initial dye concentration increased. The authors suggested that increasing the dye concentration leads to a rise in mass gradient between the adsorbent and solution, hence acting as a driver to transfer the dye ions from bulk solution to the particle surface. An increase in the proportional dye adsorption was attributed to the equilibrium shift during the clay adsorption pro-cess (Ogunmodede et al., 2015). A different study by Makhoukhi et al. (2015) also revealed that the amount of dye adsorbed increased with increasing dye concentration up to a saturation level. Makhoukhi et al. (2015) reported on Telon dyes adsorption by bis-imidazolium modified bentonite from aqueous solutions and their findings showed that all organo-Bt adsorbents showed improved capacities for dyes retention.

Rehman et al. (2013) also did a study on the uptake of BG by red clay (RC) and reported that the adsorption process was directly proportional to the initial dye concentration because it drove the mass transfer rate under a higher concentration gradient between the RC surface and the dye solution. The same explanation has been reported by other studies including Aroguz et al. (2008) and Auta and Hameed (2012). Initial dye concentration effect (20 -100 mg/L) on the adsorption of BG showed that adsorption efficiency and sorption capacity displayed opposite trends with increasing initial BG concentration. RC sorption capacity rose from 48 to 119.5 mg/g, while the adsorption efficiency declined from 96% to 47% with an increase in BG concentration from 20 mg/L to 100 mg/L, respectively. Numerous scholars similarly established comparable results using BG (Auta and Hameed, 2012, 2013; Nandi et al., 2009). Kismir and Aroguz (2011) revealed that the adsorption efficiency of BG by Saklikent mud improved with increasing initial BG concentration but their highest initial dye concentration used was 20 mg/L and it recorded a 96% removal. Auta and Hameed (2012; 2013) maintain that surfaces of the adsorbent have a fixed number of binding sites per unit mass of the sorbent. At lower initial dye concentration, the number of available sites is higher when compared to those at higher initial concentrations. As a result, majority of the dye ions are taken up by RC leading to greater percentage removal. Dye particles have to compete for the fixed number of adsorption sites at higher initial concentration hence some of dye particles cannot be taken up. The findings from the experiments confirmed that residual dye increased with the increase in initial dye concentration which resulted in lower adsorption efficacy (Nandi et al., 2009).

7.4. Effect of contact time

Researchers have done contact time studies to show a rela-tionship between the amounts of dye adsorbed onto a fixed adsorbent mass with agitation/contact time (Chinoune et al., 2016; Elmoubarki et al., 2015; Fayazi et al., 2015; Santos and Boaventura, 2016). Contact time aids in finding the optimum time at which equilibrium is reached which can later on be applied in wastewater treatment plants based on wastewater process design. Contrary to other adsorption parameters, the effect of contact time does not have a definite general trend. However, most cases show that adsorption happens rapidly at the very first few minutes of contact and then proceeds gradually until equilibrium is reached after which the percentage removal of the dye will not change.

The same can be said for Safranin dye removal by magnetic mesoporous clay (MMC) reported by Fayazi et al. (2015). The effect of agitation time on the adsorbed amount of Safranin was studied from 0 to 90 min and the results revealed that dye removal took a two-stage process, with a fast initial Safranin adsorption followed by slow adsorption. It was clear that much of the dye molecules were adsorbed during the initial 10 min where the adsorption amount (qt) was about 10.7 mg/g and nearly levelling off after 10 min such that Safranin removal remained almost constant as contact time was increased. The authors suggested that the rapid initial uptake rate was due to the rapid diffusion of the dye from aqueous solution to the MMC composite external surface. Gradually occupation of the adsorption sites by Safranin dye occurs when dye molecules are transported from the bulk phase to the inner-sphere pores of MMC. At a later stage, the slow diffusion process decreased the adsorption rate and after 30 min of shaking, a steady equilibrium state could be considered.

A more or less similar trend of results was also obtained by Ogunmodede et al. (2015) who studied how contact time would affect the amount of CR taken up by kaolin-bentonite. Their findings indicated that when contact time is increased, the amount of dye taken up was not considerably increased. CR adsorption was very quick from the start of the experiments until around 50 min where a slight increase was observed until 80 min recording the maximum CR adsorption. It can be seen that above 80 min there was almost no change in the CR adsorption. Chaari et al. (2015) had a comparable observation concerning contact time effect on dye adsorption. The results of percent uptake of DO34 by HC was investigated at time intervals ranging from 5 to 90 min and the

findings showed DO34 uptake increased with time until 60 min. Just like the other authors, the initial rapid adsorption was attributed to large number of adsorbent sites that were available for DO34 molecules and beyond 60 min, the adsorption capacity remained constant due to the saturation of adsorption sites. The overall conclusion on contact time studies is that adsorption occurs rapidly within the first few minutes of contact and then proceeds gradually until equilibrium is reached after which the dye percentage removal remains constant.

7.5. Effect of temperature

In order to determine if the adsorption process is going to occur in any adsorption process, energy and entropy values must be taken into consideration (Chen et al., 2011). The practical applicability of the process is indicated by thermodynamic parameter values. These parameters of thermodynamics on adsorption are usually obtained from the experimental data acquired at different temperatures (Chen et al., 2011). Evaluating thermodynamic parameters involves calculating the Gibbs free energy variation (ΔG), enthalpy variation (ΔH) and entropy (ΔS) according equations (1) and (2) (Yousef et al., 2011):

The standard free energy change ΔG is calculated using the following equation:

$$\Delta G = -RT \ln Ka \quad (1)$$

where Δ*G* is the free energy of sorption (kJ/mol), *T* is the temperature in Kelvin (K), *R* is the universal gas constant (8.314 J/mol/ K) and *Ka* is the sorption equilibrium constant.

The sorption equilibrium constant *Ka* can be expressed in terms of enthalpy change (ΔH) and entropy change (ΔS) as a function of temperature and is shown below: (Alver and Metin, 2012; Ma et al., 2012).

$$lnKa = \frac{\Delta H}{RT} + \frac{\Delta S}{RT} \quad (2)$$

where Δ*H* is the heat of sorption (kJ/ mol) and Δ*S* is the standard entropy change (kJ/mol/ K).

The positive values of ΔH implies that the adsorption process is endothermic, and it is an indication that the nature of the dye adsorption is predominantly physical, involving weak interaction forces. The positive values of ΔS suggest an improved chance of the solid to solution interface with some sorption system structural changes and an attraction to the adsorbate. Moreover, a positive ΔS value relates to a rise in the adsorbed species degree of freedom (Ma et al., 2012).

Temperature usually has a notable effect on reaction rate. If temperature increases, the rate of chemical reaction also increases (Mekatel et al., 2015). Hence the temperature of the aqueous solution has a vital role on the whole adsorption process. The increase or decrease of the adsorption capacity with temperature can help tell what type of adsorption took place. If the adsorption capacity increases with temperature then the adsorption is endothermic and if the adsorption capacity decreases with increasing temperature then the adsorption is an exothermic process (Zhao, et al., 2013; Zulfikar, et al., 2013; Khorramabadi et al., 2012). A number of investigations have shown that temperature plays an important role in the adsorption process (Anirudhan and Ramachandran, 2015; Chinoune, et al., 2016; Rehman, et al., 2013).

Elmoubarki et al. (2015) used Morrocan clays to adsorb MB, MG and MO from aqueous solution. These authors evaluated the temperature effect in a bid to test the capability of the clays to remove dyes from a variety of effluents, considering specific circumstances of dye wastewater. Accordingly, they did data collection at five temperatures ranging from 10 - 50 ºC. The quantities of MB, MG and MO adsorbed on the clays as function of the temperature of solution indicated that increasing solution temperature led to an increase of adsorbed MG. However, the adsorbed quantity of MO decreases significantly with an increase in temperature and lastly, the adsorption of MB was less influenced by temperature as the adsorbed amounts slightly decreases with the increase in solution temperature from 10 to 50 ºC. Thermodynamic parameters results which include the change in free energy (ΔG), enthalpy (ΔH) and entropy (ΔS) were used to define the thermodynamic behaviour of the adsorption of MB, MG and MO onto the clays. From the calculated constants it was concluded that, the adsorption was exothermic in the case of MB and MO. To further determine the type of adsorption, the magnitude of enthalpies was calculated, and the process recorded a decrease in entropy. The negative ΔS value suggested a decline in the randomness at the solid/solution interface during the adsorption. The Gibbs energy (ΔG) increased when the temperature was increased from 10 to 50 ºC indicating a decrease in feasibility of adsorption at higher temperatures. In the case of MG, the adsorption was endothermic and accompanied by a decrease in ΔG values with the increase in temperature. The MG result indicated an increase in feasibility of adsorption at higher temperatures. The ΔS values were found to be positive which suggested an increase in the randomness at the solid/solution interface during the adsorption. From all these results, it could be concluded that adsorption of methyl orange was more influenced by the change in solution temperature.

Another study to examine the influence of temperature on dye uptake was carried out by Toor and Jin (2012) using modified bentonite to remove diazo dye. They evaluated the effect of temperature on Congo Red (CR) adsorption on bentonite at 25, 30, 40, 50 and 60 ºC. The temperature impact graph showed that as temperature was increased from 25 to 60 ºC there was a minor decrease in the removal of CR. These findings revealed that the adsorption process was exothermic and lower temperatures favoured the adsorption process hence the negative H^o values. The change in enthalpy was found to be between −20 and 0 kJ mol^{-1}, indicating a physical reaction. From −400 to −80 kJ mol^{-1} chemisorption becomes predominant (Lian, et al., 2009). Similar results were also reported by Vimonses et al. (2009) and Chatterjee et al. (2009). They argue that the decline in dye removal with rising temperatures is because of poor interaction between CR and bentonite because hydrogen bonds and Van der Waals are weak. Calculating the Gibbs energy gave negative values which is indicative of a spontaneous and feasible adsorption process. This further suggests that the adsorption of CR adsorption by modified clay does not considerable change internal structure of the clay. These findings were similar to those described by Özcan et al. (2004) for the uptake of Acid Red 57 by acid activated bentonite. “The decrease in entropy implies the positive affinity of the adsorbents towards the CR adsorption” (Chatterjee et al., 2009).

7.6. Effect of ionic strength

Ionic strength is an important parameter to be investigated in adsorption experiments because it is well known that industrial wastewaters always have pollutants such as inorganic salts. The availability of such salts in solution leads to high ionic strength affecting the whole adsorption process at large (Anirudhan and Ramachandran, 2007). Usually, the variation of the concentration of salts like NaCl, KCl and $CaCl_2$ have a notable effect on the adsorption of acidic dyes. Most of the times, NaCl is used to stimulate the dying process. A study by Ma et al. (2013) to assess the removal of Congo Red, an acid dye using raw bentonite and surfactant-modified bentonite indicated that the adsorption of Congo Red, onto the negatively charged bentonite and positively charged CTABMBn was enhanced by adding the salts in the order: NaCl < KCl < CaCl2. Ionic strength increase in solution may result in the compression of the diffuse double layer on the adsorbent thus easing the electrostatic attraction and the adsorption process consequently (Li et al., 2010; Peng et al., 2006).

Kamal et al. (2014) investigated the adsorption properties of PVA/PAA/clay composite hydrogel towards crystal violet. Among many of the parameters evaluated, the effect of NaCl concentration on the adsorption capacity of the PVA/PAA and PVA/PAA/clay composite hydrogels for CV dye was also studied. The findings show that the adsorption capacities of the adsorbent decreased with increasing NaCl concentration. The findings corroborate what was also reported by Bayramoglu et al. (2009). Generally, what happens is that, as the ionic strength is increased with addition of NaCl, excessive Na^+ ions may screen the negatively charged adsorbent surfaces, leading to the reduction of electrostatic attractive force, and as a result, the cationic dye adsorption decreases. The authors concluded that NaCl addition deteriorates the performance of such prepared hydrogels for dye adsorption.

Fil et al. (2014) studied the effect of electrolyte concentrations on the removal of astrazon red violet (ARV) using montmorillonite. Unlike the above mentioned researchers who used different Cl salts, Fil et al. (2014) used different molar concentrations of NaCl solutions. The adsorption of ARV onto the montmorillonite surface was negatively affected by NaCl in aqueous solutions. Increasing the NaCl concentration from 0 mol/L - 0.1 mol/L, decreased the adsorption capacity from 194.12 mg/g to 179.05 mg/g. A possible explanation to this trend is that as ionic strength is increased electrostatic attraction between the adsorbate molecule and the adsorbent surface is reduced consequently reducing the removal efficiency. Ultimately, increasing solution ionic strength, also decreases the final pH of the suspension. As a result, positive ions increase at the montmorillonite surface, screening electrostatic interactions between charges and decreasing adsorption (Dogan et al., 2009; Weng et al., 2009).

Srivastava and Sillanpaa (2016) studied the regeneration of a basic and an acidic dye on a clay nanocomposite. Desorption study showed that among all tested regenerants (0.5 mol/L HCl, NaOH, CH_3COOH, C_2H_5OH, 1:1 mixture of C_2H_5OH: HCl, acetone and ethylene glycol), acetone proved to be the highly efficient eluent by successfully desorbing the highest amount of dye from dye loaded adsorbent. Related results were also reported by other studies (Chowdhury et al., 2009; Dave et al., 2012). Accordingly, for further adsorption-desorption cycles, acetone was selected as a regeneration medium for the adsorbent. The regenerated sorbent was efficient for the removal of both dyes (>55%) for the two adsorption-desorption cycles. Nevertheless, the third cycle showed decreased adsorption to 44% and 48% respectively for CR and MB and as a result, further cycles were not investigated.

8. Process optimization

One of the major objectives of dye adsorption studies is finding the optimum process parameters to maximize the removal of dyes. To this aim, numerical optimization is employed to determine appropriate amounts or values needed for the different parameters to attain the maximum removal efficiency which is mostly measured as percentage removal (%). Table 7 summarizes the results of optimization conditions attained by different researchers on dye adsorption using various types of clays. Such results show the reliability of the applied model for the appraisal of real conditions (Hassani et al., 2015).

9. Adsorption isotherms

The adsorbate concentration in a solution is in dynamic equilibrium with the interface of the adsorbent. Analysing equilibrium data aids in the development of mathematical models which might be useful in the quantitative description of results. The equations together with the basic assumptions of these equilibrium models can predict the adsorption ions at the same time giving important data on the adsorption mechanisms. The Langmuir and Freundlich isotherms are the most common adsorption isotherm models applied in dye adsorption studies

9.1. The Langmuir isotherm

The Langmuir isotherm model is based on the assumption that adsorption cannot proceed beyond the monolayer. It furthermore says that the adsorption of a particular molecule on a given adsorbent does not depend on the occupation of the next adsorption site (Li et al., 2011).

Expressed mathematically by Equation (3) as,

$$\frac{C_e}{q_e} = \left(\frac{1}{Q_m}\right) C_e + \frac{1}{Q_m b} \quad (1)$$

where Ce is the dye concentration at equilibrium (mg/L), Qe is the adsorbed amount of dye per mass of adsorbent at equilibrium (mg/g), b represents the Langmuir isotherm constant and Qm is the maximum adsorption capacity for a total monolayer coverage.

9.2. The Freundlich isotherm

Contrary to the Langmuir isotherm, the Freundlich isotherm describes the adsorption characteristics for heterogeneous adsorbent surfaces (Singh et al., 2015).
Expressed mathematically by Equation (4) as,

$$logQ_e = {}^{1}/_{n}\ log\ C_e + log\ K_F \quad (4)$$

K_F and 1/n are the Freundlich constants, describing the adsorption capacity and intensity respectively. The constants n and K_F are determined from the slope and the intercept respectively.

Researchers have used these two common adsorption isotherms to describe the mechanisms of dye adsorption onto various types of adsorbent surfaces. Chaari et al. (2015) applied the Langmuir and Freundlich isotherm models to study the mechanisms of adsorption of Direct Orange 34 (DO34) onto natural clay. The isotherms factors were evaluated at pH 3. By way of comparing correlation co-efficients values (R^2) for the two isotherms, the Freundlich isotherm gave the best fitting model for the adsorption of DO34 onto halloysitic clay with a high correlation coefficient value of 0.99. This is indicative of adsorption of DO34 taking place on heterogeneous surfaces (Chaari et al., 2015). These results are also the same with those obtained by Yan et al. (2015). They also applied the Langmuir and the Freundlich models to their data on acid dyes adsorption by CTMAB modified bentonite from aqueous solution. Their findings showed that the Freundlich model gave the best fit having an R^2 vale of 0.93 compared to the Langmuir model which gave an R^2 value of 0.86. These results also corroborated with other studies on the adsorption of acid dyes by clays and organoclays (Hao et al., 2014; Hameed et al., 2007; Tümsek and Avci, 2013).

It is interesting to note that some data will however conform to the Langmuir isotherms more than they will conform to the Freundlich indicating adsorption on homogenous surfaces. In another study by Abidi et al. (2015), equilibrium modelling was studied using Fouchana clay for the adsorption of Reactive Red 120 dye in the presence of CHT-Catalase.

Table 7
Optimum conditions of dye adsorption using various clays.

Clay	Dye	Experimental conditions	Optimised conditions	References
Red clay	Brilliant Green dye	pH (2-10), particle size (58-150 μm), adsorbent dose (0.3 -1.5 g), contact time (5 -1500 min), initial dye concentration (20 -100 mg/L), and temperature (25 - 65ºC)	pH = 7, contact time = 240 min, dose = 0.4 g, initial dye concentration = 20 mg/L, particle size = 58 μm and temperature = 45ºC.	Rehman et al. (2013)
Surfactant modified bentonite clay (organoclay)	Basic dyes	0.1 g of organoclay with 50 mL of various dye solutions (200-1000 mol/L) and time up to 4 h.	pH = 9.0 temperature = 30ºC. contact time = 240 min.	Anirudhan and Ramachandran (2015)
Natural clay	Direct orange 34	pH (2-8), contact time (5-90 min), and HC dose (0.3-1.5 g) and dye initial concentration (20-150 mg/L).	pH = 6.61 contact time = 60 min and dose = 1 g,	Chaari et al. (2015)
Dirty bentonite	Reactive dyes	Dose (1-5 g) Temperature (278-313 K), initial dye concentration (20-120 mg/L) and pH (2-12).	Dose = 3 g, contact time = 180 min, pH = 2 and temperature = 298 K	Chinoune et al. (2016)
Alginate-clay quasi-cryogel beads	Methylene blue	Dose (2-10 mg/mL) Temperature (20-60ºC) and initial dye concentration (0.2-1.6 mg/mL)	Dose = 8 g, contact time = 100 min, temperature = 40ºC and initial dye concentration = 0.8 mg/mL.	Uyar et al., 2016
Modified natural bentonite	Diazo dye	pH (3-11), contact time (2-30 h), and HC dose (2-26 g) and initial dye concentration (100-1000 mg/L).	Dose = 14 g, contact time = 24 h, temperature = 40ºC and initial dye concentration = 1 L and pH > 10	Toor and Jin, 2012
Stevensite-rich Moroccan clay		Dose of 1 g/L, pH (3-10), Temperature (25, 45, and 55 ºC) and initial dye (200-1000 mg/L)	Contact time = 2 h, temperature = 55ºC and initial dye concentration = 1 L and pH = 10	Elass et al., 2011
Magnetic mesoporous clay	Safranin dye	Contact time (0-90 min), dose (0.03 -0.07 g), pH (6-10), and initial dye concentration (40-80 mg/L)	Contact time = 30 min, temperature = low temperatures	Fayazi et al., 2015
Kaolin and Bentonite clay mixture		Contact time (1-80 min), pH (5-13), and initial dye concentration (75-300 mg/L)	Contact time = 50 min, initial dye concentration = 100 mg/L and pH = 10	Ogunmodede et al., 2015

The results were obtained from using the Langmuir and Freundlich isotherm models. In all cases, the Lang-muir isotherm gave the best fit compared to the Freundlich isotherm. Data fitting best to the Langmuir isotherm indicates that in the presence of CHT Catalase, the dye alone forms a monolayer on the surfaces of Fouchana clay (Abidi et al., 2015). Chinoune et al. (2016) reported on the removal of reactive dyes by dirty bentonite from aqueous solution. In this case, the Langmuir isotherms R^2 values were found considerably higher than those of the Freundlich isotherms too. Since the Langmuir isotherms fitted the experi-mental data best it showed the presence homogenous distribution of active sites on the magnesium hydroxide coated bentonite, (Be $Mg(OH)_2$) surface. This conclusion is based on the fact that the Langmuir model assumes that adsorption takes place on homogenous surfaces. Another adsorption isotherm modelling study was also done Fayazi et al. (2015) and the Langmuir and Freundlich constants calculated and reported. The adsorption of Safranin was well fitted to the Langmuir isotherm model with the higher R^2 (0.98). It indicated the adsorption took place at specific homogeneous sites within the adsorbent forming monolayer coverage of Safranin on the surface of the absorbent.

10. Desorption studies

Even though some clays have high adsorption capacities with respect to the removal of dyes, the ability of the adsorbents to be regenerated is a crucial factor to assess their reusability. Regeneration of a spent adsorbent is usually carried out in order to reuse it, avoid the cost of a new acquisition and minimizing the amount of waste. Many researchers have investigated desorption of adsorbed dye using various types of eluents. Some adsorbents can be efficiently adsorbed and reused again for many times but unfortunately some adsorbents do not perform efficiently after desorption and some materials may be lost or their structures destroyed during the desorption process.

Mahdavinia et al. (2016) used ethanol (96% V/V), 0.5 M of KCl solution, 50/50 V/V of ethanol/water mixture and 0.5 M of KCl in 50/50 V/V of ethanol/water mixture to desorb dyes from spent nanocomposites. The use of the above mentioned solutions was ineffective for desorption purposes and therefore there was a need to try other different solutions. For more practical applications of the desorption study the authors attempted to desorb the dye via a mixture of ethanol/water and KCl. The spent adsorbents were desorbed by 0.5 M of KCl in ethanol/water leading to a desorption efficiency of more than 94%. Because of the successful desorption results, Mahdavinnia and coworkers decided to carry out 5 desorption-adsorption processes using the same regeneration agent. Throughout all the regeneration cycles, the nanocomposite mCarraLap3 showed a constant dye adsorption capacity and the change in desorption efficiency and adsorption capacity for all other composites was almost negligible. In actual fact, the findings showed that the nanocomposites could be used for multiple cycles without a decrease in adsorption capacity for CV dye.

To evaluate the regeneration of sepiolite clay and study the mechanisms involved in BR sorption, Santos and Boaventura (2016) carried out desorption experiments using NaOH and HCl as regeneration agents. Desorption studies conducted for BR-loaded sepiolite showed that the maximum BR desorbed percentage was 9.4% and it was obtained for strong acidic conditions (pH 2). For higher pH values, desorption was very low and limited to 2-3%, which reflects the establishment of strong chemical bonds between the basic dye and the sepiolite in the adsorption. The results showed no feasible regeneration by using acid or alkaline solutions. The reduced colour leachability from the dye-loaded sepiolite is, on the other side, a good feature considering the disposal in landfill or reuse for other purposes, such as incorporation in construction materials or in polymeric composites (Zhou et al., 2014).

11. Conclusions

This review paper was mainly looking at the adsorption of different dyes onto various clay based adsorbents. Various materials are currently available to remove dyes from water, but clays are generally considered attractive because of their effectiveness, convenience, ease of operation, simplicity of design and for economic and environmental reasons. Performance comparison of different adsorbents is difficult because of inconsistencies in the data, principally due to different experimental conditions including pH, temperature, particle size and initial dye concentration. The review gave an extensive range of clay material adsorbents. From the literature review surveyed, it was shown that cheap, readily and locally available clay minerals could be used for effective dye adsorption from aqueous solution rather than the expensive commercial activated carbon. Low cost clay adsorbents offer quite a number of benefits that are applicable in the commercial world today and most probable a lot more in the near future. From the literature reviewed, chemically modified clay sorbents demonstrated exceptional adsorption abilities for various dyes when compared to raw clays. Regardless of a large amount of studies on clay adsorbents, there is little data containing a full study comparing the economic viability between these clay adsorbents. Even though a lot has been done on studies dealing with clay material sorbents, a great deal of work still needs to be done to predict the performance of the adsorption processes for dye adsorption in real world industrial effluents under various operating conditions and not only in the laboratory. At the present state of knowledge, it is necessary to continue investigating the potential of these natural adsorbent at and industrial scale and also their potential use after adsorption in various industries including brick manufacturing and landscaping. The benefit would be environmental by the valorisation on one hand, of the adsorbent, and on the other hand of the treated water, thus reducing the water demand. The use of these clay based alternative adsorbents would also bring economic advantages because of the low cost of the material, and potentially by its valorisation.

Acknowledgements

The authors wish to express their sincere gratitude to the University of Venda Research Directorate, Council for Scientific and Industrial Research (CSIR), Water Research Commission (WRC) and National Research Foundation (NRF) for supporting this project financially.

References

Abidi, N., Errais, E., Duplay, J., Trabelsi-Ayadi, M., 2015. Treatment of dye-containing effluent by natural clay. J. Clean. Prod. 86, 432-440.
Adensola, B., Ogundipe, K., Sangosanya, K.T., Akintola, B.D., Oluwa, A., Hassan, E., 2016. Comparative study on the biosorption of Pb(II), Cd(II) and Zn(II) using lemon grass (Cymbopogon citratus): kinetics, isotherms and thermodynamics. Chem. Int. 2, 89-102.
Adeyemo, A.A., Adeoye, I.O., Bello, O.S., 2015. Adsorption of dyes using different types of clay: a review. Appl. Water Sci. http://dx.doi.org/10.1007/s13201-015-0322-y.
Afkhami, A., Moosavi, R., 2010. Adsorptive removal of Congo red, a carcinogenic textile dye, from aqueous solutions by maghemite nanoparticles. J. Hazard. Mater 174, 398-403.
Ajbary, M., Santos, A., Morales-Florez, V., Esquivias, R., 2013. Removal of basic yel-low cationic dye by an aqueous dispersion of Moroccan stevensite. Appl. Clay. Sci. 80e81, 46-51.
Ali, I., Asim, M., Khan, T.A., 2012. Low cost adsorbents for the removal of organic pollutants from wastewater. J. Environ. Manag. 113, 170-183.
Al-Futaisi, A., Jamrah, A., Ai-Hanai, R., 2007. Aspects of cationic dye molecule adsorption to palygorskite. Desalination 214 (1-3), 327-342.
Almeida, C.A.P., Debacher, N.A., Downs, A.J., Cottet, L., Mello, C.A.D., 2009. Removal of methylene blue from coloured effluents by adsorption on montmorillonite clay. J. Colloid Interface Sci. 332, 46-53.
Alver, E., Metin, A.U., 2012. Anionic dye removal from aqueous solutions using modified zeolite: adsorption kinetics and isotherm studies. Chem. Eng. J. 200-202, 59-67.
Ambasht, R., Sillanpa, M., 2010. Water purification using magnetic assistance: a review. J. Hazard Mater 180, 38-49.
Anirudhan, T.S., Ramachandran, M., 2007. Surfactant-modified bentonite as adsor-bent for the removal of humic acid from wastewaters. Appl. Clay Sci. 35, 276-281.
Anirudhan, T.S., Ramachandran, M., 2015. Adsorptive removal of basic dyes from aqueous solutions by surfactant modified halloysite clay (organoclay): kinetic and competitive adsorption isotherm. Process Saf. Environ. Prot. 95, 215-225.
Auta, M., Hameed, B.H., 2012. Modified mesoporous clay adsorbent for adsorption isotherm and kinetics of methylene blue. Chem. Eng. J. 198-199, 219-227.
Auta, M., Hameed, B.H., 2013. Acid modified local clay beads as effective low-cost adsorbent for dynamic adsorption of methylene blue. J. Ind. Eng. Chem. 19, 1153-1161.
Auta, M., Hameed, B.H., 2014. Chitosan-clay composite as highly effective and low-cost adsorbent for batch and fixed-bed adsorption of methylene blue. Chem. Eng. J. 237, 352-361.
Aroguz, A.Z., Gulen, J., Evers, R.H., 2008. Adsorption of methylene blue from aqueous solution on pyrolyzed petrified sediment. Bioresour. Technol. 99, 1503-1508.
Artioli, Y., 2008. Adsorption. In: Erik, Sven, Brian, F. (Eds.), Encyclopedia of Ecology. Academic Press, Oxford, pp. 60-65.
Avena, M.J., De Pauli, C.P., 1998. Proton adsorption and electrokinetics of an Argentinean montmorillonite. J. Colloid Interf. Sci. 202, 195-204.
Baskaralingam, P., Pulikesi, M., Elango, D., Ramamurthi, V., Sivanesan, S., 2006. Adsorption of acid dye onto organobentonite. J. Hazard Mater 128, 138-144.
Babarinde, A., Onyiaocha, G.O., 2016. Equilibrium sorption of divalent metal ions onto groundnut (Arachis hypogaea) shell: kinetics, isotherm and thermody-namics. Chem. Int. 2, 37-46.
Balik, O.Y., Aydin, S., 2016. Coagulation/flocculation optimization and sludge pro-duction for pre-treatment of paint industry wastewater. Desalination Water Treat. 57, 12692-12699.
Bayramoglu, G., Altintas, B., Arica, M.Y., 2009. Adsorption kinetics and thermody-namic parameters of cationic dyes from aqueous solutions by using a new strong cation-exchange resin. Chem. Eng. J. 152, 339.
Benefield, D., Larry, D., Judkins, Joseph F., Barron, L., 1982. Process Chemistry for Water and Wastewater Treatment. Prentice hall, Englewood cliffs, New Jersey.
Bilal, N., Ali, S., Iqbal, M., 2014. Application of advanced oxidations processes for the treatments of textile effluents. Asian J. Chem. 26, 1882-1886.
Bhattacharyya, R., Kumar-Ray, S., 2015. Removal of Congo red and methyl violet from water using nano clay filled composite hydrogels of poly acrylic acid and polyethylene glycol. Chem. Eng. J. 260, 269-283.
Bohor, B.F., Randall, H.E., 1970. Scanning Electron Microscopy of Clays and Clay Minerals. Illinois State Geological Survey, Natural Resources Building, Urbana, Ill. 61801.
Boyd, S.A., Mortland, M.M., Chiou, C.T., 1998. Sorption characteristic of organic compounds on hexadecyltrimethylammonium-smectite. Soil Sci. Soc. Am. J. 52, 652-657.
Buthelezi, S.P., Olaniran, A.O., Pillay, B., 2012. Textile dye removal from wastewater effluents using bioflocculants produced by indigenous bacterial isolates. Mol-ecules 17, 14260-14274.
Bujdak, J., Komadel, R., 1997. Interaction of methylene blue with reduced charge montmorillonite. J. Phys. Chem. B 101, 9065-9068.
Bujdak, J., Chorvat, D., Iyi, N., 2010. Resonance energy transfer between rhodamine molecules adsorbed on layered silicate particles. J. Phys. Chem. C 114, 1246-1252.
Cadena, F., Rizvi, R., Peters, R.W., 1990. Feasibility studies for the removal of heavy metals from solution using tailored bentonite. In: Hazardous and Industrial Wastes Twenty-second Mid-Atlantic Industrial Waste Conference. Drexel University.
Cai, D.Q., Zhang, H., Tang, Y., Chu, P.K., Yu, Z.L., Wu, Z.Y., 2010. Nano-networks have better adsorption capability than nano-rods. Nano Commun. Netw. 1, 257-263.
Ceyhan, O., Baybas, D., 2001. Adsorption of some textile dyes by hexadecyl-trimethylammonium bentonite. Turk J. Chem. 25, 193-200.
Chaari, I., Moussi, B., Jamoussi, F., 2015. Interactions of the dye, C.I. direct orange 34 with natural clay. J. Alloys Compd. 647, 720-727.
Chapman, A.C., Siebold, A., 1912. On the application of adsorption to the detection and separation of certain dyes. Analyst 37, 339-345.
Chatterjee, S., Lee, D.S., Lee, M.W., Woo, S.H., 2009. Congo red adsorption from aqueous solutions by using chitosan hydrogel beads impregnated with nonionic or anionic surfactants. Bioresour. Technol. 100, 3862-3868.
Cheknane, B., Bouras, O., Baudu, M., Basly, J.P., Cherguielaine, A., 2010. Granular inorganoeorgano pillared clays (GIOCs): preparation by wet granulation, characterization and application to the removal of a Basic dye (BY28) from aqueous solutions. Chem. Eng. J. 158, 528-534.
Cheknane, B., Baudu, M., Basly, J., Bouras, O., Zermane, F., 2012. Modeling of basic green 4 dynamic sorption ono granular organoeinorgano pillared clays (GOICs) in column reactor. Chem. Eng. J. 209, 7-12.
Chen, D., Chen, J., Luan, X., Ji, H., Xia, Z., 2011. Characterization of anionecationic surfactants modified montmorillonite and its application for the removal of methyl orange. Chem. Eng. J. 171, 1150-1158.
Chen, D.M., Chen, J., Wang, X.M., Luan, X.L., Ji, H.P., Xu, F., 2011a. Adsorption of methylene blue from aqueous solution by anionic surfactant modifiedmontmorillonite. Adv. Mater. Res. 178, 29-34.

Chen, H., Zhao, J., Zhan, A.G., Jin, Y.X., 2011b. Removal capacity and adsorption mechanism of heat-treated palygorskite clay for methylene blue. Chem. Eng. J. 174, 143-150.
Chen, D., Chen, J., Luan, X., Zhiguo, X., 2016. Characterization of anionecationic surfactants modified montmorillonite and its application for the removal of methyl orange. Chem. Eng. J. 171 (3), 1150-1158.
Chinoune, K., Bentale, K., Bouberka, Z., Nadim, A., Maschke, U., 2016. Adsorption of reactive dyes from aqueous solution by dirty bentonite. Appl. Clay Sci. 123, 64-75.
Chollom, M.N., 2014. Treatment and Reuse of Reactive Dye Effluent from Textile Industry Using Membrane Technology. A thesis submitted in fulfilment of the academic requirements for the degree of Master of Technology in Engineering Durban University of Technology.
Chowdhury, A.K., Sarkar, A.D., Bandyopadhyay, A., 2009. Rice husk ash as a low cost adsorbent for the removal of methylene blue and Congo red in aqueous phases. Clean Soil Air Water 37, 581-591.
Crini, G., 2006. Non-conventional low-cost adsorbents for dye removal: a review.
Bioresour. Technol. 97, 1061-1085.
Daneshvar, N., Oladegaragoze, A., Djafarzadeh, N., 2006. Decolourization of basic dye solutions by electrocoagulation: an investigation of the effect of operational parameters. J. Hazard Mater 129, 116-122.
Dave, S., Dave, V., Tipre, D., 2012. Coconut husk as a biosorbent for methylene blue removal and its kinetics study. Adv. Environ. Res. 1, 223-236.
Dawood, S., Sen, T., 2014. Review on dye removal from its aqueous solution into alternative cost effective and non-conventional adsorbents. J. Chem. Process Eng. 1, 104.
Diaz, F.R., Santos, P., 2010. Studies on the acid activation of Brazilian smectitic clay.
Quim. Nova 24, 345-353.
Dogan, M., Karaoglu, M.H., Alkan, M., 2009. Adsorption kinetics of maxilon yellow 4GL and maxilon red GRL dyes on kaolinite. J. Hazard. Mater 165, 1142-1151.
Drouiche, N., Aoudj, S., Hecini, M., Ouslimane, T., 2011. Experimental design for the elimination of fluoride from pretreated photovoltaic wastewater by electro-coagulation. Chem. Eng. Trans. 24, 1207-1212.
Elass, K., Laachach, A., Alaoui, A., Azzi, M., 2011. Removal of methyl violet from aqueous solution using a stevensite-rich clay from Morocco. Appl. Clay Sci. 54, 90-96.
Elmoubarki, R., Mahjoubi, F.Z., Tounsadi, H., Moustadraf, J., Abdennouri, M., Zouhri, A., ElAlban, A., Barka, N., 2015. Adsorption of textile dyes on raw and decanted Moroccan clays: kinetics, equilibrium and thermodynamics. Water Resour. Industry 9, 16-29.
El-Zahhar, A.A., Awwad, N.S., El-Katori, E.E., 2014. Removal of bromophenol blue dye from industrial waste water by synthesizing polymer-clay composite. J. Mol. Liq. 199, 454-461.
Errais, E., Duplay, J., Elhabiri, M., Khodja, M., Ocampo, R., 2012. Anionic RR120 dye adsorption onto raw clay: surface properties and adsorption mechanism. Col-loids Surf. A Physicochem. Eng. Asp. 403, 69-78.
Eren, E., 2010. Adsorption performance and mechanism in binding of azo dye by raw bentonite. Clean Soil Air Water 38, 758-763.
Espantaleon, A.G., Nieto, J.A., Fernandez, M., Marsal, A., 2003. Use of activated clays in the removal of dyes and surfactants from tannery waste waters. Appl. Clay Sci. 24, 105-110, 69, 310-314.
Fan, L., Zhang, Y., Luo, C., Lu, F., Qiu, H., Sun, M., 2012. Synthesis and characterization of magnetic -cyclodextrin-chitosan nanoparticles as nano-adsorbents for removal of methyl blue. Int. J. Biol. Macromol. 50, 444-450.
Fayazi, M., Afzali, D., Taher, M.A., Mostafavi, A., Gupta, V.K., 2015. Removal of Safranin dye from aqueous solution using magnetic mesoporous clay: optimi-zation study. J. Mol. Liq. 212, 675-685.
Fil, B.A., Yilmaz, M.T., Bayar, S., Elkoca, M.T., 2014. Investigation of adsorption of the dyestuff astrazon red violet 3rn (basic violet 16) on montmorillonite clay. Braz.
Chem. Eng. 31 (1). http://dx.doi.org/10.1590/S0104-66322014000100016. Fosso-Kankeu, E., Waanders, F., Fraser, C., 2014. Bentonite clay adsorption affinity for anionic and cationic dyes. In: 6th Int'l Conf. on Green Technology, Renew-able Energy & Environmental Engg. Cape Town (SA).
Frini-Srasra, N., Srasra, E., 2009. Adsorption of quinalizarin from non-aqueous so-lution onto acid activated palygorskite. Surf. Eng. Appl. Electrochem 45, 306-311.
Gao, Q., Luo, J., Wang, X., 2015. Novel hollow a-Fe_2O_3 nanofibers via electrospinning for dye adsorption. Nanoscale Res. Lett. 10, 1-8.
Ge, F., Ye, H., Li, M.M., Zhao, B.X., 2012. Efficient removal of cationic dyes from aqueous solution by polymer-modified magnetic nanoparticles. Chem. Eng. J. 198e199, 11-17.
Ghaedi, M., Hossainian, H., Montazerozohori, M., Shokrollahi, A., Shojaipour, F., Soylak, M., Purkait, M.K., 2011. A novel acorn based adsorbent for the removal of brilliant green.
Desalination 281, 226-233.
Ghosh, R.K., Reddy, D.D., 2014. Crop residue ashes as adsorbents for basic dye (methylene blue) removal: adsorption kinetics and dynamics. Clean. Soil Air Water 42 (8), 1098-1105.
Giakisikli, G., Anthemidis, A., 2013. Magnetic materials as sorbents for metal/ metalloid preconcentration and/or separation: a review. Anal. Chim. Acta 789, 1-16.
Gomes, R.F., de Azevedo, A.C.N., Pereira, A.G.B., Muniz, E.C., Fajardo, A.R., Rodrigues, F.H.A., 2015. Fast dye removal from water by starch-based nano-composites. J. Colloid Interface Sci. 454, 200-209.
Greenwood, R., Kendall, K., 1999. Selection of suitable dispersants for aqueoussuspensions of Zirconia and Titania powders using acoustophoresis. J. Eur. Ceram. Soc. 19 (4), 479-488.
Grim, R.E., 1962. Applied Clay Mineralogy. McGraw-Hill, New York.
Gupta, V.K., Kumar, R., Nayak, A., Saleh, T.A., Barakat, M.A., 2013. Adsorptive removal of dyes from aqueous solution onto carbon nanotubes: a review. Adv. Colloid Interface Sci. 193, 24-34.
Hai, Y., Li, X., Wu, H., Zhao, S., Deligeer, W., Asuha, S., 2015. Modification of acid-activated kaolinite with TiO_2 and its use for the removal of azo dyes. Appl. Clay Sci. 114, 558-567.
Hajjaji, W., Pullar, R.C., Labrincha, J.A., Rocha, F., 2016. Aqueous Acid Orange 7 dye removal by clay and red mud mixes. Appl. Clay Sci. 126, 197-206.
Hao, Y., Yan, L., Yu, H., Yang, K., Yu, S., Shan, R., Du, B., 2014. Comparative study on adsorption of basic and acid dyes by hydroxy-aluminum pillared bentonite. J. Mol. Liq. 199, 202-207.
Han, Z.X., Zhu, Z., Wu, D.D., Wu, J., Liu, Y.R., 2014. Adsorption kinetics and ther-modynamics of acid blue 25 and methylene blue dye solutions on natural sepiolite. Synth. React. Inorg. Met. 44, 140-147.
Hanaor, D.A.H., Michelazzi, M., Leonelli, C., Sorrell, C.C., 2012. The effects of car-boxylic acids on the aqueous dispersion and electrophoretic deposition of ZrO_2. J. Eur. Ceram. Soc. 32 (1), 235-244.
Hameed, B.H., Ahmad, A.A., Aziz, N., 2007. Isotherms, kinetics and thermodynamics of acid dye adsorption on activated palm ash. Chem. Eng. J. 133, 195-203.
Hassani, A., Khataee, A., Karaca, S., Karaca, S., Kırans¸ ana, M., 2015. Adsorption of two cationic textile dyes from water with modified nanoclay: a comparative study by using central composite design. J. Environ. Chem. Eng. 3, 2738-2749.
Hashem, F.S., 2013. Removal of methylene blue by magnetite covered bentonite nano-composite. Eur. Chem. Bull. 2 (8), 524-529.
Hashemian, S., 2010. $MnFe_2O_4$/bentonite nano composite as a novel magnetic material for adsorption of acid red 138. Afr. J. Biotech. 9 (50), 8667-8671.
Heinz, R.A., Vaia, R., Krishnamoorti, B.L., 2007. Farmer, Self-assembly of alky-lammonium chains on montmorillonite: effect of chain length, head group structure, and cation exchange capacity. Chem. Mater 19, 59-68.
Hosseinzadeh, H., Zoroufi, S., Mahdavinia, G.R., 2015. Study on adsorption of cationic dye on novel kappa-carrageenan/poly(vinyl alcohol)/montmorillonite nanocomposite hydrogels. Polym. Bull. 72, 1339e1363. http://dx.doi.org/ 10.1007/s00289-015-1340-5.
Huang, R., Wang, B., Yang, B., Zheng, D., Zhang, Z., 2011. Equilibrium, kinetic and thermodynamic studies of adsorption of Cd (II) from aqueous solution onto HACC-bentonite. Desalination 280, 297-304.
Hunger, K., 2003. Industrial Dyes, Chemistry, Properties, Applications. KGaA, WILEY-VCH Verlag GmbH & Co, Weinheim.
Iqbal, M., Ahmad, I., Bhatti, I.A., 2014. Re-utilization option of industrial wastewater treated by advanced oxidation process. Pak. J. Agri. Sci 51 (4), 1041-1047.
Izuagie, A.A., Gitari, W.M., Gumbo, J.R., 2016. Synthesis and performance evaluation of Al/Fe oxide coated diatomaceous earth in groundwater defluoridation: to-wards fluorosis mitigation. J. Environ. Sci. Health Part A 1-15.
Jaafar, S.N.B., 2006. Adsorption Study e Dye Removal Using Clay. An honors thesis submitted to the University College of Engineering & Technology Malaysia.
Jamal, M.A., Muneer, M., Iqbal, M., 2015. Photo-degradation of monoazo dye blue 13 using advanced oxidation process. Chem. Int. 1, 12-16.
Javaid, M., Saleemi, A.R., Naveed, S., Zafar, M., Ramzan, N., 2011. Anaerobic treatment of desizing effluent in a mesophilic anaerobic packed bed reactor. JPIChE 39, 61-67.
Jovic-Jovicic, N., Milutinovic-Nikolic, A., Grzetic, I., Jovanovic, D., 2008. Organo-bentonite as efficient textile dye sorbent. Chem. Eng. Technol. 31, 567-574.
Kalibantonga, P.D., 2004. Adsorption of Heavy Metals from Solution by South Af-rican Industrial Clay. A thesis submitted at Tshwane University of Technology.
Kamal, H., El-Sayed, A., Sabaa, M.W., Maher, El-Dessouky M., Mohamed, M.M., 2014. Adsorption properties of PVA/PAA/clay composite hydrogel synthesized by Gamma radiation and its application in removal of crystal violet dye from its aqueous solution. J. Nucl. Tech. Appl. Sci. 2 (5), 523-537.
Kant, R., 2012. Adsorption of dye eosin from an aqueous solution on two different samples of activated carbon by static batch method. J. Water Resour. Prot. 4, 93-98.
Kavitha, D., Namasivayam, C., 2007. Experimental and kinetic studies on methylene blue adsorption by coir pith carbon.Bioresour. Technol 98, 14-21.
Khan, T., Khan, E., Shahjahan, 2015. Removal of basic dyes from aqueous solution by adsorption onto binary iron-manganese oxide coated kaolinite: non-linear isotherm and kinetics modeling. Appl. Clay Sci. 107, 70-77.
Khorramabadi, G.S., Soltani, R.D.C., Rezaee, A., Khataee, A.R., Jafari, A.J., 2012. Uti-lisation of immobilised activated sludge for the biosorption of chromium (VI). Can. J. Chem. Eng. 90, 1539.
Kismir, Y., Aroguz, A.Z., 2011. Adsorptio characteristics of the hazardous dye Bril-liant Green on Saklıkent mud. Chem. Eng. J. 172, 199-206.
Kobya, M., Bayramoglu, M., Eyvaz, M., 2007. Techno-economical evaluation of electrocoagulation for the textile wastewater using different electrode con-nections. J. Hazard Mater 148, 311-318.
Kono, H., 2015. Preparation and characterization of amphoteric cellulose hydrogels as adsorbents for the anionic dyes in aqueous solutions. Gels 1, 94-116.
Lazarevic, S., Jankovic-Castvan, I., Jovanovic, D., Milonjic, S., Janackovic, D., Petrovi, R., 2007. Adsorption of Pb^{2+}, Cd^{2+}, and Sr^{2+} ions onto natural and acid-activated sepiolites. Appl. Clay Sci. 37, 47–57.
Lazarević, I., Janković-Častvan, V., Djokić, Z., Radovanović, D., Janaćković, R., Petrović, J., 2010. Iron-modified sepiolite for Ni^{2+} sorption from aqueous solution: an equilibrium, kinetic, and thermodynamic study. Chem. Eng. Data. 55, 5681–5689.

Li, Q., Yue, Q.Y., Sun, H.J., Su, Y., Gao, B.Y., 2010. A comparative study on the prop-erties, mechanisms and process designs for the adsorption of non-ionic or anionic dyes onto cationic-polymer/bentonite. J. Environ. Manag. 91, 1601-1611.
Li, M., Yao, J., Lin, B., Yang, X., Zhang, L., Lei, L., 2013. Pentachlorophenol sorption in the cetyltrimethylammonium bromide/bentonite one-step process in single and multiple solute systems. J. Chem. Eng. Data 58, 2610-2615.
Liu, P., Zhang, L., 2007. Adsorption of dyes from aqueous solutions of suspensions with clay nano-adsorbents. Sep. Purif. Technol. 58, 32-39.
Li, Z., Chang, P., Jiang, W., Jean, J., Honga, H., 2011. Mechanism of methylene blue removal from water by swelling clays. Chem. Eng. J. 168, 1193-1200.
Li, C., Huang, B., Li, C., Chen, X., Huang, Y., 2016. In situ formation of nanoscale zero-value iron on fish-scale-based porous carbon for Cr(VI) adsorption. Water Sci. Technol. 74 (11) http://dx.doi.org/10.2166/wst.2016.077.
Liu, M., Li, W., Rong, J., et al., 2012. Novel polymer nanocomposite hydrogel with natural clay nanotubes. Colloid Polym. Sci. 290, 895. http://dx.doi.org/10.1007/ s00396-012-2588-z.
Lian, L., Guo, L., Guo, C., 2009. Adsorption of Congo red from aqueous solution on Cabentonite. J. Hazard. Mater 161, 126-131.
Liang, X., Xu, Y., Tan, X., Wang, L., Sun, Y., Lin, D., Sun, Y., Qin, X., Wang, Q., 2013. Heavy metal adsorbents mercapto and amino functionalized palygorskite: preparation and characterization. Colloids Surf. A 426, 98-105.
Liu, H., Chen, W., Liu, C., Liu, Y., Dong, C., 2014. Magnetic mesoporous clay adsor-bent: preparation, characterization and adsorption capacity for antrazine. Microporous Mesoporous Mater 194, 72-78.
Liu, Y., Wang, W.B., Wang, A.Q., 2012. Effect of dry grinding on the microstructure of palygorskite and adsorption efficiency for methylene blue. Powder Technol. 225, 124-129.
Lv, G., Li, Z., Jiang, W., Chang, P., Jean, J., Lin, K., 2011. Mechanism of acridine orange removal from water by low-charge swelling clays. Chem. Eng. J. 174, 603-611.
Ma, A., Youssef, A.M., Al-Awadhi, M.M., 2013. Adsorption of acid dyes onto bentonite and surfactant-modified bentonite. J. Anal. Bioanal. Tech. 4, 174. http://dx.doi.org/10.4172/2155-9872.1000174.
Ma, J., Jia, Y., Jing, Y., Yao, Y., Sun, J., 2012. Kinetics and thermodynamics of meth-ylene blue adsorption by cobalt-hectorite composite. Dyes Pigm. 93, 1441-1446.
Mahdavinia, G.R., Aghaie, H., Sheykhloie, H., Vardini, M.T., Etemadi, H., 2013. Syn-thesis of CarAlg/MMt nanocomposite hydrogels and adsorption of cationic crystal violet. Carbohydr. Polym. 98, 358-365.
Mahdavinia, G.R., Asgari, A., 2013. Synthesis of kappa-carrageenan-g-poly(-acrylamide)/sepiolite nanocomposite hydrogels and adsorption of cationic dye. Polym. Bull. 70, 2451. http://dx.doi.org/10.1007/s00289-013-0966-4.
Mahdavinia, G.R., Karami, S., 2015. Synthesis of magnetic carboxymethyl chitosan-gpoly(acrylamide)/laponite RD nanocomposites with enhanced dye adsorption capacity. Polym. Bull. 72, 2241-2262. http://dx.doi.org/10.1007/s00289-015-1402-8.
Mahdavinia, G.R., Massoumi, B., Jalili, K., Kiani, G., 2012a. Effect of sodium mont-morillonite nanoclay on the water absorbency and cationic dye removal of carrageenan-based nanocomposite superabsorbents. J. Polym. Res. 19, 9947. http://dx.doi.org/10.1007/s10965-012-9947-9.
Mahdavinia, G.R., Massoudi, A., Baghban, A., et al., 2012b. Novel carrageenan-based hydrogel nanocomposites containing laponite RD and their application to remove cationic dye. Iran Polym. J. 21, 609. http://dx.doi.org/10.1007/s13726-012-0066-6.
Mahdavinia, G.R., Zhale, R., Baghy, R., 2012c. Removal kinetic of cationic dye using poly (sodium acrylate)-carrageenan/Na-montmorillonite nanocomposite su-perabsorbents. J. Mater. Environ. Sci 3 (5), 895-906.
Mahdavinia, G.R., Rahmani, Z., Mosallanezhad, A., Karami, S., Shahriari, M., 2016. Effect of magnetic laponite RD on swelling and dye adsorption behaviors of k-carrageenan-based nanocomposite hydrogels. Desal. Water Treat. 57 (43), 20582-20596. http://dx.doi.org/10.1080/19443994.2015.1111808.
Makarchuk, O.V., Dontsova, T.A., Astrelin, I.M., 2016. Magnetic nanocomposites as efficient sorption materials for removing dyes from aqueous solutions. Nano-scale Res. Lett. 11 (161) http://dx.doi.org/10.1186/s11671-016-1364-2.
Makhoukhi, B., Djab, M., Didi, M.A., 2015. Adsorption of Telon dyes onto bis-imidazolium modified bentonite in aqueous solutions. J. Environ. Chem. Eng. 3, 1384-1392.
Mane, V.S., Babu, P.V.V., 2011. Studies on the adsorption of Brilliant Green dye from aqueous solution onto low-cost NaOH treated saw dust. Desalination 273, 321-329.
Masindi, V., Gitari, W.M., Ngulube, T., 2014. Defluoridation of drinking water using Al^{3+} - modified bentonite clay: optimization of fluoride adsorption conditions. Toxicol. Environ. Chem. 96 (9), 1294-1309.
Masindi, V., Gitari, W.M., Ngulube, T., 2015. Kinetics and equilibrium studies for removal of fluoride from underground water using cryptocrystalline magnesite. J. Water Reuse Desal. 1, 282-292.
Mekatel, E., Amokrane, S., Aid, A., Nibou, D., Trari, M., 2015. Adsorption of methyl orange on nanoparticles of a synthetic zeolite NaA/CuO. C. R. Chim. 18, 336-344.
Mermut, A.R., 1994. Layer charge characteristics of 2:1 silicate clay minerals. In: CMS Workshop Lectures, vol. 6. The Clay Minerals Society, Boulder, CO.
Merzouk, B., Yakoubi, M., Zongo, I., Leclerc, J.P., Paternotte, G., Pontvianne, S., et al., 2011. Effect of modification of textile wastewater composition on electro-coagulation efficiency. Desalination 275, 181-186.
Mitchell, J.K., 1993. Fundamentals of Soil Behaviour, second ed. Wiley, New York, pp. 405-445.
Miyamoto, N., Kawai, R., Kuroda, K., Ogawa, M., 2000. Adsorption and aggregation of a cationic cyanine dye on layered clay minerals. Appl. Clay Sci. 16, 161-170.
Mohan, D., Singh, K.P., Singh, G., Kumar, K., 2007. Removal of dyes from wastewater using flyash, a low-cost adsorbent. Ind. Eng. Chem. Res. 41, 3688-3695.
Moore, D.M., Reynolds, R.C., 1997. X-ray Diffraction and the Identification and Analysis of Clay Minerals. Oxford University Press, New York, NY.
Mu, B., Wang, A., 2016. Adsorption of dyes onto palygorskite and its composites: a review. J. Environ. Chem. Eng. 4, 1274-1294.
Mudzielwana, R., Gitari, W.M., Msagati, T.A.M., 2016. Characterization of smectite rich clay soils: implication for groundwater defluoridation. South Afr. J. Sci. 112 (11/12), 1-8.
Nandi, B.K., Goswami, A., Purkait, M.K., 2009. Adsorption characteristics of brilliant green dye on kaolin. J. Hazard. Mater 161, 387-395.
Ogunmodede, O.T., Ojo, A.A., Adewole, E., Adebayo, O.L., 2015. Adsorptive removal of anionic dye from aqueous solutions by mixture of Kaolin and Bentonite clay: characteristics, isotherm, kinetic and thermodynamic studies. Iran. J. Energy Environ. 6 (2), 147-153.
Oremusova, J., 2007. Manual for laboratory practice in physical chemistry for stu-dents of pharmacy. Department of Physical Chemistry, Faculty of Pharmacy, Comenius University, Bratislava, in Slovak.
Ozcan, A.S., Erdem, B., Ozcan, A., 2004. Adsorption of acid blue 193 from aqueous solutions onto Na-bentonite and DTMA-bentonite. J. Colloid Interface Sci. 280, 44-54.
Özcan, A.S., Özcan, A., 2004. Adsorption of acid dyes from aqueous solutions onto acid activated bentonite. J. Colloid Interface Sci. 276, 39-46.
Özcan, A.S., Erdem, B., Özcan, A., 2005. Adsorption of Acid Blue 193 from aqueous solutions onto BTMAebentonite. Colloids Surf. A Physicochem. Eng. Asp. 266, 73-81.
Ozcan, A., Omeroglu, C., Erdogan, Y., Ozcan, A.S., 2007. Modification of bentonite with a cationic surfactant: an adsorption study of textile dye Reactive Blue 19. J. Hazard. Mater 140, 173-179.
Pajootan, E., Arami, M., Mohammad, N., 2012. Binary system dye removal by elec-trocoagulation from synthetic and real coloured wastewaters. J. Taiwan Inst. Chem. Eng. 43, 282-290.
Peng, X., Luan, Z., Zhang, H., 2006. Montmorillonite-Cu(II)/Fe(III) oxides magnetic material as adsorbent for removal of humic acid and its thermal regeneration. Chemosphere 63, 300-306.
Peng, L., Qin, P., Lei, M., Zeng, Q., Song, H., Yang, J., Shao, J., Liao, B., Gu, J., 2012. ModifyingFe3O4 nanoparticles with humic acid for removal of Rhodamine B in water. J. Hazard. Mater 209e210, 193-198.
Peng, Y.G., Chen, D.J., Ji, J.L., Kong, Y., Wan, H.X., Yao, C., 2013. Chitosan-modified palygorskite: preparation, characterization and reactive dye removal. Appl. Clay Sci. 74, 81e86.
Pinnavaia, T., 1983. Intercalated clay catalysts. J. Sci. 220 (4595), 365-371.
Qureshi, K., Ahmad, M.Z., Bhatti, I.A., Iqbal, M., Khan, A., 2015. Cytotoxicity reduction of wastewater treated by advanced oxidation process. Chem. Int. 1, 53-59.
Rafatullah, M., Sulaiman, O., Hashim, R., Ahmad, A., 2010. Adsorption of methylene blue on low-cost adsorbents: a review. J. Hazard Mater 177 (1-3), 70-80.
Rehman, M.S.U., Munira, M., Ashfaqa, M., Rashid, N., Nazar, M.F., et al., 2013. Adsorption of Brilliant Green dye from aqueous solution onto red clay. Chem. Eng. J. 228, 54-62.
Reza-Mahdavinia, G., Aghaie, H., Sheykhloie, H., Vardini, M.T., Etemadi, H., 2013. Synthesis of CarAlg/MMt nanocomposite hydrogels and adsorption of cationic crystal violet. Carbohydr. Polym. 98, 358-365.
Robinson, T., McMullen, G., Marchant, R., Nigam, P., 2001. Remediation of dyes in textile effluent: a critical review on current treatment technologies with a proposed alternative. Bioresour. Technol. 77, 247-255.
Roulia, M., Vassiliadis, A.A., 2008. Sorption characterization of a cationic dye retained by clays and perlite. Micropor. Mesopor. Mater. 116 (1-3), 732e740.
Sabah, E., Mart, U., Çınar, M., Çelik, M.S., 2007. Zeta potentials of sepiolite suspen-sions in concentrated monovalent electrolytes. Sep. Sci. Technol. 42, 2275-2288.
Safa, Y., Bhatti, H.N., 2011. Kinetic and thermodynamic modeling for the removal of Direct Red-31 and Direct Orange-26 dyes from aqueous solutions by rice husk. Desalination 272, 313-322.
Saha, B., Das, S., Saikia, J., Das, G., 2011. Preferential and enhanced adsorption of different dyes on iron oxide nanoparticles: a comparative study. J. Phys. Chem. C 115, 8024-8033.
Santos, S.C.R., Boaventura, R.A.R., 2016. Adsorption of cationic and anionic azo dyes on sepiolite clay: equilibrium and kinetic studies in batch mode. J. Environ. Chem. Eng. 4, 1473-1483.
Santos, S.C.R., Oliveira, A.F.M., Boaventura, R.A.R., 2016. Bentonitic clay as adsorbent for the decolourisation of dyehouse effluents. J. Clean. Prod. 126, 667-676.
Sarkar, B., Xi, Y.F., Megharaj, M., Naidu, R., 2011. Orange II adsorption on paly-gorskites modified with alkyl trimethylammonium and dialkyl dimethy-lammonium bromide - an isothermal and kinetic study. Appl. Clay Sci. 51, 370-374.
Sarma, G.K., Gupta, S.S., Bhattacharyya, K.G., 2016. Adsorption of Crystal violet on raw and acid-treated montmorillonite, K10, in aqueous suspension. J. Environ. Manag. 171, 1-10.
Savic, I., Gajic, D., Stojiljkovic, S., Savic, I., di Gennaro, S., 2014. Modeming and optimization of methylene blue adsorption from aqueous solution using bentonite clay. Comput. Aided Chem. Eng. 33, 1417-1422.
Schacht, E.H., 2004. Polymer chemistry and hydrogel system. Phys. Conf. Ser. J. 3, 22

Shamraiz, U., Hussain, R.A., Badshah, A., Raza, B., Sab, S., 2016. Functional metal sulfides and selenides for the removal of hazardous dyes from water. J. Photochem. Photobiol. B Biol. 159, 33-41.
Shichi, T., Takaqi, K., 2000. Clay minerals as photochemical reaction fields. J. Photochem. Photobiol. C. Photochem. Rev. 1, 113-130.
Shirsath, S.R., Patil, A.P., Patil, R., Naik, J.B., Gogate, P.R., Sonawane, S.H., 2013. Removal of Brilliant Green from wastewater using conventional and ultrason-ically prepared poly (acrylic acid) hydrogel loaded with kaolin clay: a comparative study. Ultrason. Sonochem. 20, 914-923.
Shirsath, S.R., Hage, A.P., Zhou, M., Sonawane, S.H., Ashokkumar, M., 2011. Ultra-sound assisted preparation of nanoclay Bentonite-FeCo nanocomposites hybrid hydrogel: a potential responsive sorbent for removal of organic pollutant from water. Desalination 281, 429-437.
Shon, H., Phuntsho, S., Chaudhary, D., Vigneswaran, S., Cho, J., 2013. Nano filtration for water and wastewater treatment e a mini review. Drinking Water Eng Sci 6, 47-53.
Singh, S.A., Vemparala, B., Madras, G., 2015. Adsorption kinetics of dyes and their mixtures with Co_3O_4eZrO_2 composites. J. Environ. Chem. Eng. 3, 2684-2696.
Spark, K.M., Wells, J.D., Johnson, B.B., 1995. Characterizing trace metal adsorption on kaolinite. Eur. J. Soil Sci. 46, 633-640.
Srinivasan, R., 2011. Advances in application of natural clay and its composites in removal of biological, organic, and inorganic contaminants from drinking water. Adv. Mater. Sci. Eng., 872531
Srivastava, V., Sillanpää, M., 2016. Synthesis of malachite@ clay nanocomposite for rapid scavenging of cationic and anionic dyes from synthetic wastewater. J. Environ. Sci. http://dx.doi.org/10.1016/j.jes.2016.08.011.
Suraj, G., Iyer, C.S.P., Rugmini, S., Lalithambika, M., 1998. Adsorption of cadmium and copper by modified kaolinites. Appl. Clay Sci. 13, 293-306.
Tabak, A., Eren, E., Afsin, B., Caglar, B., 2009. Determination of adsorptive properties of a Turkish Sepiolite for removal of Reactive Blue 15 anionic dye from aqueous solutions. J. Hazard. Mater 161, 1087-1094.
Tahir, M.A., Bhatti, H.N., Iqbal, M., 2016. Solar Red and Brittle Blue direct dyes adsorption onto Eucalyptus angophoroides bark: equilibrium, kinetics and thermodynamic studies. J. Environ. Chem. Eng. 4, 2431-2439.
Tehrani-Bagha, A.R., Nickers, H., Mahmoodi, N.M., Markazi, M., Menger, F.M., 2011. The sorption of cationic dyes onto kaolin: kinetic, isotherm and thermodynamic studies. Desalination 266 (1), 274-280.
Tümsek, F., Avci, O., 2013. Investigation of kinetics and isotherm models for the acid orange 95 adsorption from aqueous solution onto natural minerals. J. Chem. Eng. Data 58, 551e559.
Tomar, V., Prasad, S., Kumar, D., 2014. Adsorptive removal of fluoride from aqueous media using citrus limonum (lemon) leaf. Microchem. J. 112, 97-103.
Toor, M., Jin, B., 2012. Adsorption characteristics, isotherm, kinetics, and diffusion of modified natural bentonite for removing diazo dye. Chem. Eng. J. 187, 79-88.
Uyar, G., Kaygusuz, F.H., Erim, B., 2016. Methylene blue removal by alginateeclay quasi-cryogel beads. React. Funct. Polym. 106, 1-7.
Vimonses, V., Lei, S., Jin, B., Chow, C.W.K., Saint, C., 2009. Kinetic study and equi-librium isotherm analysis of Congo red adsorption by clay materials. Chem. Eng. J. 148, 354-364.
Wang, W.B., Wang, F.F., Kang, Y.R., Wang, A.Q., 2015. Enhanced adsorptive removal of methylene blue from aqueous solution by alkali-activated palygorskite. Water Air Soil Pollut. 226, 83.
Wang, X., Huang, H., Li, G., 2014. Hydrothermal synthesis of 3D hollow porous Fe_3O_4 microspheres towards catalytic removal of organic pollutants. Nanoscale Res. Lett. 9, 1-5.
Wang, Y., Zeng, L., Ren, X., Song, H., Wang, A., 2010. Removal of Methyl Violet from aqueous solutions using poly (acrylic acid-co acrylamide)/attapulgite compos-ite. Environ. Sci. J. 22 (1), 7.
Watanabe, T., Miki, Y., Masuda, T., Kanai, H., Hosokawa, S., Wada, K., Inoue, M., 2011. Pore structure of c-Ga_2O_3-Al_2O_3 particles prepared by spray pyrolysis. Micro-por. Mesopor. Mater. 145, 131-140.
Weng, C.H., Lin, Y.T., Tzeng, T.W., 2009. Removal of methylene blue from aqueous solution by adsorption onto pineapple leaf powder. J. Hazard. Mater 170, 417-424.
Worch, E., 2012. Adsorption Technology in Water Treatment: Fundamentals, Pro-cesses and Modelling. Walter de Gruyter GmbH & Co. KG, Berlin/Boston.
Xu, P., Zeng, G., Huang, D., 2012. Use of iron oxide nanomaterials in wastewater treatment: a review. Sci. Total Environ. 424, 1-10.
Xue, A.L., Zhou, S.Y., Zhao, Y.J., Lu, X.P., Han, P.F., 2010. Adsorption of reactive dyes from aqueous solution by silylated palygorskite. Appl. Clay Sci. 48, 638-640.
Xue, A.L., Zhou, S.Y., Zhao, Y.J., Lu, X.P., Han, P.F., 2011. Effective NH2-grafting on attapulgite surfaces for adsorption of reactive dyes. J. Hazard. Mater 194, 7-14.
Yan, L., Qin, L., Yu, H., Li, S., Shan, R., Du, B., 2015. Adsorption of acid dyes from aqueous solution by CTMAB modified bentonite: kinetic and isotherm model-ling. J. Mol. Liq. 21, 1074-1081.
Yagub, M.T., Sen, T.K., Afroze, S., Ang, H.M., 2014. Dye and its removal from aqueous solution by adsorption: a review. Adv. Colloid Interface Sci. 209, 172-184.
Yousef, R.I., El-Eswed, B., Al-Muhtaseb, A.H., 2011. Adsorption characteristics of natural zeolites as solid adsorbents for phenol removal from aqueous solutions: kinetics, mechanism and thermodynamics studies. Chem. Eng. J. 171, 1143-1149.
Yu, X., Wei, C., Wu, H., 2015. Effect of molecular structure on the adsorption behavior of cationic dyes onto natural vermiculite. Sep. Purif. Technol. 156, 489-495.
Zhang, J., Cai, D.Q., Zhang, G.L., Cai, C.J., Zhang, C.L., Qiu, G.N., Zheng, K., Wu, Z.Y., 2013. Adsorption of methylene blue from aqueous solution onto multiparous palygorskite modified by ion beam bombardment: effect of contact time tem-perature, pH and ionic strength. Appl. Clay Sci. 83e84, 137-143.
Zhang, Y., Wang, W.B., Zhang, J.P., Liu, P., Wang, A.Q., 2015a. A comparative study about adsorption of natural palygorskite for methylene blue. Chem. Eng. J. 262, 390-398.
Zhang, Z.F., Wang, W.B., Wang, A.Q., 2015b. High-pressure homogenization associ-ated hydrothermal process of palygorskite for enhanced adsorption of methy-lene blue. Appl. Surf. Sci. 329, 306-314.
Zhang, Z.H., Zhu, H.J., Zhou, C.H., Wang, H., 2016. Geopolymer from kaolin in China: an overview. Appl. Clay Sci. 119, 31-41.
Zhao, Y., Abdullayev, E., Vasiliev, A., Lvov, Y., 2013. Halloysite nanotubule clay for efficient water purification. J. Colloid Interface Sci. 406, 121-129.
Zhou, K., Zhang, Q., Wang, B., Liu, J., Wen, P., Gui, Z., Hu, Y., 2014. The integrated utilization of typical clays in removal of organic dyes and polymer nano-composites. J. Clean. Prod. 81, 281-289.
Zhou, Z., Gunter, W.D., 1992. The nature of the surface charge of kaolinite. Clay Miner. 40, 365-368.
Zhu, L.Z., Chen, B.L., 2000. Sorption behavior of p-nitrophenol on the interface between anionecationic organobentonite and water. Environ. Sci. Technol. 34, 2997-3002.
Zollinger, H., 1987. "Fluorescent brighteners" in colour chemistry. VCH, Weinheim, pp. 203-213.
Zulfikar, M.A., 2013. Materials, Effect of temperature on adsorption of humic acid from peat water onto pyrophyllite. Int. J. Chem. Environ. Biol. Sci. 1, 88-91.

CHAPTER THREE

Application of calcined magnesite in the removal of dyes: A batch study

This chapter has been published as: Ngulube T., Gumbo J.R., Masindi V., Maity A., 2018. Calcined magnesite as an adsorbent for cationic and anionic dyes: Characterization, adsorption parameters, isotherms and kinetics study. Heliyon. 4(10), e00838. doi: 10.1016/j.heliyon. 2018.e00838.

This chapter addresses objectives (ii), (iii) and (v).

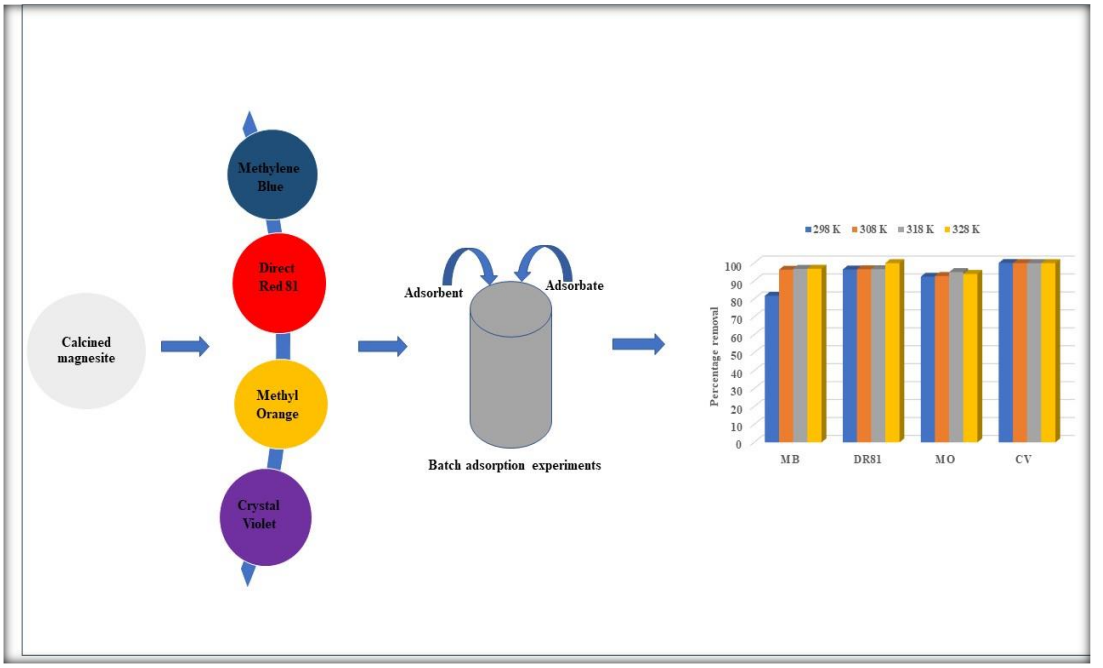

Heliyon

ELSEVIER

Received:
13 June 2018
Revised:
27 August 2018
Accepted:
27 September 2018

Cite as: T. Ngulube, J. R. Gumbo, V. Masindi, A. Maity. Calcined magnesite as an adsorbent for cationic and anionic dyes: characterization, adsorption parameters, isotherms and kinetics study. Heliyon 4 (2018) e00838. doi: 10.1016/j.heliyon.2018.e00838

Calcined magnesite as an adsorbent for cationic and anionic dyes: characterization, adsorption parameters, isotherms and kinetics study

T. Ngulube [a,*], J. R. Gumbo [b], V. Masindi [c,d], A. Maity [e,f]

[a] Department of Ecology and Resources Management, School of Environmental Sciences, University of Venda, Private bag X5050, Thohoyandou, 0950, Limpopo, South Africa

[b] Department of Hydrology and Water Resources, School of Environmental Sciences, University of Venda, Private bag X5050, Thohoyandou, 0950, Limpopo, South Africa

[c] Council for Scientific and Industrial Research (CSIR), Built Environment, Hydraulic Infrastructure Engineering, P.O BOX 395, Pretoria, 0001, South Africa

[d] Department of Environmental Sciences, School of Agriculture and Environmental Sciences, University of South Africa (UNISA), P. O. Box 392, Florida, 1710, South Africa

[e] Department of Applied Chemistry, University of Johannesburg, Johannesburg, South Africa

[f] DST/CSIR National Centre for Nanostructured Materials, Council for Scientific and Industrial Research (CSIR), Pretoria, South Africa

[*] Corresponding author.
E-mail address: tholisongulube@gmail.com (T. Ngulube).

Abstract

The ability of calcined magnesite for Methylene Blue (MB), Direct Red 81 (DR81), Methyl Orange (MO) and Crystal Violet (CV) dye removal was evaluated in this study. The experiments were designed to test the hypothesis that alkaline earth carbonates can remove dyes from water through a combination of sorption and coagulative reactions involving Mg^{2+}. To achieve that, several operational factors like residence time, dosage, adsorbate concentration and temperature were appraised. The batch study proved that calcined magnesite is effective in the treatment of MB, DR81, CV and MO contaminated water and moreover it

https://doi.org/10.1016/j.heliyon.2018.e00838

performed well in terms of colour removal. The adsorption equilibrium data were analysed by the Langmuir, Freundlich, Dubinin-Radushkevich and Temkin isotherm models, and the Dubinin-Radushkevich and Temkin models were found to be the most appropriate fit to MB and MO dyes respectively. The adsorption kinetics process primarily followed the Elovich and Pseudo-second order model, a possible indication that chemisorption was the rate limiting step during the dye uptake process. With the adsorption-desorption cycle repeated four times, the calcined magnesite regeneration efficiency for DR81 and MO loaded dyes remained very high. According to the results of this study, it can be concluded that calcined magnesite can be used effectively for the adsorption of MB, DR81, CV and MO from wastewater.

Keywords: Environmental science, Theoretical chemistry, Physical chemistry, Materials chemistry, Analytical chemistry

1. Introduction

Wastewater from numerous industries contain synthetic dyes from paper, textiles, leather and plastics (Ngulube et al., 2017). Wastewater that is discharged into natural canals and watercourses from dye manufacturing industries is a serious environmental threat (Yang et al., 2018). Even small amounts of dyes are capable of colouring huge volumes of water, thereby influencing the aesthetic value and decreasing light penetration needed for aquatic plant photosynthesis. Moreover, a lot of dyes are poisonous or carcinogenic (Uyar et al., 2016; Santos and Boaventura, 2016; Zhou et al., 2014). Hence, the elimination of dyes from wastewater is of great importance for environmental safeguard. Methods have been developed for dye removal in wastewater streams such as precipitation (Gupta et al., 2013), oxidation (Ghoreishi and Haghighi, 2003), adsorption (Gupta and Suhas, 2009), coagulation (Yagub et al., 2014) and membrane separation (Gupta and Suhas, 2009). Nonetheless, adsorption is recognized to be one of the effective techniques to treat waste-water (Ngulube et al., 2017). Activated carbon has been promoted as a good adsorbent due to its great sorption capacity for the dyes (Bello and Ahmad, 2012; Ozer et al., 2012; Malarvizhi and Ho, 2010). However, the high cost of activated carbon has led scientists to seek for low-cost adsorbents.

The removal of dyes by magnesium compounds has been proven to be a good alternative to the common adsorbents used in the treatment of industrial effluents (Bouyakoub et al., 2011), especially since conventional adsorbents like activated carbon and alum are not effective at pHs found in common wastewaters (Gao et al., 2007; Wang et al., 2009). However, the mechanisms by which dyes are responsive to removal by this kind of treatment have not been widely studied (Gao et al., 2007; Tan et al., 2000; Lee et al., 2006). Particularly, the adsorptive - coagulating mechanism that was originally proposed by Leentvaar

https://doi.org/10.1016/j.heliyon.2018.e00838

and Rebhun (1982), must be further established.

The aim of this study is then to offer some new understanding into the capability of calcined magnesite, to remove dyes from synthetic dye wastewater. The principal aim of this study was to determine its potential application in the removal of Direct Red 81 (DR81), Methylene Blue (MB), Methyl Orange (MO) and Crystal Violet (CV) from aqueous solution by employing physico-chemical processes of adsorption.

2. Experimental

2.1 Materials

Calcined magnesite used in this investigation was obtained from Folovhodwe Magnesite mine, South Africa. MB, MO and CV dyes were purchased from Rochelle chemicals, South Africa. DR81 was purchased from Sigma Aldrich, South Africa. MB, DR81, MO and CV have a maximum absorbency at wavelengths 664, 510, and 590 nm respectively. Their chemical formulas are $C_{16}H_{18}N_3ClS.xH_2O$, $C_{29}H_{19}N_2O_8S_2$, $C_{14}H_{14}N_3NaO_3S$ and $C_{25}N_3H_{30}Cl$ respectively. HCl, KCl and NaOH were also supplied by Rochelle Chemicals, South Africa.

2.2. Preparation and characterization of calcined magnesite

Calcined magnesite was milled to powder (particle size <50 μm) for 15 min at 1000 rpm by a stainless-steel vibratory ball mill (Retsch RS 200, Germany). The powdered material was kept in a zip-lock plastic bag for further use FTIR analysis of calcined magnesite before and after dye adsorption was done using a FTIR spectrometer (Bruker Alpha, Germany). The phase structure of calcined magnesite before and after dye adsorption was evaluated by a PANalytical X'Pert Pro powder diffractometer (PANalytical, Netherlands). The morphology of calcined magnesite was analyzed using a scanning electron microscope JEM - 2100 Electron Micro-scope (JEOL, USA). The solid addition method as explained by Izuagie et al. (2016) was used to carry out Point of Zero Charge (PZC). Thermal stability was analyzed by a thermo gravimetric analyzer (TGA Q500, TA instrument) under air atmosphere with a flow rate of 50 mL/min and a heating rate of 10 ^{o}C/min. The determination of surface area was done via Brunauer Emmett Teller (BET) analysis (Micromeritics Tristar II, Norcross, GA, USA).

2.3. Preparation of MB, DR81, MO and CV working solutions

The MB, DR81, CV and MO solutions were prepared by dissolving suitable amounts of dry dye powder accurately weighed on an electronic balance (RADWAG electronic balance, Wagi Elektroniczen, Poland) in deionized water

https://doi.org/10.1016/j.heliyon.2018.e00838

(ELGA, Micra Veolia Water Solution and Technologies, United Kingdom) to prepare a 1000 mg/ L stock solution. Solutions to be used during experiments were obtained by serial dilutions to get solutions at desired concentrations. The final concentration of MB, DR81, MO and CV were estimated for each sample absorbance at the wavelength corresponding to maximum absorption peak using a UV/VIS spectrophotometer (Thermoscientific Orion Aqua Matte 7000, China). A standard calibration curve, used for the transformation of absorbance information into concentrations for equilibrium studies, was plotted to calculate the dye concentration of the experiments.

The percentage removal was computed by Eq. (1):

$$Percentage\ removal = \left(\frac{C_o - C_e}{C_o}\right) \times 100 \quad (1)$$

The capacity of adsorption, Qe (mg/g) was obtained using Eq. (2):

$$Qe = \left(\frac{C_o - C_e}{m}\right) \times v \quad (2)$$

where Co and Ce are the initial and equilibrium dye concentrations in solution (mg/ L), v is the solution volume (L) and m is the weight (g) of dry adsorbent used.

2.4. Batch adsorption experiments

2.4.1. Adsorption of MB, DR81, MO and CV as a function of contact time

To evaluate the effect of contact time on MB, DR81, MO and CV the adsorption experiments were carried out by measuring 50 mL of 10 mg/L MB, DR81, MO and CV solutions into 250 mL glass Erlenmeyer flasks. Deionized water (ELGA, Micra Veolia Water Solution and Technologies, UK) was used to prepare all the synthetic dye solutions. A fixed quantity of adsorbent (1 g) was added to each flask and kept on a reciprocating table shaker (Labotec, Model 207, South Africa) then agitated for varying contact times (15, 30, 60, 90, 120, 180 min). After the equilibration time, the solutions were left to settle for 30 min and then the supernatant solution absorbance was recorded by a VIS spectrophotometer. The experiments were carried out in triplicate at room temperature (25 ^{o}C) and the mean values reported.

2.4.2. Adsorption of MB, DR81, MO and CV as a function of dosage

To evaluate the effect of adsorbent dosage on MB, DR81, MO and CV removal, 50 mL of 10 mg/L dye solution was measured into 18, 250 mL glass Erlenmeyer flasks and 0.1 g, 0.2 g, 0.4 g, 0.8 g, 1 g and 2 g of calcined magnesite were added to each flask.

https://doi.org/10.1016/j.heliyon.2018.e00838

The mixtures were then agitated at 250 rpm using a reciprocating shaker for 60 min. After the equilibration time, the solutions were left to settle for 30 min and then the supernatant solution absorbance was recorded by a VIS spectrophotometer.

2.4.3. Adsorption of MB, DR81, MO and CV as a function of dye concentration

To evaluate the effect of initial MB, DR81, MO and CV concentration on the removal capacity of calcined magnesite, samples of 50 mL of 1, 10, 15, 20, 25 and 30 mg/L MB, DR81, MO and CV solutions were measured into 18, 250 mL glass Erlenmeyer flasks and optimum dosages of calcined magnesite was added to each flask separately. The mixtures were then agitated for 60 min at 250 rpm using a reciprocating shaker. After the equilibration time, the solutions were left to settle for 30 min and then the supernatant solution absorbance was recorded by a VIS spectrophotometer.

2.4.4. Adsorption of MB, DR81, MO and CV as a function of temperature

To evaluate the effect of solution temperature on the removal capacity of calcined magnesite, samples of 50 mL of and optimum concentrations of MB, DR81, MO and CV solution were measured into 12, 250 mL glass Erlenmeyer flasks and optimum dosages of calcined magnesite were added to each flask separately. The mixtures were then agitated for 60 min at 250 rpm using the reciprocating water bath shaker set at specified temperatures (298, 308, 318, and 328 K) with each different 3 samples. After the equilibration time, the solutions were left to settle for 30 min and then the super-natant solution absorbance was recorded by a VIS spectrophotometer.

2.5. Adsorption isotherm studies

Analyzing equilibrium data assists in developing some mathematical models that are helpful in quantitatively describing results. When put together, the basic assumptions and equations of the equilibrium models give imperative data on the mechanisms of adsorption. The following models were used in this study.

2.5.1. The Langmuir isotherm model

The Langmuir isotherm has been widely used to discuss various adsorbate-adsorbent combinations for both liquid and gas phase adsorptions (Langmuir, 1918). The linear Langmuir isotherm may be represented by Eq. (3):

$$\frac{C_e}{q_e} = \left(\frac{1}{Q_m}\right) C_e + \frac{1}{Q_m b} \quad (3)$$

https://doi.org/10.1016/j.heliyon.2018.e00838

Where Ce is the equilibrium concentration (mg/L), qe is the amount adsorbed per mass of adsorbent at equilibrium (mg/g), b represents the Langmuir isotherm constant (L/mg) and Qm is the maximum adsorption capacity (mg/g) for a complete monolayer coverage.

The separation factor (R_L) Hall et al. (1966) was calculated from Eq. (4):

$$R_L = \frac{1}{(1 + bCo)} \tag{4}$$

The R_L value indicates the shape of the isotherm. R_L values between 0 and 1 indicate favorable adsorption, 0 indicates irreversible adsorption, 1 means linear adsorption while a value greater than 1 indicates an unfavorable adsorption.

2.5.2. The Freundlich isotherm model

The Freundlich model is an isotherm commonly used to describe heterogeneous systems (Freundlich, 1906). The model is represented in linear form by Eq. (5):

$$logQ_e = \frac{1}{n}\, log\, C_e + log\, K_F \tag{5}$$

K_F and 1/n are the Freundlich constants, describing the adsorption capacity and intensity respectively. The constants n and K_F are determined from the slope and the intercept of the plot log Q_e versus log C_e. When the value of n lies between 1 and 10 it represents beneficial adsorption (Aljeboree et al., 2017).

2.5.3. The Dubinin and Radushkevich isotherm model

Common isotherm Eqs. (6) and (7) used analyse the rectangularity degree of isotherms. Eq. (6) is the Dubinin Radushkevich as projected by Dubinin and Radushkevich (1947).

$$lnq_e = -K_{DR}\varepsilon^2 + ln\, q_{DR} \tag{6}$$

Where $\varepsilon = RT\, ln\left(1 + \frac{1}{C_e}\right)$ (7)

where q_{DR} (mg/g) is the adsorption capacity, K_{DR} $(mol^2/kJ^2)$is a constant related to the sorption energy (mol/k/J), ε is the Polanyi potential, T is the absolute temperature in Kelvin, R is the universal gas constant (8.314 J/mol/K).

E, which is the mean free energy of adsorption for each molecule of the adsorbate is calculated by Eq. (8)

$$E = \frac{1}{\sqrt{2K_{DR}}} \tag{8}$$

E (kJ/mol) is the mean adsorption energy indicative of the heat of adsorption, signifying a physical or a chemical adsorption process.

https://doi.org/10.1016/j.heliyon.2018.e00838

2.5.4. The Temkin isotherm model

The Temkin model as represented by Eqs. (9) and (10) was also applied in fitting the experimental data. The Temkin isotherm adopts that the adsorption heat on the surface declines linearly with the coverage adsorbate - adsorbent interaction (Temkin and Pyzhev, 1940). The Temkin adsorption isotherm linear form is given by Eq. (9):

$$q_e = \beta \ln \alpha + \beta \ln C_e \quad (9)$$

where $\beta = \frac{RT}{b}$ (10)

T is the absolute temperature in Kelvin, R is the universal gas constant (8.314 J/mol/ K), and b is the Temkin constant related to heat of adsorption (J/mol), β is Temkin constant related to maximum binding energy (J/mol) and α is the equilibrium binding constant (L/mg).

2.6. Kinetic studies

To determine the rate limiting step in adsorption processes, kinetics of adsorption in batch systems are studied (Han, 2006). To evaluate the adsorption kinetics of MB, DR81, MO and CV molecules, four adsorption kinetic models were used.

2.6.1. The pseudo first-order equation

The pseudo first-order model defines adsorption in solid-liquid systems founded on solids adsorption capacity (Ho, 1995).

Linearly, the pseudo first order model (Eq. (11)) is given as:

$$\log(q_e - q_t) = \log(q_e) - \left(\frac{k_1 t}{2.303}\right) \quad (11)$$

Where q_e (mg/g) is the capacity of adsorption at equilibrium, q_t (mg/g) is the capacity of adsorption at time t, and k_1 (1/min) is the pseudo-first-order rate constant.

2.6.2. The pseudo second order kinetics

The pseudo second-order rate equation has been used to study chemical adsorption kinetics on liquid solutions founded on solid phase adsorption (Tran et al., 2017). Linearly it is given by Eq. (12):

https://doi.org/10.1016/j.heliyon.2018.e00838

$$\frac{t}{q_t} = \left(\frac{1}{q_e}\right) t + \left(\frac{1}{k_2 q_e^2}\right) \quad (12)$$

where k_2 is the rate constant for pseudo second-order adsorption (g/mg/h) $k_2 q_e$ or h (mg/g/h) is the initial adsorption rate.

2.6.3. The Elovich model

The Elovich equation is satisfied in chemical adsorption processes and is suitable for systems with heterogeneous adsorbing surfaces (Wu et al., 2009). In reactions involving chemical adsorption of gases on a solid surface without desorption of the products, the rate decreases with time due to an increase in surface coverage (Aharoni and Tompkins, 1970). One of the most useful models for describing such activated chemical adsorption is the Elovich Eq. (13) (Juang and Chen, 1997) which is given by:

$$q_t = \frac{1}{\beta} \ln(\alpha\beta) + \frac{1}{\beta}\, lnt \quad (13)$$

where α and β are constants. The constant α (mg/g/min) considered as the initial sorption rate and β (mg/g) is the desorption constant during any one experiment and q_t (mg/g) is the amount of dye adsorbed at time t (min).

2.6.4. The intraparticle diffusion model

According to Weber and Morris (1963), if the rate-limiting step is intraparticle diffusion, a plot of solute sorbed against the square root of the contact time should yield a straight line passing through the origin (Poots et al., 1976). The most-widely applied intraparticle diffusion Eq. (14) for adsorption systems is given by Weber and Morris (1963):

$$qt = k_{id} t^{\frac{1}{2}} + C \quad (14)$$

Where kid is the intraparticle diffusion rate constant (mg/g/min) and qt is the amount of dye adsorbed at any time t (mg/g) and C is the intercept.

2.7. Regeneration studies

The regeneration potential of calcined magnesite was evaluated by using 0.01 M NaOH. An adsorption experiment was done using 2 g adsorbent in a 50 mL, 10 mg/L dye solution. The quantity of adsorbed dye was noted, and the adsorbent was dried in the oven for 12 h at 105 °C. Afterwards the adsorbent was soaked into 100 mL, 0.01 M NaOH solution and the mixture was centrifuged at 5 000 rpm for 15 min. The amount of dye desorbed into the solution was recorded. The adsorbent was again washed by 100 mL deionized water.

https://doi.org/10.1016/j.heliyon.2018.e00838

The desorbed adsorbent was again dried in the oven for 12 h at 105 °C. The dried adsorbent was again used for another adsorption experiment as described above. The same procedure using the same adsorbent was repeated three times.

3. Results and discussion

3.1. Adsorbent characterization

3.1.1. Point of zero charge (PZC) analysis

The point of zero charge (PZC) designates a pH wherein the net total particle charge is zero. PZC is among the most significant parameters helpful in the description of variable-charge surfaces. When the adsorbent is in a solution of pH higher than its PZC, the adsorbent's surface will be negatively charged and consequently display the capability of exchanging cations, whereas, if its pH is below its PZC, the adsorbent will mostly retain anions (Ngulube et al., 2016). Fig. 1 shows that calcined magne-site has a PZC at around pH 12. Like observations were made by Han et al. (1998) on MgO. They pointed out that, the point of zero charge of magnesium oxide is well documented and is usually pH 12. Calcined magnesite is highly alkaline when in aqueous solution. During the adsorption experiments, after equilibration with the four different dyes, the final solution pH of the dyes ranged from around 10 -11. pH results during the variation of contact time with the acidic and basic dyes are shown in Table 1:

The general observation was that despite being used in acidic or alkaline conditions, the introduction of calcined magnesite would change the aqueous solution to highly alkaline. Based on that, there was no further need to evaluate the influence of solution pH on the removal of the various dyes using calcined magnesite. Since this current adsorbent does not yield an acceptable pH for effluent discharge, it then becomes imperative for the wastewater to be neutralized by an acid to bring the pH of the contents into the acceptable range before disposal.

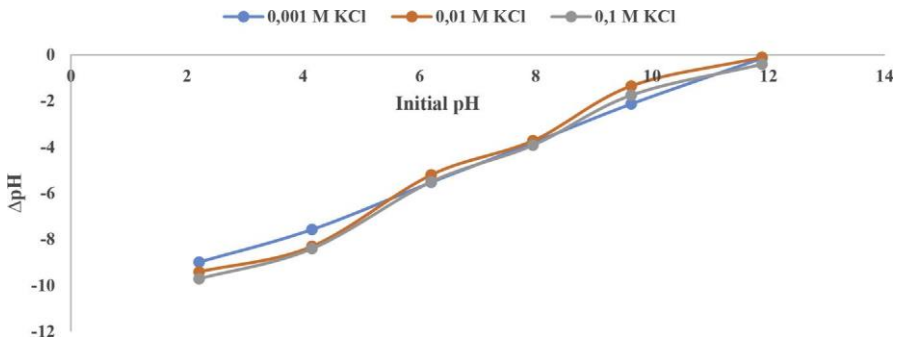

Fig. 1. Point of Zero Charge of calcined magnesite.

https://doi.org/10.1016/j.heliyon.2018.e00838

Table 1. pH values before and after dye adsorption.

Dye	pH before adsorption	pH after adsorption
MB	10.63	11.99
DR81	8.24	11.86
MO	8.99	12.59
CV	10.39	11.70

3.1.2. X ray diffraction (XRD) analysis

The XRD patterns of the calcined magnesite sample showed that the major mineral constituent of the sample is periclase, which is basically a cubic form of magnesium oxide (MgO). Fig. 2 shows the crystal-chemical structure of calcined magnesite as analyzed by XRD.

XRD patterns of calcined magnesite are shown in Fig. 3(a). The sharp peaks in the XRD patterns imply good crystallinity of the sample. The identification of the patterns confirms the material to be largely periclase, this was also observed by Masindi and Gitari (2016) for cryptocrystalline magnesite. The diffraction patterns of the raw calcined magnesite and MB, DR81, MO and CV reacted calcined magnesite show that calcined magnesite had some minor but significant changes after MB, DR81, MO and CV adsorption. The raw calcined magnesite diffractogram shows the presence of periclase (MgO) in notable amounts at approximately (32, 45, 50 and 75) $^{o}2\Theta$, quartz (SiO_2) and periclase at about 32 $^{o}2\Theta$ and magnesite ($MgCO_3$) at 38 $^{o}2\Theta$. Initial studies on the crystal structures of various carbonate materials also reported essentially the same mineralogy as observed for the material used in this study (Effenberger et al., 1981). After MB, DR81, MO and CV adsorption, the intensity of the characteristic basal peak at 50.25 $^{o}2\Theta$ was reduced and slightly

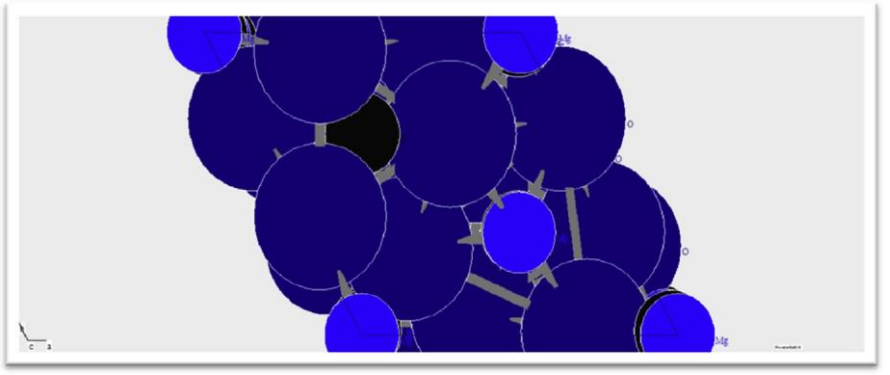

Fig. 2. Crystal-chemical structure of calcined magnesite (Light blue represents Mg; Dark blue represents O; Black represents C).

https://doi.org/10.1016/j.heliyon.2018.e00838

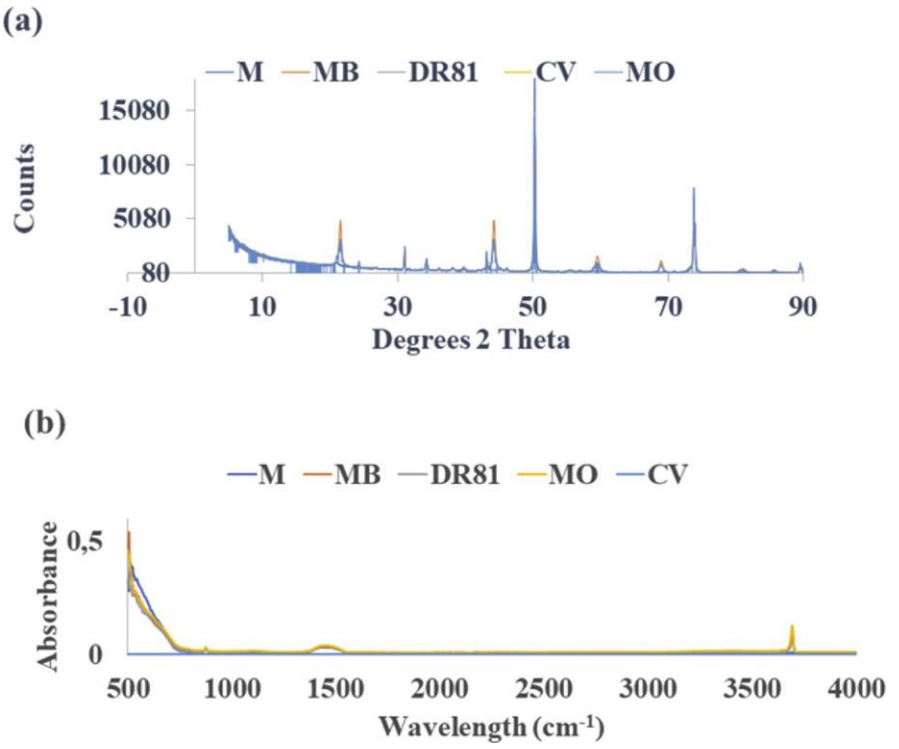

Fig. 3. (a) XRD diffractogram of raw and MB, DR81, MO and CV reacted calcined magnesite (b) FTIR spectra of raw and MB, DR81, MO and CV reacted calcined magnesite.

shifted to 51.24 º2Θ. The shift and decrease in intensity indicate structural change in calcined magnesite is a result of the formation of brucite (Mg (OH)$_2$). MgO can react with water (aqueous solution of dyes) to form Mg(OH)$_2$ according to the equation

$$MgO + H_2O \rightarrow Mg(OH)_2 \quad (15)$$

Thus, the presence of brucite (Mg (OH)$_2$) after adsorption of the dye could be a result of the hydroxylation reaction between the MgO with the aqueous solution of dyes. Brucite formation as a new material is also seen with new peaks at (21.57, 45.00, 60.66, 69.99 and 72.81) º2Θ. This is evidence of a precipitation re-action taking place with hydroxides precipitating out of the solution. Similar re-sults were obtained by Bouyakoub et al. (2011) when using MgCl to remove a reactive dye from textile waste water. Their results showed that brucite particles were formed when MgCl$_2$ was applied to the textile wastewaters. This means that on contact with dyes, calcined magnesite reacted and changed in mineralogy as evidenced by the results. After reaction with DR81, there was also a notable increase of calcite from 1.79 to 7.42%. Another carbonate mineral in the form of dolomite CaMg(CO$_3$)$_2$ was also formed in small quantities on the DR81 and MO loaded calcined magnesite.

https://doi.org/10.1016/j.heliyon.2018.e00838

3.1.3. Fourier transform infra-red analysis

The FTIR spectra for raw and MB, DR81, MO and CV treated calcined magnesite is shown in Fig. 3(b). Since the FTIR spectra of both the raw and MB, DR81, MO and CV treated calcined magnesite were more similar, only MB, DR81, MO and CV reacted calcined magnesite spectra were used to highlight the changes that occurred after adsorption. The FTIR spectroscopic studies confirm the results of XRD studies. After MB, DR81, MO and CV reaction, a brucite bending vibration corresponding to 3694 cm^{-1} was observed. The formation of brucite as seen on the FTIR spectrum corroborates the results reported on XRD, wherein new brucite peaks were seen. This new band could be used as evidence for adsorption of MB, DR81, MO and CV on calcined magnesite which further certifies the successful adsorption of MB, DR81, MO and CV by calcined magnesite. Similar developments of new bands were also observed on other studies after adsorbents interacted with the dye solution (Li et al., 2017; Wang et al., 2013). From the FTIR spectra of raw and MB, DR81, MO and CV reacted calcined magnesite it can be affirmed that these spectra are more similar, they only differ on the development of a new band at 3694 cm^{-1}. Raw magnesite shows a system of bands characteristic of periclase stretching vibration corresponding to band 1450 and 880 cm^{-1} (Masindi et al., 2015). The vibration at 1450 cm^{-1}, also supports the presence of carbonate materials including $CaCO_3$ (calcite) and $MgCO_3$ (magnesite). These results confirm the mineralogical composition as given by the XRD analysis which depicts the presence of periclase.

3.1.4. Thermal gravimetric analysis (TGA)

The results of the thermal treatments of raw calcined magnesite and after adsorption of MB, DR81, MO and CV using the thermogravimetric analysis are shown in Fig. 4. The thermogram of raw calcined magnesite (a) shows a multi stage decomposition process. The decomposition process contains three phases with weight loss between 299 - 367 ^oC, 410 - 435 ^oC and 619 -742 ^oC. The changes can be explained in terms of the decomposition of magnesite as per Eq. (16).

$$Magnesite + dolomite + calcite + heat \rightarrow dolomite + calcite + MgO + CO_2 \quad (16)$$

DR81 (c), MO (d) and CV (e) loaded thermograms showed a similar trend but different to that of the raw calcined magnesite (a) and MB (b) loaded calcined magnesite. This type of curve is exhibited by samples that undergo two mass losses, in this case, between 350 and 404 ^oC, and between 650 - 750 ^oC. On heating at temperatures above 350 C, a rapid and continual weight loss to approximately 400 ^oC is observed in all 3 samples, after which, a steadier change is observed in the 650 - 750 ^oC temperature range. This weight loss up to 400 ^oC can be ascribed to hydroxylated water loss (Knowles et al., 2017) bound to the dye adsorbed calcined magnesite.

https://doi.org/10.1016/j.heliyon.2018.e00838

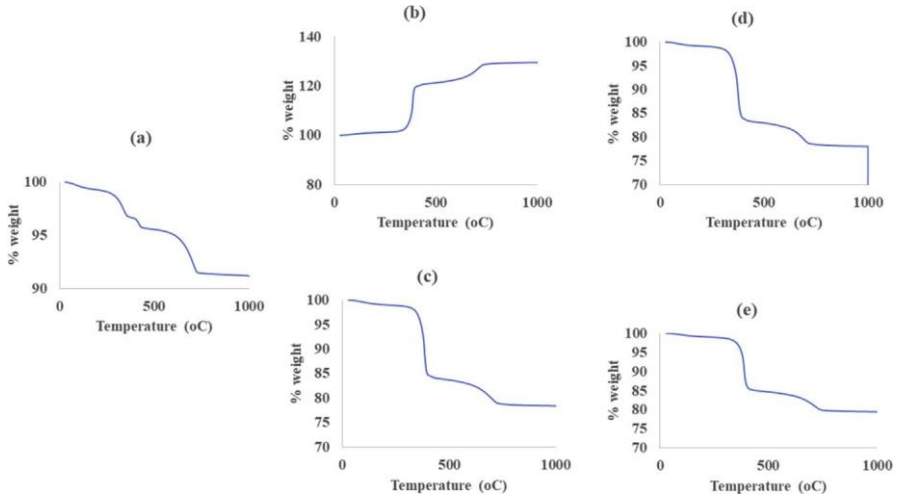

Fig. 4. Thermograms of (a) - raw calcined magnesite and (b) - MB, (c) - DR81, (d) - MO, (e) - CV-adsorbed calcined magnesite.

The second decomposition phase can be due to possible transformation of the mineral phases via the loss of other volatile compounds.

There is an interesting observation with respect to MB loaded calcined magnesite (b). Contrary to (a), (c), (d) and (e), this thermogram shows weight gain rather than weight loss. This kind of curve is possible where there are numerous reactions as the temperature rises. The weight increase is a result of surface oxidation reactions (Loganathan et al., 2017), whereas the weight reduction with increase in temperature corresponds to material decomposition.

3.1.5. Scanning electron microscopy (SEM) analysis

The SEM images of raw and MB, DR81, MO and CV reacted calcined magnesite are shown in Fig. 5 at X 50 000 and X 25 000. The raw calcined magnesite images (a) and (b) appear to have definite hexagonal and rectangular shapes with different sizes. This is perfectly portrayed by image (a) which shows conspicuous

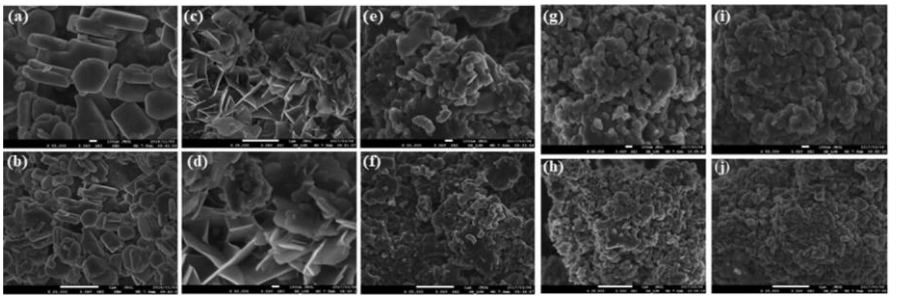

Fig. 5. SEM images of (a & b) - raw, (c & d) - MB, (e & f) - DR81, (g & h) - CV and (i & j) - MO reacted calcined magnesite nanosheet particles at different magnifications (X 50 000 and 25 000).

https://doi.org/10.1016/j.heliyon.2018.e00838

quadrangular and rod like particles. On the contrary, images of the MB - (c) & (d), CV - (g) & (h) and MO (i) & (j) reacted calcined magnesite have a significantly different appearance in both size and shape. After MB, CV and MO reaction the SEM images (c, d, g, h, i and j), particles appear to be broken down into small and medium size particles without a distinct shape. Worth noting is the eye-catching difference of DR81 reacted calcined magnesite images (e) and (f). Images (e) and (f) show irregular shaped flakes with sharp edges that are have characteristic leafy structure images. Most of the raw calcined magnesite particles are < 200 nm in size. After the reaction with MB, DR81, MO and CV a reduction in particle sizes to < 50 nm is observed, although some bigger sized particles were still seen. In the process of reacting in aqueous solution, MgO continuously dissolves and forms Mg $(OH)_2$ (as evidenced by XRD results) on the surface of the parent particles. As the reaction proceeds, the larger particles of MgO are dissolved, and the particle size is gradually reduced. The surfaces of other particles seem to have been sufficiently transformed through aggregate particles created, yet others appeared to have a fibrous nature. This same observation was noted by Sarma et al. (2016). The transformation of the surface topography is evidence of MB, DR81, MO and CV being loaded onto calcined magnesite.

3.1.6. Brunauer-Emmett-Teller (BET) analysis

Surface area is amongst the utmost significant physical properties that limit the quality and efficacy of an adsorbent. Variances of surface area and particle porosity seriously impact its performance. The surface area of particles ultimately determines its adsorption capacity. Table 2 shows that calcined magnesite has a BET surface area of 10.73 m^2/g. After the adsorption of dyes, the surface area of calcined magnesite was reduced in the order: RDR81 > RMB > RMO > RCV. When compared to other clay-based adsorbents used for dye removal, calcined magnesite has comparatively lower surface area (Ngulube et al., 2017). The major reason for the high adsorption capacity of adsorbent materials is their high surface areas. If an adsorbent material

Table 2. Surface areas of raw (R), MB, DR81, MO and CV reacted calcined magnesite nanosheet.

	Single point surface area (m^2/g)	BET surface area (m^2/g)	Langmuir surface area (m^2/g)
R	10.5895	10.7305	14.6564
RMB	8.1462	8.2205	11.1543
RDR81	9.4009	9.4891	12.8352
RCV	6.3461	6.3613	8.6613
RMO	6.4828	6.4434	8.7557

https://doi.org/10.1016/j.heliyon.2018.e00838

has a higher surface area, it means that it will also have a higher adsorption capacity compared to clays with lower surface areas (Muller, 2010). However, this notion may not always be the case for some materials as exemplified by other studies (Chaari et al., 2015; Hai et al., 2015). The former study showed that halloysite had a surface area of 20 m^2/g and therefore producing an adsorption capacity of 7.75 mg/g which is comparable to the present study. However, the latter study by Hai et al. (2015) shows that acid activated kaolinite had an exceptional high surface area of 358.6 m^2/g but it produced a low adsorption capacity of 12.36 mg/g. Therefore, it can be established that other characteristics of an adsorbent material other than its surface area played a vital role in the adsorption of the four dyes.

3.2. Optimization of adsorption conditions

3.2.1. Contact time

The rate of contaminants removal by adsorbents gives data that is essential in the prediction of the time needed to treat contaminated water consequently giving information on adsorption efficiency of the adsorption system (Yagub et al., 2014). Percentage dye removal with time is presented in Fig. 6(a). The graph shows that removal capacity of calcined magnesite increases slightly by increasing contact time for MB, DR81 and CV. For MO, there was a slight fall at 30 minutes and a rise again to the general trend after 60 minutes. The high percentage noted at first for MO dye could be due to all active sites taking up the dye ions at the initial stages. For all dyes, after 60 minutes of contact time, the percentage removal dropped, and no significant further change was observed till 180 minutes, hence 60 minutes of contact time was chosen as the optimum contact time for further experiments. The hypothetical justification to this trend can be credited to the amount of active adsorbent sites (Ismail and AbdelKareem, 2015). The rapid removal rate at the early

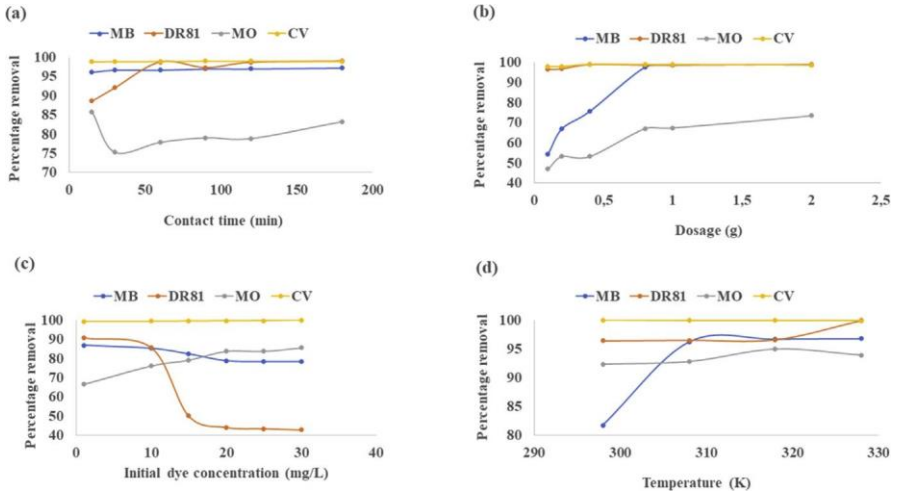

Fig. 6. Removal of MB, DR81, MO and CV by calcined magnesite as a function of (a) - contact time; (b) - dosage; (c) - initial dye concentration (d) - temperature.

https://doi.org/10.1016/j.heliyon.2018.e00838

stage is likely due to the accessibility of a great number of active sites on the surface of the adsorbent. Alike results were observed on other adsorbents reported for dye removal (Elmoubarki et al., 2015; Amuda et al., 2014).

3.2.2. Adsorbent mass

Fig. 6(b) shows MB, DR81, MO and CV dye adsorption as a function of calcined magnesite dosage. Clearly, from Fig. 6(b), increasing the dosage of the adsorbent also increases the percentage dye removal. It is expected that increasing the dosage of the adsorbent increases the amount of available adsorption sites available to take up more dye molecules hence resulting in the percentage removal of dyes also increasing (Sarma et al., 2016; Chaari et al., 2015). Rehman et al. (2013) also reported on a direct association between percentage dye removal and dosage of the adsorbent. The percentage removal increased from 67 to 94, at a dosage of 0.3-1.5 g/L. A similar adsorption pattern with adsorbent amount was also given by Mane and Babu (2011) and Safa and Bhatti (2011). Adding the adsorbent quantity, increases the obtainable adsorption spaces to a definite level against a certain number of dye molecules (Ghaedi et al., 2011). The optimum dosages of 0.1 g for DR81 and CV and 2 g for MB and MO were chosen for the following experiments.

3.2.3. Initial dye concentration

The trend in the percent MB, DR81, MO and CV removal with initial dye concentration is reported in Fig. 6(c). The percent CV and MO removal was directly proportional to the initial concentration within the evaluated initial concentration range of 1-30 mg/L. Hence CV and MO concentration was the sorption rate driving force at the given concentration range. A similar trend was reported by Rehman et al. (2013) on the removal of Brilliant Green dye by red clay. The authors revealed that the process of adsorption was directly proportional to the concentration of dyes as it drove the mass transfer rate below a greater gradient of concentration between the dye solution and the surface of clay. The same elucidation was reported by other authors including Aroguz et al. (2008) and Auta and Hameed (2012). On the contrary, MB and DR81 percentage removal declined with the increased initial dye concentration indicating that MB and DR81 adsorption relied on the number of active sites that are available for taking up MB and DR81 ions. Similar trends of reduced adsorption capacity by increasing initial dye concentration were also described before (Tahir et al., 2016; Ullah et al., 2013).

3.2.4. Temperature

The influence of temperature on MB, DR81, MO and CV removal by calcined magnesite is presented in Fig. 6(d). Experimental results show that as temperature was increased from 298-328 K, percentage dye removal

https://doi.org/10.1016/j.heliyon.2018.e00838

slightly increased for MB and DR81 dyes. The improved dye removal with increase in temperature may be credited to kinetic effects due to enhanced diffusion of molecules or it can be attributed to new adsorption sites being "activated" (Zhou et al., 2014) on calcined magnesite at higher temperature. It seemed that the increase of temperature improved the diffusivity of dye molecules on water causing the increase of their movement into the pores of calcined magnesite (Ngulube et al., 2017). For MO and CV dye, it was observed that the differences in temperature had a negligible influence on the dye removal. Sivakumar et al. (2014a,b) also reported an insignificant percent dye removal at the different evaluated temperatures. Based on that, it was concluded that there was no need to adjust the temperatures for dye removal experiments hence 298 K (room temperature) was fixed as the optimum temperature to be used in subsequent experiment as this temperature is common for many water resources.

3.3. Isotherm studies

The batch adsorption studies were designed to evaluate the efficiency of calcined magnesite for the removal of MB, DR81, MO and CV from aqueous solution. The equilibrium data obtained was used to analyze the adsorption systems in view of the Langmuir, Freundlich, Dubinin Radushkevich and Temkin isotherm models. The isotherm constants of Eqs. (3), (4), (5), (6), (7), (8), (9), (10) are very valuable factors used to predict adsorption capacities and mass transfer relations to envisage the design and plan of batch reactors (Thilagavathy and Santhi, 2014). The equilibrium data for calculating isotherm constants were obtained by evaluating the effect of MB, DR81, MO and CV initial concentration on percentage dye removal. The isotherm model's validity was confirmed by comparing the R^2 values and comparison of calculated and experimental adsorption capacities. Examination of the data shows that all the four adsorption models could not perfectly describe the uptake of the dyes. However, the Dubinin Radushkevich and Temkin isotherms fitted better to MB and MO adsorption data respectively compared to all other isotherm models tested though the R^2 values of Freundlich and Dubinin Radushkevich models for MB adsorption were close to each other. Hence both isotherms may be held responsible for guiding MB adsorption, but it is also note worth noting that the best fit also means that both experimental adsorption capacity and calculated adsorption capacity are close to each other. In this case, the Dubinin Radushkevich isotherm adsorption capacity was closer to experimental adsorption capacity than the Freundlich hence the choice of the Dubinin Radushkevich as the best fit. The Dubinin Radushkevich isotherm is generally applied to express the adsorption mechanism with a Gaussian energy distribution onto a heterogeneous surface (Dubinin, 1960) whereas the Temkin isotherm assumes that the bonding energy of adsorption decreases linearly with increasing surface coverage (Temkin and Pyzhev, 1940). From the calculated isotherm model parameters for the Dubinin Radushkevich model, provided in Table 3 the mean free energy (E) was found to be 510.93 KJ/mol indicating a chemisorption

https://doi.org/10.1016/j.heliyon.2018.e00838

Table 3. Parameters of the adsorption isotherms for the system of calcined magnesite.

	MB	DR81	MO	CV
Langmuir	R^2 = 0.003	R^2 = 0.4644	R^2 = 0.3888	R^2 = 0.0028
Freundlich	R^2 = 0.9359	R^2 = 0.0348	R^2 = 0.8079	R^2 = 0.0627
	Qm exp = 0.39 (mg/g)			
	K_F = 0.0947 (mg/g)			
	n = 1.0189			
Dubinin Radushkevich	R^2 = 0.9559	R^2 = 0.0304	R^2 = 0.8588	R^2 = 0.0627
	Qm exp = 0.39 (mg/g)			
	Qm cal = 0.271(mg/g)			
	K_{DR} = 0.0000019 (mol^2/Kj^2)			
	E = 510.93 (kJ/mol)			
Temkin	R^2 = 0.8975	R^2 = 0.0778	R^2 = 0.9399	R^2 = 0.0627
			β = 0.4586 (J/mol)	
			α = 0.7523 (L/mg)	
			b = 5402.47 (J/mol)	

process for MB onto a heterogenous surface. If there are any adsorbate - adsorbate interactions, they are best described by the Temkin isotherm. The Temkin isotherm plots for MO adsorption on calcined magnesite was linear with an R^2 of 0.94 demonstrating that adsorbate - adsorbate and adsorbate - adsorbent interactions both control the dye removal process. The parameters of the Temkin model are presented in Table 3 show a higher value for b (5402.47 J/mol) which is an indication of the heat of sorption signifying a chemical adsorption for MO uptake.

3.4. Kinetic studies

To study the adsorption mechanisms like chemical reaction and mass transfer, four kinetic models were used to analyze the rate data. The adsorption parameters of the four kinetic models are presented in Table 4.

The batch adsorption system examined in this study aims to determine if it is suitable to be applied in treating field wastewater. The performance and cost of adsorbents including the mode of application are significant factors controlling the process efficiency (Zhou et al., 2015). For that reason, the adsorption capacity and the time taken to reach equilibrium become the most imperative parameters to determine in such studies. The adsorption rate was tested using four kinetic models to understand possible mechanisms involved in the adsorption process. The conformity between experimental data and the model predicted values was expressed by the correlation coefficients R^2 (R^2 values close or equal to 1). A relatively high R^2 value indicates that the model successfully describes the adsorption kinetics. The parameters of the four kinetic models are presented in Table 4. The pseudo first order model yielded relatively low R^2 values hence its

https://doi.org/10.1016/j.heliyon.2018.e00838

Table 4. The pseudo first order, pseudo second order, intra particle diffusion and Elovich kinetic model parameters for adsorption of MB, DR81, MO and CV onto calcined magnesite.

Parameter	MB	DR81	M0	CV
Pseudo first order				
R^2	0.7930	0.0893	#N/A	#N/A
Pseudo second order				
Qe (mg/g) experimental	0.3932	12.5561	0.6416	14.9907
Qe (mg/g) calculated	0.2271	14.8148	0.4291	0.5209
k_2 (g/mg/h)	0.0069	$1.10E^{-17}$	0.0001	0.0271
R^2	0.9600	1	1	0.9898
Intraparticle diffusion				
Kid (mg/g/min)	0.2457	0.2306	0.7871	1.0056
C	0.8406	1.0834	0.3175	0.2486
R^2	1	1	0.9999	1
Elovich				
a (mg/g/min)	1.3692	1.9050	0.5186	0.2854
b (mg/g)	1.713	1.8308	0.5239	0.4171
R^2	1	0.9999	0.996	1

applicability was dismissed. However, the other three models gave high R^2 values in the order; intra particle diffusion > Elovich > pseudo second order as shown in Table 4. For the intra particle diffusion model to be valid, the plot of Qt versus $t^{0.5}$ should be linear and pass through the origin (Guo et al., 2015). The fitting results (provided in the supplementary material) shows a linear regression, however, the plot did not pass through the origin ($C \neq 0$) which contradicted the validity of the intraparticle diffusion model suggesting that the adsorption of the dyes was not entirely controlled by intraparticle diffusion (Ugbe and Ikudayisi, 2017).

The Elovich equation is satisfied in chemical adsorption processes and is suitable for systems with heterogeneous adsorbing surfaces (Aharoni and Tompkins, 1970). As shown by the R^2 values indicated in Table 4, the Elovich equation was successfully used to describe second e order kinetics behavior that concurs with the nature of chemical adsorption, if the actual solid surfaces are energetically heterogeneous (Senthilkumar et al., 2010). The results from the Elovich model corroborates those from isotherm modelling because they confirm that adsorption took place on heterogenous surfaces as evidenced by the Dubinin Radushkevich and Freundlich model fit on MB adsorption. Moreover, the proven applicability of the Elovich model signified the role of chemisorption as probably one of the basic rates limiting mechanisms during the adsorption process. This also concurs with the best fit shown by the pseudo second order model. The pseudo second order model basically supports chemisorption (Ngulube et al., 2017). Consequently, it can be

https://doi.org/10.1016/j.heliyon.2018.e00838

determined that the rate limiting step in the adsorption of the four dyes is possibly chemisorption involving valence forces, occurring possibly due to electron sharing and/or exchange between calcined magnesite and dye ions in solution. The calculated and experimental adsorption capacities for MB, DR81 and MO were also close to each other confirming the best fit of the pseudo-second-order model. However, there was a significant difference between the calculated and experimental adsorption capacity with regards to CV which could possibly mean that the uptake of CV was not entirely controlled by chemisorption as explained in the mechanisms of adsorption of different dyes on Section 3.6.

3.5. Regeneration studies

Excellent regeneration capability of an adsorbent is a crucial factor after the adsorption of dyes because it allows the reuse of the adsorbent. 0.1 M NaOH was used as an eluent in this study. The four dyes showed 2 different trends with each successive regeneration cycle. The general observation with regenera-tion experiments is that the more the adsorbent is regenerated and used for adsorption experiments, the more the adsorbent loses its adsorption capacity. This is the observation seen with MB and CV loaded calcined magnesite as seen in Fig. 7. Regeneration of CV loaded calcined magnesite proved ineffective just after one adsorption experiment whereas that of MB loaded calcined magnesite decreased to zero after 2 cycles. The decreased leaching of colour from the CV loaded calcined magnesite is, on the other hand, a good characteristic, bearing in mind what would happen after disposal in landfills or reusing for other uses including integration in polymeric composites and construction materials (Ngulube et al., 2017). On the other hand, regenerating DR81 and MO loaded calcined magnesite with 0.1 M NaOH enhanced the adsorbent dye removal capacity with each successive cycle. The regenerated adsorbents were shown to be effective even after 3 cycles.

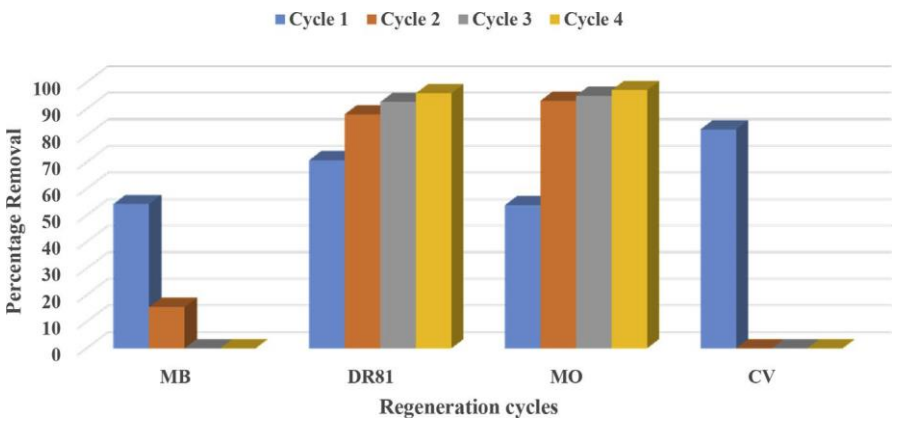

Fig. 7. Regeneration test of calcined magnesite.

https://doi.org/10.1016/j.heliyon.2018.e00838

It is shown that the percentage removal for each cycle was remarkably high proving that NaOH is an exceptional eluent to regenerate relevant adsorbents. Zhou et al. (2016) also recorded surprisingly high values of percentage removal with successive regeneration cycles. This behavior indicated that adsorption of DR81 and MO was chemical in nature. Adsorption was reversible and adsorbed DR81 and MO could be completely recovered with the alkaline solution. A possible explanation to this is that DR81 and MO dyes are acidic and reacting with alkaline solution leads to electrostatic interactions between the negatively and positively charged ions hence the reversible reactions.

3.6. Proposed mechanisms explaining the uptake of MB, DR81, MO and CV by calcined magnesite

Various factors like the adsorbent nature (physicochemical characteristics of the adsorbent) affect contaminants removal from water. The traditional theory of physical chemistry postulates that adsorption is a surface effect, Moreover, adsorption can be separated into chemical and physical depending on the nature of the inter-action between the adsorbate and adsorbent (Saad et al., 2015). For physical adsorption, the main interactions are the Van der Waals' (VDW) forces between the adsorbent and adsorbate (Han et al., 2016). For chemisorption, the attraction force present between adsorbent and adsorbate have almost equal strength as chemical bonds and these are strong covalent bonds involving electron exchange. From the results obtained from the kinetic models, it is evident that MB, DR81, MO and CV were taken up by calcined magnesite particles via a chemical reaction. However, a further differentiation can be made between the acidic dyes (DR81 and MO) and basic dyes (MB and CV). The main mechanisms that controlled DR81 and MO uptake by magnesium nanoparticles include charge neutralization, electrostatic interaction and adsorptive coagulating mechanism. As shown in Fig. 3(a), the XRD study displays that the adsorbent is mainly made up of periclase which is principally magnesium hydroxide. It is also further revealed that the raw mate-rial is almost transformed into $Mg(OH)_2$ precipitate in the colour removal process. The precipitate structure offers a huge surface area for adsorption and a positive electrostatic surface charge, enabling the precipitate to be a significant and efficient coagulant. Hence, it can be inferred that calcined magnesite decolourizes the coloured aqueous solution via adsorptive coagulating mechanism and charge neutralization.

When oxides and hydroxides of Mg and Ca ions are in solution, they give out elec-trical charges which are involved in the dye removal processes. Charge neutralization is defined as a state in which the particles' net electrical charge in aqueous solution have been canceled by the adsorption of an equal number of opposite

https://doi.org/10.1016/j.heliyon.2018.e00838

charges (Wang et al., 2009). Magnesium carbonate is among inorganic coagulants that usually work via charge neutralization. Once the metal-based coagulants are in aqueous solution, they dissociate, and metal ions are formed. In the case of magne-sium carbonate, these liberated Mg ions and OH ions react with the dye molecules to make several polymeric and monomeric hydrolyzed species. Metal adsorption hy-drolyzed products on the colloid surface causes charge neutralization bringing about van der Walls forces (O'Melia and Weber, 1972). Magnesium, with its divalent cations, is effective for neutralizing the negative charge of DR81 and MO dyes. Accord-ing to a process respectively schematized as follows:

$$Mineral\ ion\ (Mg^{2+})\ \text{Positive charge}\ \leftrightarrow Dye\ organic\ fraction\ (SO_3^{2-})\ \text{Negative charge} \quad (16)$$

$$Mg^{2+} + SO_3^{2-} \leftrightarrow MgSO_4 \quad (17)$$

There was an electrostatic interaction strong electrostatic attraction existing between the positively charged magnesium ion and the negatively charged dye molecules as shown by Eqs. (17) and (18), which could enhance the uptake of acidic dyes.

The nature of functional groups (hydrophobic/hydrophilic) present on the surface of the adsorbent lead to various interaction like hydrogen bonding and electrostatic attractions. This factor could be the one that played a role in the uptake of the basic dyes. As discussed in the FTIR characterization results, the bands at 3600-3700 cm $^{-1}$ which are associated with OH groups adsorbed water shifted after dye adsorption indicating that the hydroxyl groups might have played an important role in the adsorption process. These modifications indicate the definite electrostatic, hydrogen bonding and dipole and ion-induced dipole forces among the functional groups of dye molecules and hydroxyls, Furthermore, as MB and CV molecules have C = C double bonds and benzene rings with π electrons, it could have π-π interaction with calcined magnesite in aqueous solution.

3.7. Performance evaluation

The maximum adsorption capacities of adsorbent materials for MB, DR81, MO and CV dye removal are listed in Table 5. It was observed that the maximum adsorption capacity of calcined magnesite is significantly comparative with the others reported in Table 5. The significance of the present study is to obtain maximum adsorption capacity at ambient temperature without modifying the natural adsorption conditions and the adsorbent itself. Most adsorbents with significantly high adsorption capacities are chemically modified but natural and/or raw materials have lower adsorption capacities. Nonetheless, calcined magnesite managed to achieve colour removal as shown in the images provided in supplementary materials.

https://doi.org/10.1016/j.heliyon.2018.e00838

Table 5. Comparison of adsorption capacity of various adsorbents for MB, DR81, MO and CV.

Adsorbent	Adsorption capacity (mg/g)	Dye	Reference
Calcined magnesite	0.39	MB	Present study
Calcined magnesite	12.56	DR81	Present study
Calcined magnesite	0.64	MO	Present study
Calcined magnesite	14.99	CV	Present study
Zn-MOF	0.75	MB	Sun et al. (2013)
Brazil nut shells	7.81	MB	Modesto et al. (2010)
Raw clay beads	58.02	MB	Auta and Hameed (2012)
Swelling clays	65	MB	Li et al. (2011)
Graphene oxide	714	MB	Yang et al. (2011)
Argemone mexicana	2.4	DR81	Khamparia and Jaspal (2016)
Bamboo Sawdust	6.43	DR81	Khan et al. (2012)
Pumice	10.56	DR81	Hossein and Behzad (2012)
Balsamodendron Caudatum wood waste	5.0354	DR81	Sivakumar et al. (2014a,b)
MgNiAl-CO_3	118.5	MO	Zaghouane-Boudiaf et al. (2012)
Activated carbon	21.42	MO	Chennouf-Abdellatif et al. (2017)
Chitosan/MgO composite	60	MO	Haldorai and Shim (2014)
Mineral-based porous granulated material	80	MO	Wang et al. (2015)
TLAC/Chitosan composite	2.375	CV	Kumari et al. (2017)
Walled carbon nanotubes	90.52	CV	Sabna et al. (2015)
Subbituminous coal	6.25	CV	Schoonen and Schoonen (2014)
$SnFe_2O_4$@activated carbon magnetic nanocomposite	158.73	CV	Rai et al. (2015)

4. Conclusion

Calcined magnesite was successfully employed to remove of MB, DR81, MO and CV from aqueous solution. Results of the adsorption showed that MB, DR81, MO and CV dye removal improved with an increase in contact time and adsorbent dosage. Of the two kinetic models applied to the equilibrium data, the pseudo-second-order kinetic model could predict the adsorption kinetics well. Furthermore, the use of calcined magnesite is economically practical particularly because it can be easily regenerated and reused afterwards. The results of this paper also provide more insight on the mechanisms involved when magnesium solutions are applied for discolouration of dye effluents. The mechanism of removal can be ascribed to electrostatic interaction, charge neutralization and adsorptive coagulating mechanisms. The application of magnesite for

https://doi.org/10.1016/j.heliyon.2018.e00838

wastewater treatment seems to signify a capable substitute of conventional adsorbents because the optimum dose and production of sludge are very low compared to those accomplished by several natural adsorbents. After contacting dyes with calcined magnesite, a colourless aqueous solution was observed. Such standards conform with the environmental standards on wastewater disposal in surface waters. Since the magnesite material showed an excellent dye removal capacity on a batch study, it become imperative to investigate its performance in a continuous fixed bed column mode in order assess the potential use in real wastewater. The employed calcined magnesite adsorbent proved to be effective in removing the dyes from water and demonstrated that it can be a hopeful answer to dye wastewater treatment problem.

Declarations

Author contribution statement

T. Ngulube: Conceived and designed the experiments; Performed the experiments; Analyzed and interpreted the data; Wrote the paper.

J.R Gumbo, V Masindi: Conceived and designed the experiments; Analyzed and in-terpreted the data; Contributed reagents, materials, analysis tools or data.

A. Maity: Conceived and designed the experiments; Analyzed and interpreted the data.

Funding statement

This work was supported by the Director of Research and Innovation, University of Venda, National Research Foundation (NRF), Water Research Commission (WRC).

Competing interest statement

The authors declare no conflict of interest.

Additional information

Supplementary content related to this article has been published online at https://doi.org/10.1016/j.heliyon.2018.e00838.

References

Aharoni, C., Tompkins, F.C., 1970. Kinetics of adsorption and desorption and the Elovich equation. In: Eley, D.D., Pines, H., Weisz, P.B. (Eds.), Advances in Catal-ysis and Related Subjects, vol. 21. Academic Press, New York, pp. 1- 49.

https://doi.org/10.1016/j.heliyon.2018.e00838

Aljeboree, A.M., Abbas, N., Alshirifi, A.N., Alkaim, A.F., 2017. Kinetics and equi-librium study for the adsorption of textile dyes on coconut shell activated carbon. Arab. J. Chem. 10, S3381-S3393.

Amuda, O.S., Olayiwola, A., Alade, A.O., Farombi, A.G., Adebisi, S.A., 2014. Adsorption of methylene blue from aqueous solution using steam-activated carbon produced from Lantana camara stem. J. Environ. Protect. 5, 1352-1363.

Aroguz, A.Z., Gulen, J., Evers, R.H., 2008. Adsorption of methylene blue from aqueous solution on pyrolyzed petrified sediment. Bioresour. Technol. 99, 1503-1508.

Auta, M., Hameed, B.H., 2012. Modified mesoporous clay adsorbent for adsorption isotherm and kinetics of methylene blue. Chem. Eng. J. 198-199, 219-227.

Bello, O.S., Ahmad, M.A., 2012. Coconut (Cocos nucifera) shell based activated carbon for the removal of malachite green dye from aqueous solutions. Sep. Sci. Technol. 47 (6), 903-912.

Bouyakoub, A.Z., Lartiges, B.S., Ouhib, R., Kacha, S., El Samrani, A.G., Ghanbaja, J., Barres, O., 2011. $MnCl_2$ and $MgCl_2$ for the removal of reactive dye Levafix Brilliant Blue EBRA from synthetic textile wastewaters: an adsorp-tion/aggregation mechanism. J. Hazard Mater. 187, 264-273.

Chaari, I., Moussi, B., Jamoussi, F., 2015. Interactions of the dye, C.I. direct orange 34 with natural clay. J. Alloy. Compd. 647, 720-727.

Chennouf-Abdellatif, Z., Cheknane, B., Zermane, F., Gaigneaux, E.M., Mohammedi, O., Bouchenafa-Saib, N., 2017. Equilibrium and kinetic studies of methyl orange and Rhodamine B adsorption onto prepared activated carbon based on synthetic and agricultural wastes. Desalination Water Treat. 67, 284-291.

Dubinin, M.M., 1960. The potential theory of adsorption of gases and vapors for adsorbents with energetically non-uniform surface. Chem. Rev. 60, 235-266.

Dubinin, M.M., Radushkevich, L.V., 1947. Evaluation of microporous materials with a new isotherm. Dokl. Akad. Nauk SSSR 55, 331-334.

Effenberger, H., Mereiter, K., Zemann, J., 1981. Crystal structure refinements of magnesite, calcite, rhodochrosite, siderite, smithonite, and dolomite, with discus-sion of some aspects of the stereochemistry of calcite type carbonates. Z. Krist. 156, 233-243.

Elmoubarki, R., Mahjoubi, F.Z., Tounsadi, H., Moustadraf, J., Abdennouri, M., Zouhri, A., ElAlban, A., Barka, N., 2015. Adsorption of textile dyes on raw andde-canted Moroccan clays: kinetics, equilibrium and thermodynamics. Water Resour. Ind. 9, 16-29.

https://doi.org/10.1016/j.heliyon.2018.e00838

Freundlich, H.Z., 1906. Over the adsorption in solution. J. Phys. Chem. 57A, 385-470.

Gao, B.Y., Yue, Q.Y., Wang, Y., Zhou, W.Z., 2007. Colour removal from dye-containing wastewater by magnesium chloride. J. Environ. Manag. 82 (2), 167-172.

Ghaedi, M., Hossainian, H., Montazerozohori, M., Shokrollahi, A., Shojaipour, F., Soylak, M., Purkait, M.K., 2011. A novel acorn-based adsorbent for the removal of brilliant green. Desalination 281, 226-233.

Ghoreishi, S., Haghighi, R., 2003. Chemical catalytic reaction and biological oxida-tion for treatment of non-biodegradable textile effluent. Chem. Eng. J. 95 (1), 163-169.

Gupta, V.K., Kumar, R., Nayak, A., Saleh, T.A., Barakat, M.A., 2013. Adsorptive removal of dyes from aqueous solution onto carbon nanotubes: a review. Adv. Colloid Interface Sci. 193-194, 24-34.

Gupta, V.K., Suhas, 2009. Application of low-cost adsorbents for dye removal - A review. J. Environ. Manag. 90, 2313-2342.

Guo, Z., Liu, X., Huang, H., 2015. Kinetics and thermodynamics of reserpine adsorption onto strong acidic cationic exchange fiber. PloS One 10 (9), 0138619.

Hai, Y., Li, X., Wu, H., Zhao, S., Deligeer, W., Asuha, S., 2015. Modification of acid activated kaolinite with TiO_2 and its use for the removal of azo dyes. Appl. Clay Sci. 114, 558-567.

Haldorai, Y., Shim, J.J., 2014. An efficient removal of methyl orange dye from aqueous solution by adsorption onto chitosan/MgO composite: a novel reusable adsorbent. Appl. Surf. Sci. 292, 447-453.

Hall, K.R., Eagleton, L.C., Acrivos, A., Vermeulen, T., 1966. Pore- and solid-diffusion kinetics in fixed-bed adsorption under constant-pattern conditions. Ind. Eng. Chem. Fundam. 5 (2), 212-223.

Han, S., Hou, W., Zhaag, C., Sun, D., Huang, X., Wang, C., 1998. Structure and the point of zero charge of magnesium aluminium hydroxide. J. Chem. Soc. Faraday Trans. 94 (7), 915-918.

Han, H., Wei, W., Jiang, Z., Lu, J., Zhu, J., Xie, J., 2016. Removal of cationic dyes from aqueous solution by adsorption onto hydrophobic/hydrophilic silica aerogel. Colloid. Surface. Physicochem. Eng. Aspect. 509, 539-549.

Han, R., 2006. Removal of copper (II) and lead (II) from aqueous solution by man-ganese oxide coated sand. J. Hazard Mater. 137 (1), 384-395.

https://doi.org/10.1016/j.heliyon.2018.e00838

Ho, Y.S., 1995. Adsorption of Heavy Metals from Waste Streams by Peat. PhD Thesis. University of Birmingham, Birmingham, UK.

Hossein, M.A., Behzad, H., 2012. Removal of reactive red 120 and direct red 81 dyes from aqueous solutions by pumice. Res. J. Chem. Environ. 16 (1), 62-68.

Ismail, Z.Z., AbdelKareem, H.N., 2015. Sustainable approach for recycling waste lamb and chicken bones for fluoride removal from water followed by reusing fluoride-bearing waste in concrete. Waste Manag. 45, 66-75.

Izuagie, A.A., Gitari, W.M., Gumbo, J.R., 2016. Synthesis and performance eval-uation of Al/Fe oxide coated diatomaceous earth in groundwater defluoridation: to-wards fluorosis mitigation. J. Environ. Sci. Health Part A 1-15.

Juang, R.S., Chen, M.L., 1997. Application of the Elovich equation to the kinetics of metal sorption with solvent-impregnated resins. Ind. Eng. Chem. Res. 36, 813-820.

Khamparia, S., Jaspal, D., 2016. Adsorptive removal of direct red 81 dye from aqueous solution onto Argemone mexicana. Sustain. Environ. Res. 26, 117-123.

Khan, T.A., Dahiya, S., Ali, I., 2012. Removal of direct red 81 dye from aqueous solution by native and citric acid modified bamboo sawdust - kinetic study and equilibrium isotherm analyses. Gazi Univ. J. Sci. 25 (1), 59-87.

Knowles, K.V., Yaya, A., Tiburu, E.K., Vickers, M.E., Efavi, J.K., Onwona-Agyeman, B., Knowles, K.M., 2017. Characterisation and identification of local kaolin clay from Ghana: a potential material for electroporcelain insulator fabrica-tion. Appl. Clay Sci. 150, 125-130.

Kumari, H.J., Krishnamoorthy, P., Arumugam, T.K., Radhakrishnan, S., Vasudevan, D., 2017. An efficient removal of crystal violet dye from waste water by adsorption onto TLAC/Chitosan composite: a novel low-cost adsorbent. Int. J. Biol. Macromol. 96, 324-333.

Langmuir, I., 1918. The adsorption of gases on plane surfaces of glass, mica and platinum. J. Am. Chem. Soc. 40, 1361-1403.

Lee, J.W., Choi, S.P., Thiruvenkatachari, R., Shim, W.G., Moon, H., 2006. Evalu-ation of the performance of adsorption and coagulation processes for the maximum removal of reactive dyes. Dyes Pigments 69 (3), 196-203.

Leentvaar, J., Rebhun, M., 1982. Effect of magnesium and calcium precipitation on coagulationeflocculation with lime. Water Res. 16, 655-662.

Li, X., Zhao, Y., Xi, B., Meng, X., Gong, B., Li, R., Peng, X., Liu, H., 2017. Decol-ourization of MB by a new clay-supported nanoscale zero-valentiron: synergetic effect, efficiency optimization and mechanism. J. Environ. Sci. 52, 8-17.

https://doi.org/10.1016/j.heliyon.2018.e00838

Li, Z., Chang, P., Jiang, W., Jean, J., Honga, H., 2011. Mechanism of methylene blue removal from water by swelling clays. Chem. Eng. J. 168, 1193-1200.

Loganathan, S., Valapa, R.B., Mishra, R.K., Pugazhenthi, G., Thomas, S., 2017. Thermogravimetric analysis for characterization of nanomaterials. In: Thermal and Rheological Measurement Techniques for Nanomaterials Characterization, first ed., vol. 4. Elsevier, pp. 68-107.

Malarvizhi, R., Ho, Y.S., 2010. The influence of pH and the structure of the dye molecules on adsorption isotherm modeling using activated carbon. Desalination 264 (1), 97-101.

Mane, V.S., Babu, P.V.V., 2011. Studies on the adsorption of Brilliant Green dye from aqueous solution onto low-cost NaOH treated saw dust. Desalination 273, 321-329.

Masindi, V., Gitari, W.M., 2016. Removal of arsenic from wastewaters by crypto-crystalline magnesite: complimenting experimental results with modelling. J. Clean. Prod. 113, 318e324. http://hdl.handle.net/10204/8485.

Masindi, V., Gitari, M.W., Tutu, H., De Beer, M., 2015. Fate of inorganic contam-inants post treatment of acid mine drainage by calcined magnesite: complimenting experimental results with a geochemical model. J. Environ. Chem. Eng.

Modesto, S., Andrade, H.M.C., Soares, L.F., Pires, R., 2010. Brazil nut shells as a new biosorbent to remove methylene blue and indigo carmine from aqueous solu-tions. J. Hazard Mater. 174, 84-92.

Muller, B.R., 2010. Effect of particle size and surface area on the adsorption of albumin-bonded bilirubin on activated carbon. Carbon 48, 3607-3615.

Ngulube, T., Gumbo, J.R., Masindi, V., Maity, A., 2017. An update on synthetic dyes adsorption onto clay-based minerals: a state-of-art review. J. Environ. Manag. 191, 35-57.

Ngulube, T., Gitari, M.W., Tutu, H., 2016. Defluoridation of groundwater using mixed Mukondeni clay soils. Water Sci. Technol. Water Supply 17 (2), 480-492.

O'Melia, R., Weber, W.J., 1972. Physicochemical Process for Water Quality Con-trol. Wiley Publication, New York.

Ozer, C., Imamoglu, M., Turhan, Y., Boysan, F., 2012. Removal of methylene blue from aqueous solutions using phosphoric acid activated carbon produced from ha-zelnut husks. Toxicol. Environ. Chem. 94 (7), 1283-1293.

https://doi.org/10.1016/j.heliyon.2018.e00838

Poots, V.J.P., McKay, G., Healy, J.J., 1976. The removal of acid dye from effluent, using natural adsorbents: I. Peat. Water Res. 10, 1061-1066.

Rai, P., Gautam, R.K., Banerjee, S., Rawat, V., Chattopadhyaya, M.C., 2015. Syn-thesis and characterization of a novel $SnFe_2O_4$@activated carbon magnetic nano-composite and its effectiveness in the removal of crystal violet from aqueous solution. J. Environ. Chem. Eng. 3 (4), 2281-2291.

Rehman, M.S.U., Munira, M., Ashfaqa, M., Rashid, N., Nazar, M.F., Danish, M., Han, J., 2013. Adsorption of Brilliant Green dye from aqueous solution onto red clay. Chem. Eng. J. 228, 54-62.

Saad, N., Al-Mawla, M., Moubarak, E., Al-Ghoul, M., El-Rassy, H., 2015. Surface-functionalized silica aerogels and alcogels for methylene blue adsorption. RSC Adv. 5, 6111-6122.

Sabna, V., Thampi, S.G., Chandrakaran, S., 2015. Adsorption of crystal violet onto functionalised multi-walled carbon nanotubes: equilibrium and kinetic studies. Eco-toxicol. Environ. Saf. 134 (2), 390-397.

Safa, Y., Bhatti, H.N., 2011. Kinetic and thermodynamic modelling for the removal of Direct Red-31 and Direct Orange-26 dyes from aqueous solutions by rice husk. Desalination 272, 313-322.

Santos, S.C.R., Boaventura, R.A.R., 2016. Adsorption of cationic and anionic azo dyes on sepiolite clay: equilibrium and kinetic studies in batch mode. J. Environ. Chem. Eng. 4, 1473-1483.

Sarma, G.K., Gupta, S.S., Bhattacharyya, K.G., 2016. Adsorption of Crystal violet on raw and acid-treated montmorillonite, K10, in aqueous suspension. J. Environ. Manag. 171, 1-10.

Schoonen, M.A., Schoonen, J.M.T., 2014. Removal of crystal violet from aqueous solutions using coal. J. Colloid Interface Sci. 422, 1-8.

Senthilkumar, S., Krishna, S.K., Kalaamani, P., Subburamaan, C.V., Ganapathy Subramaniam, N., Kang, T.W., 2010. Approach for the adsorption of organophos-phorous pesticides from aqueous solution using “Waste” jute fiber carbon. E-J. Chem. 7 (S1), S511-S519.

Sivakumar, B., Nithya, P., Karthikeyan, S., Kannan, C., 2014a. Kinetics, equilib-rium and isotherms of direct red 81 removal from aqueous solution using balsamo-dendron caudatum wood waste activated nanoporous carbon. Rasayan J. Chem. 7(2), 161169.

https://doi.org/10.1016/j.heliyon.2018.e00838

Sivakumar, S., Muthirulan, P., Meenakshi Sundaram, M., 2014b. Adsorption ki-netic and isotherm studies of Azure A on various activated carbons derived from agricultural wastes. Arab. J. Chem.

Sun, C., Wang, X., Qin, C., Jin, J., Su, Z., Huang, P., Shao, K., 2013. Solvatochro-mic behavior of chiral mesoporous metal e organic frameworks and their applica-tion for sensing small molecules and separating cationic dyes. Chem. Eur. J. 19, 3639-3645.

Tahir, M.A., Bhatti, H.N., Iqbal, M., 2016. Solar Red and Brittle Blue direct dyes adsorption onto Eucalyptus angophoroides bark: equilibrium, kinetics and thermo-dynamic studies. J. Environ. Chem. Eng. 4, 2431-2439.

Tan, B.H., Teng, T.T., Mohd-Omar, A.K., 2000. Removal of dyes and industrial dye wastes by magnesium chloride. Water Res. 34 (2), 597-601.

Temkin, M.I., Pyzhev, V., 1940. Kinetic of ammonia synthesis on promoted iron catalyst. Acta Physiochim. USSR 12, 327-356.

Thilagavathy, P., Santhi, T., 2014. Kinetics, isotherms and equilibrium study of Co adsorption from single and binary aqueous solutions by Acacia nilotica leaf car-bon. Chin. J. Chem. Eng. 22 (11-12), 1193-1198.

Tran, H.N., You, S., Hosseini-Bandegharaei, A., Chao, H., 2017. Mistakes and in-consistencies regarding adsorption of contaminants from aqueous solutions: a critical review. Water Res. 120, 88 -116.

Ugbe, F.A., Ikudayisi, V.A., 2017. The kinetics of eosin yellow removal from aqueous solution using pineapple peels. Edorium J. Waste Manag. 2, 5-11.

Ullah, I., Nadeem, R., Iqbal, M., Manzoor, Q., 2013. Biosorption of chromium onto native and immobilized sugarcane bagasse waste biomass. Ecol. Eng. 60, 99-107.

Uyar, G., Kaygusuz, F.H., Erim, B., 2016. Methylene blue removal by alginatee clay quasi-cryogel beads. React. Funct. Polym. 106, 1-7.

Wang, E., Lei, S., Zhang, S., Huang, T., Zhong, L., 2015. Removal of methyl orange from aqueous solution by mineral-based porous granulated material. Wuhan Univ. Technol.-Mater. Sci. Edit. 30, 185-192.

Wang, Q., Luan, Z., Wei, N., Li, J., Liu, C., 2009. The colour removal of dye waste-water by magnesium chloride/red mud (MRM) from aqueous solution. J. Hazard Mater. 170 (2-3), 690-698.

Wang, T., Su, J., Jin, X., Chen, Z., Megharaj, M., Naidu, R., 2013. Functional clay supported bimetallic nZVI/Pd nanoparticles used for removal of methyl orange from aqueous solution. J. Hazard Mater. 262, 819-825.

https://doi.org/10.1016/j.heliyon.2018.e00838

Weber, J.W.J., Morris, J.C., 1963. Kinetics of adsorption on carbon from solution. J. Sanit. Eng. Div. ASCE 89 (SA2), 31-59.

Wu, F., Tseng, R., Juang, R., 2009. Characteristics of Elovich equation used for the analysis of adsorption kinetics in dye-chitosan systems. Chem. Eng. J. 150, 366-373.

Yagub, M.T., Sen, T.K., Afroze, S., Ang, H.M., 2014. Dye and its removal from aqueous solution by adsorption: a review. Adv. Colloid Interface Sci. 209, 172-184.

Yang, R., Li, D., Li, A., Yang, H., 2018. Adsorption properties and mechanisms of palygorskite for removal of various ionic dyes from water. Appl. Clay Sci. 151, 20-28.

Yang, S., Chen, S., Chang, Y., Cao, A., Liu, Y., Wang, H., 2011. Removal of methylene blue from aqueous solution by graphene oxide. J. Colloid Interface Sci. 359, 24-29.

Zaghouane-Boudiaf, H., Boutahala, M., Arab, L., 2012. Removal of MO from aqueous solution by uncalcined and calcined MgNiAl layered double hydrox-ides (LDHs). Chem. Eng. J. 187, 142-149.

Zhou, K., Zhang, Q., Wang, B., Liu, J., Wen, P., Gui, Z., Hu, Y., 2014. The inte-grated utilization of typical clays in removal of organic dyes and polymer nanocom-posites. J. Clean. Prod. 81, 281-289.

Zhou, Q., Gao, Q., Luo, W., Yan, C., Ji, Z., Duan, P., 2015. One-step synthesis of amino functionalized attapulgite clay nanoparticles adsorbent by hydrothermal carbonization of chitosan for removal of methylene blue from wastewater. Colloid. Surf. A Physicochem. Eng. Asp. 470, 248-257.

Zhou, Y., Zhou, L., Zhang, X., Chen, Y., 2016. Preparation of zeolitic imidazolate framework-8/graphene oxide composites with enhanced VOCs adsorption capacity. Micropor. Mesopor. Mat. 225, 488-493.

https://doi.org/10.1016/j.heliyon.2018.e00838

CHAPTER FOUR

Application of halloysite in the removal of dyes: A batch study.

This chapter has been accepted for publication in Clay Minerals - Journal of Fine Particle Science as: Ngulube T., Gumbo J.R., Masindi V., Maity A., 2019. Evaluation of the efficacy of halloysite nanotubes in the removal of acidic and basic dyes from aqueous solution.

This chapter addresses objectives (ii), (iii) and (v).

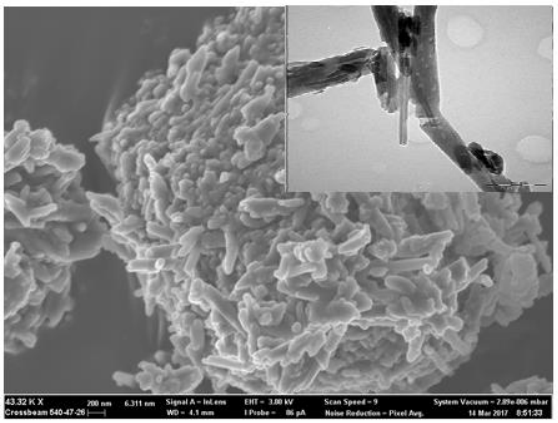

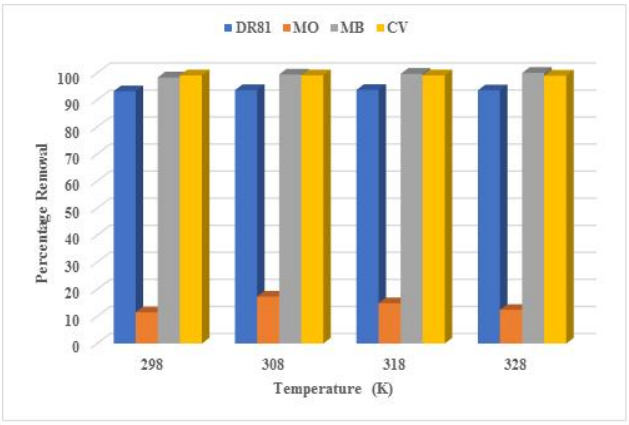

Evaluation of the efficacy of halloysite nanotubes in the removal of acidic and basic dyes from aqueous solution

♣Tholiso Ngulube [1], Jabulani Ray Gumbo[2], Vhahangwele Masindi [3&4] and Arjun Maity [5]

[1]Department of Ecology and Resources Management, School of Environmental Sciences, University of Venda, Private bag X5050, Thohoyandou, 0950, Limpopo, South Africa.
[2]Department of Hydrology and Water Resources, School of Environmental Sciences, University of Venda, Private bag X5050, Thohoyandou, 0950, Limpopo, South Africa

[3]Council for Scientific and Industrial Research (CSIR), Built Environment, Hydraulic Infrastructure Engineering, P.O BOX 395, Pretoria, 0001, South Africa.

[4]Department of Environmental Sciences, School of Agriculture and Environmental Sciences, University of South Africa (UNISA), P. O. Box 392, Florida, 1710, South Africa

[5]Smart Polymers Group, Polymers and Composites, Council for Scientific and Industrial Research (CSIR), Pretoria, South Africa

ABSTRACT

The present work describes the removal of Direct Red 81 (DR81), Methyl Orange (MO), Methylene Blue (MB), and Crystal violet (CV) from aqueous solution using halloysite nanotubes. The clay mineral was physico-chemically characterized using various methods. The influences of pH, interaction time, initial dyes concentration, adsorbent amount and temperature on adsorption were monitored and explained. As prevalently reported, acidic pH conditions favor the adsorption of pollutants from aqueous systems by clay materials but the highest percent removal on this study was possible over a wide range of pH conditions (pH ≥ 2 – 12). Adsorption was very rapid, and equilibrium was attained in 30 min. For all the four dyes studied, chemical reaction seemed significant as the rate-controlling step and the pseudo-second order chemical reaction kinetics provided the best correlation of the experimental data. Thermodynamically, the adsorption process was spontaneous with the Gibbs energy decreasing with rise in temperature. The results suggest that halloysite would be suitable for removing dyes from aqueous solution. This was further attested by using the halloysite nanotubes for the removal of complex dyes from printing and ink industry effluents.

Keywords: halloysite nanotubes, acidic and basic dyes, adsorption, kinetics, isotherms, thermodynamics.

1 INTRODUCTION

Coloured, toxic industrial waste is increasingly becoming a social and environmental problem. Via aquatic pathways, contaminants can spread through living organisms (Ngulube et al., 2017). This has made scientists to develop numerous techniques to eliminate dyes from

♣ Corresponding author: Email; tholisongulube@gmail.com

wastewater (Yang et al., 2018). Adsorption is among the methods used for water treatment because of low startup costs, less complicated design and ease of operation and implementation even in small plants (Mu and Wang, 2016). Because of stringent laws concerning the removal of dyes from wastewaters before their discharge into the aquatic environment and costly conventional adsorbents, there is a growing tendency to develop new, acceptable and low-cost adsorbents with improved adsorption properties and are inexpensive to regenerate (Yagub et al., 2014).

Various available, abundant and naturally occurring materials have been explored as adsorbents for dye treatment (Sarma et al., 2016; Santos et al., 2016). Great attention is growing towards natural adsorbents, preferably the development of an adsorbent demonstrating both low cost and high adsorption capacity for removing contaminants from polluted waters. Though a variety of sorbents have been used for water decontamination, naturally available clays have been the adsorbents of choice in most developing countries (Adebowale et al., 2014; Kausar et al., 2018). It is extremely important to choose a technique that is cheap and requires minor workload. Using clay minerals and soils fits well with the above-mentioned parameters.

Halloysite clay is one of these inexpensive adsorbents applied for decolourization of dyed wastewater. Halloysite ($Al_2Si_2O_5(OH)_4 \cdot nH_2O$) was originally defined as a dioctahedral 1:1 clay mineral belonging to the kaolin group by Berthier (1826). Halloysite clay has a similar structure as kaolinite but it is rolled in tubes with a diameter of 50 nm and a length of 1000 nm (Słomkiewicz et al., 2015). The value of n is zero for kaolinite and up to 4 for halloysite. Halloysite clay displays higher adsorption capacity for both acidic and basic dyes because of the presence of a negative SiO_2 outmost and positive Al_2O_3 innermost surface; thus, it has effective bivalent adsorbancy (Zhao et al., 2013).

The objective of the present study was to evaluate the adsorption of 2 anionic and 2 cationic dyes, Direct Red 81 (DR81), Methyl Orange (MO), Methylene Blue (MB) and Crystal violet (CV) respectively which are usually used in the textile industry, and to evaluate the influence of several parameters on the adsorption capacity of halloysite clay. After which, adsorption kinetics and isotherm studies were undertaken to determine the adsorption capacity of the clay. Many studies have been done on the removal of dyes using halloysite under different experimental conditions. However, most of the studies focus on an individual dye and only focus on synthetic dye solutions. In this study, halloysite clay was tested across four different dyes (two cationic and two anionic). This provided an opportunity to deliver a comparative

analysis on how the halloysite material works with differently charged dyes under the same experimental conditions. There are still few studies that test their adsorbent materials on real coloured industrial effluent. For this study, a step further was taken to test the halloysite material on real industrial wastewater to ascertain the feasibility of the adsorbent in the real-world applicability.

2 MATERIALS AND METHODS

2.1 Materials

Halloysite nanoclay – kaolin clay was purchased from Sigma Aldrich (South Africa). MO, MB, CV, HCl, KCl and NaOH pellets were purchased from Rochelle Chemicals (South Africa). DR81 was purchased from Sigma Aldrich (South Africa). Real industrial effluent was collected from a printing and ink industry.

2.2 Batch removal studies

Deionised water (ELGA, Micra Veolia Water Solution and Technologies, UK) was used to prepare dye solutions. The dye solutions were prepared separately by dissolving appropriate amounts of dry powder dye accurately weighed on an electronic balance (RADWAG electronic balance, Wagi Elektroniczen, Poland) in deionized water to prepare a stock solution (1000 mg/L). Experimental solutions were obtained by serial dilutions to obtain the working solutions at desired concentrations. The final concentration of dyes was estimated for each sample through absorbance at the wavelength corresponding to the maximum absorption peak (λmax = 510, 505, 664 and 590 nm for DR81, MO, MB and CV respectively) using a spectrophotometer (Thermoscientific Orion Aqua Matte 7000, China). Adsorption experiments were performed to investigate the removal of dyes as a function of solution pH (2, 4, 6, 8, 10 and 12), initial dye concentration (1, 5, 10, 20, 30 and 40 mg/L), temperature (25, 35, 45 and 55 ^{o}C), contact time (10, 15, 20, 30, 60 and 90 min) and adsorbent dosage (0.1, 0.2, 0.4, 0.8, 1.0 and 2 g). A batch adsorption study was carried out in 250 mL glass erlenmeyer flasks containing 50 mL dye solution of desired concentrations. The solution pH was adjusted using either 0.1 M of HCl or 0.1 M NaOH solution. The solutions were shaken on a reciprocating table shaker (Labotec, Model 207, South Africa) at various time intervals at 250 rpm. After the equilibration time, the solutions were left to settle for 30 min and the supernatant solution absorbance was recorded by a VIS spectrophotometer. The corresponding dye concentration was obtained using a constructed calibration graph from prepared standard solutions. All the

experiments besides that of temperature variation were carried out at room temperature (25 ± 3 ^{o}C). To verify the reproducibility of the results, the experiments were carried out in triplicate and the mean values were reported.

2.3 Characterization

X-ray diffraction patterns of halloysite were acquired on a PANalytical X'Pert PRO-diffractometer. To determine the functional groups of halloysite, spectra were recorded using FTIR spectrometer (Bruker, Alpha, USA). Transmission Electron Microscope (TEM) images were acquired with a JEOL JEM-2100F Field Emission (JEOL, Japan). Point of zero charge (PZC) was determined by solid addition method as described by Izuagie et al. (2016). Surface area was determined using Brunauer Emmett Teller (BET) analysis (Micromeritics Tristar II, Norcross, GA, USA). Characterization of wastewater was done using an Inductively Coupled Plasma Mass Spectrometry (ICP-MS) (7500ce, Agilent, Alpharetta, GA, USA).

2.4 Adsorbent regeneration

The regeneration potential of halloysite was evaluated by using 0.01 M NaOH. An adsorption experiment was done using 2 g clay, 50 mL volume of solution and 10 mg/L concentration of each dye. The amount of dye adsorbed was noted and the adsorbent was dried in the oven for 12 h at 105 ^{o}C. The adsorbent was then soaked in 50 mL, 0.01 M NaOH solution and the mixture was centrifuged at 5 000 rpm for 15 min. The adsorbent was washed using 50 mL MilliQ water. The desorbed adsorbent was then dried in the oven for 12 h at 105 ^{o}C and then cooled in a desiccator. The dried adsorbent was used for another adsorption experiment as described above. The same procedure using the same adsorbent was repeated three times. A blank sample made up of deionized water was used for comparison purposes.

3 RESULTS AND DISCUSSIONS

3.1 Characterization

3.1.1 X-ray Diffraction study

X-ray diffraction pattern of raw halloysite and DR81-MO-MB-CV–adsorbed halloysite is shown in Figure 1.

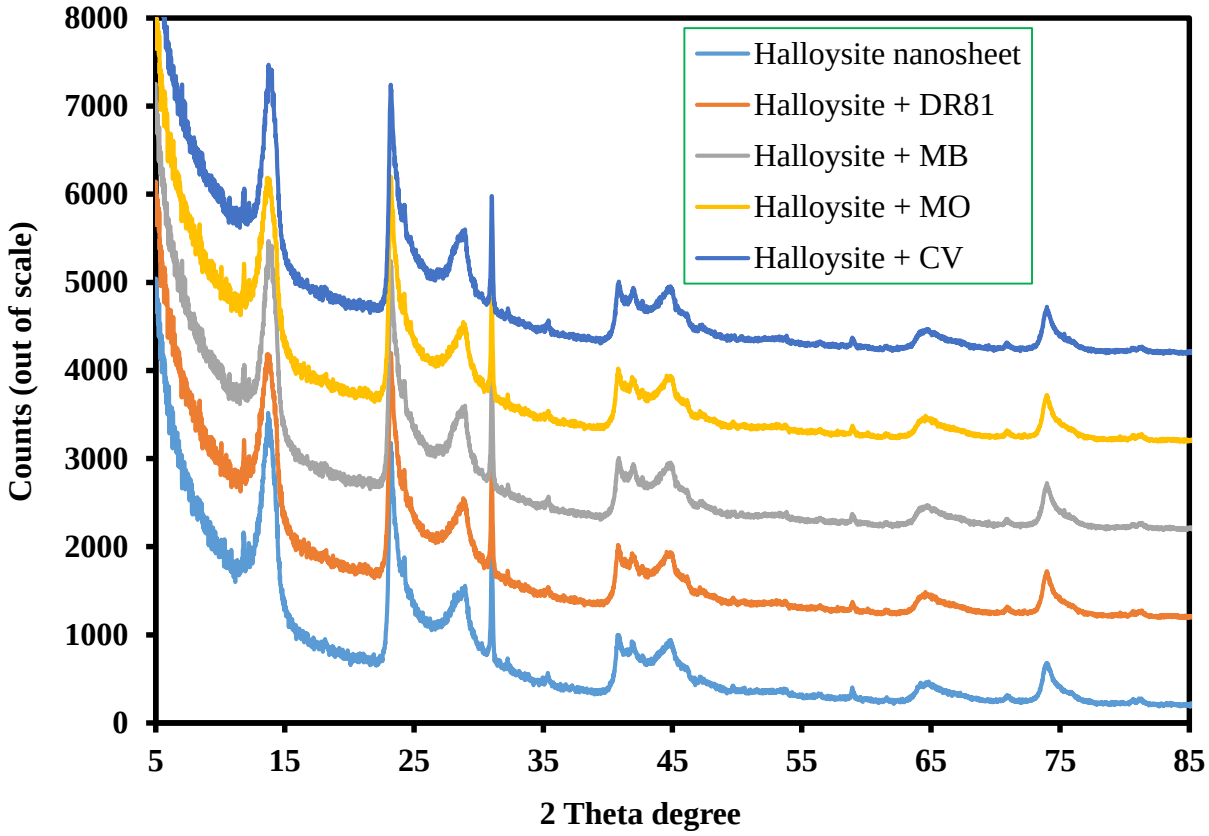

Figure 1. X-ray diffraction pattern of raw halloysite and DR81-MO-MB-CV -adsorbed halloysite,

The crystal structures of raw halloysite and dye adsorbed halloysite were studied by X-ray diffraction. As shown in Figure 1, there is no significant difference between raw halloysite and dye adsorbed halloysite. The diffractograms showed sharp peaks at 13.95, 23.23 and 31.02° (2θ). The results agree with the previous reports on halloysite nanotubes (Liu et al., 2015; Jiang et al., 2015). The identified peaks are characteristic of quartz (SiO_2), kaolinite ($Al_2Si_2O_5OH_4$) and halloysite ($Al_2Si_2O_5OH_4$) (Zhang et al., 2012). The similarity of raw halloysite and dye adsorbed halloysite diffractograms shows that the dye adsorption process did not alter the crystallogy and major mineral phase of halloysite.

3.1.2 Fourier Transform InfraRed study

FTIR spectra of raw halloysite and DR81-MO-MB-CV -adsorbed halloysite are shown in Figure 2.

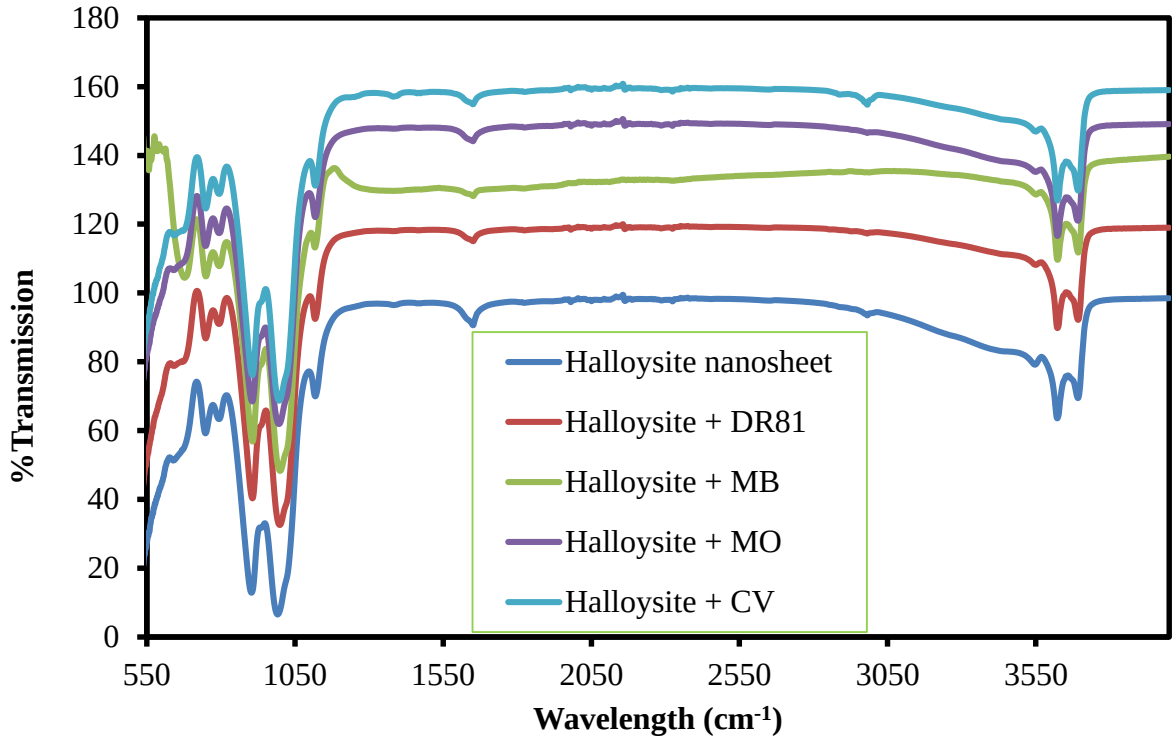

Figure 2. FTIR spectra of raw halloysite and DR81-MO-MB-CV -adsorbed halloysite

The FTIR spectra in the range 4050 – 550 cm^{-1} is shown in Figure 2. The FTIR spectra of the halloysite displayed bands that are representative of kaolin minerals related to the OH-stretching region (3700 cm^{-1}) (Luo et al., 2010) and bands associated with stretching and bending vibrations of aluminosilicate framework (~1200 cm^{-1}) (Prokop et al., 2015). Xie et al. (2011) also reported double peaks at 3696 and 3623 cm^{-1} for halloysite nanotubes and the authors mentioned that the peaks were due to the stretching vibrations of hydroxyl groups at the surface of the nanotubes. FTIR analysis is an important tool to identify the characteristic functional groups that might be responsible for dye binding (D'Souza et al., 2008). The FTIR spectra of unloaded and dye loaded halloysite are shown in Figure 2 and it is very clear that there is no notable difference between the peaks before and after adsorption. Since no significant difference is noted, it can be said that the functional groups (hydroxyl and aluminosilicate) noted in the FTIR spectra were not well involved in the dye removal process of the four dyes.

3.1.3 Transmission Electron Microscopy studies.

TEM images of (A) & (B)-raw halloysite and (C)-DR81, (D)-MO, (E)-MB, (F)-CV adsorbed halloysite are shown in Figure 3. Raw halloysite images (A and B) present predominate halloysite nanotubes, among which exhibit some hollow rod like structures (Ahmed et al., 2010). The lengths of halloysite nanotubes are between 500 –700 nm, and their inner diameter and outer diameters are 40 – 60 nm. The images clearly indicate empty lumens of halloysite with some rod like structures found inside the empty lumens. This is clearly visible in image (C) and (F). When the images of raw halloysite (A and B) are compared with the dye adsorbed images (C) – (F), additional material has been added to the walls of the tubes on the dye adsorbed halloysite. More shades of dark material are observed in the images (C) – (F) and this is a confirmation of dyes being adsorbed onto the interlays of the clay. However, the halloysite material still maintains its tubular structure even after dye adsorption.

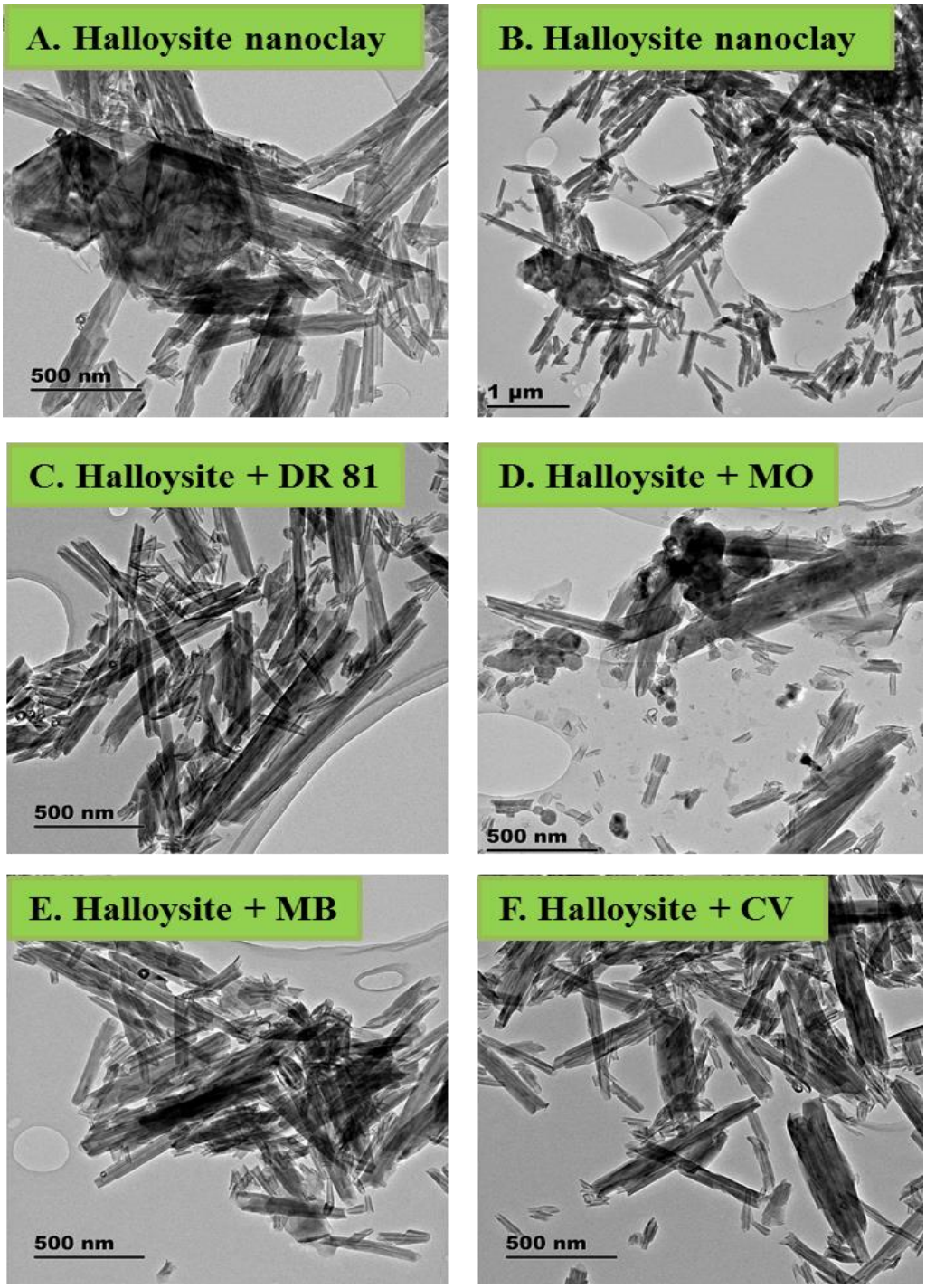

Figure 3. TEM images of (A) & (B)-raw halloysite and (C)-DR81, (D)-MO, (E)-MB, (F)-CV adsorbed halloysite.

3.1.4 Scanning Electron Microscopy.

SEM images of (A–B)-raw halloysite and (C)-DR81, (D)-MO, (E)-MB, (F)-CV adsorbed halloysite are shown in Figure 4.

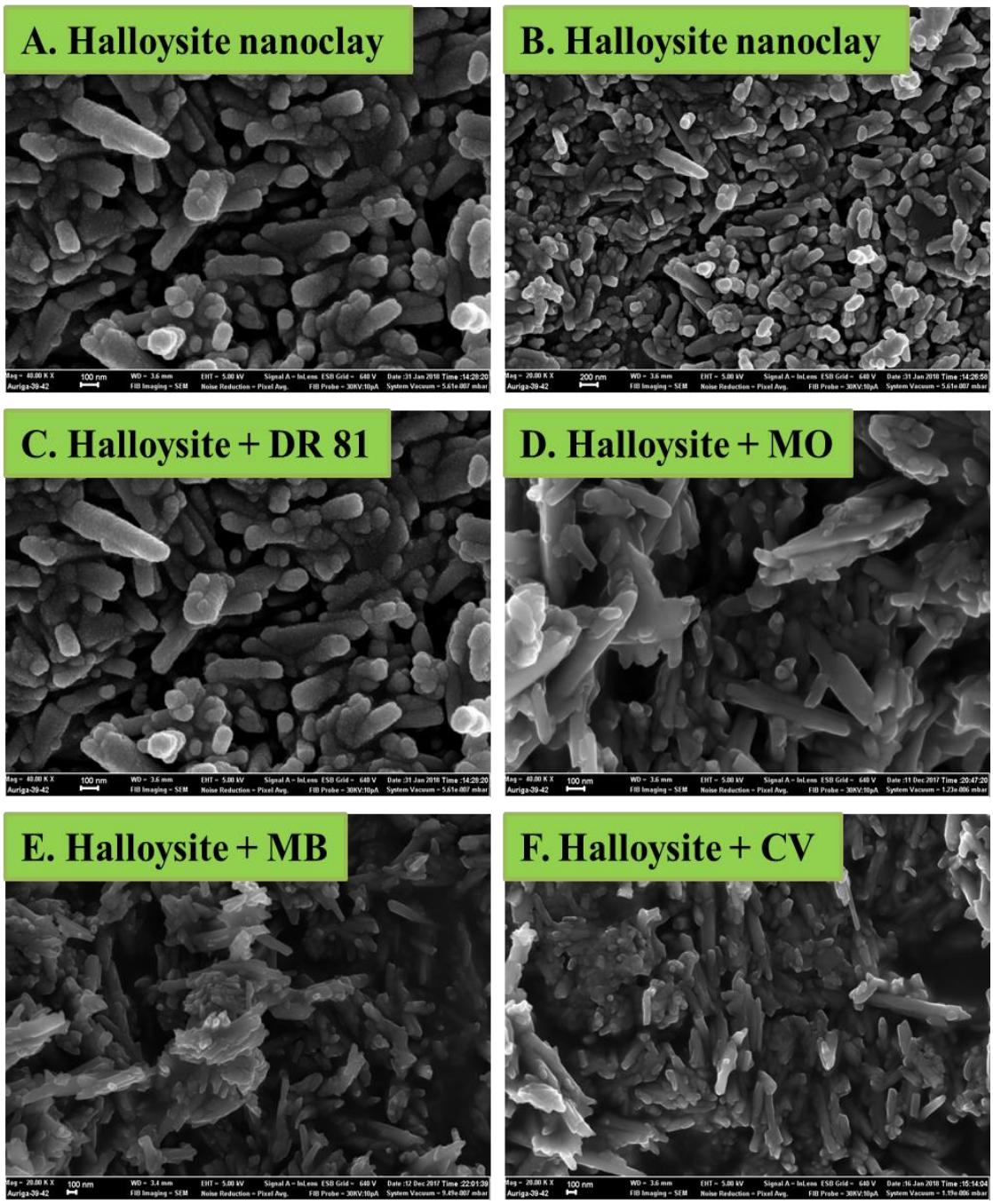

Figure 4. SEM images of (A–B)-raw halloysite and (C)-DR81, (D)-MO, (E)-MB, (F)-CV adsorbed halloysite

Scanning electron microscopy (SEM) was used to view the morphology and fundamental physical properties on the surface of halloysite before and after dye adsorption. Generally, halloysite contains agglomerates of nanotubes with some irregularities in diameter, wall thickness and a fibrous morphology (Kamble et al., 2012). The SEM images of unloaded and dye loaded halloysite are shown in Figure 4(A)-(B) and (C)-(F), respectively. The surface morphology indicates that unloaded halloysite has an uneven surface, but smoother surface

compared to the dye adsorbed halloysite. The SEM images showed that after dye adsorption, the surface morphology changed considerably, which indicates that dye molecules adsorbed onto the surface and inside the available spaces because a more uniform surface in loaded halloysite is observed especially for MB adsorbed halloysite - (E) and CV adsorbed halloysite - (F). Previous studies also revealed that the surface of the adsorbent changed to a more homogenous form versus unloaded adsorbent in loaded adsorbents (Sarma et al., 2016). The appearance of MO - (D) and CV - (F) adsorbed halloysite however has a different morphology. The images show rod like structures of the clay clearly confirming the tubular structure of halloysite. Image (D) shows a homogenous surface but with flakes that are fluffy in appearance with different sizes and shapes. The fibrous surface topography of the clays is expected to increase the degree of unsaturation of the surface with dangled bonds and free valences, thus amassing the total surface area of the clay (Ngulube et al., 2017).

3.1.5 Brunauer–Emmett–Teller (BET) analysis.

High adsorption capacities of clay materials are largely due to their high surface areas (Cadena et al., 1990). Various studies have demonstrated that the surface area of a clay is directly proportional to the adsorption capacity of the clay (Sarma et al., 2016; Santos et al., 2016). As shown in Table 1, halloysite has a BET surface area of 41.94 m^2/g which is comparable higher compared to other clays. Several studies on dye adsorption have reported on clay surface area and these include: Montmorillonite, kaolinite and Na-bentonite with surface areas of 42.71, 18.40 and 12.74 m^2/g respectively (Park et al., 2011; Gu et al., 2014; Sari and Tuzen, 2014). Comparison between raw halloysite (H) and dye adsorbed halloysite (HDR81, HMO, HMB and HCV) showed an increase in surface area after dye adsorption and the highest surface area was observed for HMO. High specific surface area is associated with high soil-water-contaminant interaction, which indicates high reactivity (Pennel, 2016). Theoretical relationships for surfaces of various particle geometries show that surface area is controlled by the smallest dimension of the particle. There is a double effect of particle size on specific surfaces such that as the particle size decreases, surface area increases not only due to the inverse relationship between specific surface and size, but also because the shape of small particles tends towards platy and rod-like geometries (Santamarina et al., 2002). After adsorption of the four dyes, there is a clear change in the shape of the particles (SEM images, Figure 4), particularly with the DR81 adsorbed halloysite showing platy geometries hence this could be the cause of the increase of the surface area after dye adsorption. Previous studies have shown that kaolinite pores are more open, and this gives a greater pore diameter of slit-

shaped pores of the structure (Boukhemkhem and Rida, 2017). As explained under 3.1.4, the fibrous surface topography of the clays is expected to increase the degree of unsaturation of the surface with dangled bonds and free valences, thus amassing the total surface area of the clay (Ngulube et al., 2017).

Table 1. Surface areas of raw halloysite (H), DR81 adsorbed halloysite (HDR81), MO adsorbed halloysite (HMO), MB adsorbed halloysite (HMB) and CV adsorbed halloysite (HCV).

	Single point surface area (m^2/g)	**BET Surface Area (m^2/g)**	**Langmuir Surface Area (m^2/g)**
Halloysite	40.9725	41.9418	57.4141
HDR81	44.7224	45.8406	62.7893
HMO	45.4613	46.6220	64.9594
HMB	42.4226	43.5305	60.9756
HCV	42.8736	43.9718	60.3304

3.2 Batch removal studies

The effect of contact time, adsorbent dosage, initial concentration, pH, temperature, and point of zero charge (PZC) is shown in Figure 5.

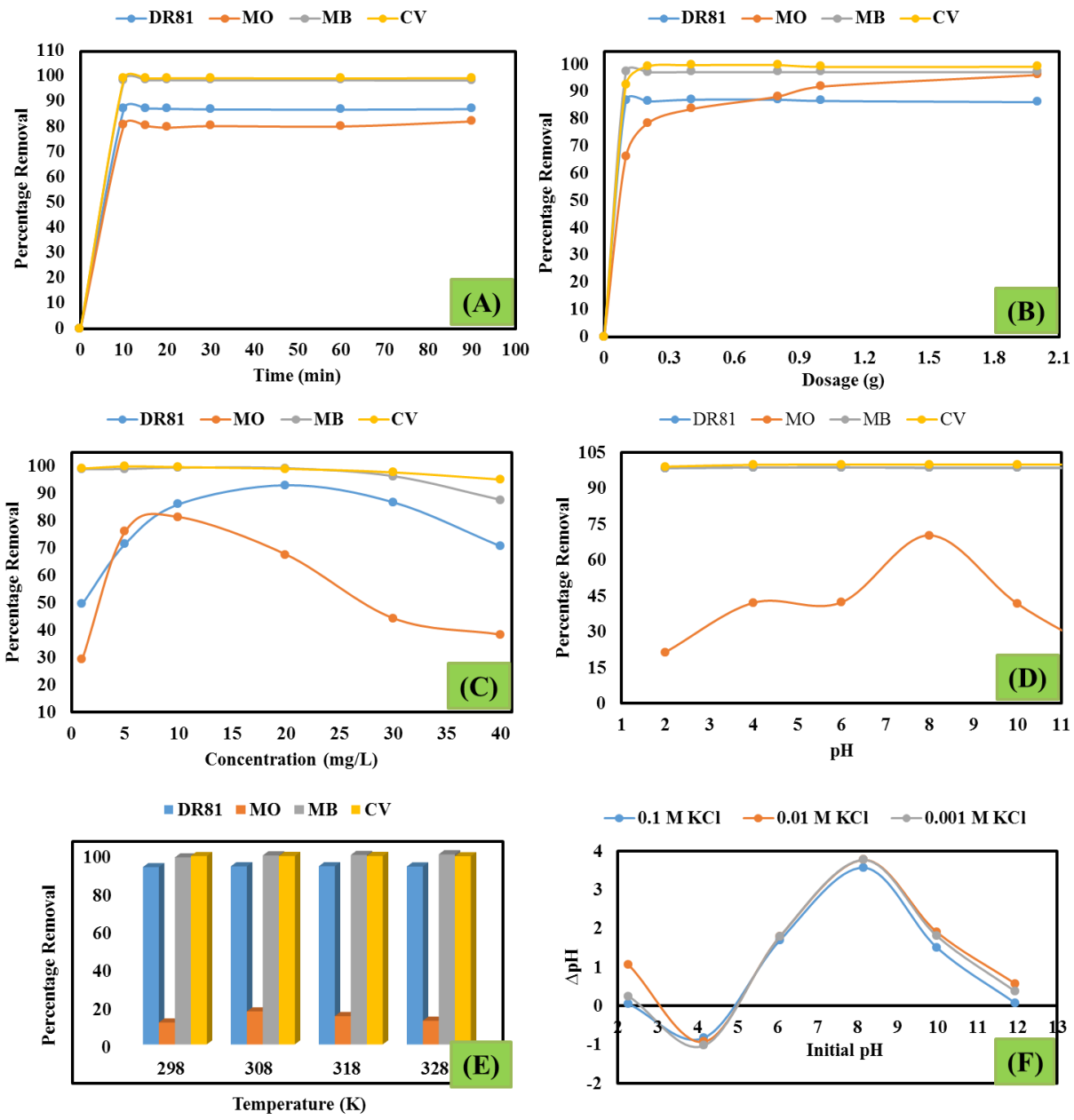

Figure 5. Removal of DR81, MO, MB and CV by halloysite as a function of (A)-contact time, (B)- dosage, (C)-initial dye concentration and (D)-pH, (F) – temperature and (F) – Halloysite Point of Zero Charge

3.2.1 Effect of time.

Contact time helps in determining the optimum time at which equilibrium is attained. Depending on wastewater process design, this information can be used in wastewater treatment plants. The results of tests done to determine the equilibrium time are shown in Figure 5 (A). The percentage removal shows that the adsorption of all dyes was almost the same for all the contact times used. The percentage removal decreased insignificantly linearly with time. The

range of percentage removal of MB and CV was from 98% to 99% whereas that of DR81 ranged from 86% to 87% and finally that of MO was the lowest ranging from 79% to 90%. The near constant percent removal values after 30 min indicates that the adsorbent was approaching its optimum performance hence 30 min was selected as the optimum contact time for subsequent experiments.

3.2.2 Effect of adsorbent dose.

Sorbent dosage has a substantial effect on adsorption processes and the effect is shown in Figure 5(B). It is observed that increasing the adsorbent dose increased the percentage removal of the dyes. Ciesielczyk et al. (2017) reported the same trend for their study. Increasing adsorbent dosage at a constant volume and dye concentration leads to the saturation of adsorption sites. Due to particulate interaction, such as formation of aggregates at higher doses there might be a decrease in adsorption capacity because aggregation would lead to a decrease in total surface area of the adsorbent and decreased diffusion path length (Sarma et al., 2016).

3.2.3 Effect of initial dye concentration.

The effect of initial dye concentration is shown in Figure 3(C). By increasing initial dye concentration to 20 mg/L, the percentage removal of DR81 and MO increased after which a reduction was observed from 20 mg/L - 40 mg/L. However, the percentage removal of CV and MB showed a different trend of a gradual decrease as the initial dye concentration was increased from 1– 40 mg/L. Similar trends have been reported previously (Anirudhan and Ramachandran, 2015; Yu et al., 2015) where the concentration of the dye is a driving force to overcome mass transfer resistance of dye molecules between the solid and the aqueous phases. Low concentrations of dye have more active adsorption sites available for adsorption hence at this stage adsorption is independent of initial concentration. However, as the concentration is increased the available sites are occupied and ultimately a decrease in dye removal is observed (Ogunmodede et al., 2015).

3.2.4 Effect of pH.

pH affects the adsorption of dyes due to the effect it has on the surface characteristics of the adsorbent (Ngulube et al., 2018). The pH of a solution pH determines the degree of protonation of hydroxide exchange sites and the adsorbate hence influencing the specific charge of exchange sites and eventually the adsorption tendency of the adsorbent (Tomar et al., 2014). Results from this study (Figure 5D) show that, for DR81, MB and CV, pH had a negligible

influence in the percentage removal of the dyes because from pH 2 – pH 12, the percentage removal was almost the same. Alike results showing negligible pH influence were also described by Santos et al. (2016). For MO, maximum percentage removal was observed to be 70.24 % at pH 8, the percentage removal was below 40% for all other pHs. MO molecules have different charges at different pHs (Subbaiah and Kim, 2016). The dissociation constant (pKa) for MO is 3.46 (Arshadi et al., 2016), hence MO species will mainly exist as monovalent anions at this equilibrium pH. Below and above this pH, MO will go through a protonation process determining the charge it carries. Due to the protonation reaction ($\equiv RN(CH_3)_2 + H^+ \rightarrow \equiv RNH^+(CH_3)_2$), MO is positively charged at pH < 3.76 (Yao et al., 2018). On one hand, halloysite surface is also positively charged hence the poor adsorption because of repulsive forces of same charged particles. As pH is increased, it becomes clear that MO has fewer positive charges thus the enhanced MO adsorption on halloysite is accredited to hydrogen bonding, electrostatic attraction and strong surface complexation (Xiang et al., 2014). At alkaline pHs up to 12, the electrostatic repulsion and OH^- competition leads to a decrease in the adsorption of anions (Cheah et al., 2013).

3.2.5 Effect of temperature.

Generally, temperature has a significant effect on reaction rate. When temperature rises, chemical reaction rate also increases (Mekatel et al., 2015). Therefore, temperature plays a crucial role in adsorption processes. The rise or fall of adsorption capacity with temperature determines the adsorption type. An increase in adsorption capacity with temperature shows an endothermic reaction whereas a decrease in adsorption capacity with increasing temperature symbolizes an exothermic process (Zulfikar, 2013). The effect of temperature on dye adsorption was investigated and the results are shown in Figure 5(F). The results showed that the increase or decrease of temperature did not have a considerable effect on the percentage removal of all four dyes indicating that there is no need to adjust temperature for halloysite to effectively remove dyes from aqueous solution.

3.2.6 Point of zero charge studies.

Point of zero charge (pHpzc) is one of the important factors that can help tell the type of surface-active centers on the adsorbent which aid in adsorption processes (Yagub et al., 2014). Positively charged dye adsorption is enhanced at pH > pHpzc due to the presence of functional groups like hydroxide ions whereas, negatively charged dye adsorption is enhanced at pH < pHpzc where the surface of the adsorbent is positively charged (Ngulube et al., 2017). When

the pH is higher than the PZC, the surface charge of halloysite is negative, while it is positive when the pH is lower than the PZC. Figure 5(F) shows that the PZC of halloysite is 5. According to the PZC results, it is expected that the adsorption of MB and CV be highest pH > 5 and that of DR81 and MO highest at pH < 5. However, Figure 5(D) shows that the variation of pH had a negligible influence in the percentage removal of the dyes except MO dye. This could mean that the adsorption of the other three dyes was not predominantly affected by surface charges of halloysite.

3.3 Treatment of real industrial effluent

The process of adsorption was also applied to a sample of real textile effluent as shown in Figure 6.

Figure 6. Real industrial effluent before and after treatment with halloysite nanoclay.

The raw wastewater physical characterization of a textile mill wastewater was carried out for colour, Total Dissolved Solids, Electrical Conductivity, Turbidity, Total Suspended Solids and pH. The results of the wastewater characteristics before and after treatment with halloysite nanoclay are presented in Table 2. Characterization of wastewater indicate that the wastewater is categorized under high strength wastewater (Benefield, 2002). After treatment with halloysite clay, the wastewater could be characterized under medium strength wastewater. The experiment was carried out at the optimum conditions determined on the batch study. The dye removal efficiency was satisfactory recording a 79.25, 90.01, 92.22 and 92.22% removal at the absorbance value of DR81, MO, MB and CV respectively. The removal of colour can also be

observed from Figure 6 where a colour change before and after halloysite is seen changing from black to milky white.

Table 2. Characterization of actual industrial effluent

Analyzer parameter	**Industrial effluent before treatment with halloysite**	**Industrial effluent after treatment with halloysite**
Total dissolved solids, TDS (mg/L)	1219	1068
Total suspended solids, TSS (mg/L)	918	785
Electrical Conductivity (µS/m)	1764	1504
Turbidity (NTU FNU)	0.01	246
pH	8.77	8.20
Colour	black	milky white

3.3 Adsorption kinetics studies

Adsorption kinetics are important in determining the effectiveness of adsorption. In this study, two models were used to predict the adsorption kinetics of DR81, MO, MB and CV onto halloysite.

3.3.1 The pseudo first order model.

The pseudo first order kinetic model has been widely used to predict dye adsorption kinetics. A linear form of pseudo-first-order model was described by Ho and McKay (1998) and it can be expressed as:

$$\log(q_e - q_t) = \log(q_e) - \left(\frac{k_1 t}{2.303}\right) \qquad (1)$$

Where q_e (mg/g) is the adsorption capacity at equilibrium, q_t (mg/g) is the adsorption capacity at time t, and K_1(1/min) is the rate constant.

3.3.2 Pseudo second order model.

The pseudo second order model, which has been applied for analyzing chemisorption kinetics from liquid solutions based on solid phase sorption (Ho, 2006) is linearly expressed as:

$$\frac{t}{q_t} = \left(\frac{1}{q_e}\right) t + \left(\frac{1}{k_2 q_e^2}\right) \ldots \ldots \ldots (2)$$

Where q_e (mg/g) is the capacity of adsorption at equilibrium, q_t (mg/g) is the capacity of adsorption at time t, k_2 is the rate constant (g/mg/h), $k_2 q_e^2$ (mg/g/h) is the initial adsorption rate.

The conformity between experimental data and model predicted values was expressed by the coefficient of determination R^2. The experimental data could not fit the pseudo first order model hence its application was dismissed. The curves of the plots are given in the supplementary material and the calculated kinetic parameters and the corresponding linear regression coefficient of determination R^2 values are summarized in Table 3. There is a good agreement between experimental and calculated Qe for DR81 and MB dyes. The correlation coefficients for the pseudo second-order kinetics model (R^2) are all equal to 1, indicating the applicability of this kinetic model and the second-order nature of the adsorption process of the dyes onto halloysite clay. These results imply that chemisorption mechanism may play an important role for the adsorption of DR81, MO, MB and CV.

Table 3. The pseudo first order and pseudo second order parameters for adsorption of DR81, MO, MB and CV onto halloysite

Parameter	**DR81**	**MO**	**MB**	**CV**
Pseudo first order				
R^2	#N/A	#N/A	#N/A	#N/A
Pseudo second order				
Qe (mg/g) experimental	4.3553	0.2055	4.9219	1.2419
Qe (mg/g) calculated	4.3668	4.7847	4.9285	5.2192
k_2 (g/mg/h)	0.0001	1154329.94	6.0725	630.56
R^2	1	1	1	1

3.4 Adsorption isotherm studies

An adsorption isotherm describes the relationship between the amount of adsorbate adsorbed by the adsorbent and the remaining adsorbate concentration in the solution. Adsorption equilibrium studies were done using two adsorption isotherms.

3.4.1 The Langmuir isotherm.

This describes the formation of a monolayer adsorbate on the outer surface of the adsorbent, and after that no further adsorption takes place (Langmuir, 1918). Based upon these assumptions, Langmuir represented the following equation:

$$\frac{C_e}{q_e} = \left(\frac{1}{Q_m}\right) C_e + \frac{1}{Q_m b} \quad \ldots\ldots (3)$$

Where *Ce* is the equilibrium concentration (mg/L), *Qe* is the amount adsorbed at equilibrium (mg/g), *b* represents the Langmuir isotherm constant (L/mg) and *Qm* is the maximum adsorption capacity (mg/g) for a complete monolayer coverage.

The separation factor (R_L) was calculated from this relationship:

$$\mathrm{R_L} = \frac{1}{(1 + bCo)} \quad \ldots\ldots (4)$$

$\mathrm{R_L}$ values between 0 and 1 indicate favourable adsorption, 0 indicates irreversible adsorption, 1 means linear adsorption while a value greater than 1 indicates an unfavorable adsorption.

3.4.2 The Freundlich isotherm.

The Freundlich model is an isotherm commonly used to describe heterogeneous systems (Freundlich, 1906). The model is represented in linear form as:

$$log Q_e = \frac{1}{n}\, log\, C_e + log\, K_F \quad \ldots\ldots (5)$$

K_F (mg/g) and *n* are the Freundlich constants, describing the adsorption capacity and intensity respectively. The constants *n* and K_F are determined from the slope and the intercept of the plot $log\ Q_e$ versus $log\ C_e$. When the value of n lies between 1 and 10 it represents beneficial adsorption (Kadirvelu and Namasivayam, 2000).

The equation parameters of the equilibrium models give insight into the adsorption mechanism, the surface properties and affinity of the adsorbent. From a comparison of the correlation coefficients values, the Langmuir isotherm gave high coefficients of determination for MO, MB and CV dyes and it seemed to be the best fitting model for adsorption of the dyes onto halloysite (Table 4). The Freundlich isotherm gave low coefficients of determination for all the dyes hence the parameters of the Langmuir isotherm were taken into consideration to try and describe the mechanisms of adsorption. The dimensionless equilibrium separation factor, R_L, which is used to estimate whether the adsorption process is favorable ($0 < R_L < 1$), linear ($R_L = 1$), unfavorable ($R_L > 1$) or irreversible ($R_L = 0$) was considered. The R_L values for all the dyes were less than 1. The values show that adsorption of the dyes was a favorable process.

Table 4. Parameters of the Langmuir adsorption isotherms for the system of DR81, MO, MB and CV adsorption onto halloysite clay

Parameters	**DR81**	**MO**	**MB**	**CV**
		Langmuir isotherm		
Qm cal (mg/g)	67.57	104.17	185.16	5.22
Qm exp (mg/g)	14.11	0.38	17.51	4.75
Ka (L/mg)	85.25	110.82	119.45	12.08
R_L	0.3719	0.2775	0.1777	0.8846
R^2	0.0083	0.8033	0.9969	0.9784
		Freundlich isotherm		
R^2	0.6589	0.6321	0.7975	0.8093
n	0.8599	1.2097	0.1831	1.8278
***K_F* (mg/g)**	1.7037	0.0428	12.4824	4.3642

3.5 Thermodynamic studies

Values of thermodynamic parameters are the actual indicators for practical application of a process (Yakout and Elsherif, 2010). ΔG^o (kJ/mol), as well as enthalpy: ΔH^o (kJ/mol) and entropy ΔS^o (J/mol/ K) were determined by using the following equations.

The standard free energy change ΔG was calculated using the following equation:

$$\Delta G^O = -RT \ln Ka \quad \ldots\ldots (6)$$

where ΔG is the free energy of sorption (kJ/mol), T is the temperature in Kelvin (K), R is the universal gas constant (8.314 J/mol/ K) and Ka is the sorption equilibrium constant.

The sorption equilibrium constant Ka can be expressed in terms of enthalpy change (ΔH) and entropy change (ΔS) as a function of temperature and is shown below:

$$lnKa = \frac{\Delta H^O}{RT} + \frac{\Delta S^O}{RT} \ldots\ldots\ldots\ldots\ldots\ldots\ldots\ldots (7)$$

where ΔH^O is the heat of sorption (kJ/ mol) and ΔS^O is the standard entropy change (kJ/mol/ K).

Table 5. Thermodynamic parameters for the system of DR81, MO, MB and CV adsorption onto halloysite clay

Parameters	DR81	MO	MB	CV
ΔGº kJ/mol	-15341.01	-7242.34	-4560.09	-12917.68
ΔHº (kJ/mol)	-25776.73	3745.21	547.29	219.57
ΔSº (kJ/mol/K)	-5.22	4.59	23.22	4.23
Ka (L/g)	331189.87	4.57	1.26	1.09

The corresponding values for thermodynamic parameters have been calculated and given in Table 5. The values show that the enthalpy of activation, ΔHº, is positive for all the dyes except for DR81. Positive values for the enthalpy of activation indicate that activation of the adsorption process for MO, MB and CV is endothermic whereas that of DR81 is exothermic because the values is negative. The free energy is spontaneous (negative ΔGº) for all the dyes and the negative value for entropy, ΔSº, for DR81 indicates that no significant changes occurs at the activation stage. However, for MO, MB and CV, the entropy values were positive indicating that there was a change in the internal structure of the halloysite material during the adsorption process (Ofomaja et al., 2010).

3.6 Regeneration studies

Regeneration feasibility of halloysite clay for the removal of acidic and basic dyes from aqueous solution is shown in Figure 7.

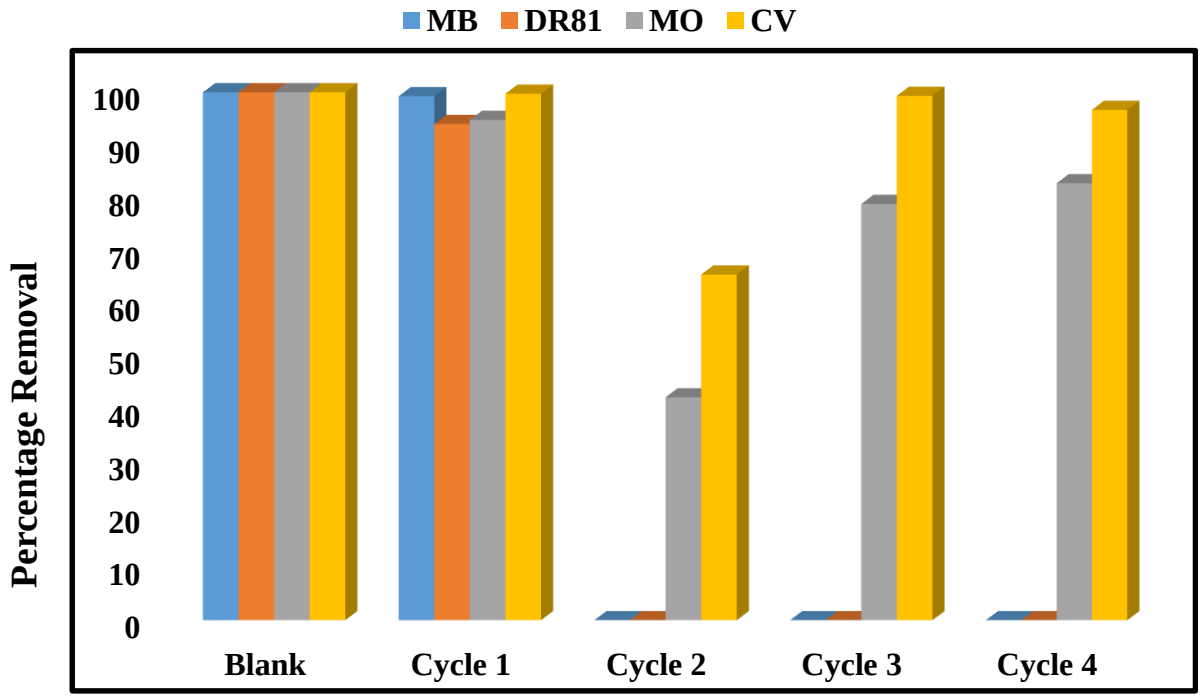

Figure 7. Regeneration of halloysite clay

As can be seen from Figure 7, the spent adsorbent has less adsorption capacity as compared to the fresh adsorbent. There is however an interesting observation with regards to the different dyes. MB and DR81 adsorbed clays show a similar trend whereas CV and MO adsorbed clays show a slightly different trend. The former shows that after one adsorption experiment, the spent adsorbent lost its capacity to remove dyes on successive experiments. The latter trend shows that, adsorption capacity decreased after the 1st regeneration cycle but for successive cycles, the percentage removal increased as the halloysite was being regenerated. This behavior showed that CV and MO adsorption is chemical in nature. Adsorption was reversible and adsorbed CV and MO could be completely recovered with the alkaline solution. A likely explanation could be that MO is an acidic dye and therefore there will be electrostatic interactions with the alkaline solution hence the reversible reactions. CV is an organic compound that is water-soluble, and it contains a violet cation. Adding NaOH converts the cation into a carbonyl base and the polarity of oxygen also makes the alpha hydrogens of carbonyl compounds much more acidic hence possible electrostatic attractions between an acid and a base (Cannon et al., 1994).

3.7 Adsorption mechanisms

Results of the adsorption studies and characterization analysis allow us to highlight some issues of major importance in the adsorption of the anionic and cationic dyes on the halloysite clay. These results can furthermore help us to propose processes involved during the adsorption process. For clays, it is expected that the solution pH and ultimately PZC influences the adsorption of anionic and cationic molecules depending on the extent of protonation of the adsorbate and adsorbent. According to the PZC results, it is anticipated that the adsorption of MB and CV be highest pH > 5 and that of DR81 and MO highest at pH < 5. However, Figure 5D shows that the variation of pH had a negligible influence in the percentage removal of the dyes except for MO dye probable meaning that the solution pH did not cause a notable protonation of the ions in solution hence the negligible impact of pH in the dye uptake process. The same can also be said from FTIR results, no notable activity or change of the functional groups was seen before and after adsorption of the dyes.

Nonetheless, the overall observation was that out of the four dyes, MO had the lowest percent dye removal. Molecular size of the adsorbing components also affects adsorption. Large molecules might not be adsorbed because their size prevents their diffusion into the pores of the adsorbent. The chemical formulas and molecular weights of DR81, MB, CV and MO are $C_{29}H_{19}N_2O_8S_2$ (675.598 g/mol), $C_{16}H_{18}N_3ClS.xH_2O$ (319.85 g/mol), $C_{25}N_3H_{30}Cl$ (407.979 g/mol) and $C_{14}H_{14}N_3NaO_3S$ (327.334 g/mol) respectively. From the dyes, MO is the second smallest molecule and hence if molecular size affected the adsorption of the dyes, MO would have presented a higher percent removal compared to MB and DR81.

Since well, the dye uptake could not be explained in terms of molecular weights, pH variation or characterization results, the adsorption mechanism will have to be discussed in the light of the isotherms and kinetics modelling results. The pseudo second order model gave the best fit with the experimental data for all the four dyes whereas the Langmuir isotherm model described well the adsorption of MB, CV and MO but not that of DR81. Hence, the adsorption mechanisms may involve complexation or ion exchange between the dye ions and the surface ions or SiO_2 or Al_2O_3 groups on the clay surfaces. The halloysite clay was observed to have relatively high Langmuir adsorption capacities for all the dyes and therefore, most of the dye ions might have been held in a monolayer on the clay surface.

According to Errais et al. (2012), depending on the type of clay, the possible processes involved in dye adsorption can be summed up in the following processes:

Process 1: The polyvalent metal cations (Si^{4+} by Al^{3+}) adsorbed on edge sites of the clay, contribute to the surface charge being positive, hence forming bridges between the particles of the clay and organic anions, allowing anionic dyes like DR81 to be adsorbed.

Process 2: In basic pH conditions and at the particle edges of dissociated aluminol groups, OH groups may be substituted by anions (Errais et al., 2012).

Process 3: Halloysite is a kaolinite clay and these clays have a net layer charge of zero (Sarma et al., 2011). However, a small net negative charge may arise from broken edges on the clay crystals. This negative charge may be responsible for holding the cations to the clay surface through coulombic interactions. The charge on the edges is due to protonation or deprotonation of surface hydroxyl groups (Kausar et al., 2018).

In general, the uptake of dye molecules by clay minerals is due to the trapping of dye molecules by exchangeable ions and protonated sheet edges of the clay.

3.8 Comparison with other studies

Table 6 illustrates the comparison of adsorption capacities of halloysite with other clay-based adsorbents. As observed, the adsorption capacity of halloysite clay used for this study was comparatively higher than other adsorption capacities of other halloysite clays for the removal of MO, MB, and DR81. However, for CV dye, it was notable lower. This difference could be because of the different operational parameters used during the adsorption experiments and due to various chemical modifications performed on the clay before use. Thus, this adsorbent can be considered as an effective option for the removal of both acidic and basic dyes from aqueous media.

Table 6. Adsorption capacities for different adsorbent materials used to remove dyes

Adsorbent	Adsorption capacity (mg/g)	Dye	Reference
Halloysite clay	104.17	Methyl Orange	Present study
Halloysite clay	185.16	Methylene blue	Present study
Halloysite clay	5.22	Crystal Violet	Present study
Halloysite clay	67.57	Direct Red 81	Present study
HDTMA modified halloysites	91.74	Methyl orange	Liu et al., 2012
Halloysite nanotubes	54.85	Neutral Red	Luo et al., 2010
Halloysite nanotubes	113.64	Methyl violet	Liu et al., 2011
Chitosan halloysite composite	68.92	Methylene Blue	Peng et al., 2015
Magnetic halloysite nanotubules	37.38	Methylene Blue	Xie et al., 2011
Magnetic halloysite nanotubules	31.21	Nile Red	Xie et al., 2011
Magnetic halloysite nanotubules	0.68	Methyl orange	Xie et al., 2011

4 CONCLUSIONS

The removal of DR81, MO, MB and CV from aqueous solution was carried out using halloysite clay as an adsorbent. The optimum contact time for the interaction of the adsorbent with dye effluent was 30 min. Two kinetic models i.e pseudo first-order and pseudo second-order models were used to test the adsorption mechanism and the best fit was observed with the pseudo second order model with a perfect coefficient of determination (R^2 =1) for all dyes. Adsorption isotherm modelling obeyed the Langmuir model more compared to the Freundlich model in the order MB > CV > MO > DR81. Ordinary, untreated clay was an effective material in the adsorption of acidic and basic dyes at room temperature (25 ± 3 ºC) and pH of the solution.

The results have established good potential for the halloysite clay to be used as an adsorbent for the removal of dyes from wastewater.

ACKNOWLEDGEMENT

The authors wish to thank the University of Venda, National Research Foundation (NRF), Water Research Commission (WRC) for funding.

REFERENCES

Adebowale K.O., Olu-Owolabi B.I., Chigbundu. E.C. 2014. Removal of Safranin-O from Aqueous Solution by Adsorption onto Kaolinite Clay. Journal of Encapsulation and Adsorption Sciences. 4, 89 –104.

Ahmed S., Rasul M.G., Martens W.N., Brown R., Hashib, M.A. 2010. Heterogeneous photocatalytic degradation of phenols n wastewater: A review on current status and developments, Desalination. 261, 3–18.

Anirudhan T.S., Ramachandran M., 2015. Adsorptive removal of basic dyes from aqueous solutions by surfactant modified halloysite clay (organoclay): kinetic and competitive adsorption isotherm. Process Safety and Environmental Protection. 95, 215–225.

Arshadi M., Mousavini F., Amiri M.J., Faraji A.R., 2016. Adsorption of methyl orange and salicylic acid on a nano-transition metal composite: Kinetics, thermodynamic and electrochemical studies. Journal of Colloid and Interface Science. 483, 118–131.

Benefield L.A., 2002. Wastewater quality/strength/content. Wastewater Management Program. Washington State Department of Health. WAC 246-272-11501(3).1–18.
Berthier P., 1826. Analyse de l'halloysite. Annales de Chimie et de Physique. 32, 332–335

Boukhemkhem A., Rida K., 2017. Improvement adsorption capacity of methylene blue onto modified Tamazert kaolin. Adsorption Science and Technology. doi.org/10.1177/0263617416684835.

Cadena F., Rizvi R., Peters R.W., 1990. Feasibility studies for the removal of heavy metals from solution using tailored bentonite. In: Hazardous and Industrial Wastes Twenty-second Mid-Atlantic Industrial Waste Conference. Drexel University.

Cheah W., Hosseini S., Khan M.A., Chuah T.G., Choong T.S.Y., 2013. Carbon coated monolith, a mesoporous material for the removal of methyl orange from aqueous phase: adsorption and desorption studies. Chemical Engineering Journal. 215–216, 747–754.

Ciesielczyk F., Bartczak P., Zdarta J., Jesionowski T., 2017. Active MgO-SiO_2 hybrid material for organic dye removal: A mechanism and interaction study of the adsorption of C.I. Acid Blue 29 and C.I. Basic Blue 9. Journal of Environmental Management. 204, 123–135.

D'Souza L., Devi P., Divya S.M.P., Naik C.G., 2008. Use of Fourier Transform Infrared (FTIR) Spectroscopy to Study Cadmium-Induced Changes in Padina Tetrastromatica (Hauck). Analytical Chemical Insights. 3, 135–143.

Errais E., Duplaya J., Elhabiri M., Khodja M., Ocampo R., Baltenweck-Guyot R., Darragi F., 2012. Anionic RR120 dye adsorption onto raw clay: Surface properties and adsorption mechanism. Colloids and Surfaces A: Physicochemical Engineering Aspects. 403, 69 – 78.

Freundlich H.Z.,1906. Over the adsorption in solution. Journal of Physical Chemistry. 57A, 385–470.

Gu Z., Gao M., Luo Z., Lu L., Ye Y., Liu, Y., 2014. Bis-pyridinium dibromides modified organobentonite for the removal of aniline from wastewater: a positive role of π-π polar interaction. Applied Surface Science, 290, 107–115.

Ho, Y.S., McKay, G., 1998. A comparison of chemisorption kinetic models applied to pollutant removal on various sorbents. Process Safety and Environmental Protection. 76(4), 332–340.

Ho Y.S., 2006. Review of second-order models for adsorption systems. Journal of Hazardous Materials B. 136, 68–689.

Izuagie A.A., Gitari W.M., Gumbo, J.R., 2016. Synthesis and performance evaluation of Al/Fe oxide coated diatomaceous earth in groundwater defluoridation: towards fluorosis mitigation. Journal of Environmental Science and Health A. 1–15, 810–824.

Jiang L., Huang Y., Liu T., 2015. Enhanced visible-light photocatalytic performance of electrospun carbon-doped TiO_2/ halloysite nanotube hybrid nanofibers. Journal of Colloid and Interface Science. 439, 62–68.

Kadirvelu K., Namasivayam C., 2000. Agricutural By-Product as Metal Adsorbent: Sorption of Lead (II) from Aqueous Solution onto Coirpith Carbon. Environmental Technolog. 21(10). 1091–1097

Kamble R., Ghag M., Gaikawad, S., Panda, B.J., 2012. Halloysite Nanotubes and Applications: A Review. Journal of Advanced Scient Research. 3(2), 25–29.

Kausar A., Iqbal M., Javeda A., Aftab K., Nazli Z., Bhatti H.N., Nouren S., 2018. Dyes adsorption using clay and modified clay: A review. Journal of Molecular Liquids. 256, 395–407.

Langmuir I., 1918. The adsorption of gases on plane surfaces of glass, mica and platinum, Journal of the American Chemical Society. 40, 1361–1403.

Liu R., Zhang B., Mei D., Zhang H., Liu J., 2011. Adsorption of methyl violet from aqueous solution by halloysite nanotubes. Desalination. 268, 111–116.

Liu M.X., Zhang Y., Zhou C.R., 2013. Nanocomposites of halloysite and polylactide. Applied Clay Science, 75-76, 52–59.

Liu M., Jia Z., Jia D., Zhou, C., 2014. Recent Advanced in Research of Halloyiste Nanotubes-Polymer Nanocomposites. Progress in Polymer Science. 39, 1498–1525.

Luo P., Zhao Y.F., Zhang B., Liu J.D., Yang Y., Liu J.F., 2010. Study on the adsorption of Neutral Red from aqueous solution onto halloysite nanotubes. Water Research. 44, 1489–1497.

Mekatel E., Amokrane S., Aid A., Nibou D., Trari, M., 2015. Adsorption of methyl orange on nanoparticles of a synthetic zeolite NaA/CuO. Comptes Rendus Chimie. 18, 336–344.

Mu B., Wang, A., 2016. Adsorption of dyes onto palygorskite and its composites: a review. Journal of Environmental Chemical Engineering. 4, 1274 –1294.

Nandi B., Goswami A., Purkait M., 2009. Removal of cationic dyes from aqueous solutions by kaolin: kinetic and equilibrium studies. Applied Clay Sciences. 42, 583–590.

Ngulube T., Gumbo J.R., Masindi V., Maity A., 2017. An update on synthetic dyes adsorption onto clay-based minerals: A state-of-art review. Journal of Environmental Management. 191, 35–57.

Ngulube T., Gumbo J.R., Masindi V., Maity A., 2018. Calcined magnesite as an adsorbent for cationic and anionic dyes: characterization, adsorption parameters, isotherms and kinetics study. Heliyon. 4, e00838.

Ofomaja A.E., 2010. Intraparticle diffusion process for lead (II) biosorption onto mansonia wood sawdust. Bioresource Technology. 101, 5868–5876.

Ogunmodede O.T., Ojo A.A., Adewole E., Adebayo O.L.,2015) Adso.rptive removal of anionic dye from aqueous solutions by mixture of Kaolin and Bentonite clay: characteristics, isotherm, kinetic and thermodynamic studies. Iranian Journal of Energy and Environment. 6 (2), 147–153.

Park Y., Ayoko G.A., Frost R.L., 2011. Characterisation of organoclays and adsorption of p-nitrophenol: environmental application. Journal of Colloid Interface Science. 360, 440–456.

Peng Q., Liu M., Zheng, J., Zhou C., 2015. Adsorption of dyes in aqueous solutions by chitosan–halloysite nanotubes composite hydrogel beads. Microporous and Mesoporous Materials. 201, 190–201.

Pennell K.D., 2016. Specific Surface Area. Pp. 1–8 in: Reference Module in Earth Systems and Environmental Sciences Publisher (A.E. Scott, editor) Elsevier, USA.

Prokop A., Maziarz P., Matusik J., 2015. Removal of selected anions by raw halloysite and smectite clay. Geology, Geophysics and Environment. 41(1), 125–126.

Sari A., Tuzen M. (2014) Cd (II) adsorption from aqueous solution by raw and modified kaolinite. Applied Clay Sciences. 88–89, 63–72.

Sarma G.K., Gupta S.S., Bhattacharyya K.G., 2016. Adsorption of Crystal violet on raw and acid-treated montmorillonite, K10, in aqueous suspension. Journal of Environmental Management. 171, 1–10.

Sarma G.K., Gupta S.S., Bhattacharyya K.G., 2011. Methylene Blue Adsorption on Natural and Modified Clays. Separation Science and Technology, 46(10), 1602–1614.

Santamarina J.C., Klein K.A., Wang Y., Prencke E., 2002. Specific surface: Determination and relevance. Canadian Geotechnical Journal. 39, 233–241.

Santos S.C.R., Oliveira A.F.M., Boaventura R.A.R., 2016. Bentonitic clay as adsorbent for the decolourisation of dyehouse effluents. *Journal of Cleaner Production,* **126,** 667–676.

Słomkiewicz P.M., Szczepanik B., Garnuszek M., 2015. Determination of adsorption isotherms of aniline and 4-chloroaniline on halloysite adsorbent by inverse liquid chromatography. Applied Clay Science. 114, 221–228.

Subbaiah M.V., Kim D.S., 2016. Adsorption of methyl orange from aqueous solution by aminated pumpkin seed powder: Kinetics, isotherms, and thermodynamic studies. Ecotoxicology and Environmental Safety. 128, 109–17.

Tomar V., Prasad S., Kumar D., 2014. Adsorptive removal of fluoride from aqueous media using citrus limonum (lemon) leaf. Microchemal Journal. 112, 97–103.

Xiang W., Zhang G.K., Zhang Y.L., Tang D.D., Wang J.T., 2014. Synthesis and characterization of cotton-like Ca–Al–La composite as an adsorbent for fluoride removal. Chemical Engineering Journal. 250, 423–430.

Xie Y., Qian D., Wu D., Ma X., 2011. Magnetic halloysite nanotubes/iron oxide composites for the adsorption of dyes. Chemical Engineering Journal. 168, 959–963.

Yagub M.T., Sen T.K., Afroze S., Ang H.M. (2014) Dye and its removal from aqueous solution by adsorption: a review. Advanced Colloid Interface Science. 209, 172–184.

Yakout S.M., Elsherif E., 2010. Batch kinetics, isotherm and thermodynamic studies of adsorption of strontium from aqueous solutions onto low cost rice-straw based carbons. Carbon – Scince and Technology. 1, 144 –153.

Yang R., Li D., Li A., Yang H., 2018. Adsorption properties and mechanisms of palygorskite for removal of various ionic dyes from water. Applied Clay Science. 151, 20–28.

Zhang Y., Fua L., Yang H., 2012. Insights into the physicochemical aspects from natural halloysite to silica nanotubes. Colloids and Surfaces A: Physicochemical Engineering Aspects. 414, 115–119.

Zhao M., Liu P., 2008. Adsorption Behavior of Methylene Blue on Halloysite Nanotubes. Microporous and Mesoporous Materials. 112(1-3), 419–424.

Zhao Y., Abdullayev E., Vasiliv A., Lvov Y., 2013. Halloysite nanotubule clay for efficient water purification. Journal of Colloid and Interface Science. 406,121–129.

Zulfikar M.A., 2013. Materials, Effect of temperature on adsorption of humic acid from peat water onto pyrophyllite. International Journal of Chemical Environmental and Biological Sciences. 1, 88-91.

CHAPTER FIVE

Application of calcined magnesite – halloysite clay nanocomposite in the removal of dyes: A batch study.

This chapter is under review for publication in Chemical Sciences Journal as: Ngulube T., Gumbo J.R., Masindi V., Maity A., 2018. Mechanochemical-synthesis of a super-performing nanocomposite and its application on the removal of cationic and anionic dyes. Chemical Sciences Journal.

This chapter addresses objectives (i), (ii), (iii) and (v).

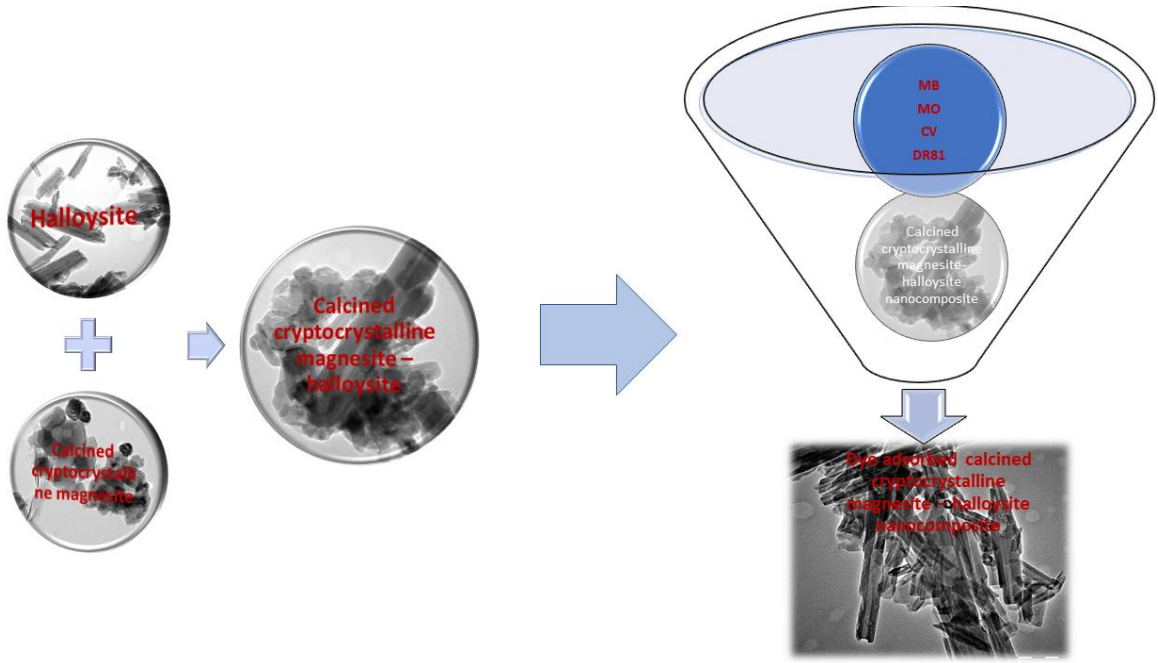

Mechanochemical-synthesis of a super-performing nanocomposite and its application on the removal of cationic and anionic dyes

♣Tholiso Ngulube [1], Jabulani Ray Gumbo[2], Vhahangwele Masindi [3&4] and Arjun Maity[5&6]

[1] Department of Ecology and Resources Management, School of Environmental Sciences, University of Venda, Private bag X5050, Thohoyandou, 0950, Limpopo, South Africa. Tel: +27159628563, Email: tholisongulube@gmail.com

[2] Department of Hydrology and Water Resources, School of Environmental Sciences, University of Venda, Private bag X5050, Thohoyandou, 09 50, Limpopo, South Africa.

[3] Council for Scientific and Industrial Research (CSIR), Built Environment, Hydraulic Infrastructure Engineering, P.O BOX 395, Pretoria, 0001, South Africa.

[4] Department of Environmental Sciences, School of Agriculture and Environmental Sciences, University of South Africa (UNISA), P. O. Box 392, Florida, 1710, South Africa

[5] Department of Applied Chemistry, University of Johannesburg, Johannesburg, South Africa

[6] DST/CSIR National Centre for Nanostructured Materials, Council for Scientific and Industrial Research (CSIR), Pretoria, South Africa

Abstract

Attaining inexpensive and clean water is one of the biggest worldwide challenges of this era because the population is growing fast and producing large amounts of wastewater making freshwater a rare resource. In this novel study, mechanochemical-synthesis of a super-performing nanocomposite and its application on the removal of cationic and anionic dyes was explored. Targeted dyes were Direct Red 81 (DR81), Methylene Blue (MB), Crystal Violet (CV) and Methyl Orange (MO). A batch experimental approach was used to fulfil the goals of this study. Evaluated parameters include time, dosage, concentration, pH and temperature. Optimization studies revealed that, 75 min were adequate for the removal of dyes at specified dosage, concentration, pH and temperature. The adsorption behavior of the nanocomposite was fitted to four isotherm models and the data fitted the Langmuir isotherm well. Data fitting best to the Langmuir isotherm indicates that the dyes formed a monolayer on the surfaces of the nanocomposite. The fit of the Langmuir isotherm model was in the order MB (R^2 = 0.9766) > CV (R^2 = 0.9623) > DR81 (R^2 = 0.9623) > MO (R^2 = 0.6157). The kinetics modelling data was also fitted to four kinetic models and the data fitted the pseudo second order model and the intra particle diffusion model best with R^2 values of 1. Thermodynamic studies gave negative ΔG values for all the dyes suggesting that the dye adsorption process was spontaneous and

♣ Corresponding author: Email: tholisongulube@gmail.com

thermodynamically favorable. Furthermore, the nanocomposite exhibited high stability during 4 adsorption-desorption cycles. The results showed that the highest experimental maximum adsorption capacity was 19.89 mg/g for DR81 dye. The combination of high adsorption capacity, short equilibrium time and high stability, indicates that the prepared nanocomposite is an excellent adsorbent material for the removal of both anionic and cationic dyes from wastewaters.

Keywords: Ball milling, mechanochemical synthesis, magnesite, halloysite, nanocomposite, dye removal.

1 Introduction

Dye wastewaters are complex and consists of concentrated waste streams, which contain a wide and varied range of dyes and their metabolites (Sarma et al., 2016). This wastewater contains non-biodegradable constituents and the impartation of colour to water disturbs aquatic life by hindering the infiltration of sunlight to benthic fauna and flora thus deterring the process of photosynthesis (Uyar et al., 2016). On exposure to living organisms, dyes can produce great harm to aquatic biota because they are associated with carcinogenicity. Furthermore, the colour imparted by dyes to water bodies has an adverse aesthetic effect (Rangabhashiyam et al., 2013; Zhou et al., 2014; Santos and Boaventura, 2016). Due to the complexity of dye wastewater, some industrial companies do not meet wastewater discharge standards, causing detrimental problems if the wastewater is discharged into the sewerage system and into the environment (Ngulube et al., 2017). Unless the wastewater is properly treated before it is discharged, it will contaminate the natural aquatic environment (Ianos et al., 2018). The goal for effluent discharge into the environment as per South African guidelines is to attain water that is of good quality, which is suitable for use and a healthy aquatic ecosystem which is sustainable (DEA, 2014).

Many investigations have been done on the remediation of dye wastewater (Ciesielczyk et al., 2017; Qiu et al., 2018; Yang et al., 2018). However, low cost techniques that can be used by small scale industries are hardly available. Conventional advanced wastewater treatment methods like electrolysis, ion exchange and membrane separation are costly (Singh et al., 2015; Yousef et al., 2015; Hajjaji et al., 2016) and hence the driving force is to search for creative, low cost and environmentally sound ways of treating wastewater as environmental laws and requirements are becoming more stringent. This calls for research efforts to develop an

industrially feasible, cost effective and environmentally compatible adsorbent for wastewater treatment.

Adsorbents synthesized from inorganic materials like clays, modified metal oxide including CaO, MgO, SiO_2 and Al_2O_3 are mostly used in adsorption processes of removing dyes from wastewater (Ciesielczyk et al., 2017). These adsorbents have the capacity to remove a combination of acidic, basic and reactive dyes from water. Several studies have been done on the removal of colour from aqueous solutions and the outcomes show that such adsorbents are effective in the remediation of coloured wastewater (Shokry et al., 2014; Zhan et al., 2014; Dadfarnia et al., 2015). The pros of combining different metal oxides is that they can form good fusion systems with excellent adsorption capacities. Furthermore, modification of their surfaces increases their capability of taking up various organic pollutants. These modification techniques make it possible to obtain more active adsorption sites by increasing surface areas and providing suitable physical structures allowing the effective binding of organic pollutants like dyes (Rasalingam et al., 2013).

In this work, a new adsorbent was prepared from calcined cryptocrystalline magnesite and halloysite nanotubes. These two inorganic earth materials also contain metal oxides including MgO, CaO, SiO_2 and Fe_2O_3 which have proved to be effective in dye remediation studies. A fast and easy method involving vibratory ball milling was employed for calcined cryptocrystalline magnesite - halloysite nanoclay composite CCM-HNC preparation. The adsorption capability of the composite was tested to remove Direct Red 81 (DR81), Methylene Blue (MB), Crystal Violet (CV) and Methyl Orange (MO) from aqueous solution. Thereafter, adsorption isotherm and kinetics studies were done to evaluate the mechanisms governing dye removal.

2 Materials and methods

2.1 Materials

Calcined cryptocrystalline magnesite was collected from Sterkfontein carbonate group Pty (Ltd). Halloysite nanotubes were purchased from Sigma Aldrich Pty (Ltd). Other chemical reagents such as NaOH pellets, KCl, HCl, DR81, MB, CV and MO were purchased from Rochelle Chemicals Pty (Ltd) (South Africa). Real industrial effluent was collected from a printing and ink industry.

2.2 Synthesis of the nanocomposite

Different ratios (1:1; 2:1; 1:2) of calcined cryptocrystalline magnesite and halloysite nanotubes composite were mixed and then milled using a vibratory ball mill (Retsch RS 200) (stainless-steel) using the optimized conditions described by Masindi et al. (2014).

2.3 Characterization of the adsorbent materials and field water

X-ray diffraction patterns were acquired on a PANalytical X'Pert PRO-diffractometer. Transmission Electron Microscopy (TEM) images were acquired with a JEOL JEM-2100F Field Emission Transmission Electron Microscope (JEOL, Japan). Scanning Electron Microscopy (SEM) images were acquired on a Zeiss Ultra Plus and Zeiss Cross Beam 540 Field Emission Scanning Electron microscopes (Carl Zeiss, Germany). To determine the functional groups of the nanocomposite, spectra were recorded using FTIR spectrometer, Bruker Alpha model, Platinum ATR (Germany). The thermal stability of the adsorbent was investigated, using a Thermo Gravimetric Analyser (TGA Q500, TA instrument) under air atmosphere with a flow rate of 50 mL/min and a heating rate of 10 °C/min. Surface area was determined using Brunauer EmmettTeller (BET) analysis (Micromeritics Tristar II, Norcross, GA, USA). Point of zero charge (PZC) was determined by solid addition method as described by Izuagie et al. (2016). Characterization of wastewater was done using an Inductively Coupled Plasma Mass Spectrometry (ICP-MS) (7500ce, Agilent, Alpharetta, GA, USA). The pH, EC and TDS of the aqueous solutions were determined by using a CRISON MM40 multimeter probe for pH, EC, TDS and temperature. Turbidity was measured by a Lovibond TB250-WL Handheld Turbidity Meter.

2.4 Optimization studies

Visible spectrophotometric analysis of DR81, MB, CV and MO by CCM-HNC prepared in this work were conducted using Thermo Scientific Orion Aqua matte 7000 visible spectrophotometer at the wavelength of 505, 664, 590 and 510 nm at which DR81, MB, CV and MO respectively show maximum light absorption. DR81, MB, CV and MO adsorption by the prepared CCM-HNC was investigated by adding 50 mL of 5 mg/L DR81, MB, CV and MO solution into 3, 250 mL glass Erlenmeyer flasks. 1 g of CCM-HNC was added into the flasks and the mixtures were equilibrated by agitating them on a table shaker for 15 min. After equilibrium, the solutions were allocated 30 min to settle after which the supernatant solution was collected, and its absorbance recorded. The procedure was repeated for other

determinations but with equilibration time of 30, 45, 60, 75 and 90 min. Consequently, the contact time which resulted in the highest DR81, MB, CV and MO percentage removal (%) was chosen for all successive experiments. The same procedure was repeated for different dosages (0.1, 0.5, 1, 1.5, 2, and 3 g) with time and initial dye concentration kept contant. For the variation of initial dye concentrations (1, 2, 3, 4, 5 and 6 mg/L for CV and MO, (1, 5, 10, 15, 20 and 30 mg/L for MB) and (5, 10, 20, 30, 40 and 50 mg/L for DR81) time and dosage were kept constant. For temperature variation (298, 308, 318 and 328 K), time, dosage and initial dye concentration were kept contant. The influence of initial DR81, MB, CV and MO solution pH on the equilibrium uptake of DR81, MB, CV and MO ions were evaluated over a pH range of 2 – 12 in a batch mode. During this experiment, time, dosage and initial dye concentration were kept constant. The solution pH was adjusted using either 0.1 M of HCl or 0.1 M NaOH solution. All the experiments besides that of temperature variation were done at room temperature (25 ± 3 ^{o}C). To validate the reproducibility of the results, the experiments were done in triplicate and the mean values were recorded.

2.5 Mathematical modelling

2.5.1 Adsorption isotherm

In the quest intended to find novel adsorbents and to develop model adsorption systems, it is crucial to create the best applicable mathematical depiction of the adsorption equilibrium over the entire experimental conditions (Sarma et al., 2016). Adsorption isotherms are thought of as the most fitting system in this aspect, but the rationality of the assumptions resulting from the isotherms are determined by the appropriateness of a model to define a certain state. For this work, the adsorption data were tested with reference to the Freundlich (1906), Langmuir (1916), Dubinin (1975) and Temkin and Pyzhev (1940) models.

2.5.1.1 Langmuir Isotherm

The Langmuir isotherm (Equation 1), assumes that beyond the monolayer, adsorption cannot proceed, and the occupation of neighboring sites does not affect the ability of a molecule to be adsorbed at a given site (Langmuir, 1918).

The Hanese -Woolf linearization of the Langmuir model (Tran et al., 2017) is as follows:

$$\frac{C_e}{q_e} = \left(\frac{1}{Q_m}\right) C_e + \frac{1}{Q_m b} \quad \text{..... (1)}$$

Where Ce (mg/L) is the concentration at equilibrium, Qe (mg/g) is adsorbed dye per mass of adsorbent at equilibrium, b signifies the Langmuir isotherm constant and Qm (mg/g) is the Langmuir adsorption capacity.

If the Langmuir model sufficiently describes the experimental data, it is important to compute the separation factor (R_L), given by:

$$R_L = \frac{1}{1 + bC_0} \qquad (2)$$

where R_L is a constant separation factor (dimensionless) of the solid-liquid adsorption system, b is the Langmuir equilibrium constant, and Co (mg/L) is the initial adsorbate concentration.

2.5.1.2 Freundlich Isotherm

This isotherm is mainly used to define adsorption process occurring on heterogeneous surfaces (Singh et al., 2015).
It can be expressed by a linear mathematical equation as follows:

$$logQ_e = \frac{1}{n} \log C_e + \log K_F \qquad (3)$$

Where n and K_F are the Freundlich constants, describing the adsorption intensity and capacity respectively.

2.5.1.3 Dubinin–Radushkevich (DR) Isotherm

The DR is mostly practical in expressing adsorption mechanisms onto a heterogeneous surface through a Gaussian energy distribution (Dabrowski, 2001). Compared to the Langmuir isotherm, the DR isotherm is more general because it does not assume a constant adsorption potential or a homogenous surface (Daifullah et al., 2007).

The linearized DR isotherm is expressed as follows:

$$lnq_e = -KDR^{\varepsilon^2} + \ln q_{DR} \qquad (4)$$

$$\varepsilon = RT \ln\left(1 + \frac{1}{C_e}\right) \qquad (5)$$

By inserting Equation (4) into Equation (5), Equation (6) can be obtained:

$$lnq_e = -K_{DR} RT \ln\left(1 + \frac{1}{C_e}\right) + \ln q_{DR} \qquad (6)$$

where qe and Ce are concentration at equilibrium and initial concentration respectively, K_{RD} (mol^2/kJ^2) is a constant associated with adsorption energy, q_{RD} (mg/g) is the adsorption capacity, ε is the Polanyi potential, R is the gas constant and T is the temperature in Kelvin.

2.5.1.4 Temkin Isotherm

Equation (7) representing the Temkin isotherm adopts that adsorption heat of molecules in layers decreases linearly with coverage because of adsorbent - adsorbate interactions (Temkin and Pyzhev, 1940).

The Temkin equation is linearly given as follows:

$$q_e = \beta \ln \alpha + \beta \ln C_e \quad \ldots\ldots (7)$$

where $\beta = \frac{RT}{b}$ ……(8)

β (J/mol) is the Temkin constant describing the maximum binding energy, α (L/mg), is the equilibrium binding constant, T(K) is the absolute temperature, R (8.314 J/mol/K), is the universal gas constant and b (J/mg) is the Temkin constant associated with the heat of adsorption.

2.6 Adsorption kinetics

The process of adsorption is dependent on time; hence it becomes imperative to know the adsorption rate for design purposes of wastewater treatment systems (Buamah et al., 2013). The experimental data of the DR81, MB, CV and MO adsorption onto CCM-HNC were evaluated by fitting the data onto the pseudo first-order (Lagergren model) and the pseudo second-order kinetic models.

2.6.1 The pseudo first-order kinetic model

The equation defines adsorption occurring in liquid-solid systems based on the solids' adsorption capacity.

The pseudo first order model (Wu et al., 2017) can be linearly expressed as follows:

$$\log(q_e - q_t) = \log(q_e) - \left(\frac{k_1 t}{2.303}\right) \quad \ldots\ldots (9)$$

Where q_e (mg/g) is the adsorption capacity at equilibrium, q_t (mg/g) is the adsorption capacity at time t, and *K* (1/min) is the rate constant of pseudo-first-order.

2.6.2 The pseudo second order kinetic model

The pseudo second-order model (Tran et al., 2017), is applied to analyze chemisorption kinetics from liquid solutions based on solid phase sorption. It is linearly expressed as:

$$\frac{t}{q_t} = \left(\frac{1}{q_e}\right) t + \left(\frac{1}{k_2 q_e^2}\right) \ldots \ldots \ldots (10)$$

where k_2 is the rate constant for pseudo second-order adsorption (g/mg/h), $k_2 q_e$ or h (mg/g/h) is the initial adsorption rate.

2.6.3. Intraparticle diffusion model

A plot of solute adsorbed against the square root of contact time should produce a straight line passing through the origin, if the rate-limiting step is intraparticle diffusion (Poots et al., 1976). The widely applied intraparticle diffusion equation for adsorption systems is given by Weber and Morris (1963):

$$qt = k_{id} t^{\frac{1}{2}} + C \ldots \ldots \ldots (11)$$

Where *qt* (mg/g) is the amount of dye adsorbed at any time *t*, *kid* (mg/g/min) is intraparticle diffusion rate constant and *C* is the intercept.

2.6.4 The Elovich model

The Elovich model is used to describe activated chemical adsorption processes occurring on heterogeneous surfaces (Aharoni and Tompkins, 1970). The Elovich equation (Juang and Chen, 1997), is given by

$$q_t = \frac{1}{b} \ln(ab) + \frac{1}{b} \; lnt \ldots \ldots \ldots (12)$$

where qt (mg/g) is the amount of dye adsorbed at time t (min), *a* (mg/g/min) and *b* (g/mg) are the Elovich constants relating to the initial adsorption rate and the extent of surface coverage and activation energy for chemisorption respectively.

2.7 Thermodynamic studies

Energy and entropy values must be considered in adsorption systems to determine processes that will occur spontaneously. Thermodynamic parameters values assist in indicating practical application of the process (Yakout and Elsherif, 2010). Thermodynamic parameters like Gibbs free energy ΔG (kJ/mol), enthalpy ΔH (kJ/mol) and entropy ΔS (J/mol/ K) were calculated using the following equations:

$$\Delta G = -RT \ln Ka \quad (13)$$

where ΔG is the free energy of adsorption (kJ/mol), T is the temperature in Kelvin (K), R is the universal gas constant (8.314 J/mol/ K) and Ka is the sorption equilibrium constant.

$$lnKa = \frac{\Delta H}{RT} + \frac{\Delta S}{RT} \quad (14)$$

where ΔH is the heat of sorption (kJ/ mol) and ΔS is the standard entropy change (kJ/mol/ K).

2.8 Regeneration studies

To determine the regeneration potential of CCM-HNC 0.01 M NaOH solution was used. A solid to liquid ratio of 2 g/50 mL, 10 mg/L dye solution was used to perform the adsorption – desorption experiments.

3 Results and discussion

3.1 Characterization of CCM-HNC

3.1.1 X-ray Diffraction analysis

Figure 1 shows an XRD diffractogram of raw and DR81, MB, CV and MO reacted CCM-HNC.

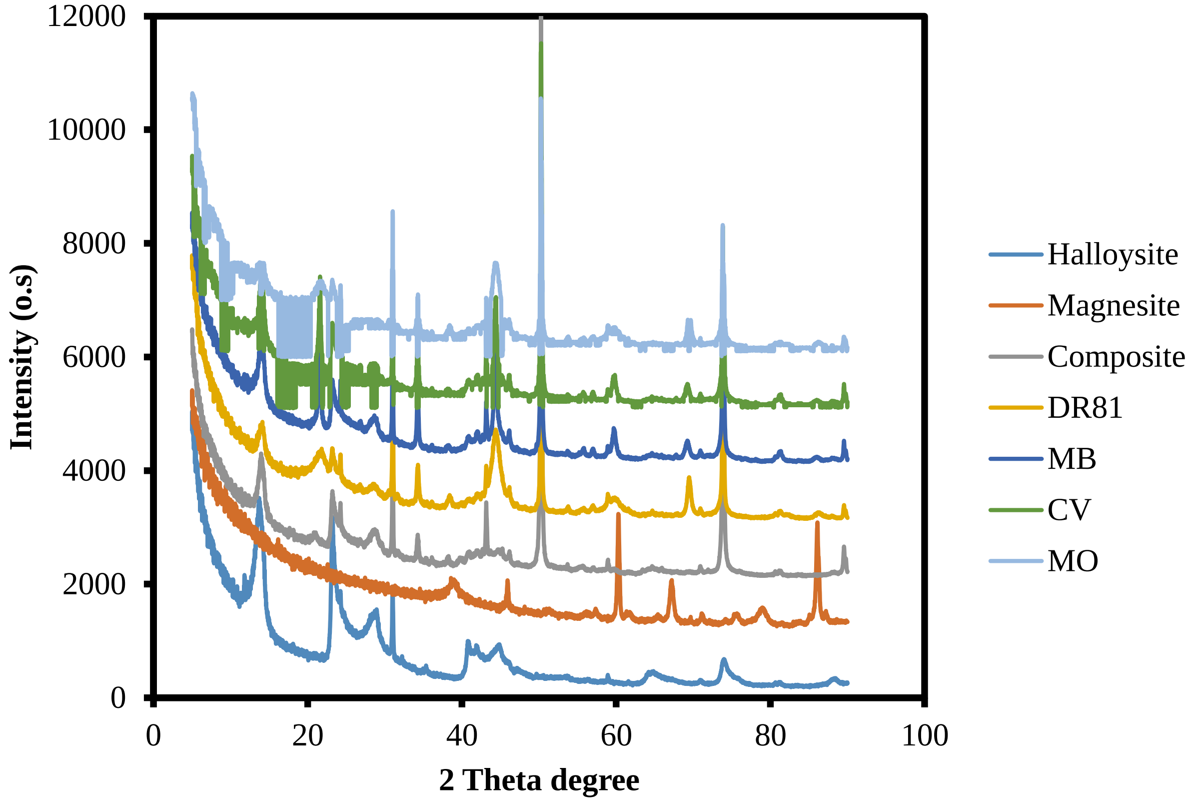

Figure 1: XRD diffractogram of raw and DR81, MB, CV and MO reacted CCM-HNC

The peak list from XRD analysis of the nanocomposite material shows the presence of quartz, periclase, brucite, calcite, magnesite, halloysite and kaolinite (**Figure 1**). The diffraction pattern exhibited a crystal line structure with an intense reflection at 50, 26° and 73.83° (2θ) characteristic of brucite, quartz and periclase. These are materials coming from the magnesite part of the composite material. Masindi et al. (2016) had the same observation for cryptocrystalline magnesite. On the other hand, the nanocomposite diffractogram showed sharp peaks at 13.95, 23.23 and 31.02° (2θ). The identified peaks are characteristic of quartz and halloysite (Zhang et al., 2012). These materials also characterize the availability of halloysite in the nanocomposite sample. Differentiating between the raw nanocomposite material and the DR81, MB, CV and MO reacted CCM-HNC shows that the characteristic materials remained the same before and after dye adsorption. However, a reduction in percentage weight after dye adsorption was observed for periclase and quartz whereas that of brucite and calcite increased. The increase in brucite composition could be as result of MgO reacting in aqueous solution according to the equation:

$$MgO + H_2O \rightarrow Mg(OH)_2 \ldots\ldots\ldots\ldots\ldots\ldots\ldots\ldots\ldots\ldots\ldots\ldots\ldots\ldots\ldots\ldots\ldots\ldots\ldots\ldots\ldots\ldots\ldots (15)$$

Accordingly, the occurrence of brucite ($Mg(OH)_2$) after dye adsorption could have resulted from the hydroxylation reaction.

3.1.2 Morphology of the synthesized composite

The morphological properties of raw magnesite nanosheets, halloysite nanotubes and their nanocomposite are shown in Figure 2.

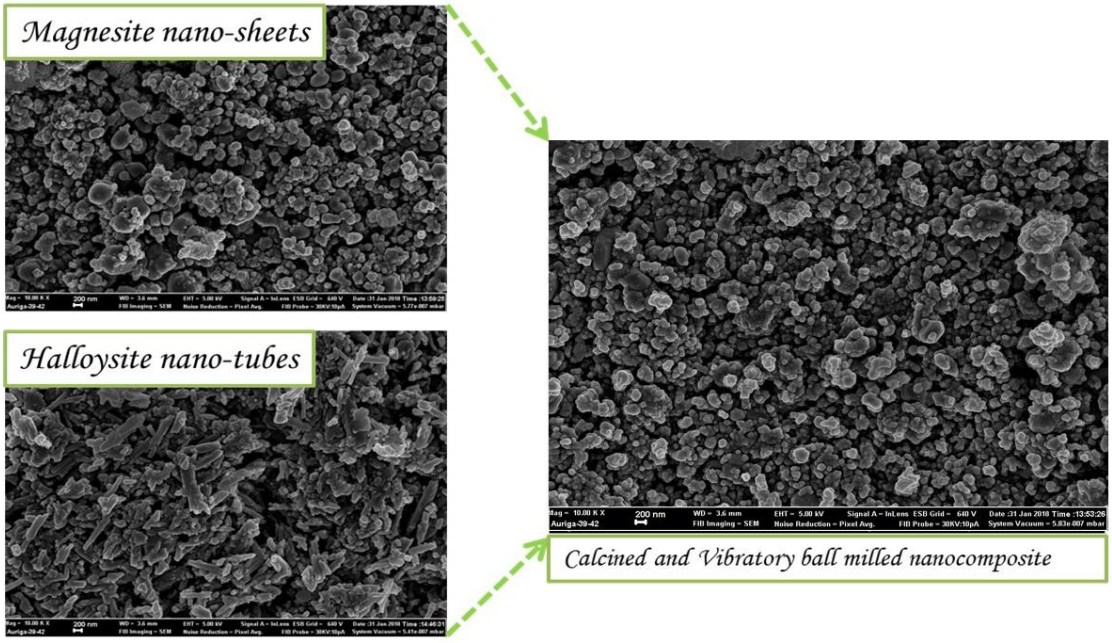

Figure 2: The morphological properties of raw magnesite nanosheets, halloysite nanotubes and their nanocomposite

The morphological structures of the raw nanocomposite and DR81, MB, CV and MO reacted nanocomposite are shown in Figure 3 (A – H).

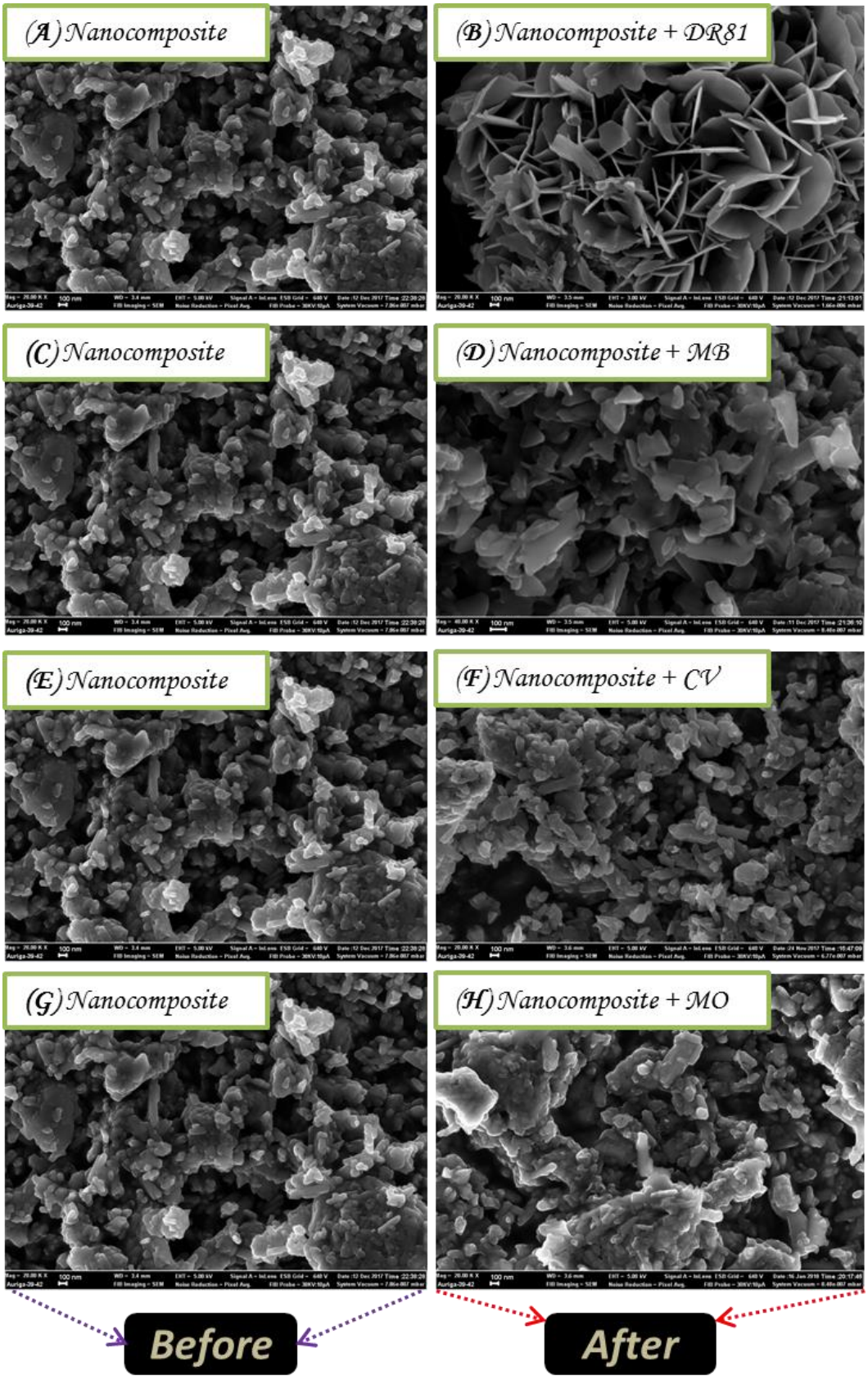

Figure 3 (A – H): The morphological structures of the raw nanocomposite and DR81, MB, CV and MO reacted nanocomposite

As shown in **Figure 3**, images of the raw CCM-HNC show aggregated particles some compacting together forming lumps. On the contrary DR81- reacted CCM-HNC images (B) display uneven shaped flakes with sharp edges that have distinctive leafy structures. The images reveal a flowery like structure. Worth noting is that images of the DR81 reacted CCM-HNC are significantly different from all the other images. Then, the MB reacted CCM-HNC (D) shows irregular shaped structures and the particles also appear to be very small in size too. CV reacted CCM-HNC (F) shows small particles aggregated together into a clump whereas a different observation is seen with MO reacted CCM-HNC (H) which show a rather fair distribution of particles across the surface. The particles are very small in size and shaped like rods. The eye-catching differences between the raw and dye reacted CCM-HNC could be as a result of reactions that took place between the adsorbent and adsorbate hence different morphological structures.

3.1.3 FTIR Analysis

The FTIR spectra for individual magnesite and halloysite materials, their composite and DR81, MB, CV and MO-reacted CCM-HNC are shown in **Figure 4.**

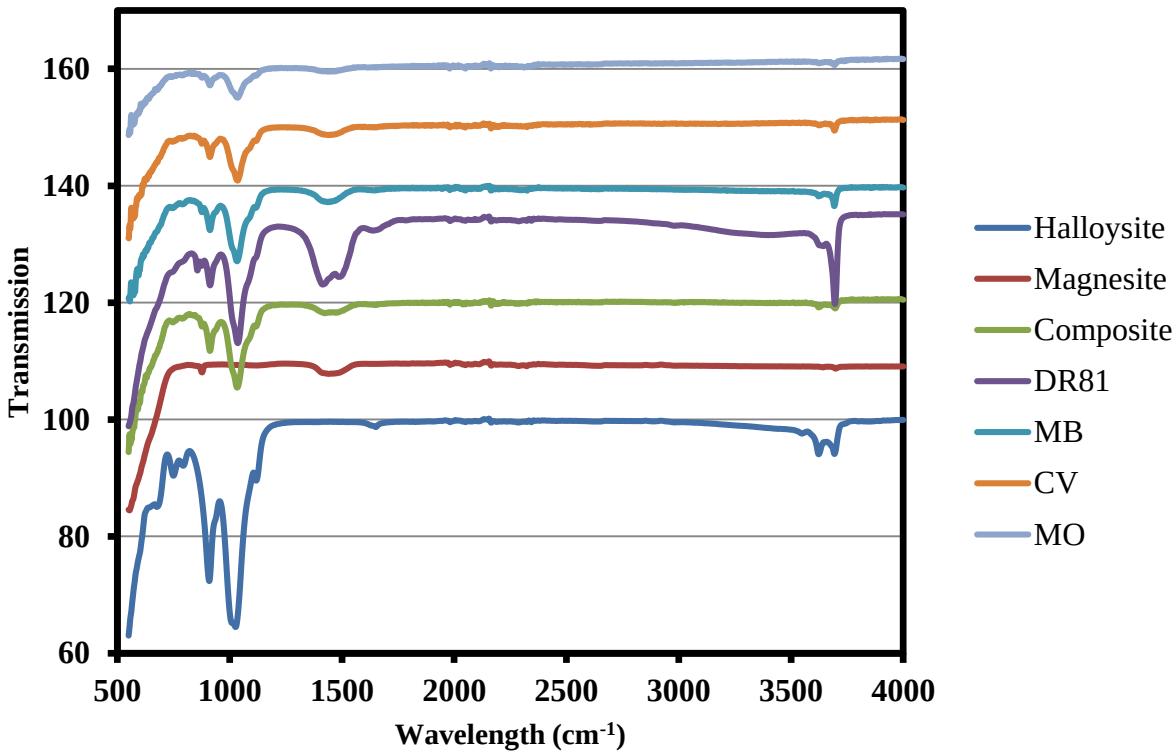

Figure 4: The FTIR spectra for individual magnesite and halloysite materials, their composite, and DR81, MB, CV and MO-reacted CCM-HNC

As shown in Figure 4, the FTIR results confirm the XRD study results. The FTIR spectroscopic study shows a system of bands characteristic of aluminisilicate materials and brucite. The various peaks are representative of the following: brucite at 3702 cm^{-1}, periclase at 900 cm^{-1} (Masindi et al., 2015). The FTIR spectra also showed stretching vibrations corresponding to kaolin group minerals associated with the OH-stretching region (3700 cm^{-1}) (Luo et al., 2010) and bending vibrations related to aluminosilicate framework (~1000 cm^{-1}) (Prokop et al., 2015). A major difference is shown between the raw and DR81, MB, CV and MO reacted CCM-HNC especially for the MB and CV reacted CCM-HNC where the transmittance significantly increased at around 1000 cm^{-1}. Since FTIR studies are vital in detecting characteristic functional groups in control of dye binding, it can be said that the functional groups where there is higher transmittance at approximately 900, 1000 and 3700 cm^{-1} being brucite, aluminosilicate and hydroxyl groups took part in the dye uptake process.

3.1.4 Brunauer–Emmett–Teller (BET) analysis

The surface areas of raw nanocomposite and the dye reacted nanocomposite is presented in **Table 1.**

Table 1: The surface areas of raw nanocomposite and the dye reacted nanocomposite

Material	Single point surface area (m^2/g)	BET Surface Area (m^2/g)	Langmuir Surface Area(m^2/g)
Magnesite	10.5895	10.7305	14.6564
Halloysite	40.9725	41.9418	57.4141
Composite	17.9525	18.1753	25.3153
CDR81	20.0207	20.2766	28.2623
CMB	16.9215	17.0475	23.6503
CCV	16.2217	16.3875	22.7491
CMO	18.3067	18.4533	25.5784

Surface area is a surface phenomenon and it is dependent on the size of particles, the smaller the particle size, the higher the surface area and the bigger the particle size the smaller the surface area. Specific surface area of clay soils provides sites in which molecules in solution can bind through weak van der Waal forces. As shown in Table 1, CCM-HNC has a BET surface area that is higher than that of magnesite alone but lower than that of halloysite. CCM-HNC has a BET surface area of 18.18 m^2/g. There is a notable difference shown after the material was used for the adsorption of dyes. Results show that the surface area increased after

the adsorption of DR81 and MO dye and decreased after the adsorption of CV and MB. The surface area decrease of the nanocomposites after CV and MB adsorption should be credited to an increased proportion of less porous calcined cryptocrystalline magnesite after dye reaction (Zhou et al., 2016). Since CV and MB are cationic dyes, they must have reacted more with the negatively charged clay particles by electrostatic attraction leaving out the calcined cryptocrystalline magnesite particles which are less porous when compared to halloysite clay. An increase in surface area after the adsorption of DR81 and MO dye could be because of the effect which particle shapes has on surface area and particle size. When particle size decreases, the shapes of the particles change and ultimately surface area increases (Santamarina et al., 2002). As observed from the SEM images, after dye adsorption, there was a notable change in the shape of the particles, which could have led to different dimensions of particles leading to an increase in surface area.

3.2 Optimization studies

3.2.1 Optimization of the synthesis of the adsorbent material

To optimize the conditions for fabricating the composite that would effectively remove dyes from aqueous solution, a dye adsorption experiment was carried out at each stage of optimization to determine which conditions gave the highest dye removal. Three ratios of the calcined cryptocrystalline magnesite and halloysite nanotubes respectively (1:1; 2:1; 1:2) were evaluated. The results for the removal of dyes as a function of ratios are presented in **Figure 5**.

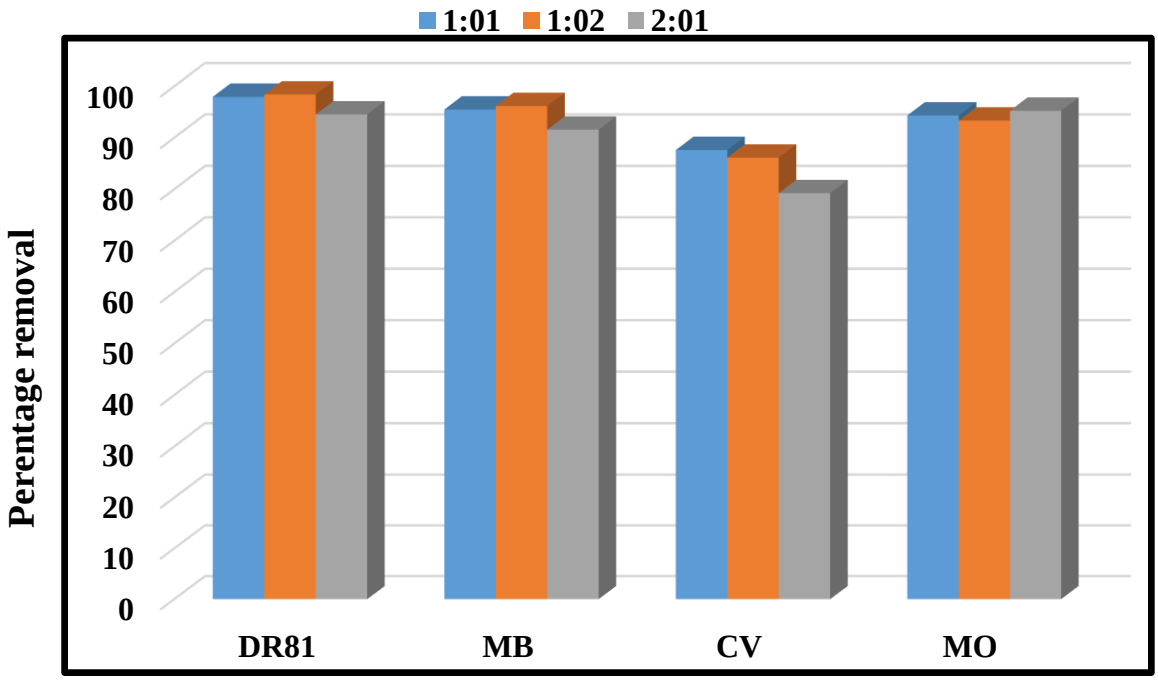

Figure 5: Removal of DR81, MB, CV and MO by the nanocomposite as a function of ratios (120 min contact time, 5mg/L adsorbate concentration, room temperature, 2 g adsorbent dosage; 250 rpm shaking speed)

As shown in **Figure 5**, between ratios 1:1 and 1:2 there is no substantial difference between the percentage removals of the dyes and moreover these two ratios present a notably higher percentage removal compared to the 2:1 ratio. Based on that, the ratio of 1:1 was chosen as the optimum ratio to synthesize the nanocomposite.

3.2.2 DR81, MB, CV and MO adsorption by CCM-HNC

The optimization results for the removal of DR81, MB, CV and MO as a function of various operational parameters and PZC are shown in **Figure 6**.

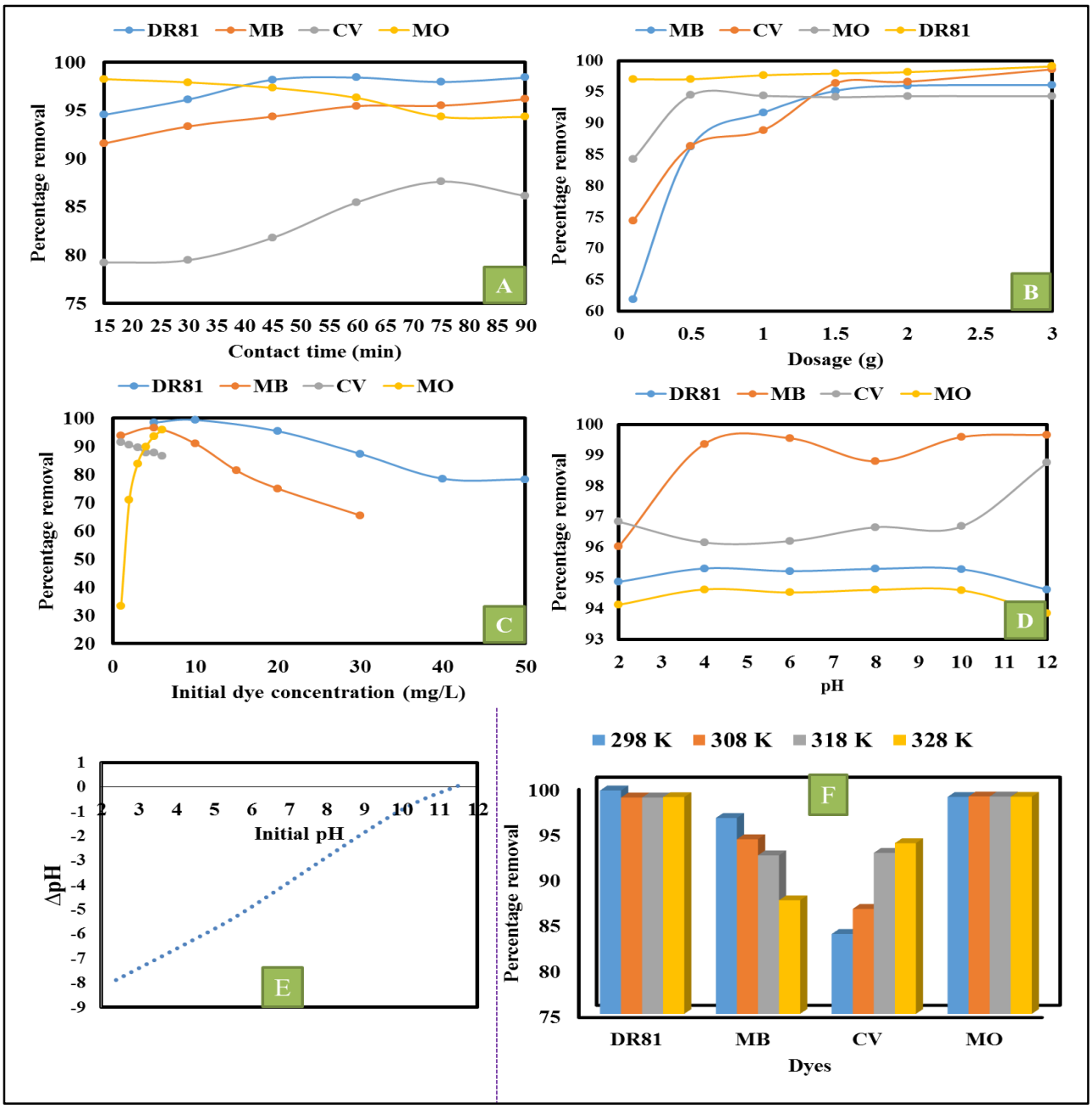

Figure 6: The optimization results for the removal of cationic and anionic dyes as a function of different operational parameters and PZC

Effect of contact time

As presented in **Figure 6A**, the removal capacity of CCM-HNC generally increases as the contact time is increased. The percentage removal for DR81, MB and CV started to decrease after 60 minutes whereas the initial percentage removal decrease for MO was at 45 minutes. The overall observation is that across the studied contact times, the percentage removal of CV dye was lower (<85%) whereas that of DR81, MB and MO were above 90%. Hypothetically,

this trend can be attributed to the number of free adsorbent sites accessible for adsorption (Ismail and AbdelKareem, 2015). The rate of dye removal at the early stages is rapid because of the accessibility of the unoccupied adsorbent sites. Similar results showing rapid adsorption at early stages have also been reported in other studies (Amuda et al., 2014; Öden and Özdem, 2014).

Effect of dosage

As displayed in **Figure 6B**, it was seen that the quantity of DR81, MB, CV and MO taken up by CCM-HNC increased with adsorbent dosage increase. It is interesting to note that, even at the least dosage of 0.1 g, CCM-HNC removed above 97 % of DR81 and its percentage removal remained notably high compared to other dyes. The increase in DR81, MB, CV and MO removal with dosage is probable driven by the improved obtainability of adsorbent sites (Goswami and Purkait, 2012; Balouch et al., 2013; Vinati et al., 2015).

Effect of initial DR81, MB, CV and **MO concentration**

As shown in **Figure 6C**, it is shown that the amount of DR81, MB and CV adsorbed declines with increase in the initial dye concentration which indicates that the adsorption process relies on the number of actives sites that are available for taking up DR81, MB and CV ions. When the adsorbate concentration is low, surface active sites / DR81, MB and CV ions ratio is high, therefore, the adsorbate could interact with the adsorbent to occupy the binding sites on the sorbent surface adequately thereby being removed from the solution. Some studies have also reported similar results (Amin, 2009; Gong et al., 2013; Amuda et al., 2014). As the DR81, MB and CV concentration increases, the amount of active adsorption sites become limited hence the observed decrease in percentage removal. On the contrary, MO percentage removal showed an opposite trend wherein there was a direct proportion between the percentage removal and initial dye concentration. It is observed that as MO is increased, the percentage removal also increases. Adsorption sites are available for occupation at lower initial dye concentration hence adsorption becomes independent of initial dye concentration. On the other hand, dye removal at higher concentration, depends on the initial concentration because the active sites would have been occupied due to large amounts of dye molecules (Özer et al., 2007). It should be noted that for MO and CV, the concentrations after contacting these dyes with the adsorbent above 6 mg/L were above range on the visible spectrophotometer hence the initial concentration variation for the two dyes was limited to 6 mg/L. This shows the range within which CCM-HNC can work on different dyes.

Effect of pH

Amongst most essential parameters to evaluate the adsorption process, pH accounts for the greatest part mainly because it influences charged ions distribution on the surface of the adsorbent. However, with CCM-HNC, varying the pH of the DR81, MB, CV and MO solution had a negligible effect on the removal of the dye as displayed by **Figure 6D**. The difference between the highest percentage removal (96.7%: pH=10: MB) and the lowest percentage removal (94.1%: pH=12: MO) is only 2.6% and in terms of colour visibility that was negligible. It can also be noted that as pH was varied the percentage removals of DR81, and MO did not vary a lot. However minor variations were observed for MB and CV dyes. The latter dyes are basic dyes whereas the former are acidic dyes. In that regard there was no need to adjust pH for subsequent experiments.

Point of Zero Charge Analysis

In adsorption systems, determining the pH dependent surface charge characteristics of the adsorbent material is crucial because it helps to determine pH conditions in favor of adsorption applications. In that regard, PZC becomes a significant property of nanocomposite–water interface to be assessed in technical adsorption systems (Mahmood et al., 2011; Samad et al., 2014). Numerous PZC values for basic and mixed oxide nanostructures have been reported in literature (Kosmulski, 2011; Singh et al., 2014) As shown in **Figure 6E**, CCM-HNC has a point of zero charge at pH = 11.65. This means that the surface of CCM-HNC is positively charged at pH values below 11.65 and negatively charged at pH values above 11.65. It is expected that, the percentage removal of the cationic dyes (MB and CV) be greater at pH above 11.65 and that of the anionic dyes (DR81 and MO) be greater at pH below 11.65. However, from Figure 6D, which shows the influence of pH on the percentage removal of the four dyes, there was no notable difference in the removal of dyes below and above pH 11.65. It therefore means that the removal of the dye from aqueous solution by CCM-HNC was not entirely controlled by ion exchange processes between the adsorbent material and the adsorbate.

Effect of temperature

As shown in **Figure 6F**, DR81, MB, CV and MO ion uptake capacities were evaluated as a function of temperature to select the most favorable temperature for the uptake of DR81, MB, CV and MO by CCM-HNC. Three different trends are observed with respect to the four dyes. The first trend is that the adsorption of the acidic dyes (DR81 and MO) was less affected by

changes in temperature because the percentage removal slightly decreased as the solution temperature was increased from 298 K to 328 K. The second trend is that of direct proportional relationship between temperature and percentage exhibited by CV and the last trend is that of an inverse relationship between temperature and percentage displayed by MB. The rise or decline of percentage removal with temperature assists in determining the type of adsorption (Ngulube aet al., 2017). If the percentage removal is directly proportional to temperature, that signifies an endothermic adsorption process whereas an inverse relationship between percentage removal and temperature signifies an exothermic process (Khorramabadi et al., 2012; Zhao et al., 2013; Zulfikar, 2013). On that basis, the adsorption of DR81, MB and CV were an exothermic process whereas that of CV was an endothermic process. As observed from **Figure 6F**, the % dye removal of CV by CCM-HNC was found to rise from 83.76 – 93.71 with rising temperature from 298 K to 328 K. This information shows that the movement of dye molecules improved with the rise in temperature (Shahryari et al., 2010). However, the percentage removal of MB decreased from 96.47 – 87.45 with rising temperature from 298 K to 328 K. Similar results of a reduction in dye percentage removal with rise in solution temperature were also reported in literature (Chatterjee et al., 2009; Vimonses et al., 2009). The reason why dye removal decreases as temperatures increase is the poor interaction between the dye and the adsorbent because hydrogen bonds and Van der Waals forces are weak.

3.3 Treatment of real industrial effluent

In general, textile wastewater is highly coloured, (specifically the dyeing and printing effluent) has a high pH and COD and contains a mixture of inorganic salts and a variety of inorganic molecules. The concentration of contaminants, especially in deep shades may greatly exceed effluent permissible limits. The parameters of the industrial wastewater used in this study are shown in Table 2.

Table 2. Characterization of real industrial effluent before and after treatment with calcined magnesite, halloysite nanoclay and the corresponding nanocomposite

Parameter	SA General standards (DWS)	Before treatment	After treatment with calcined magnesite	After treatment with halloysite nanoclay	After treatment with nanocomposite
TDS (mg/L)	25	1219	865	1068	630
TSS (mg/L)	90	918	613	785	432
EC (µS/m)	70000-150000	1764	1216	1504	889
Turbidity (NTU)	-	0.01	14.79	246	20.3
pH	6-9	8.77	11.79	8.20	11.81
Colour	colourless	black	colourless	milky white	colourless
Na (mg/L)	90	165	201	149	169
Cr (µg/L)	50	0.12	0.13	0.12	0.11
Fe (µg/L)	300	0.27	<0.025	0.031	<0.025
Mn (µg/L)	100	0.044	<0.025	0.031	<0.025
Zn (mg/L)	300	0.5	0.033	0.063	0.048
K (mg/L)	-	37	56	44	98
Mg (mg/L)	-	8	<1.0	10	1
Ca (mg/L)	-	20	108	35	5

In the present work, real printing and ink effluent was subjected to the process of adsorption using the optimized conditions achieved in the batch adsorption study. Characterization of wastewater indicate that the wastewater is categorized under high strength wastewater (Benefield, 2002). After treatment with the three adsorbent materials, the wastewater could be characterized under medium strength wastewater.

In all the analysis, done, it appears that most of the measured values of the physical parameters do not meet the South African discharge standards of industrial wastewater as provided for by the Department of Water and Sanitation (DWS). Only the EC values lie within permissible limits of industrial wastewater discharge. However, the values of the metal concentration

excluding that of Na lie within the permissible limits. It can be also noted that there is considerable heterogeneity in the results, showing variations of the degree of adsorption from one adsorbent to another. In terms of pH, only the effluent treated with halloysite remained within permissible limits (5.5 < pH < 9.5). The effluent treated with calcined magnesite and the nanocomposite was found to be highly alkaline therefore it is recommended that before discharge into the environment, the effluent be neutralized to meet wastewater requirements on pH. In terms of colour, (as shown in the images on **Figure 7**) an opposite trend was shown. The effluent treated with halloysite showed a milky white colour whereas that treated with calcined magnesite and the nanocomposite was colourless as recommended by DWS guidelines.

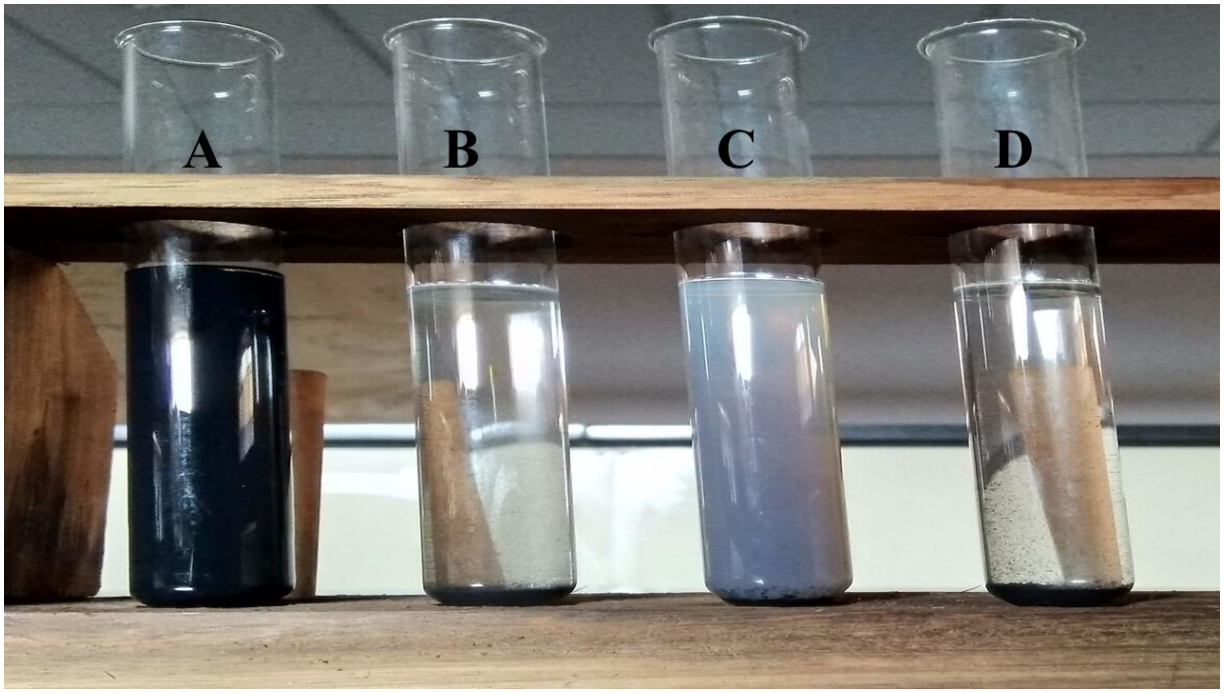

Figure 7. Real industrial effluent before and after treatment: **A** - real industrial effluent before treatment, **B** - real industrial effluent after treatment with calcined magnesite, **C** - real industrial effluent after treatment with halloysite clay, **D** - real industrial effluent after treatment with calcined magnesite- halloysite clay nanocomposite.

3.4 Adsorption isotherm modelling

Analyzing equilibrium data from isotherm models aids in describing results quantitatively. Isotherm coefficients of the isotherm models are essential parameters for calculating adsorption capacities and for integrating mass transfer relationships to predict the design of batch reactors (Chatterjee et al., 2009). Values of the isotherm constants were calculated from slopes and

intercepts of the different isotherm plots using regression analysis and presented in **Table 3** and **4.**

Table 3: Langmuir, Freundlich, Dubinin-Radushkevich and Temkin isotherm parameters for the adsorption of DR81, MB, CV and MO onto CCM-HNC

	DR81	**MB**	**CV**	**MO**
Langmuir	y = 0.0525x+0.0421 R^2 = 0.9623	y = 1.4127x+1.9171 R^2 = 0.9766	y = 3.469x+3.5698 R^2 = 0.9724	y = 154.2x-50.942 R^2 = 0.6157
Freundlich	y = 0.3318x+0.9337 R^2 = 0.8973	y = 0.5245x-0.6292 R^2 = 0.8812	y = 0.7675x-0.8063 R^2 =0.9975	y = -2.5959x- 2.2105 R^2 =0.7938
DBK	y = 0.588x+2.8184 R^2 = 0.8745	y = 0.9707x – 0.4365 R^2 = 0.9491	y = 09872x – 1.2823 R^2 = 0.9979	y = 3.612x-7.28 R^2 = 0.7637
Temkin	y = 2.8166x+10.695 R^2 = 0.9285	y = 0.1126x+0.336 R^2 =0.9754	y = 0.0468x+0.129 R^2 = 0.9547	y = -0.14x-0.042 R^2 = 0.9912

Table 4: Langmuir isotherm parameters for the adsorption of DR81, MB, CV and MO onto CCM-HNC

	Qm_{exp} (mg/g)	**Qm_{cal} (mg/g)**	**b (L/mg)**	**R_L**	**R^2**
DR81	19.89	0.0019	0.0451	0.6892	0.9623
MB	0.6547	0.7079	0.3693	0.2131	0.9766
CV	0.1296	0.2883	0.0808	0.5531	0.9724
MO	0.1436	0.0065	-0.0001	1.0010	0.6157

The cogency of isotherms is verified by comparing calculated and experimental data. On the basis of correlation coefficients (R^2) provided in **Table 3**, it is observed that the best fit over the entire range of models is given by the Langmuir model. The fit of the Langmuir isotherm model was in the order MB > CV > DR81 > MO.

When data fits best to the Langmuir isotherm, it shows that the dyes form a monolayer on the surfaces of CCM-HNC (Thilagavathy and Santhi, 2014). The dimensionless equilibrium separation factor (R_L), was used to estimate whether the adsorption process was favorable ($0 < R_L < 1$), linear ($R_L = 1$), unfavorable ($R_L > 1$) or irreversible ($R_L = 0$). The R_L values for DR81, MB and CV are 0.6892, 0.2131 and 0.5531 respectively (**Table 4**). The values show that the adsorption of these three dyes was a favorable process. However, the R_L value for MO was 1.0010 (= 1) which means that the adsorption of MO onto CCM-HNC was linear. This is further substantiated by the very low R^2 value for MO (0.6157), indicating that adsorption of the MO

dye did not best conform to the Langmuir isotherm. Comparing the experimental and calculated adsorption capacities showed that it was only the Qm values of MB which were closer to one another thereby corroborating the order of the R^2 fit of the Langmuir isotherm model (MB > CV > DR81 > MO).

3.5 Adsorption kinetics modelling

The process of adsorption is dependent on time; hence it becomes imperative to know the adsorption rate for design purposes (Izuagie et al., 2016). The experimental data of DR81, MB, CV and MO adsorption onto CCM-HNC were evaluated by fitting the data onto the pseudo first-order, pseudo second-order, intra particle diffusion and Elovich kinetic models. The values for the various parameters attained from fitting kinetic data on the model curve are listed in **Table 5**.

Table 5: Pseudo-second-order and Intra particle diffusion kinetic model parameters for the adsorption of DR81, MB, CV and MO onto CCM-HNC

Parameters	**DR81**	**MB**	**CV**	**MO**
Pseudo-first-order	y=0 R2= #N/A	y=0 R^2 = #N/A	y = -0.0138x+ 0.3243 R^2 = 0.1543	y = 2E-0.5x-0.0826 R^2 = 2E-0.5
Pseudo-second-order	y = 4.0647x R^2 = 1	y = 4.1594x R^2 = 1	y = 4.6436 R^2 =1	y = 0.0424 R^2 =1
Intra particle diffusion	y = 0.9826x-0.2414 R^2 =1	y = 0.9688x-0.2346 R^2 =1	y = 0.9119x-0.2078 R^2 =1	y = 9.805x-24.031 R^2 =1
Elovich	y = 156.14x-34.167 R^2 =0.8748	y = 155.02x-32.781 R^2 = 0.9897	y = 66.705x-10.085 R^2 = 0.822	y = -1.3639x+36.68 R^2 = 0.8008

Applying the pseudo-second-order kinetic model equation to the adsorption experimental data converged well with excellent R^2 values (R^2 = 1) for all four dyes as shown in **Table 5**. A straight line confirmed the suitability of the pseudo-second-order kinetic model for the description of DR81, MB, CV and MO onto CCM-HNC from aqueous solution. The pseudo-second-order kinetic model best fit could be indicating that chemisorption could possibly be the rate determining step in the adsorption process (Ngulube et al., 2018).

From a comparison of the coefficients of determination values (R^2) for the four kinetic models, the Intraparticle diffusion model also gave high correlation coefficients for DR81, MB, CV and MO. If the plot passes through the origin and the regression of Qt versus $t^{0.5}$ is linear, it is assumed that intraparticle diffusion is the sole rate-controlling step (Ofomaja, 2010; Guo et al., 2015). The fitting results show a linear regression; nevertheless, the intercept was not at zero

(C≠ 0). This is in contradiction with the intra-particle diffusion model validity. This suggests that DR81, MB, CV and MO adsorption onto CCM-HNC could not have been entirely governed by intraparticle diffusion (Abdus-Salam et al., 2017).

3.6 Thermodynamic study

To assess if adsorption process was feasible, thermodynamic parameters were evaluated and are shown in **Table 6.** The values of ΔG, ΔH and ΔS were obtained from the slope and intercept of the Van Hoff's plot of ln (Ka) vs 1/T (Zhou et al., 2014).

Table 6: Thermodynamic parameters for the system of DR81, MB, CV and MO adsorption onto CCM-HNC

Parameters	DR81	MB	CV	MO
ΔG kJ/mol	-17161.4	-15830.36	-17043.84	-19.79
ΔH (kJ/mol)	7390.56	-692481.37	1654.48	7E-25
ΔS (kJ/mol/K)	10.19	-20.76	-20.76	7.986

The values indicate that ΔH (enthalpy of activation) is positive for all the dyes except for MB. Positive values for the enthalpy of activation indicate that activation of the adsorption process for MO, DR81 and CV was endothermic whereas that of MB was exothermic because the value is negative. Moreover, the values of ΔH for MB and MO were not higher than 40 kJ/mol, signifying a physical adsorption process whereas that of DR81 and CV was a chemical process. ΔG for all the dyes were negative suggesting that the dye adsorption process was spontaneous and thermodynamically favourable and the negative value for entropy, ΔS, for MB and CV indicates that no vital changes happened during the activation stage. However, for DR81 and MO, the entropy values were positive indicating that there was an internal structural change in the composite material in the process of adsorption (Ofomaja et al., 2010).

3.7 Regeneration study

The reusability of adsorbents was performed by measuring the percentage removal of CCM-HNC during consecutive adsorption-desorption cycles (**Figure 8**).

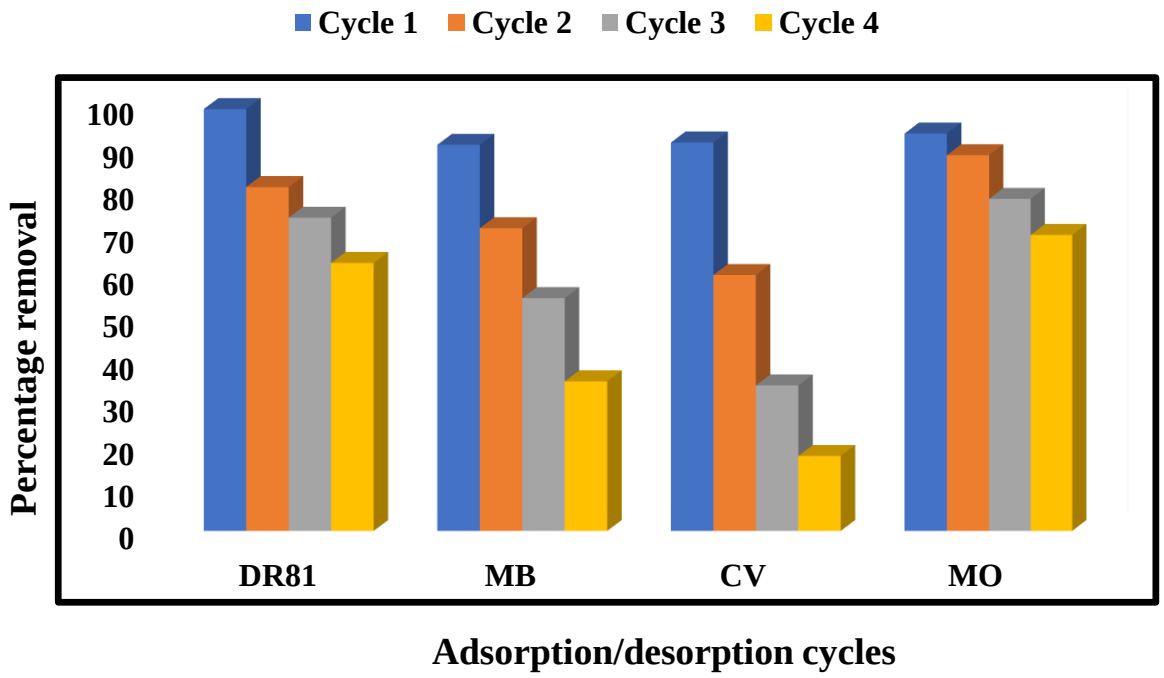

Figure 8: Regeneration of CCM-HNC

From **Figure 8**, it can be observed that with each consecutive cycle, the percentage removal of each dye decreased but 2 clear trends can be differentiated between the four dyes. It is shown that with DR81 and MO, the decrease with removal capacity is gradual whereas that of MB and CV is rapid. A possible reason is that DR81 and MO are acidic dyes whereas MB and CV are basic dyes, therefore there will be repulsive forces between the basic eluent used (NaOH) with the basic dyes such that, the adsorbed dyes remain in the matrices of the nanocomposite hence it cannot adsorb more dyes with each successive cycle. On the other hand, NaOH can react with the acidic dyes via electrostatic forces hence the acidic dyes-adsorbed nanocomposite is easily regenerated and maintains high percentage removal of dyes during consecutive adsorption-desorption cycles. These results clearly demonstrated the stability and good reusability of the nanocomposite prepared in this work.

4 Proposed mechanism

Several factors play a role in the adsorption of dye molecules onto an adsorbent. The type of functional groups found on the adsorbent's surface lead to numerous interactions such as electrostatic attractions and hydrogen bonding. Based on the FTIR results we can attempt to describe the adsorption mechanism involved during the interactions between CCM-HNC and the basic and acidic dyes. FTIR analysis study results suggest that there are two clear trends in the mechanisms of the interactions between the anionic (DR81 and MO) and the cationic dyes

(MB and CV). In aqueous solution, the acidic dyes take the form of anions (negatively charged ions) hence electrostatic repulsion occurs between these dyes and the negatively charged adsorbent surface. As shown earlier in the FTIR study, the stretching vibrations at 3600 – 3700 cm^{-1} corresponding to OH groups appeared to have shifted after dye adsorption indicative of the participation of hydroxyl groups during the adsorption process. The shifts in these bands also indicate the anionic dyes and the adsorbent interactions were physical in nature based on hydrogen bonding. This occurs between the adsorbent's hydroxyl groups and the -OH and -NH_2 groups in the dyes. The basic dyes trend indicates that the interactions between the surface of the adsorbent and the dyes are chemical. It seems that there is a formation of covalent bonds between oxides (CaO, MgO and SO_2,) available on the adsorbent surface with hydroxyl groups and the positively charged basic dye ions. These results agree with prior studies (Jesionowski et al., 2011; Fu et al., 2015; Wawrzkiewicz et al., 2015; Ciesielczyk et al., 2018), where authors revealed that the mechanism with which organic dyes interact with synthetic oxide adsorbents relies on the functional groups available on the dyes and the adsorbent's surface.

5 Comparison of the performance in dye removal between the raw individual materials and the synthesized nanocomposite

Recently, nanocomposite materials have been studied extensively because of their potential applications in wastewater treatment. Moreover, advantages possessed by each component and their combined properties also display some attractive features important in various applications. In this study, the performance of CCM-HNC was evaluated. This nanocomposite was synthesized by combining calcined cryptocrystalline magnesite and halloysite via mechanical modification using a vibratory ball miller. Evaluating the performance of the nanocomposite material on the removal of DR81, MB, CV and MO against the performance of its individual component (**Figure 9**) showed that the halloysite nanotubes performed extremely well more than the other two materials. The performance was in the order: halloysite > calcined cryptocrystalline magnesite > CCM-HNC. However, the highest adsorption capacity was observed for the nanocomposite material on the removal of DR81. Therefore, the synergestic effect of combining magnesite and halloysite was more favourable for DR81 dye compared to the others. Furthermore, it was shown that all three materials performed exceptionally well in the removal of DR81 however, calcined magnesite performed well for the removal of CV and halloysite performed well for the removal of MB.

It should however be highlighted that compared to the individual components of the nanocomposite, the synergistic effects had a positive effect on the ability of the nanocomposite to be regenerated for use again in adsorption processes. From the 3 separate regeneration studies, it was noted that when halloysite was used, after the second cycle, MB and DR81 adsorbed clays lost their effectiveness. The same was observed with the magnesite where the MB and CV adsorbed materials were no longer effective after the second and first regeneration cycle for the respective dyes. However, the nanocomposite material could be regenerated upto three times for all the four tested dyes.

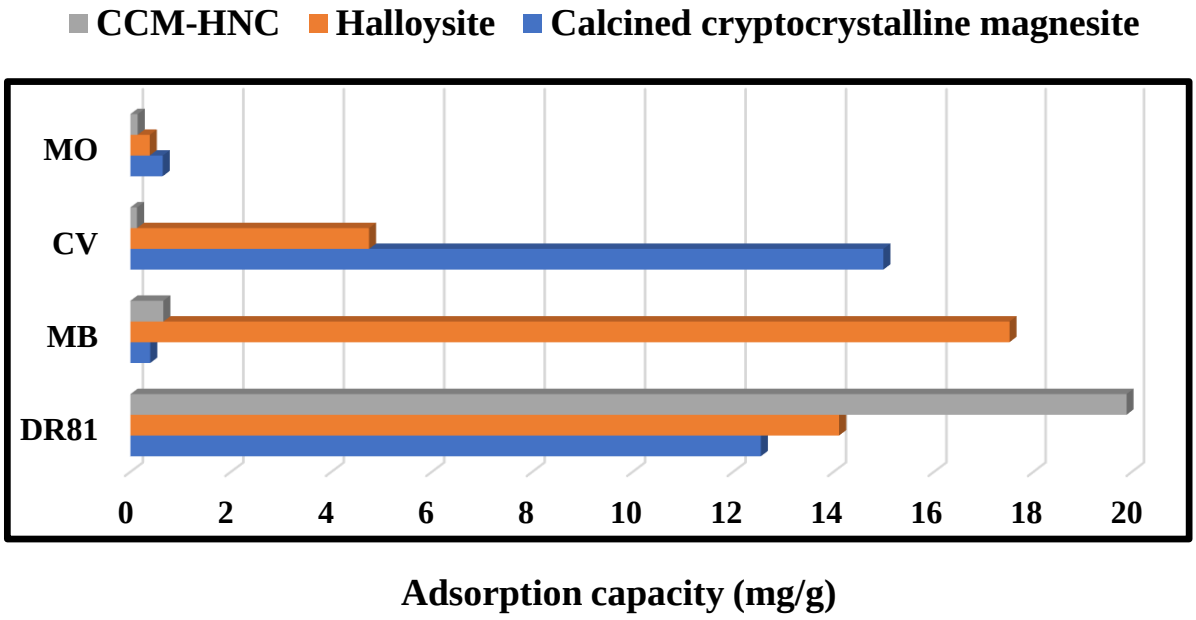

Figure 9: Comparison of maximum experimental adsorption capacities of cryptocrystalline magnesite, halloysite nanotubes, and CCM-HNC on the removal of DR81, MB, CV and MO

6 Comparison of the nanocomposite with other adsorbents

The maximum adsorption capacity of the CCM-HNC at room temperature was 19.89 mg/g for DR81 and considerably lower compared to most composite adsorbents reported in **Table 7**. It should however be noted that the mechanisms of dye adsorption onto different adsorbents are subject to the adsorbent's chemical properties and the physico-chemical experimental conditions used, including initial dye concentration, solution pH and temperature of the solution. Hence the differences in these affect the adsorption capacities of different adsorbents.

Table 7: Comparison of adsorption capacity of various adsorbents for DR81, MB, CV and MO adsorption

Adsorbent	**Adsorption capacity (mg/g)**	**Dye**	**Reference**
CCM-HNC	19.89	DR81	Present study
CCM-HNC	0.6547	MB	Present study
CCM-HNC	0.1296	CV	Present study
CCM-HNC	0.1436	MO	Present study
Magnetic halloysite-iron oxide nanocomposite	11.2	Naphthol green B	Riahi-Madvaar et al., 2017
Iron oxide/sepiolite magnetite composite	18.48	Safranin dye	Fayazi et al., 2015
Magnetite/carbon nanocomposite	83.42	MB	Iano et al., 2018
Chitosan/Fe_3O_4/graphene oxide nanocomposite	30.10	MB	Tran et al., 2017(a)
Sol-gel derived MgO-SiO_2 hybrid	44.9	C.I. Acid Blue 29	Ciesielczyk et al., 2017
Fe_3O_4-MNPs-AC	78.76	MB	Bagheri et al., 2017
Magnetic chitosan/claybeads	82	MB	Bée et al., 2017
Polyacrylamide-bentonite composite	144.60	MB	Anirudhan et al., 2009
Palygorskite/bentonite composite	44.95	MB	Mu and Wang et al., 2016
Magnesium hydroxide coated bentonite	40.22	Procion blue HP	Chinoune et al., 2016
Magnetic g-Fe_2O_3/SiO_2 (M-gFS) nanocomposite	26.62	MB	Chen et al., 2016
kaolin-bentonite clay	71.43	Congo red	Ogunmodede et al. 2015
SiO_2@MgO composite	2244.85	Crystal violet	Pei et al., 2015

7 Conclusion

A nanocomposite material was successfully synthesized from calcined cryptocrystalline magnesite and halloysite nanotubes. The synthesized nanocomposite was employed for the adsorption of DR81, MB, CV and MO dyes. On a comparative basis the nanocomposite showed the highest uptake for DR81 which could be attributed to the possible synergistic effect of electrostatic attractions from the halloysite clay and the coagulative mechanism of the magnesite material. The optimization adsorption study of the four dyes showed that equilibration time was reached after 75 min, the initial dye concentration and solution temperature had an obvious effect on the dye adsorption process, but the solution pH showed a negligible effect of the percentage removal of the dyes. The results of Langmuir model fitting to experiment data showed that adsorption took place on a homogenous surface of the composite material. The kinetic modeling data fitted well to both the pseudo-second-order kinetic model and the intraparticle diffusion model. The thermodynamic study gave negative ΔG for all the dyes suggesting that the dye adsorption process was spontaneous and thermodynamically favorable. The primary adsorption mechanisms involved in the removal of the dyes included electrostatic interaction and hydrogen-bonding formations. After four cycles of adsorption-desorption CCM-HNC presented an appreciable removal efficiency for the four dyes, demonstrating its good potential of regeneration and reuse. The advantages of the synthesised nanocomposite in this study compared to other nanocomposites used as adsorbents in literature are: the natural occurrence of the raw materials, quick reaction period, simplicity of the preparation technique accompanied by the capability to remove both acidic and basic dyes from aqueous solution and the good possibility to be regenerated and reused. The fabrication of the nanocomposite material via vibratory ball milling proved to be an easy and effective method and the resultant materials showed good dye removal efficiencies and therefore CCM-HNC can be applied for wastewater treatment purposes.

Acknowledgements

The authors wish to thank the Director of Research and Innovation, University of Venda, National Research Foundation (NRF) and Water Research Commission (WRC) for funding, the Council for Scientific and Industrial Research (CSIR) for extending all facilities required for this research.

References

Abdus-Salam N., Itiola A.D., 2012. Potential application of termite mound for adsorption and removal of Pb (II) from aqueous solutions. Journal of the Iranian Chemical Society. 9, 373 – 382.

Aharoni C., Tompkins F.C., 1970. Kinetics of adsorption and desorption and the Elovich equation, in: D.D. Eley, H. Pines, P.B. Weisz (Eds.), Advances in Catalysis and Related Subjects, vol. 21, Academic Press, New York, 1- 49.

Amin N.K., 2009. Removal of Direct Blue-106 Dye from Aqueous Solution Using New Activated Carbons Developed from Pomegranate Peel: Adsorption Equilibrium and Kinetics. Journal of Hazardous Materials. 165(1-3), 52-62.

Amuda O.S., Olayiwola A.O., Alade A.O., Farombi A.G., Adebisi S.A., 2014. Adsorption of Methylene Blue from Aqueous Solution Using Steam-Activated Carbon Produced from Lantana camara Stem. Journal of Environmental Protection. 5,1352-1363.

Anirudhan T.S., Ramachandran M., 2015. Adsorptive removal of basic dyes from aqueous solutions by surfactant modified halloysite clay (organoclay): kinetic and competitive adsorption isotherm. Process Safe Environ. Prot. 95, 215-225.

Bagheri A.R., Ghaedi M., Asfaram A., Bazrafshan A.A., Jannesar R., 2017. Comparative study on ultrasonic assisted adsorption of dyes from single system onto Fe_3O_4 magnetite nanoparticles loaded on activated carbon: experimental design methodology. Ultrason. Sonochem. 34, 294 - 304.

Balouch A.M., Kolachi F.N., Talpur H., Khan I., Bhanger M.I., 2013. Sorption kinetics, isotherm and thermodynamic modelling of defluoridation of groundwater using natural adsorbents. Am. J. Anal. Chem. 4, 221–228.

Bée A., Layaly L., Mbolantenaina R., Welschbillig M., Talbot D., 2017. Magnetic chitosan/claybeads: A magsorbent for the removal of cationic dye from water. Journal of Magnetism and Magnetic Materials. 421, 59-64.

Benefield L.A., 2002. Wastewater quality/strength/content. Wastewater Management Program. Washington State Department of Health. WAC 246-272-11501(3),1–18.

Buamah R., Mensah A., Salifu A., 2013. Adsorption of fluoride from aqueous solution using low cost adsorbent. Water Science and Technology: Water Supply13(2), 238-248.

Chatterjee S., Lee D.S., Lee M.W., Woo S.H., 2009. Congo red adsorption from aqueous solutions by using chitosan hydrogel beads impregnated with non-ionic or anionic surfactants. Bioresour. Techno. 100, 3862 - 3868.

Chen D., Zeng Z., Zeng Y., Zhang F., Wang A., 2016. Removal of methylene blue and mechanism on magnetic g-Fe_2O_3/SiO_2 nanocomposite from aqueous solution, Water Resour. Invest. 15, 1-13.

Chinoune K,, Bentale K,, Bouberka Z,, Nadim A,, Maschke U., 2016. Adsorption of reactive dyes from aqueous solution by dirty bentonite. Appl. Clay Sci. 123, 64 -75.

Ciesielczyk F., Bartczak P., Zdarta J., Jesionowski T., 2017. Active MgO-SiO_2 hybrid material for organic dye removal: A mechanism and interaction study of the adsorption of C.I. Acid Blue 29 and C.I. Basic Blue 9. Journal of Environmental Management. 204, 123-135.

Dabrowski A., 2001. Adsorption from theory to practice. Adv Colloid Interface Sci. 93, 135–224.

Dadfarnia S., Haji S.A.M., Moradi S.E., Emami S., 2015. Methyl red removal from water by iron-based metal-organic frameworks loaded onto iron oxide nanoparticle adsorbent. Appl. Surf. Sci. 330, 85-93.

Daifullah A.A.M., Yakout S.M., Elreefy S.A., 2007. Adsorption of fluoride in aqueous solutions using KMnO4-modified activated carbon derived from steam pyrolysis of rice straw. Journal of Hazardous Materials. 147, 633–643.

Department of Environmental Affairs (2014) National Guideline for the Discharge of Effluent from Land-based Sources into the Coastal Environment. Pretoria, South Africa. RP101/2014. RP101/2014 ISBN: 978-0-621-42619-9.

Dubinin M.M., 1960. The potential theory of adsorption of gases and vapors for adsorbents with energetically non-uniform surface. Chem. Rev. 60, 235–266.

Fayazi M., Afzali D., Taher M.A., Mostafavi A., Gupta V.K., 2015. Removal of Safranin dye from aqueous solution using magnetic mesoporous clay: optimization study. J. Mol. Liq. 212, 675 - 685.

Freundlich H.Z., 1906. Over the adsorption in solution, J. Phys. Chem. 57A, 385–470.

Fu J., Chen Z., Wang M., Liu S., Zhang J., Zhang J., Han R., Xu Q., 2015. Adsorption of methylene blue by a high-efficiency adsorbent (polydopamine microspheres): kinetics, isotherm, thermodynamics and mechanism analysis. Chem. Eng. J. 259, 53-61.

Gong L., Sun W., Kong L., 2013. Adsorption of Methylene Blue by NaOH-modified Dead Leaves of Plane Trees. Computational Water, Energy, and Environmental Engineering. 2, 13-19.

Goswami A., Purkait M.K., 2012. The defluoridation of water by acidic alumina. Chem. Eng. Res. Des, 90, 2316–2324.

Guo Z., Liu X., Huang H., 2015. Kinetics and Thermodynamics of Reserpine Adsorption onto Strong Acidic Cationic Exchange Fiber. PLoS ONE, 10(9), 0138619. https://doi.org/10.1371/journal.pone.0138619.

Hajjaji W., Pullar R.C., Labrincha J.A., Rocha F., 2016. Aqueous Acid Orange 7 dye removal by clay and red mud mixes. Applied Clay Science. 126, 197–206.

Ianos R., Pacurariu C., Muntean S.G., Muntean, E., Nistor M.A., Niznanský D., 2018. Combustion synthesis of iron oxide/carbon nanocomposites, efficient adsorbents for anionic and cationic dyes removal from wastewaters. Journal of Alloys and Compounds. 741, 1235-1246.

Ismail Z.Z., AbdelKareem H.N., 2015. Sustainable approach for recycling waste lamband chicken bones for fluoride removal from water followed by reusing fluoride-bearing waste in concrete. Waste Management. 45, 66 -75.

Izuagie A.A., Gitari W.M., Gumbo J.R., 2016. Synthesis and performance evaluation of Al/Fe oxide coated diatomaceous earth in groundwater defluoridation: towards fluorosis mitigation. J. Environ. Sci. Health Part A. 1-15.

Jesionowski T., Przybylska A., Kurc B., Ciesielczyk F., 2011. Hybrid pigments preparation via adsorption of C.I. Mordant Red 3 on both unmodified and aminosilane functionalised silica supports. Dyes Pigm. 89, 127-136.

Juang R.S. Chen M.L., 1997. Application of the Elovich equation to the kinetics of metal sorption with solvent-impregnated resins. Ind. Eng. Chem. Res. 36, 813–820.

Khorramabadi G.S., Soltani R.D.C., Rezaee A., Khataee A.R., Jafari A.J., 2012. Utilisation of immobilised activated sludge for the biosorption of chromium (VI). Can. J. Chem. Eng. 90, 1539.

Kosmulski M., 2011. The pH-dependent surface charging and points of zero charge V. Update, J. Colloid. Interf. Sci. 353, 1–15.

Langmuir I., 1918. The adsorption of gases on plane surfaces of glass, mica and platinum. J. Am. Chem. Soc. 40, 1362-1403.

Luo P., Zhao Y.F., Zhang B., Liu J.D., Yang Y., Liu J.F. 2010. Study on the adsorption of Neutral Red from aqueous solution onto halloysite nanotubes. Water Research. 44, 1489-1497.

Mahmood T., Mahmood T., Tahir M., Muhammad S., Saddique T., Abdul, N.N., Alum A.A., 2011. Comparison of Different Methods for the Point of Zero Charge Determination of NiO. Industrial & Engineering Chemistry Research, 50(17), 10017–10023.

Masindi V., Gitari M.W., 2016. Removal of boron from aqueous solution using cryptocrystalline magnesite. Journal of Water Reuse and Desalination. doi: 10.2166/wrd.2016.012.

Masindi V., Gitari M.W., Tutu H., De Beer M., 2014. Application of magnesite–bentonite clay composite as an alternative technology for removal of arsenic from industrial effluents. Toxicol. Environ. Chem. 96, 1435–1451.

Masindi V., Gitari M.W., Tutu H., De Beer M., 2015. Removal of boron from aqueous solution using magnesite and halloysite clay composite. Desalin. Water Treat. 1–11.

Mohammed M.A., Shitu A., Ibrahim A., 2014. Removal of Methylene Blue Using Low Cost Adsorbent: A Review. Research Journal of Chemical Sciences. 4(1), 91-102.

Mu B., Wang A., 2016. Adsorption of dyes onto palygorskite and its composites: a review. J. Environ. Chem. Eng. 4, 1274 -1294.

Ngulube T., Gumbo J.R., Masindi V., Maity A., 2017. An update on synthetic dyes adsorption onto clay-based minerals: A state-of-art review. Journal of Environmental Management. 191, 35-57.

Ngulube T., Gumbo J.R., Masindi V., Maity A., 2018. Calcined magnesite as an adsorbent for cationic and anionic dyes: characterization, adsorption parameters, isotherms and kinetics study. Heliyon. 4, e00838.

Öden M.K., Özdem C.R., 2014. Removal of Methylene Blue Dye from Aqueous Solution Using Natural Boron Ore and Leach Waste Material: Adsorption Optimization. International Journal of Current Research and Academic Review. 1, 66 -71.

Ofomaja A.E., 2010. Intraparticle diffusion process for lead (II) biosorption onto mansonia wood sawdust. Bioresource Technology. 101, 5868–5876.

Ogunmodede O.T., Ojo A.A., Adewole E., Adebayo O.L., 2015. Adsorptive removal of anionic dye from aqueous solutions by mixture of Kaolin and Bentonite clay: characteristics, isotherm, kinetic and thermodynamic studies. Iran. J. Energy Environ. 6 (2), 147- 153.

Özer D., Dursun G., Özer A., 2007. Methylene Blue Ad-sorption from Aqueous Solution by Dehydrated Peanut Hull. Journal of Hazardous Materials. 144 (1-2) 171-179.

Pei Y.Y., Wang M., Tian D., Xu X.F., Yuan L.J., 2015. Synthesis of core – shell SiO_2 @MgO with flower like morphology for removal of crystal violet in water. J. Colloid Interface Sci. 453, 194 -201.

Poots V.J.P., McKay G., Healy J.J., 1976. The removal of acid dye from effluent, using natural adsorbents: I. Peat. Water Res. 10, 1061–1066.

Prokop A., Maziarz P., Matusik J., 2015. Removal of selected anions by raw halloysite and smectite clay. Geology, Geophysics and Environment. 41 (1), 125 – 126.

Qiu Z., Kong X., Yuan J., Shen Y., Zhu B., Zhu L., Yao, Z., Tang C.Y., 2018. Cross-linked PVC/hyperbranched polyester composite hollow fiber membranes for dye removal. Reactive and Functional Polymers, 122, 51–59.

Rangabhashiyam S., Anu N., Selvaraju N., 2013. Sequestration of dye from textile industry wastewater using agricultural waste products as adsorbents. J. Environ. Chem. Eng. 1, 629-641.

Rasalingam S.1., Peng R., Koodali R.T., 2013. An investigation into the effect of porosities on the adsorption of rhodamine B using titania-silica mixed oxide xerogels. Journal of Environmental Management. 128, 530-539.

Riahi-Madvaar R., Taher M.A., Fazelirad H., 2017. Synthesis and characterization of magnetic halloysite-iron oxide nanocomposite and its application for naphthol green B removal. Appl. Clay Sci. 137, 101–106.

Samad JE, Hashim S, Ma S, Regalbuto JR (2014) Determining surface composition of mixed oxides with pH. J Colloid Interface Sci 436:204-210. doi: 10.1016/j.jcis.2014.07.050.

Santamarina J.C., Klein K.A., Wang Y., Prencke E., 2002. Specific surface: Determination and relevance. Canadian Geotechnical Journal. 39, 233–241.

Santos S.C.R., Boaventura R.A.R., 2016. Adsorption of cationic and anionic azo dyes on sepiolite clay: Equilibrium and kinetic studies in batch mode. Journal of Environmental Chemical Engineering. 4, 1473–1483.

Sarma G.K., Gupta S.S., Bhattacharyya K.G., 2016. Adsorption of Crystal violet on raw and acid-treated montmorillonite, K10, in aqueous suspension. Journal of Environmental Management. 171, 1-10.

Shahryari Z., Goharrizi A.S., Azadi M., 2010. Experimental study of methylene blue adsorption from aqueous solutions onto carbon nano tubes. International Journal of Water Resources and Environmental Engineering. 2 (2) 16-28.

Shokry H.H., Elkady M.F., El-Shazly A.H., Bamufleh H.S., 2014. Formulation of synthesized zinc oxide nanopowder into hybrid beads for dye separation. J. Nanomater. 1-14. Article ID 967492.

Singh D, Guatam RK, Kumar R, Shukla BK, Shankar V, Krishna V (2014) Citric acid coated magnetic nanoparticles: synthesis, characterization and application in removal of Cd(II) ions from aqueous solution. J. Water. Process. Eng 4:233–241.

Singh R.L., Singh P.K., Singh R.P., 2015. Enzymatic decolourization and degradation of azo dyes - a review. Int. Biodeterior. Biodegrad. 104, 21–31.

Temkin M.I., Pyzhev V., 1940. Kinetic of ammonia synthesis on promoted iron catalyst, Acta physiochim. USSR, 12, 327-356.

Thilagavathy P., Santhi T., 2014. Kinetics, Isotherms and Equilibrium Study of Co(II) Adsorption from Single and Binary Aqueous Solutions by Acacia nilotica Leaf Carbon. Chinese Journal of Chemical Engineering. 22 (11-12), 1193-1198.

Tran H.N., You S., Hosseini-Bandegharaei A., Chao H., 2017. Mistakes and inconsistencies regarding adsorption of contaminants from aqueous solutions: A critical review. Water Research. 120, 88-116.

Tran H.V., Bui L.T., Dinh T.T., Le D.H., Huynh C.D., Trinh A.X., 2017 (a). Graphene oxide/ Fe_3O_4/chitosan nanocomposite: a recoverable and recyclable adsorbent for organic dyes removal. Application to methylene blue, Mater. Res. Express 4. 035701, https://doi.org/10.1088/2053-1591/aa6096.

Uyar G., Kaygusuz F.H., Erim B., 2016. Methylene blue removal by alginate–clay quasi-cryogel beads. Reactive and Functional Polymers. 106, 1–7.

Vimonses V., Lei S., Jin B., Chow C.W.K., Saint C., 2009. Kinetic study and equilibrium isotherm analysis of Congo red adsorption by clay materials. Chem. Eng. J. 148, 354 -364.

Vinati A., Mahanty B., Behera S.K., 2015. Clay and clay minerals for fluoride removal from water: a state-of-the-art review. Applied Clay Science. 114, 340–348.

Wawrzkiewicz M., Wisniewska M., Gun'ko V.M., Zarko V.I., 2015. Adsorptive removal of acid, reactive and direct dyes from aqueous solutions and wastewater using mixed silica-alumina oxide. Powder Technol. 278, 306 -315.

Weber J.W.J., Morris J.C., 1963. Kinetics of adsorption on carbon from solution. J. Sanit. Eng. Div. ASCE 89 (SA2), 31-59.

Wu, Z., Zhong H., Yuan X., Wang H., Wang L., Chen X., Zeng G., Wu Y., 2017. Reply for comment on “Adsorptive removal of methylene blue by rhamnolipidfunctionalized graphene oxide from wastewater”. Water Res. 108, 464-465.

Yang R., Li D., Li A., Yang H., 2018. Adsorption properties and mechanisms of palygorskite for removal of various ionic dyes from water. Applied Clay Science. 151, 20-28.

Yakout S.M., Elsherif E., 2010. Batch kinetics, isotherm and thermodynamic studies of adsorption of strontium from aqueous solutions onto low cost rice-straw based carbons. Carbon – Sci. Tech. 1, 144 – 153.

Yousef A., Brooks R.M., El-Halwany M.M., Barakat N.A.M., EL-Newehy M.H., Kim H.Y., 2015. Cu0-decorated, carbon-doped rutile TiO_2 nanofibers via one step electrospinning: effective photocatalyst for azo dyes degradation under solar light. Chem. Eng. Process. 95, 202–207.

Zhan H.Y., Jiang Y.F., Ma Q.Z., 2014. Determination of adsorption characteristics of metal oxide nanomaterials: application as adsorbents. Analytic. Lett. 47, 871-884.

Zhang Y., Chen Y., Zhang H., Zhang B., Liu J., 2013. Potent antibacterial activity of a novel silver nanoparticle-halloysite nanotube nanocomposite powder. Journal of Inorganic Biochemistry. 118, 59-64.

Zhao Y., Abdullayev E., Vasiliev A., Lvov Y., 2013. Halloysite nanotubule clay for efficient water purification. J. Colloid Interface Sci. 406, 121-129.

Zhou Y., Zhou L., Zhang X., Chen Y., 2016. Preparation of zeolitic imidazolate framework-8/graphene oxide composites with enhanced VOCs adsorption capacity, Micropor. Mesopor. Mat. 225, 488-493.

Zhou Y., Zhang M., Wang X., Huang Q., Min Y., Ma T., Niu J., 2014. Removal of crystal violet by a novel cellulose-based adsorbent: comparison with native cellulose. Ind. Eng. Chem. Res. 53, 5498-5506.

Zulfikar M.A., 2013. Materials, Effect of temperature on adsorption of humic acid from peat water onto pyrophyllite. Int. J. Chem. Environ. Biol. Sci. 1, 88-91.

CHAPTER SIX

Application of calcined magnesite, halloysite nanoclay and calcined magnesite – halloysite clay nanocomposite in the removal of dyes: A column study.

This chapter has been prepared for submission to a peer reviewed journal as: Ngulube, T., Gumbo, J.R., Masindi, V., Maity, A., 2019. Exceptional removal of DR81 dye from aqueous solution: A fixed column study.

This chapter addresses objective (v).

Exceptional removal of Direct Red 81 dye from aqueous solution: A fixed column study

♣T. Ngulube [a], J.R Gumbo[b], V Masindi [c&d] and A. Maity [e&f].

[a] Department of Ecology and Resources Management, School of Environmental Sciences, University of Venda, Private bag X5050, Thohoyandou, 0950, Limpopo, South Africa. Tel: +27159628563, Email: tholisongulube@gmail.com

[b] Department of Hydrology and Water Resources, School of Environmental Sciences, University of Venda, Private bag X5050, Thohoyandou, 09 50, Limpopo, South Africa.

[c] Council for Scientific and Industrial Research (CSIR), Built Environment, Hydraulic Infrastructure Engineering, P.O BOX 395, Pretoria, 0001, South Africa.

[d] Department of Environmental Sciences, School of Agriculture and Environmental Sciences, University of South Africa (UNISA), P. O. Box 392, Florida, 1710, South Africa

[e] Department of Applied Chemistry, University of Johannesburg, Johannesburg, South Africa

[f] DST/CSIR National Centre for Nanostructured Materials, Council for Scientific and Industrial Research (CSIR), Pretoria, South Africa

Abstract

An approach to remediate dyed wastewater and reduce environmental pollution is the use of a permeable reactive barrier with adsorbent materials. In this study, the adsorption of Direct Red 81 (DR81) ions was conducted in a continuous flow fixed-bed column by using three adsorbent materials namely calcined magnesite, halloysite nanoclay and calcined magnesite - halloysite nanocomposite. The adsorbent's column performance was evaluated by manipulating the adsorbent bed height, flow rate of the dye solution and influent dye concentration. The increase in bed height increased the amount of adsorbent used, thus increasing the total removal of DR81 ions and prolonged the lifespan of the column. However, the increase in flow rate and influent concentration resulted in the shortened lifespan of the column. The column system which showed the best performance (maximum bed capacity = 51.7319 mg) was that of the nanocomposite material with a bed height of 4 cm, flow rate of 3 mL/min and 10 mg/L influent concentration. Moreover, a large volume of DR81 dye solution (2694 mL) was successfully decolourized using the nanocomposite material. Expressed through breakthrough curves, the packed-bed DR81 adsorption data of calcined magnesite and halloysite nanoclay showed consistency with the ideal s-shape. The kinetic data was analysed by the Thomas model and Adams-Bohart models. Low coefficient of determination values ($R^2 < 0.97$) were determined indicating that the experimental data did not conform very well to the models though the experimental data from halloysite nanomaterial provided a better fit compared to calcined

♣ Corresponding author: Email; tholisongulube@gmail.com

magnesite and the nanocomposite material. The study revealed the applicability of calcined magnesite- halloysite nanoclay composite in a fixed bed column for the removal of DR81 dye from aqueous solution.

Keywords: adsorption, breakthrough curve, continuous flow, nanocomposite, DR81 dye.

1 Introduction

Batch processes are vital for evaluating thermodynamic and kinetic parameters for adsorption reactions and the interaction between the pollutant and the adsorbent. They give essential information about the sorbent-sorbate interaction in terms of adsorption capacities and kinetics (Nouh et al., 2010). Batch adsorption systems are usually applied to treat small volumes of wastewater in the laboratory. These are limited because of the use of small vessel tests used on table shakers. For that reason, batch systems tend to be less suitable to be applied at an industrial scale where large volumes of water are continuously used. The industrial use of adsorbents screened using batch adsorption studies generally involves fixed-bed sorption (Maria and Mansur, 2017). In a continuous column set up, the sorbate is endlessly flowing though an adsorbent, thus offering a concentration gradient required between the adsorbate and adsorbent for adsorption to occur (Jia et al., 2014).

Column systems are normally applied in decontamination processeses that involve removing toxic organic compounds by way of ion exchange in a fixed bed through adsorption. In a batch set up, the sorbent and sorbate are in contact for a certain time pending equilibrium (Ahmad and Hameed, 2010). On the other hand, equilibrium is never attained at any stage in a column set up because the sorbate continuously enters and leaves the system. When the sorbate flows down the column, the upper part of the packed adsorbent (feed zone), becomes saturated and the low concentration of adsorbate comes into contact with fresh adsorbent at the bottom of the packing (Futalan et al., 2011). The overall column performance is determined by the service time, which is the time the sorbate breaks through the adsorbent in the column bed and is spotted in the effluent. During this time, the column flow can be stopped because the column is said to be saturated (Himanshu and Vashi 2015). From an economic and process control point of view, continuous column systems are the most suitable mode of adsorption systems. The column adsorption system is typically characterized by breakthrough curves, which are illustrations of the contaminant effluent concentration against time profile in a fixed-bed column (Han et al., 2008).

The breakthrough curve concept describes fixed-bed columns in terms of a priori design and their optimization. A breakthrough curve demonstrates the behaviour of a fixed-bed column from the point of view of the contaminant quantity that can be retained and is generally expressed in terms of a normalized concentration defined as the ratio of the effluent concentration to inlet concentration, as a function of flow time or volume of the effluent for the fixed-bed depth. In addition, breakthrough curve prediction through mathematical models is a useful tool for scale-up and design purposes.

In the previous chapters, calcined magnesite, halloysite nanoclay and calcined magnesite-halloysite nanocomposite showed high adsorption capacity for DR81 dye. On that basis, DR81 was chosen as a model dye to perform column adsorption experiments using the three different adsorbents. Because batch adsorption studies are usually not applicable to most industrial treatment systems, fixed bed column studies were done to study the effect of flow rate, bed height and initial dye concentration.

2 Materials and Methods

2.1 Column adsorption experiments

Continuous adsorption experiments in a fixed-bed column were conducted in a perspex glass column (3.5 cm internal diameter and 75 cm height), packed with a known quantity of adsorbent material. At the bottom of the column, inert glass beads were packed followed by a layer of glass wool. The column was set up as shown in Figure 1. Experiments were conducted, at a bed height of 4 cm, flow rate of 3 mL/min, 5 mL/min and 7 mL/min and the initial dye concentration was fixed at 10 mg/L. To investigate the effect of bed height, experiments were carried out at three different bed heights of 1.5 cm, 3 cm and 4 cm. The inlet flow rate was fixed at 3 mL/min by use of peristaltic pump (Gilson Mini puls evolution, 52F, USA) and a solution of fixed initial dye concentration (10 mg/L) was made to flow downwards through the column. To study the effect of initial dye concentration, the column was packed with the adsorbent materials to a height of 4 cm and dye solution of required concentration (5 mg/L, 10 mg/L and 20 mg/L) was made to flow through the column at a rate of 3 mL/min. The dye solutions at the outlet of the column were collected at regular time intervals and the final dye concentration was measured using a UV–vis spectrophotometer (Thermo Scientific Orion Aqua matte 7000, China). All the experiments were carried out at room temperature (28±^{o}C).

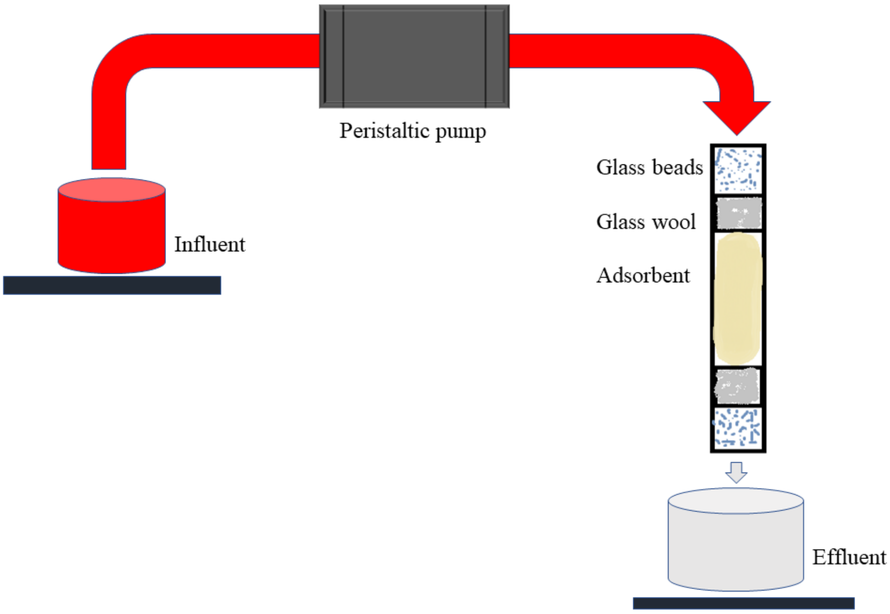

Figure 1. Schematic representation of the continuous fixed-bed column test apparatus

2.2 Mathematical description of Fixed Bed Column Studies

The breakthrough curve of a continuous fixed-bed system is used to evaluate the column performance.

The effluent volume is calculated using equation 1:

$$V_{eff} = Qt_{total} \ldots \ldots \ldots \ldots \ldots (1)$$

Where, V_{eff} is effluent volume collected (mL), Q is volumetric flow rate (mL/min) t_{total} is total flow time (min).

The maximum bed capacity for a given flow rate and feed concentration is given by equation 2:

$$q_{total} = \frac{Q\int C_{ad} dt}{1000} \ldots \ldots \ldots \ldots \ldots (2)$$

Where, q_{total} is maximum bed capacity (mg), Q is inlet flow rate (mL/min) Cad is adsorbed dye concentration (mg/g). The value of integral is obtained from the area under the curve of adsorbed dye concentration versus time.

The total amount of dye sent to the column is given by the equation 3:

$$M_{total} = \frac{C_o Q t_{total}}{1000} \dots\dots\dots\dots\dots\dots\dots\dots\dots\dots\dots\dots\dots\dots\dots\dots\dots\dots\dots\dots\dots\dots\dots\dots\dots\dots\dots\dots (3)$$

Where, M_{total} is total amount of dye sent to the column (mg), C_o is initial dye concentration (mg/g), Q is volumetric flow rate (mL/min), t_{total} is total flow time (min).

Total percentage of dye removal is given by the following equation:

$$\%\ Removal = \frac{q_{total}}{M_{total}}\ 100 \dots\dots\dots\dots\dots\dots\dots\dots\dots\dots\dots\dots\dots\dots\dots\dots\dots\dots\dots\dots\dots\dots\dots\dots. (4)$$

Where, q_{total} is maximum bed capacity (mg), M_{total} is total amount of dye sent to the column (mg).

Equilibrium dye uptake in the column is given by the following equation:

$$q_{eq(xp)} = \frac{q_{total}}{x} \dots\dots\dots\dots\dots\dots\dots\dots\dots\dots\dots\dots\dots\dots\dots\dots\dots\dots\dots\dots\dots\dots\dots\dots\dots\dots\dots. (5)$$

Where, qeq(exp) is equilibrium dye uptake (mg/gm), x is amount of adsorbent in the column (mg).

2.3 Modelling of Fixed Bed Column Studies

Many models have been proposed for the evaluation of the efficiency and applicability of column models for operations at industrial level. In the present work, adsorption data from the fixed bed column studies was analyzed using the Thomas and Adams-Bohart model.

2.3.1 The Thomas model

The Thomas model is based on the mass transfer model which assumes that dye migrates from the solution to the film around the particle and diffuses through the liquid film to the surface of the adsorbent. This is followed by intraparticle diffusion and adsorption on active sites (Rouf and Nagapadma, 2015). The linear form of Thomas model for adsorption is given by:

$$\ln\left(\frac{C_0}{C_t} - 1\right) = \frac{K_{TH} q_e x}{Q} - K_{TH} C_0 t \dots\dots\dots\dots\dots\dots\dots\dots\dots\dots\dots\dots\dots\dots\dots\dots\dots\dots\dots\dots\dots (6)$$

Where, C_o is initial dye concentration, mg/L; C_t is effluent dye concentration at time t; mg/L K_{TH} is Thomas model constant, L/min.mg; q_e is prediction adsorption capacity, mg/g; x is mass of adsorbent, gm; Q is inlet flow concentration, mL/min. The value of K_{TH} and q_e are determined from slope and intercept of a plot of $\ln\left(\frac{C_0}{C_t} - 1\right)$ versus t.

2.3.2 The Adams-Bohart model

The Adams-Bohart model assumes that the rate of adsorption is proportional to the residual concentration of the adsorbent and concentration of adsorbing species (Ling et al., 2016). This model is used for describing the initial part of the break through curve. The linear form of Adams-Bohart model is given by the following equation:

$$\ln\left(\frac{C_0}{C_t}\right) = K_{AB}C_0\,t - \frac{K_{AB}N_0Z}{U_0} \dots\dots\dots\dots\dots\dots\dots\dots\dots\dots\dots\dots (7)$$

Where, C_0 is initial dye concentration, mg/L; C_t is concentration of effluent at time t, mg/L; Z is bed depth, cm; N_0 is maximum dye uptake capacity per unit volume of adsorbent column, mg/L; U_0 is linear velocity of influent dye solution, cm/min; K_{AB} is Adams-Bohart rate constant, L/mg.min, The values of K_{AB} and N_0 are determined from the slope and intercept of $\ln\left(\frac{C_0}{C_t}\right)$ versus t.

3 Results and discussion

3.1 Column adsorption studies

The ratio of effluent DR81 concentration to the DR81 influent concentration against the flow time, which was the breakthrough curve was plotted in order to study the performance of the three adsorbents at various adsorbent bed heights, flow rates and DR81 influent concentrations.

3.1.1 Effect of influent concentration

The effect of DR81 influent concentration on the breakthrough curve was studied by varying the influent concentration at 5mg/L, 10 mg/L and 20 mg/L and the breakthrough curve is shown in Figure 1.

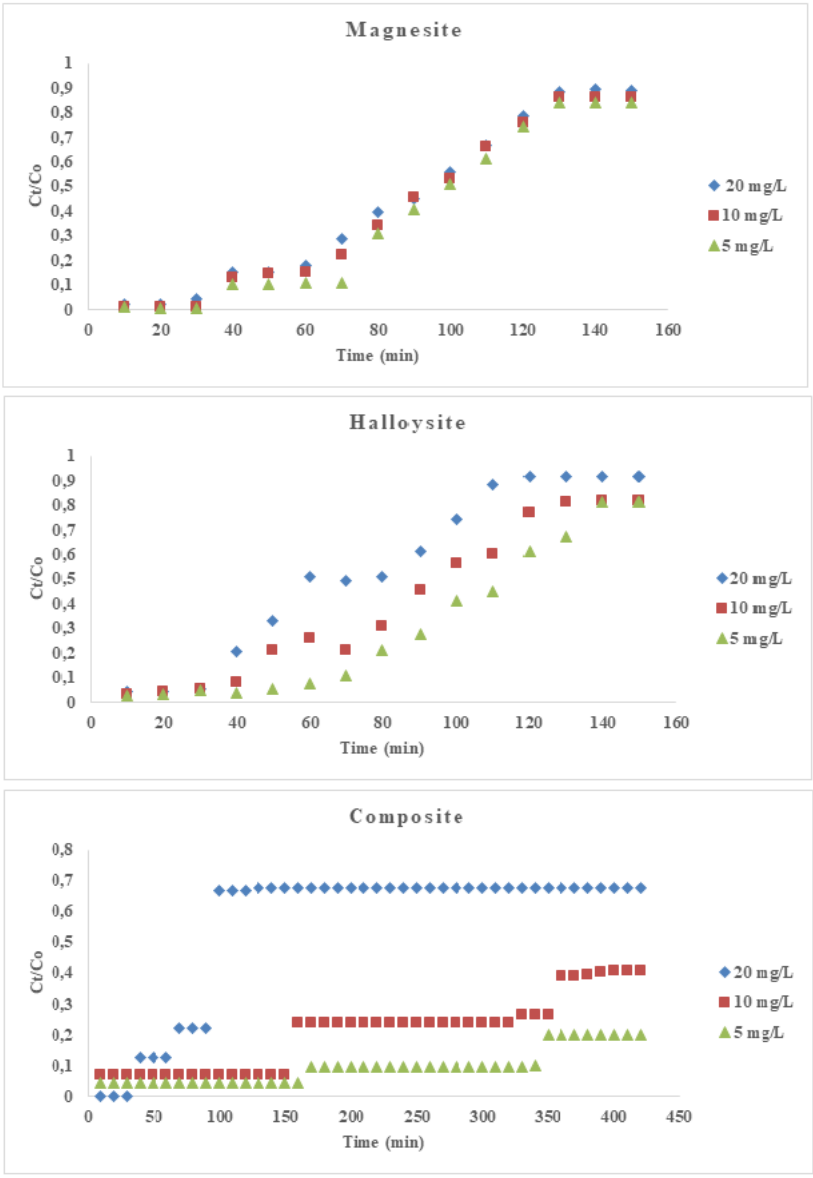

Figure 2: Breakthrough curves of calcined magnesite, halloysite nanoclay and nanocomposite material vs influent concentration

From Figure 2, the highest influent concentration of 20 mg/L showed the steepest slope of the 3 breakthrough curves. There is, however, variation between the adsorbents regarding saturation times. Calcined magnesite and halloysite nanoclay reached saturation at around 140 min, however the nanocomposite material column system ran almost 3 times longer than that of calcined magnesite and halloysite nanoclay. Usually, column studies are terminated when the column reaches exhaustion/saturation (Nwabanne and Igbokwe, 2015). However, there is an interesting observation made on the nanocomposite material i.e it does not reach exhaustion point, the material was effective in decolourizing DR81 dye for a longer period of time until such a time when the column could not yield enough effluent for analysis. Therefore, the

column system was stopped due to insufficient yield caused by blockage/clogging rather than reaching saturation.

Several studies have reported on partial saturation and/or blockage of the column during adsorption processes (Li et al., 2003; Kocyba, 2006; Arpanaei, 2008; Lin et al., 2015). Some studies have been conducted to investigate the mechanisms involved in the adsorption of organic pollutants on mesoporous materials, with a special focus on the roles of pore blocking and they report that pore blockage is mainly caused by larger molecules, which adsorb in larger pores and constrict, possibly completely blocking the entrance to smaller pores (Lin et al., 2015). Another report showed that when activated carbon is used at a water plant, organics collect on its surface. Residual of the chemicals used for treatment react either with the activated carbon surface or with the adsorbed organics. These reactions show that oxides may form as reaction products. These surface oxides form at the entrance to the micropores, which results in partial blockage of those pores and ultimate stoppage to the column (Doll, 1980).

In the case of the present study, blockage of the column system might have been due to the interactions between the adsorbent material and the DR81 dye in aqueous solution. XRD characterization results from the batch studies showed that after DR81 adsorption with the nanocomposite material, there was a production of brucite mineral in large quantities as well as notable amounts of calcite, dolomite and magnesite. Brucite which is basically, magnesium hydroxide is very sparingly insoluble in water and group 2 carbonates are also less soluble in water hence the column fouling might have been due to the collection of insoluble materials, which led to blocking, high back pressure and the need to stop column loading. Analysis of the adsorbent layer after discontinuing the column explicitly revealed blockage caused by fine particles forming a very hard brick of adsorbent material. It is important to emphasize that this blockage aspect before saturation, seen on the nanocomposite material was observed on all subsequent experiments using the nanocomposite material.

Figure 2 shows that, the larger the concentration of dye, the steeper is the break through curve. Steeper breakthrough slopes shown on high influent concentrations indicate that concentration has an effect on the saturation rate and thus reducing the break through time. With increase in dye concentration, the driving force for mass transfer will also increase. This results in a decreased adsorption zone (Rouf and Nagapadma, 2015). A decrease in influent concentration gave an extended breakthrough curve because a lower concentration gradient caused slower transportation due to a decrease in diffusion coefficient or mass transfer coefficient (Tan,

2008). Results from Table 1 show that, the calcined magnesite material treated more volume of influent compared to halloysite nanoclay and the nanocomposite material. In terms of the maximum bed capacity, the nanocomposite material recorded the highest capacity (10.31 mg) at an influent concentration of 10 mg/L.

Table 1: Effect of influent concentration on adsorption

Influent concentration (mg/L)	**Qtotal (mg)**	**Qeq(exp) (mg/gm)**	**Mtotal (mg)**	**% Dye Removal**	**Veff (mL)**
		Calcined magnesite			
5	2.1060	0.1404	2.25	93.60	1158
10	3.7349	0.2489	4.50	82.99	1250
20	10.2645	0.6843	9.00	43.84	1348
		Halloysite nanoclay			
5	3.2475	0.2165	3.25	99.9230	250
10	6.3900	0.4260	6.50	98.3076	275
20	9.8325	0.6555	10.0	98.3250	280
		Nanocomposite			
5	6.2785	0.4185	6.30	99.6587	810
10	10.3067	0.6871	12.6	81.7997	820
20	8.1773	0.5451	25.2	32.4496	815

3.1.2 Effect of Bed Height on Adsorption

The effect of bed height on adsorption was evaluated by varying the bed height from 1.5 cm to 4 cm as shown in Figure 3.

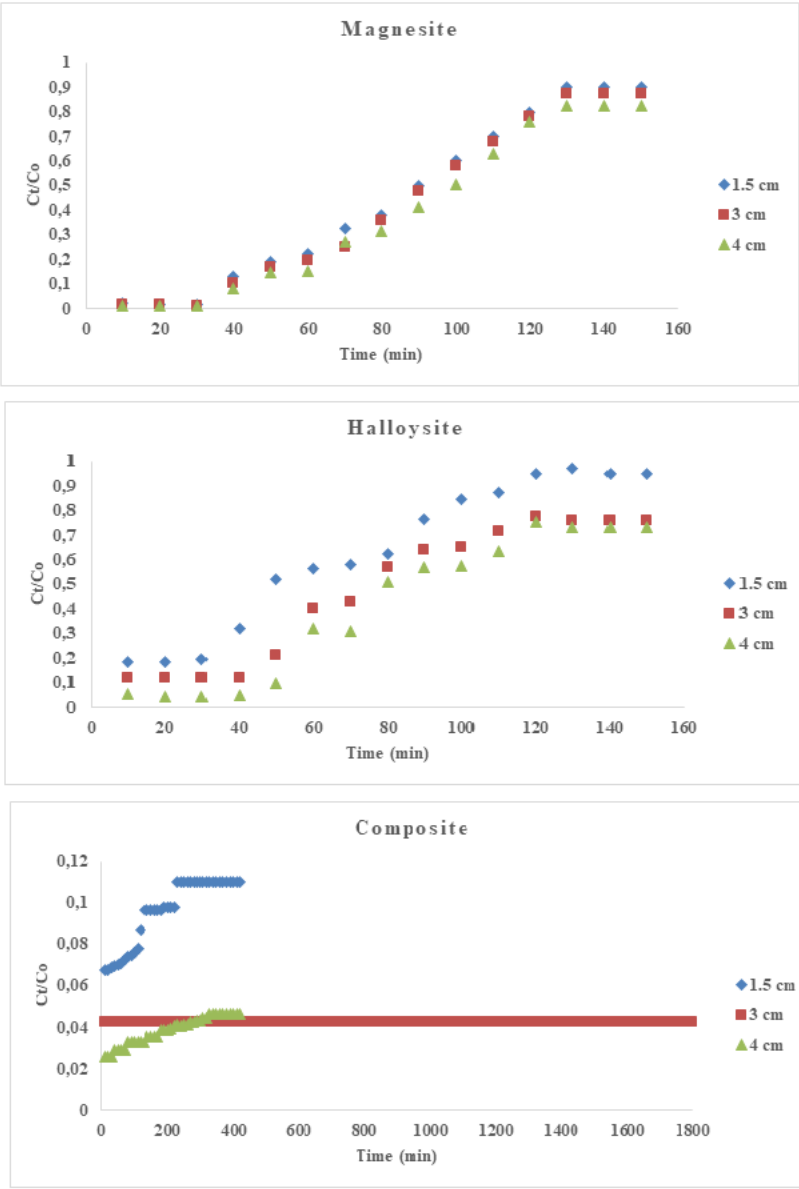

Figure 3: Breakthrough curves of calcined magnesite, halloysite nanoclay and the nanocomposite material vs bed height.

As the bed height increased, dye solution had more time to come in contact with the adsorbent. This resulted in higher % dye removal as shown in Table 2, ultimately leading to lower dye concentration in the effluent. The increase in bed height significantly affected the column performance by slowing the exhaustion time for halloysite nanoclay and calcined magnesite materials (Lim and Aris, 2014). The column breakthrough and the performance of adsorbent bed were both significantly affected by the length of bed height. From calcined magnesite and halloysite nanoclay breakthrough curves, it can be observed that the slope of the breakthrough curve decreased with increase in bed height, which resulted in a higher mass transfer zone. The break through curves were steeper at lower bed height. It should however be noted that, the

nanocomposite adsorbent gave a different trend compared to the other two adsorbents. It is seen that a bed height of 3 cm, the ratio of Ct/Ce did not change with time, it rather remained constant from the 10th minute to 1800th minute. It can also be seen that at that same bed height, the column ran for a longer period of 30 h compared to 1.5 and 4 cm which only operated for 7 h, though all the colums were stopped due to blockage rather than saturation. The column parameters attained from bed height effect are given in Table 2. As the bed height was increased, the total adsorption capacity of the bed also increased. More active sites are available for adsorption at higher bed heights and this leads to increased dye removal (Ling et al., 2016).

Table 2: Effect of bed height on adsorption

Bed height (cm)	**Qtotal (mg)**	**Qeq(exp) (mg/gm)**	**Mtotal (mg)**	**% Dye Removal**	**Veff (mL)**
		Calcined magnesite			
1.5	3.5414	0.7082	4.5	78.6993	684
3	3.6515	0.3652	4.5	81.1460	690
4	3.7079	0.2471	4.5	82.3993	696
		Halloysite nanoclay			
1.5	2.4599	0.4919	3.75	65.5986	172
3	2.3549	0.2355	3.75	62.7986	179
4	2.3999	0.1599	3.75	63.9986	184
		Nanocomposite			
1.5	10.5461	2.1092	12.6	83.6997	2694
3	51.7319	5.1732	54.0	95.7999	2700
4	12.0959	0.8064	12.6	95.9997	2712

3.1.2 Effect of flow rate

The effect of DR81 solution volumetric flow rate on the breakthrough curve was evaluated using three different flow rates: 3 mL/min, 5 mL/min and 7 mL/min. On varying the inlet flow rate from 3 mL/min to 7 mL/min, the following trend was observed on break through curves as shown in Figure 4.

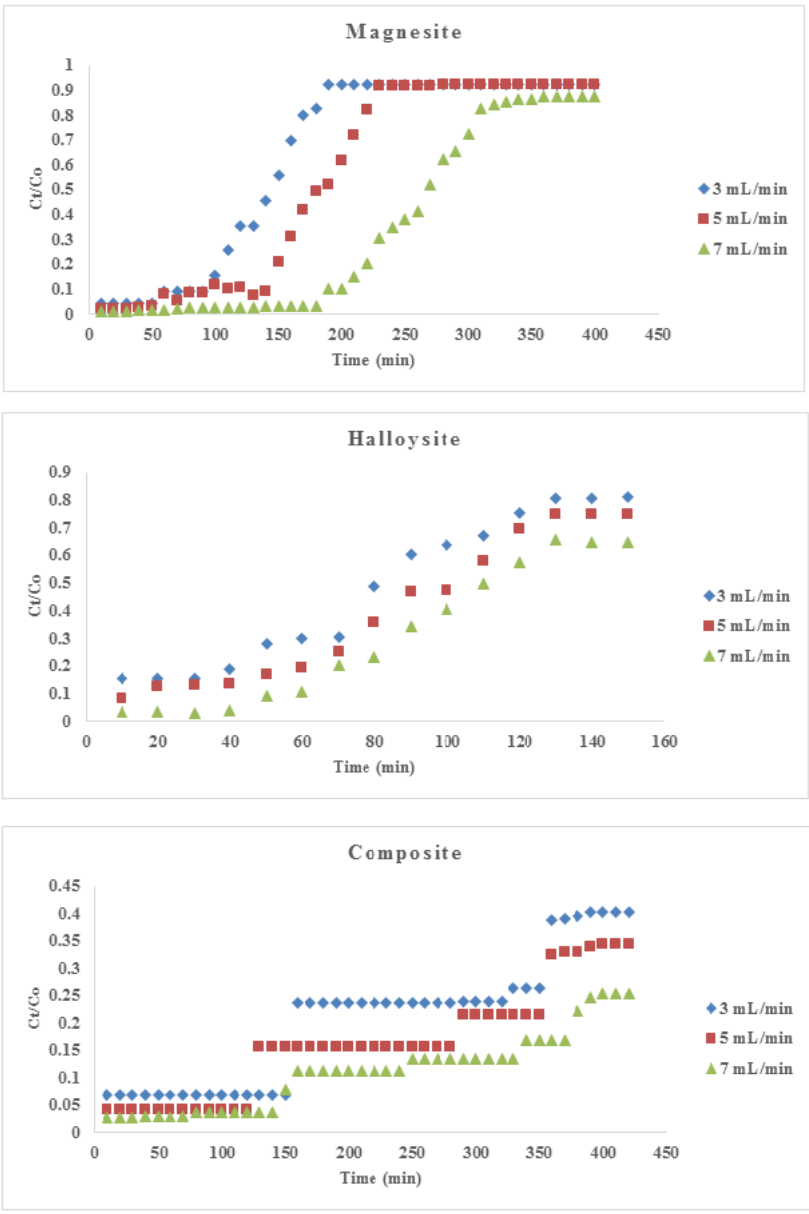

Figure 4: Breakthrough curves of calcined magnesite, halloysite nanoclay and the nanocomposite material vs influent flow rate

The column system with the fastest flow rate of 7 mL/min showed a gradual increase in breakthrough curve especially for the calcined magnesite material. The breakthrough curve became steeper as the flow rate was increased due to the lower contact time between the adsorbate and adsorbent (Setshedi et al., 2015). There is not enough time for the adsorption equilibrium to be achieved at higher flow rates therefore, the DR81 solution left the column before equilibrium was obtained (Janet et al., 2015). Increasing the flow rate gave rise to a shorter time for saturation. It can also be noted that the column system loaded with halloysite nanoclay had a shorter life span compared to that of calcined magnesite and nanocomposite. The column parameters attained from inlet flow rate effect are given in Table 3.

Table 3: Effect of inlet flow rate on adsorption

Flow rate (mL/min)	Qtotal (mg)	Qeq(exp) (mg/gm)	Mtotal (mg)	% Dye Removal	Veff (mL)
		Magnesite			
3	10.3823	0.6921	12.6	82.3997	666
5	17.1779	1.1452	21.0	81.7997	752
7	24.1667	1.6110	29.4	82.1997	868
		Halloysite			
3	2.0744	0.1382	2.25	92.1986	220
5	3.3899	0.3389	3.75	90.3986	344
7	4.5254	0.3016	5.25	86.1986	408
		Composite			
3	12.0477	0.8032	12.6	95.6166	666
5	19.8239	1.3216	21.0	94.3997	745
7	27.6065	0.1737	29.4	93.8997	896

From Table 3, the slowest flow rate of 3 mL/min achieved the highest % removal in all the 3 adsorbent column systems but the overall highest % removal was achieved by the nanocomposite adsorbent. On the other hand, the adsorption capacity of the adsorbents increased as the flow rate was decreased. The performance of the column was remarkably influenced by the flow rate as it affected the contact time between the adsorbate and adsorbent. The DR81 ions had longer time to diffuse through the pores and achieved a higher percent removal when the flow rate was decreased (Janet et al 2015; Ling et al., 2016). At higher flow rates, the decrease in liquid film surrounding the adsorbent particles led to the reduction of the boundary layer and the mass transfer resistance in adsorption processes (Lo´pez-Cervantes et al., 2018).

3.2 Adsorption modelling for breakthrough curves

3.2.1 Thomas model

The Thomas model has been applied in many studies to evaluate packed bed adsorption kinetics (Sivakumar and Palanisamy, 2009; Rouf and Nagapadma, 2015; Ling et al., 2016). The Thomas kinetic coefficient, (K_{TH}) and the bed adsorption capacity (q_e) were determined from the In[(Co/Ce)-1] against t plot. The results of the kinetic parameters are given in Table 4. The

Thomas rate constant and the adsorption capacity are largely dependent on flow rate. From Table 3, it is observed that as flow rate increases, the adsorption capacity represented by qe also increased. The same trend of increase with increasing flow rate is also seen with K_{TH}. Similar results were also reported by Sivakumar and Palanisamy (2009) and Nwabanne and Igbokwe (2012). Low coefficients of determination values were determined indicating that the experimental data did not conform well to the Thomas model. Comparison of the R^2 values amongst the three adsorbent materials showed that the Thomas model fitted more to the experimental data of halloysite nanoclay material.

Table 4: Thomas Model Parameters Using Linear Regression Analysis

Q (mL/min)	H (cm)	Co (mg/L)	q_e (mg/gm)	K_{TH} (L/min.mg)	R^2
		Calcined magnesite			
3	4	10	1.8769	0.0026	0.6548
5	4	10	3.1282	0.0044	0.9321
7	4	10	4.3794	0.0096	0.7365
3	3	10	3.1565	0.0025	0.6552
3	1.5	10	5.4960	0.0023	0.6527
3	4	5	1.7809	0.0021	0.7547
3	4	20	1.8774	0.0031	0.6822
		Halloysite nanoclay			
3	4	10	1.0348	0.0023	0.8313
5	4	10	1.7246	0.0048	0.8523
7	4	10	2.4145	0.0075	0.8544
3	3	10	1.2000	0.0014	0.9282
3	1.5	10	1.3286	0.0010	0.9163
3	4	5	1.0667	0.0021	0.8795
3	4	20	1.0000	0.0024	0.8098
		Nanocomposite			
3	4	10	0.6633	0.0002	0.8507
5	4	10	1.1054	0.0004	0.9051
7	4	10	1.5476	0.0006	0.9020
3	3	10	1.5E-14	0.00017	7E-16
3	1.5	10	5.2941	0.0006	0.8123
3	4	5	2.5143	0.0007	0.7079
3	4	20	3.6333	0.0006	0.3993

3.2.2 Adam-Bohart model

The Adam-Bohart model is used to predict the breakthrough activities for initial part of the adsorption process (Ling et al., 2016). The adsorption capacity of the adsorbent (N_o), and the

Adam-Bohart model rate constant (K_{AB}) were determined from the plot [ln (Ct/Co) versus t] and presented in Table 5.

Table 5: Adams-Bohart Model Parameters Using Linear Regression Analysis

Flow rate (mL/min)	**Bed Height (cm)**	**Dye concentration (mg/L)**	**N_0 (mg/gm)**	**K_{AB} (L/min.mg)**	**R^2**
		Calcined magnesite			
3	4	10	129.230	0.0223	0.6363
5	4	10	92.3348	0.0284	0.9230
7	4	10	53.7418	0.0341	0.8793
3	3	10	1956.15	0.0033	0.8454
3	1.5	10	316.262	0.0309	0.8381
3	4	5	134.349	0.0294	0.8992
3	4	20	154.859	0.0386	0.8267
		Halloysite nanoclay			
3	4	10	24.1034	0.1110	0.8280
5	4	10	17.2198	0.1521	0.9054
7	4	10	10.4200	0.1943	0.8883
3	3	10	401.174	0.0281	0.8408
3	1.5	10	572.522	0.0138	0.8609
3	4	5	136.227	0.0247	0.8038
3	4	20	185.177	0.0287	0.9674
		Nanocomposite			
3	4	10	450.5431	0.0054	0.8359
5	4	10	322.6111	0.0073	0.8596
7	4	10	193.5667	0.0088	0.9011
3	3	10	1.09E+16	5E-17	3E-15
3	1.5	10	7592.77	0.0013	0.8103
3	4	5	877.273	0.0043	0.8576
3	4	20	517.429	0.0085	0.3468

The results show that the adsorption capacity decreased with increase in flow rate but increased with increase in bed height and dye concentration. The column which recorded the highest adsorption capacity (7592.77 mg/gm) was that of the nanocomposite material with a bed height of 1.5 cm, 3 mL/min flow rate and a 10 mg/L dye concentration. The values of corresponding coefficients K_{AB} increased with increase in flow rate, bed height and dye concentration. The decrease in adsorption capacity with flow rate is because of the lower residence time of solute in the column (Rouf and Nagapadma, 2015). Based on R^2 values, the Adam-Bohart model was overall fitted better with the halloysite nanoclay than the calcined magnesite and nanocomposite materials.

4 Conclusions

In the present study, calcined magnesite, halloysite nanoclay and calcined magnesite-halloysite nanocomposite were used in column experiments to decolourize DR81 synthetic dye solution. Based on the experimental results of the column study, the following conclusions were drawn. Firstly, all three adsorbents can be used as adsorbents for the removal of DR81 dye from solution. However, in terms of column duration and colour removal the nanocomposite adsorbent performed exceptionally well compared to the halloysite nanoclay and calcined magnesite material. Despite the exceptional dye removal by the nanocomposite material, it should be quickly highlighted that for all the experiments performed using the nanocomposite adsorbent, the overall system was compromised by formation of insoluble compounds, that caused blockage of the column hence its inability to reach saturation. This column blockage can be a limitation to the application of this promising nanocomposite material for commercialization purposes hence the need to investigate further on procedures that can enable achievement of hydraulic conductivity with special regard to the mineral materials that explicitly depicted a tendency for blockage during the adsorption process.

The performance of the adsorbent materials in the column study based on the maximum bed capacity was in the order: nanocomposite adsorbent > calcined magnesite adsorbent > halloysite nanoclay adsorbent. The maximum capacity of column was found to be about 51.73 mg DR81 per gram of the nanocomposite adsorbent for a flow rate of 3 mL/min, initial concentration of 10 mg/L and 4 cm bed height. Moreover, adsorption was dependent on bed height, influent DR81 concentration and volumetric flow rate. When the bed height was decreased, the removal percentage was decreased and the total weight of DR81 adsorbed in the column also decreased. The study revealed that the synergestic effects of combining calcined

magnesite and halloysite nanoclay to make a nanocomposite material had a superiority effect on the removal of DR81 dye because the nanocomposite material performed well when compared to calcined magnesite and halloysite nanoclay individually.

References

Ahmad A.A., Hameed B.H., 2010. Fixed-bed adsorption of reactive azo dye onto granular activated carbon prepared from waste. Journal of Hazardous Materials. 175(1–3), 298–303.

Doull J., Borzelleca J.F., Engelbrecht R.S., Hoel D.G., 1980. Drinking Water and Health, Volume 2. Washington: National Academy Press.

Futalan C.M., Kan C.C., Dalida M.L., et al. 2011. Fixed-bed column studies on the removal of copper using chitosan immobilized on bentonite. Carbohydrate Polymers. 83(2), 697–704.

Han R., Ding D., Xu Y., et al. 2008. Use of rice husk for the adsorption of Congo red from aqueous solution in column mode. Bioresource Technology. 99(8), 2938–2946.

Himanshu P., Vashi R.T., 2015. Fixed-Bed Column Studies of Dyeing Mill Wastewater Treatment Using Naturally Prepared Adsorbents. Pp 127 – 145. In Characterization and Treatment of Textile Wastewater. Butterworth-Heinemann: USA.

Janet A., Kumaresan R., Uma M.S., 2015. Removal of dyes in adsorption column. Journal of Chemical and Pharmaceutical Research. 7(3), 1718-1723.

Jia D.M., Li Y.P., Li Y.J., Li Y.G., Li C.H., 2014. Fixed bed adsorption of 2-naphthalenesulfonic acid from aqueous solution by composite resin. Water Environ Res. 86(2), 99-103.

Kocyba J., 2006. Pilot trials with columns filled with reactive materials for stormwater treatment. MSC thesis submitted to Warsaw Agricultural University.

Li Q.L., Snoeyink V.L., Mariñas B.J., Campos C., 2003. Pore blockage effect of NOM on atrazine adsorption kinetics of PAC: The roles of PAC pore size distribution and NOM molecular weight. Water Res. 37, 4863- 4872.

Lim A.P., Aris A.Z., 2014. Continuous fixed-bed column study and adsorption modeling: Removal of cadmium (II) and lead (II) ions in aqueous solution by dead calcareous skeletons. Biochem. Eng. J. 87, 50-61.

Lin D., Hu L., Xing B., You H., Loy D.A., 2015. Mechanisms of Competitive Adsorption Organic Pollutants on Hexylene-Bridged Polysilsesquioxane. Materials. 8, 5806-5817.

Ling C.P., Tan I.A.W., Lim L.LP., 2016. Fixed-bed Column Study for Adsorption of Cadmium on Oil Palm Shell-derived Activated Carbon. Journal of Applied Science & Process Engineering. 3(2), 60- 71.

Lo´pez-Cervantes J., Sa´nchez-Machado D.I., Sa´nchez-Duarte R.G., Correa-Murrieta M.A., 2018. Study of a fixed-bed column in the adsorption of an azo dye from an aqueous medium using a chitosan–glutaraldehyde biosorbent. Adsorption Science & Technology. 36(1–2), 215–232.

Maria M.E., Mansur M.B., 2017. Mathematical modelling of manganese adsorption onto bone char in a continuous fixed bed column incorporating backmixing and shriking core approaches. Brazilian Journal of Chemical Engineering. 34 (3), 901 – 909.

Nouh S.A., Lau, K.K., Shariff, A.M., 2010. Modeling and simulation of fixed bed adsorption column using integrated CFD approach. Journal of Applied Sciences, 10(24), 3229-3235.

Nwabanne J. T., Igbokwe, P. K., 2012. Adsorption Performance of Packed Bed Column for the removal of Lead (ii) using oil Palm Fibre. International Journal of Applied Science and Technology. 2(5), 106-115.

Rouf S., Nagapadma M. 2015. Modeling of Fixed Bed Column Studies for Adsorption of Azo Dye on Chitosan Impregnated with a Cationic Surfactant. International Journal of Scientific & Engineering Research. 6(2), 538- 545.

Setshedi K.Z., Bhaumik M., Onyango M.S., Maity A., 2015. High-performance towards Cr (VI) removal using multi-active sites of polypyrrole–graphene oxide nanocomposites: Batch and column studies. Chemical Engineering Journal. 262, 921–931.

Sivakumar P., Palanisamy, P. N. 2009. Adsorption studies of basic Red 29 by a non-conventional activated carbon prepared from Euphorbia antiquorum L. International Journal of Chem. Tec. Research. 1(3), 502-510.

Tan I.A.W., 2008. Preparation, characterization and evaluation of mesoporous activated carbons derived from agricultural by-products for adsorption of methylene blue and 2,4,6-trichlorophenol, PhD Dissertation, University Science Malaysia.

CHAPTER SEVEN

Thesis Conclusions

This study was based on several objectives and therefore the conclusions will be drawn in accordance with the objectives.

- Firstly, a nanocomposite adsorbent was successfully prepared through a simple physical method employing a vibratory ball mill to blend the two adsorbent materials namely calcined magnesite and halloysite nanoclay. The successful fusion of the two raw materials to create a novel adsorbent material is evidenced in the characterization results.

- Characterisation results showed that the surface areas of calcined magnesite, halloysite nanoclay and the corresponding nanocomposite ranged from 6 – 47 m^2/g before and after adsorption. The general observation was that, the surface area decreased after dye adsorption which could possibly be due to the constriction of pores from occupation by dye particles. XRD results showed that periclase forms a large part of the calcined magnesite whereas halloysite nanoclay results showed a large presence of quartz and kaolinite and lastly, the nanocomposite material showed the presence of minerals as observed in calcined magnesite and halloysite nanoclay with an additional development of new materials like brucite and calcite further affirming a novel prepared adsorbent. SEM analysis showed more similar morphologies but worth noting is the eye-catching difference of the adsorbent materials after DR81 adsorption. In contrast to the usual definite spherical and rectangular shapes with different sizes of most clays, after reacting with DR81, the adsorbents have a striking different morphology characterised by irregular shaped flakes with sharp edges that have characteristic leafy structure images.

- Results from the use of calcined magnesite, halloysite nanoclay and the corresponding nanocomposite for the removal of MB, DR81, MO and CV dyes showed that, based on the experimental adsorption capacities from the batch adsorption experiments, the order of maximal performance was halloysite nanoclay > calcined magnesite > nanocomposite. Furthermore, in terms of the dyes, the greatest removal was recorded in the following order: DR81 > CV > MB > MO. The batch adsorption study showed that the optimum conditions for removing the four dyes were in the range: time (30 – 60 min), dosage (0.1- 2 g), initial dye concentration (6 – 40 mg/L), temperature (room temperature) and pH (2 - 12). Overall, on the batch adsorption study, based on experimental adsorption capacities and not on adsorption isotherm calculated adsorption capacities, the maximum removal was observed where calcined magnesite – halloysite nanocomposite was used to remove DR81 from solution recording 19.89 mg/g adsorption capacity.

- The column adsorption system showed that the nanocomposite material gave the best results with the best performance given by the column with a bed height of 4 cm, flow rate of 3 mL/min and 10 mg/L influent concentration recording a 51.73 mg maximum bed capacity. The order of best performance from the three materials used in the column study was: nanocomposite > calcined magnesite > halloysite nanoclay. Worthnoting is the fact that the nanocomposite material performed very well in terms of dye removal, but its lifespan was compromised by the formation of insoluble compounds, that caused blockage of the column hence its inability to reach saturation.

- Describing the mechanisms of adsorption by modelling showed that of the four adsorption isotherm models used in the batch study, no single isotherm model fitted all dyes across the three adsorbents used however the Langmuir model could describe the adsorption of the dyes onto halloysite nanoclay and the nanocomposite. On the other hand, the pseudo second order model of rate kinetics perfectly suited all data with accordance to the four dyes and three adsorbents, implying that chemisorption was possible the rate limiting step in the removal of the dyes from aqueous solution. To describe the mechanisms of adsorption for the column study, the Thomas model and the Adams-Bohart model were applied and both the models could not provide a perfect fit to the experimental data (R^2 values less than 0.97). However, comparison of the R^2

values obtained from both models showed a better fit for the halloysite nanoclay than the nanocomposite material and calcined magnesite materials.

- From the large number of published literature reviewed, it was observed that the mechanism of dyes on various adsorbents depend on the chemical nature of the materials and various physico-chemical experimental conditions such as solution pH, initial dye concentration, adsorbent dosage and temperature of the solution. Therefore, these factors are to be considered while evaluating the performance of adsorbent materials in contrast to others. The overall observation based on experimental adsorption capacities and not on calculated adsorption capacities is that the adsorbent materials used in this study performed well, though when compared to chemically modified adsorbents, they had fairly lower adsorption capacities.

- The general observation with regeneration experiments is that the more the adsorbent is regenerated and used for adsorption experiments, the more the adsorbent loses its adsorption capacity. This was true for the halloysite nanoclay material and the nanocomposite material. Calcined magnesite, however showed a different trend with regards to DR81 and MO dyes where the spent adsorbent had higher adsorption capacity as compared to fresh adsorbent. Overall, there was a general trend between the acidic dyes and the basic dyes. A possible reason is that DR81 and MO are acidic dyes whereas MB and CV are basic dyes, therefore there will be repulsive forces between the basic eluent used (NaOH) with the basic dyes such that the adsorbed dyes remain in the matrices of the adsorbent hence it cannot adsorb more dyes with each successive cycle. Nonetheless, the nanocomposite material exhibited high stability during the 4 regeneration cycles.

- It was a general observation that, with all three adsorbent materials, pH had a negligible influence on the removal of the tested dyes. However, it was also observed that when calcined magnesite was applied for dye removal the resultant solution was highly alkaline. Since this current adsorbent does not yield an acceptable pH for effluent discharge, it then becomes imperative for the wastewater to be neutralized by an acid to bring the pH of the effluents into the acceptable range before disposal.

- To conclude, a novel nanocomposite was prepared as an adsorbent for the removal of synthetic dyes from two natural clay-based materials without major chemical modifications. The study was based on the hypothesis that a nanocomposite prepared from calcined magnesite and halloysite nanoclay using a vibratory milling technique can successfully remove selected cationic and anionic dyes from aqueous solution. Results from this study proved the hypothesis right because it was observed that the nanocomposite material successfully decolourized both synthetic dye solutions and real industrial effluent from a printing industry. Furthermore, the application of the prepared nanocomposite material was successfully commissioned for a fixed column set up which has high feasibility for upgrading to industrial set up. In overall, based on the batch and column tests, the study revealed that the synergestic effects of combining calcined magnesite and halloysite nanoclay to make a nanocomposite material had a superiority effect on the removal of DR81 dye as the nanocomposite material performed well when compared to calcined magnesite and halloysite nanoclay individually towards DR81 dye.

Recommendations for future work

It is hoped that the present work will spur further research and advances in the wastewater treatment field and lead to the widespread application of adsorption in the removal of dyes from wastewater. Based on the gaps found in this study, the research described in this thesis could be continued in several ways.

- First, the present study is limited to the removal of dyes, in principle, the removal of colour from wastewater. However, the results provided in this thesis can act as a base for the removal of not just dyes but other water pollutants from industrial wastewater.

- In the future, a study is recommended to concentrate on overcoming the problem associated with adsorbent compaction during the column adsorption experiments which leads to blockage of the system and ultimately no production of effluent even when the adsorbent material is still efficiently removing colour from aqueous solution. The broad aim of such a study would be to develop a better understanding of how the hydrodynamics in adsorbent columns are affected by fluid distribution, to understand

the mechanisms behind adsorbate – adsorbent interaction and thus to find new solutions for better adsorbent design and column operation.

- Possible industrial application of this system raises issues to be explored. Results from column studies point towards the feasibility of the efficiency of these materials in fixed bed columns even in large industrial batch reactors. However, this work also raises questions as to whether significant improvements cannot still be made. In particular, the effect of different design parameters including distributor geometry and dimensions, and effluent outlet designs, the quality of the flow introduced, and its relation to scalability must still be investigated, both with model and real wastewater.

- Finally, disposal of adsorbent materials is one of the problems associated with the adsorption process. Regeneration can reduce the need of new adsorbent and reduce the problem of disposal of used adsorbent but overtime, the adsorbent might get exhausted and be rendered useless for adsorption processes. In that regard, post-adsorption methods of manufacture of value-added key products can be applied. In our case, with natural clay-based materials, these can be used to make bricks and clay pottery for decorative purposes. It is recommended that spent adsorbents be disposed of in licenced disposal landfills. Results from TGA analysis show that the adsorbent materials are stable to temperatures below 250 ^{o}C and regeneration studies showed that water causes minimal leaching but for precautionary measures the landfills must be protected from rainfall to prevent the possibility of generating contaminated storm water runoff.

APPENDICES

Appendix A: Supplementary materials for published chapters

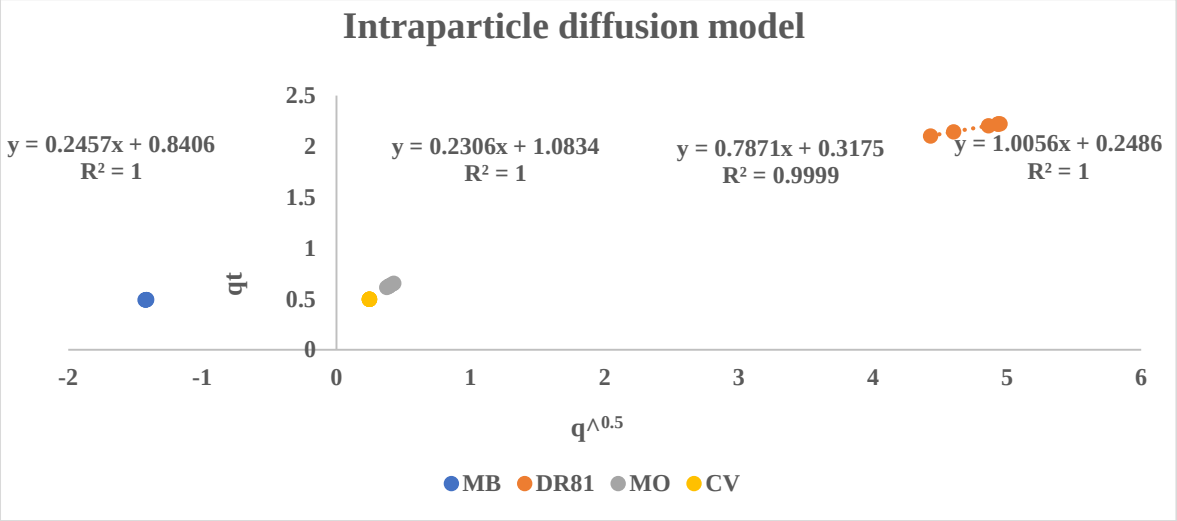

Figure S1: The intra particle diffusion model plot of Qt versus $t^{0.5}$ for calcined magnesite

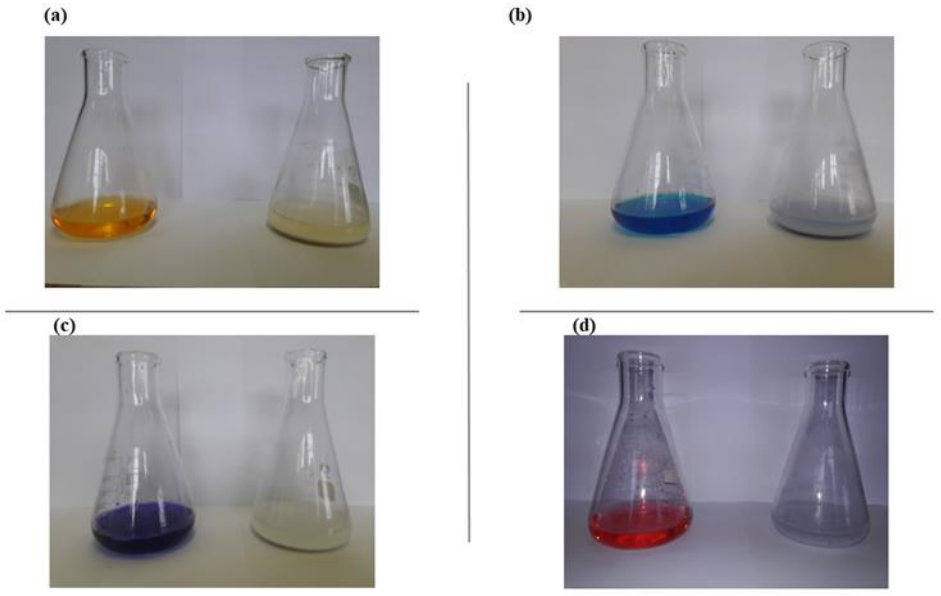

Figure S2: Images showing colour removal before and after adsorption by calcined magnesite on (a) – MO; (b) – MB; (c) – CV; (d) – DR81

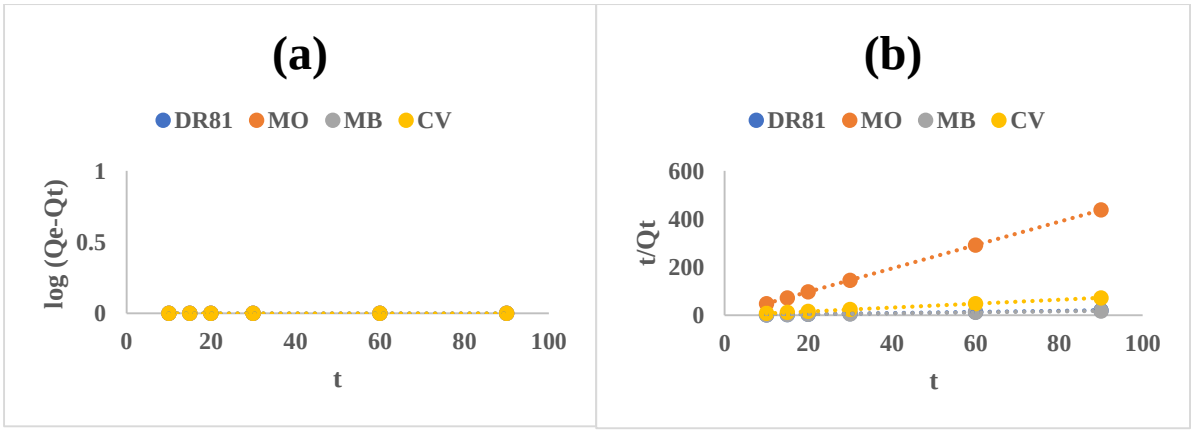

Figure S3: (a) The pseudo first order (b) the pseudo second order for adsorption of DR81, MO, MB and CV onto halloysite.

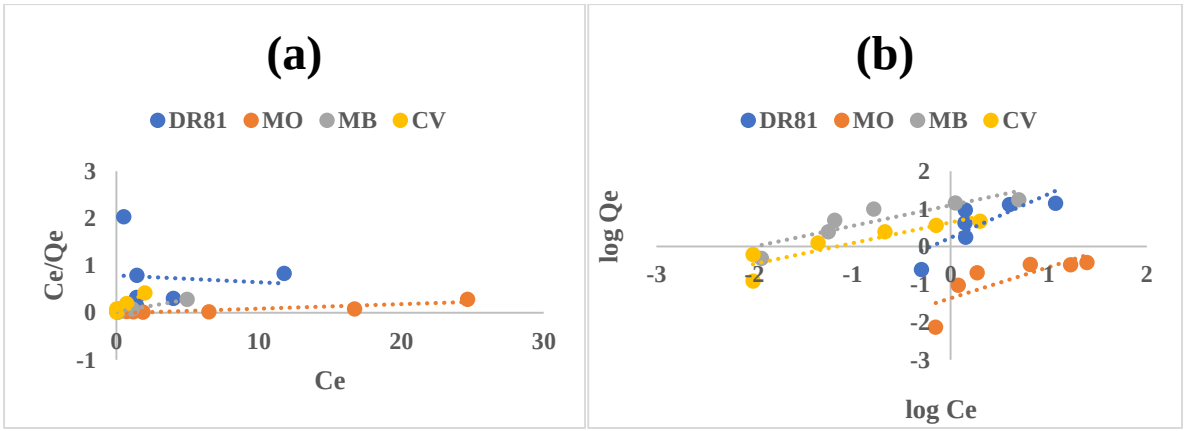

Figure S4: (a)- Langmuir (b) - Freundlich adsorption isotherm models of DR81, MO, MB and CV dyes onto halloysite.

Appendix B: Effect of various parameters on dye removal

B1: Percent removal (% R) and final pH (pH_f) of dye solutions after treatment with calcined magnesite

Table 1.1: Effect of contact time (min)

	% R				pH_f			
Time	MB	DR81	MO	CV	MB	DR81	MO	CV
15	96.05	88.63	85.82	98.79	11.90	11.58	12.75	11.61
30	96.61	92.04	75.29	98.87	12.03	11.83	12.74	11.75
60	96.61	98.75	77.87	98.90	12.02	11.87	12.72	11.73
90	96.95	97.27	79.06	98.98	12.01	11.85	12.77	11.81
120	96.95	98.63	78.86	98.96	12.02	11.92	12.65	11.73
180	97.18	98.97	83.23	98.92	11.96	11.86	12.69	11.72

Table 1.2: Effect of adsorbent dosage (g)

	% R				pH_f			
Dosage	MB	DR81	MO	CV	MB	DR81	MO	CV
0.1	54.26	96.70	46.92	98.01	11.18	12.08	11.72	11.54
0.2	66.92	96.93	53.17	98.02	12.09	12.38	11.83	12.11
0.4	75.53	98.86	53.17	99.02	12.51	12.85	12.03	12.45
0.8	97.48	98.63	67.06	98.98	12.82	13.19	12.31	12.75
1	98.70	98.63	67.36	98.98	12.90	13.27	12.37	12.85
2	98.72	98.97	73.41	98.74	13.4	13.41	12.36	13.01

Table 1.3: Effect of initial dye concentration (mg/L)

	% R				pH_f			
Conc	MB	DR81	MO	CV	MB	DR81	MO	CV
1	86.81	90.75	66.46	99.28	13.14	10.58	12.57	11.13
10	85.21	85.68	76.04	99.37	13.23	11.02	12.70	11.11
15	82.37	50.11	79.08	99.47	13.31	11.12	12.63	11.13
20	78.83	44.09	83.69	99.57	13.30	11.08	12.67	11.11
25	78.44	43.40	83.68	99.63	13.41	11.09	12.71	11.69
30	78.44	42.78	85.54	99.93	13.35	11.12	12.60	11.70

Table 1.4: Effect of solution temperature (K)

	% R			pH_f				
Temp	MB	DR81	MO	CV	MB	DR81	MO	CV
298	81.71	96.36	92.32	99.99	13.23	11.24	12.65	11.86
308	96.22	96.47	92.76	99.89	13.26	10.85	12.65	11.51
318	96.70	96.55	94.90	99.89	13.32	10.74	12.64	11.69
328	96.78	99.9	93.88	99.88	13.24	10.35	12.28	11.63

B2: Percent removal (% R) and final pH (pH_f) of dye solutions after treatment with halloysite nanoclay

Table 2.1: Effect of contact time (min)

	% R				pH_f			
Conc	DR81	MO	MB	CV	DR81	MO	MB	CV
10	87.33	80.82	98.46	99.25	6.92	6.16	6.30	7.79
15	87.33	80.36	98.51	99.20	7.03	6.26	6.32	7.37
20	87.21	79.75	98.55	99.32	7.24	6.43	6.37	6.72
30	86.99	80.36	98.48	99.328	7.42	6.51	6.44	6.27
60	86.88	80.21	98.51	99.23	7.23	6.57	6.50	6.29
90	87.10	82.20	98.43	99.35	7.09	6.61	6.44	6.41

Table 2.2: Effect of adsorbent dosage (g)

	% R				pH_f			
Dose	DR81	MO	MB	CV	DR81	MO	MB	CV
0.1	86.88	66.25	97.32	92.65	7.62	5.29	5.82	5.99
0.2	86.54	78.52	97.25	99.41	7.19	5.62	5.88	5.95
0.4	87.21	83.74	97.32	99.90	7.42	5.60	5.94	6.20
0.8	87.21	88.34	97.32	99.93	7.62	5.64	6.11	6.72
1	86.77	92.02	97.35	99.27	7.79	5.67	6.24	7.26
2	86.32	96.31	97.32	99.32	7.81	5.69	6.31	8.26

Table 2.3: Effect of initial dye concentration (mg/L)

	% R				pH_f			
Conc	DR81	MO	MB	CV	DR81	MO	MB	CV
1	49.55	29.44	98.81	99.03	7.85	5.55	5.89	7.41
5	71.52	76.07	98.86	99.80	7.56	5.63	5.83	7.08
10	85.98	81.28	99.33	99.55	7.13	5.67	5.66	6.50
20	92.93	67.56	99.17	98.92	6.86	5.78	5.63	5.86
30	86.65	44.27	96.25	97.62	7.02	5.84	5.48	5.70
40	70.57	38.34	87.57	95.00	7.18	5.91	5.41	5.36

Table 2.4: Effect of pH

	% R				pH_f			
pH	DR81	MO	MB	CV	DR81	MO	MB	CV
2	98.38	21.31	98.38	98.97	2.59	2.33	2.41	2.56
4	98.61	42.02	98.61	99.72	6.33	4.40	4.83	5.03
6	98.66	42.17	98.66	99.82	6.50	6.59	4.90	5.80
8	98.45	70.24	98.45	99.81	6.64	8.44	5.42	5.90
10	98.43	41.71	98.43	99.87	9.01	10.02	7.12	6.40
12	98.42	20.55	98.42	99.73	11.67	12.01	11.35	11.29

Table 2.5: Effect of solution temperature (K)

	% R				pH_f			
Temp	DR81	MO	MB	CV	DR81	MO	MB	CV
298	93.21	11.50	98.34	99.07	6.64	5.63	5.69	6.02
308	93.66	17.33	99.40	99.09	6.17	5.54	5.51	6.12
318	93.72	14.87	99.64	99.09	6.24	5.69	5.64	6.32
328	93.55	12.42	99.99	98.95	6.24	5.52	5.94	5.92

B3: Percent removal (% R) and final pH (pH_f) of dye solutions after treatment with calcined magnesite-halloysite nanoclay nanocomposite

Table 3.1: Effect of contact time (min)

	% R				pH_f			
Time	DR81	MB	CV	MO	DR81	MB	CV	MO
15	94.54	91.58	79.22	98.25	10.26	9.64	10.46	9.36
30	96.13	93.34	79.47	97.91	10.27	9.83	10.51	9.41
45	98.18	94.36	81.79	97.34	10.31	9.80	10.63	9.42
60	98.40	95.45	85.47	96.30	10.36	9.82	10.64	9.50
75	97.95	95.49	87.61	94.33	10.41	9.71	10.70	9.55
90	98.40	96.16	86.13	94.33	10.51	9.73	10.73	9.55

Table 3.2: Effect of adsorbent dosage (g)

	% R				pH_f			
Dose	DR81	MB	CV	MO	DR81	MB	CV	MO
0.1	97.04	61.89	74.39	84.27	10.37	9.48	10.54	9.15
0.5	97.04	86.20	86.37	94.49	10.58	9.72	10.60	9.58
1	97.68	91.69	88.90	94.38	10.59	9.83	10.75	9.77
1.5	97.95	95.18	96.41	94.17	10.59	9.88	10.86	9.71
2	98.18	96.01	96.65	94.33	10.62	9.92	10.88	9.86
3	99.09	96.12	98.62	94.33	10.62	9.93	10.97	9.93

Table 3.3: Effect of initial dye concentration (mg/L)

	% R					pH_f			
Conc	CV	MO	**Conc**	MB	**Conc**	DR81	CV	MO	MB	DR81
1	91.47	33.24	**1**	93.79	**5**	98.40	10.15	9.72	9.52	9.76
2	90.40	71.03	**5**	96.46	**10**	99.31	10.34	9.78	9.70	10.02
3	89.51	83.84	**10**	90.94	**20**	95.34	10.35	9.82	9.73	10.06
4	87.79	89.79	**15**	81.37	**30**	87.31	10.41	9.83	9.77	10.12
5	87.61	93.57	**20**	74.98	**40**	87.3	10.40	9.85	9.80	10.10
6	86.46	95.71	**30**	65.47	**50**	78.26	10.39	9.85	9.91	10.18

Table 3.4: Effect of pH

	% R				pH_f			
pH	DR81	MB	CV		DR81	MB	CV	MO
2	94.86	96.01	96.82	94.12	10.36	9.62	10.24	9.47
4	95.30	99.36	96.15	94.62	10.44	10.97	10.35	10.00
6	95.21	99.54	96.19	94.52	10.48	10.98	10.43	9.76
8	95.29	98.79	96.65	94.60	10.56	11.03	10.41	9.91
10	95.28	99.58	96.67	94.59	10.63	11.04	10.38	9.85
12	94.61	99.66	98.74	93.83	10.71	11.74	10.68	10.67

Table 3.5: Effect of solution temperature (K)

	% R				pH_f			
Temp	DR81	MB	CV	MO	DR81	MB	CV	MO
298	99.47	96.46	83.75	98.77	10.56	9.85	10.35	9.83
308	98.70	94.13	86.50	98.82	10.61	9.88	10.41	9.92
318	98.70	92.37	92.64	98.81	10.60	9.91	10.44	9.88
328	98.75	87.44	93.70	98.79	10.59	9.90	10.38	9.86